

Some pages of this thesis may have been removed for copyright restrictions.

If you have discovered material in Aston Research Explorer which is unlawful e.g. breaches copyright, (either yours or that of a third party) or any other law, including but not limited to those relating to patent, trademark, confidentiality, data protection, obscenity, defamation, libel, then please read our [Takedown policy](#) and contact the service immediately (openaccess@aston.ac.uk)

**SOLIDS MIXING AND
SEGREGATION IN A GAS
SPOUT-FLUID BED
- EFFECT OF THE
DISTRIBUTOR DESIGN**

Afzal Elahi Qureshi

Doctor of Philosophy

The University of Aston in Birmingham

May, 1990

This copy of the thesis has been supplied on the condition that anyone who consults it is understood to recognise that its copyright rests with its author and that no quotation from the thesis and no information derived from it may be published without the author's prior, written consent.

The University of Aston in Birmingham

**SOLIDS MIXING AND SEGREGATION IN A GAS SPOUT-FLUID BED-
EFFECT OF THE DISTRIBUTOR DESIGN**

AFZAL ELAHI QURESHI

Doctor of Philosophy

1990

SUMMARY

This work is concerned with the assessment of a newer version of the spout-fluid bed where the gas is supplied from a common plenum and the distributor controls the operational phenomenon. Thus the main body of the work deals with the effect of the distributor design on the mixing and segregation of solids in a gas spout-fluid bed. The effect of distributor design in the conventional fluidised bed and of variation of the gas inlet diameter in a spouted bed was also briefly investigated for purposes of comparison. Large particles were selected for study because they are becoming increasingly important in industrial fluidised beds but have not been thoroughly investigated. The mean particle diameters of the fraction ranged from 550 to 2400 μm , and their specific gravity from 0.97 to 2.45. Only work carried out with binary systems is reported here. The effects of air velocity, particle properties, bed height, the relative amount of jetsam and flotsam and initial conditions on the steady-state concentration profiles were assessed with selected distributors. The work is divided into three sections. Sections I and II deal with the fluidised bed and spouted bed systems.

Section III covers the development of the spout-fluid bed and its behaviour with reference to distributor design and it is shown how benefits of both spouting and fluidising phenomena can be exploited. In the fluidisation zone, better mixing is achieved by distributors which produce a large initial bubble diameter. Some common features exist between the behaviour of unidensity jetsam-rich systems and different density flotsam-rich systems. The shape factor does not seem to have an affect as long as it is only restricted to the minor component. However, in the case of the major component, particle shape significantly affects the final results. Studies of aspect ratio showed that there is a maxima (1.5) above which slugging occurs and the effect of the distributor design is nullified. A mixing number was developed for unidensity spherical rich systems, which proved to be extremely useful in quantifying the variation in mixing and segregation with changes in distributor design.

Key words: Concentration profile, jetsam, flotsam, fluidisation, spouting, spout-fluidising velocity, developed zone, undeveloped zone, dip value.

ACKNOWLEDGEMENT

I wish to express my sincere appreciation to Dr. E. L. Smith, Head of the Department of Chemical Engineering and Applied Chemistry for his patience, guidance, and continuing support throughout this research work and for his critical review of this manuscript.

The author also wishes to thank the University of Aston in Birmingham for providing financial assistance and research facilities and the Chief Technician and his staff for their assistance with equipment.

Finally, the author wishes to express his gratitude to his family for their continuing support and encouragement throughout this research work.

TABLE OF CONTENTS

<u>CHAPTERS</u>	<u>D E S C R I P T I O N</u>	<u>PAGE</u>
	List of Tables	8
	List of Figure	9
	Notations	22
CHAPTER 1	INTRODUCTION	26
	<i>SECTION 1</i>	28
CHAPTER 2	FLUIDISED BEDS	29
	2.1 The Phenomenon of Fluidisation	29
	2.2 Minimum Fluidisation Velocity	31
	2.3 The Two-Phase Theory	33
	2.4 Bubble Dynamics	34
	2.5 Solids Motion	37
	2.6 Literature review - Solids Mixing and Segregation	39
	2.6.1 Rowe and Nienow et al.	39
	2.6.2 Burgess et al (1977)	48
	2.6.3 Fan and Chang (1979)	51
	2.6.4. Geldart, Baeyens, Pope and Van de Wijer (1980)	52
	2.6.5. Daw (1985)	53
	2.6.6. Rice and Brainvoich (1986)	56
	2.6.7. Beeckmans and Stahl (1987)	57
	2.7. The Effect of the Gas Distributor Design on the Mixing and Segregation Phenomena in Gas-Fluidised Beds.	58
	2.8. Quality of Fluidisation	59
	2.9 Literature Review - effect of the Distributor Design	64
	2.9.1. Naimer (1982)	64
	2.9.2. Whitehead, Dent and Close (1983)	65
	2.9.3. Feng, Chen and Whiting (1984)	66
CHAPTER 3	EXPERIMENTAL EQUIPMENT	68

3.1.	Experimental Equipment	68
3.2.	The Solids	72
3.3.	Electrostatic Effects	72
3.4.	The Sampling Procedure	74
3.5	Sample Analysis	74
3.6	Mixing Index	76
CHAPTER 4	FLUIDISED BED - EXPERIMENTAL RESULTS	77
4.1	Measurement of the Minimum Fluidising Velocity - Procedure	77
	Minimum Fluidising Velocity - Experimental Results	78
4.2	The Procedure for Mixing / Segregation Experiments	80
4.3	Distributor Plates	81
4.4.	Review of the Experimental Programme	85
4.5.	Experimental Results	85
4.5.1.	The ABS Cylinders / Polybeads System	85
	Effect of the distributor design	87
	Effect of the Initial Condition	88
	Effect of the Superficial Velocity	89
4.5.2.	The Ballotini 1090 / Ballotini 550 System	92
	Effect of the Distributor Design	92
	Effect of the Initial Condition	93
4.5.3.	The Ballotini 1090 / Polybeads 1850 System	94
	Effect of the Distributor Design	94
	Effect of the Superficial Air Velocity	95
	Effect of the Aspect Ratio (Ra)	98
4.5.4.	The ABS Cylinders / Polycylinders System	99
	Effect of the Distributor Design	99
	Effect of the Superficial Velocity	100
	Effect of the Initial Condition	101
4.5.5.	The Polybeads 1550 / Polybeads 925 System	102
	Effect of the Distributor Design	102
	Effect of the Superficial Velocity	103
	Effect of the Initial Condition	106

CHAPTER 5	DISCUSSION, CONCLUSIONS & RECOMMENDATIONS	107
5.1	Discussion	107
5.2	Conclusion	111
5.3	Recommendations for Future Work	112
	<i>SECTION 11</i>	114
CHAPTER 6	THE SPOUTED BED	115
6.1	Introduction	115
6.2	Literature Review	117
	6.2.1. Berquin (1964)	117
	6.2.2. Mathur (1972)	117
	6.2.3. Piccinni, Bernhard, Campagna and Vallena (1977)	118
	6.2.4. Robinson and Waldie (1978)	118
	6.2.5. Cook and Bridgwater (1979)	118
	6.2.6. McNab and Bridgwater (1979)	118
	6.2.5. Kutluoglu et al (1983)	119
	6.2.6. Uemaki et al (1983)	120
6.3.	Summary of Previous Segregation Studies	121
CHAPTER 7	THE SPOUTED BED - EXPERIMENTAL RESULTS	123
7.1	The Procedure for Minimum Spouting Velocity Experiments	123
	7.1.1. Minimum Spouting Velocity - Experimental Results	123
7.2.	The Experimental Strategy	127
7.3.	Interpretation of the Experimental Data	127
7.4.	Experimental Results	128
	7.4.1. The ABS Cylinders / Polybeads System	128
	Effect of Orifice Size	128
	Effect of the Spouting Velocity	135
	Effect of the Initial Condition	136
	Effect of the Aspect Ratio (Ra)	136
	7.4.2. The Ballotini 1090 / Polybeads 1850 System	137
	Effect of Orifice Size	138
	Effect of the Spouting Velocity	142

	Effect of the Initial Condition	143
	Effect of the Aspect Ratio (Ra)	144
7.4.3.	The ABS Cylinders / Polycylinders System	145
	Effect of Orifice Size	145
	Effect of the Spouting Velocity	145
	Effect of the Aspect Ratio (Ra)	147
7.4.4.	The Polybeads 1550 / Polybeads 925 System	148
	Effect of Orifice Size	148
	Effect of the Initial Condition	153
CHAPTER 8	DISCUSSION, CONCLUSIONS	
	& RECOMMENDATIONS	155
8.1.	Discussion	155
8.2.	Conclusions	158
8.3.	Recommendations for Future Work	158
	<i>SECTION III</i>	160
CHAPTER 9	THE SPOUT-FLUID BED	161
9.1	Introduction	161
9.2	Flow Regimes	163
9.3	The Author's Spout-fluid Bed System	166
CHAPTER 10	SPOUT-FLUID BED - EXPERIMENTAL RESULTS	171
10.1	Measurement of the Minimum	
	Spout-fluidisation Velocity	171
	Experimental Results	171
10.2	Flow Regimes	174
10.3	The Experimental Strategy -	
	Solids Mixing / Segregation	178
10.4.	Experimental Results -	
	Solids Mixing /. Segregation	180
10.4.1.	The ABS Cylinders / Polybeads System	180
	Effect of Distributor Design	181
	Analysis of the Data	
	- The Mixing Number, S	185
	Effect of the Initial Condition	188
	Effect of the Superficial Air Velocity	190

	Effect of Aspect Ratio (Ra)	192
	Effect of the Jetsam Concentration	201
10.4.2.	The Ballotini 1090/ Ballotini 550 System	203
	Effect of the Distributor Design	203
	Effect of the Initial Condition	206
	Analysis of the Data	
	- mixing Number (s)	210
10.4.3.	The Ballotini 1090 / Polybeads 1850 System	211
	Effect of Distributor design	211
	Effect of the Initial condition	215
	Effect of the Superficial Air Velocity	217
10.4.4.	The ABS Cylinders / Polycylinders System	219
	Effect of Distributor Design	220
	Effect of the Initial Condition	223
	Effect of the Superficial Air Velocity	225
	Effect of the Aspect Ratio (Ra)	227
10.4.5.	The Polybeads 1550 / Polybeads 925 System	229
	Effect of Distributor Design	229
	Effect of the Initial Condition	235
	Effect of the Superficial Air Velocity	235
	Analysis of the Data	
	- The Mixing Number, S	239
CHAPTER 11	DISCUSSION, CONCLUSIONS	
	& RECOMMENDATIONS	240
11.1	Discussion	240
11.2.	Conclusions	244
11.3.	Recommendations for Future Work	249
REFERENCES		252
APPENDIX 1		262
APPENDIX 2		263
APPENDIX 3		264

LIST OF TABLES

TABLE NO.	D E S C R I P T I O N	PAGE
3.1	Physical properties of the experimental solids	73
4.1	Summary of the minimum fluidising velocities - for the binary systems	80
4.2	The distributor plates (Bed diameter 138 mm)	83
4.3	Mixtures used	86
5.1	Mixing indices for the binary systems tested	109
7.1.	Summary of the minimum spouting velocities - for the binary systems	126
7.2	Summary of operating variables (ABS Cylinders / Polycylinders 1090)	129
7.3	Summary of operating variables (Polycylinders 1550 / Polycylinders 925)	149
9.1.	Details of the central and peripheral orifices for distributors	169
10.1.	Summary of the minimum spout-fluidising velocities	175
10.2.	Calculations of mixing number, S (ABS Cylinders / Polybeads 1090)	187
10.3.	Calculation of the mixing number, S (ABS Cylinders / Polybeads 1090)	189
10.4	Experimental data and mixing number, S	202
10.5	Calculation of the mixing number, S	210
10.6	Experimental data and mixing number, S	239

LIST OF FIGURES

Fig No.	D e s c r i p t i o n	Page
2.1	Six basic flow patterns in Gas-Solid systems (adapted from Kunii and Levenspiel (1969))	30
2.2	Pressure drop verses velocity curves representing various types of fluidisation (adapted from Geldart (1986))	32
2.3.	The basic features of two-phase theory for gas fluidised beds (adapted from Kunii and Levenspiel (1969))	34
2.4.	The gas flow patterns around bubble as described by the theories of Davidson (1961) and Pyle and Rose (1965)) (adapted from Kunii and Levenspiel (1969))	36
2.5.	Solid classification as described by Geldart	39
2.6.	Segregation patterns and mixing index for close-sieved binary mixtures (adapted from Rowe et al. (1972b))	41
2.7.	Illustration of the assumptions made by Gibilaro and Rowe (1974) in their steady-state segregation model.	43
2.8.	Variation of mixing index with excess gas velocity (adapted from Nienow et al. (1978))	47
2.9.	Wake mixing model; with component. (adapted from Burgess et al. (1977))	50
2.10.	Well mixed wake bulk flow representation. (adapted from Burgess et al. (1977))	50
2.11.	Effect of the type of distributor on the quality of fluidisation. (adapted from Kunii and Levenspiel ((1969))	60

2.12.	Zenz's idealised jet-to-bubble emergence pattern (adapted from Zenz (1968))	61
2.13.	Modes of gas discharge in gas-solid fluidised bed (adapted from Massimilla in "Fluidisation" by Davidson, Harrison and Clift (1985))	63
3.1.	Schematic arrangement of the experimental apparatus	69
3.2.	Adjustible pressure probe for measuring pressure at arbitrary radial positions in the fluidised bed	70
3.3.	Photograph of the column and pressure probe used.	71.
3.4.	Vacuum sampling device used to remove samples from the slumped bed.	75
4.1.	The two defluidisation procedures. (adapted from Cheung, (1976))	78
4.2.	U_{mf} curve - Polybeads 1550	79
4.3.	U_{mf} curve of Polybeads 1550 / Polybeads 925	79
4.4.	Pressure drop across the various distributors used	83
4.5.	Photograph showing the distributors used in the fluidised bed systems.	84
4.6.	Effect of four distributors on the concentration profile (Segregated - ABS Cylinders / Polybeads system)	87
4.7.	Effect of four distributors on the concentration profile (Well mixed - ABS Cylinder / Polybeads system)	88
4.8a.	Effect of initial concentration with Perforated plate 2 (ABS Cylinder / Polybeads system)	90

4.8b.	Effect of initial concentration with Perforated plate 3 (ABS Cylinder / Polybeads system)	90
4.9	Effect of U_0 on concentration profile with Perforated plate 2 (ABS Clylinder / Polybeads system)	91
4.10.	Effect of U_0 on the concentration profile with Standpipe type plate (ABS Cylinder/Polybeads system)	91
4.11.	Concentration profiles obtained with four distributors (Well mixed Ballotini 1090 / Ballotini 550 system)	93
4.12.	Effect of the initial condition with Perforated plate 2 (Ballotini 1090 / Ballotini 550 system)	94
4.13.	Concentration profiles with three distributors (Ballotini 1090 / Polybeads 1850 system)	95
4.14.	Effect of U_0 on the concentration profile with porous plate (Ballotini 1090 / Polybeads 1850 system)	97
4.15.	Effect of U_0 on the concentration profiles with porous plate (Ballotini 1090 / Polybeads 1850 system)	97
4.16.	Similarity in concentration profiles at two different U_0 values using porous plate (Ballotini 1090 / Polybeads 1850 system)	98
4.17.	Effect of the aspect ratio on the concentration profile using porous plate (Well mixed - Ballotini 1090 / Polybeads 1850 system)	99
4.18.	Concentration profiles with five distributors (ABS Cylinders / Polycylinders system)	100
4.19.	Effect of U_0 on the concentration profiles with perforated plate 3 (ABS Cylinders / Polycylinders system)	101
4.20.	Effect of the initial condition on the concentration	

	profile (ABS Cylinders / Polybeads system)	102
4.21.	Effect of the distributor design on the concentration profiles (ABS Cylinder / Polycylinders system)	103
4.22.	Physical appearance of the bed as observed at different velocities (Polybeads 1550 /Polybeads 925 System)	104
4.23.	Effect of the superficial air velocity with perforated plate 2 (Polybeads 1550 / Polybeads 925 System)	105
4.24.	Effect of the initial condition with perforated plate 2 (Polybeads 1550 / Polybeads 925 System)	106
5.1	Transition from Jet-to-Bubble as visible at the Bed wall using perforated plate	108
5.2	Formation of Bubbles with porous plate as visible from Bed wall	108
5.3	Jets emerging from standpipes as visible from below the distributor	108
6.1.	Schematic diagram of a spouted bed. (adapted from Mathur and Epstein (1974))	116
7.1.	U_{ms} plot for Polybeads 1400 -1700	124
7.2.	U_{ms} plot for red Polycylinder	124
7.3.	Minimum spouting velocity of Polycylinder / ABS Cylinder (weight ratio 90% / 10%)	125
7.4.	A typical concentration profile - ABS Cylinder / Polybeads 1090	127
7.5.	Inlet orifice diameter vs log of spouting velocity	

	(ABS Cylinder / Polybeads 1090)	129
7.6.	Effect of the inlet orifice diameter on the conc. profile (Segregated - ABS Cylinder / Polybeads System)	130
7.7.	Effect of the inlet orifice diameter on the conc. profile (Segregated: ABS Cylinder / Polybeads System)	132
7.8.	Effect of the inlet orifice diameter on the conc. profile (Segregated: ABS Cylinder / Polybeads System)	132
7.9.	Relationship between inlet orifice diameter vs mixing number (MI) (ABS Cylinders / Polybeads System)	134
7.10.	A sectional view of the spouted bed	134
7.11.	Effect of the superficial air velocity on the conc. profile (ABS Cylinders / Polybeads System)	135
7.12.	Effect of the initial condition on the conc. profile (ABS Cylinders / Polybeads System)	136
7.13.	Effect of the aspect ratio (Ra) (ABS Cylinder / Polybeads System)	137
7.14.	A typical concentration profile (Ballotini 1090 / polybeads 1850 System)	139
7.15.	Spout penetration with 10 mm diameter orifice inlet (Ballotini 1090 / Polybeads 1850 System)	139
7.16.	Effect of inlet orifice diameter on the conc. profile (Ballotini 1090 / Polybeads 1850 System)	140
7.17.	Physical appearance of the spouted bed with 14 mm diameter air inlet orifice	141
7.18.	Physical appearance of the spouted bed with 10 mm diameter air inlet orifice.	141

7.19.	Effect of the superficial air velocity on the conc. profile (Ballotini 1090 /Polybeads 1850 System)	142
7.20.	Effect of the initial jetsam position on the concentration profiles (Ballotini 1090 / Polybeads 1850 System)	143
7.21.	Effect of the aspect ratio (Ra) on the conc. profile (Ballotini 1090 / Polybeads 1850 system0)	144
7.22.	Effect of the inlet orifice diameter on the conc. profile (ABS Cylinders / Polycylinders System)	146
7.23.	Effect of the spouting velocity (ABS Cylinders / Polycylinders system)	146
7.24.	Effect of the aspect ratio (Ra) (ABS Cylinders / Polycylinders system)	148
7.25.	Inlet orifice diameter vs log (U_{Oj}) (Polybeads 1550 / Polybeads 925 System)	149
7.26.	A typical concentration profile (Polybeads 1550 / Polybeads 925 System)	151
7.27.	Effect of the inlet orifice diameter on the conc. profile (Segregated - Polybeads 1550 / Polybeads 925 System)	151
7.28.	Effect of the inlet orifice diameter on the conc. profile (Segregated - Polybeads 1550 / Polybeads 925 System)	152
7.29.	Effect of the inlet orifice diameter on the flotsam concentration band (Polybeads 1550 / Polybeads 925 System)	153
7.30.	Effect of the initial condition (Polybeads 1550 / Polybeads 925 System)	154
8.1.	The spouted bed as observed	156

9.1.	Spout-fluidised bed (adapted from Chatterjee (1970))	162
9.2.	Regimes map for polystyrene particles (adapted from (Sutanto 1983))	164
9.3.	Physical appearance of the various flow regimes in spout-fluidisation (adapted from Sutanto (1983))	167
9.4.	Photograph showing Distributors used.	170
10.1.	Minimum spout-fluid velocity curve for Polycylinders	172
10.2.	Minimum spout-fluid velocity curve for Polybeads 1550 / Polybeads 925 (90% / 10%)	172
10.3.	Effect of distributor design on the minimum spout-fluidising velocity.	173
10.4.	Effect of the aspect ratio (Ra) on the minimum spout-fluidising velocity.	174
10.5.	Physical appearance of the various flow regimes as observed	177
10.6.	Physical appearance of the various flow regimes with deeper bed at $H_b = 39.0$ cm	179
10.7.	Effect of the central orifice diameter variation on the conc. profile (Segregated -ABS Cylinders / Polybeads System)	182
10.8.	Effect of the peripheral orifices on the conc. profile (Segregated - ABS Cylinders / Polybeads System)	182
10.9.	Similar conc. profiles obtained with two different distributors. (Segregated - ABS Cylinders / Polybeads System)	184
10.10.	Effect of the peripheral orifice configuration on the conc. profile.(Segregated - ABS Cylinders /	

	Polybeads System)	184
10.11.	Effect of the peripheral orifices on the conc. profile (Segregated - ABS Cylinders / Polybeads System)	185
10.12.	Four conc. profiles with best distributors. (Segregated - ABS Cylinders / Polybeads System)	187
10.13.	Effect of the peripheral orifice variation (well mixed - ABS Cylinders / Polybeads System)	188
10.14.	Effect of the initial condition on the conc. profile (ABS Cylinders / Polybeads System)	190
10.15.	Effect of the superficial air velocity on the conc. profile (Dist.5, Segregated - ABS Cylinders / Polybeads System)	191
10.16.	Effect of the superficial air velocity on the conc. profile (Dist.7, Segregated - ABS Cylinders / Polybeads System)	192
10.17.	Effect of aspect ratio (Ra) on the conc. profile . @ Ra = 0.6 (Dist.2, Segregated - ABS Cylinders / Polybeads System)	193
10.18.	Effect of aspect ratio (Ra) on the conc. profile. @ Ra = 1.1 (Dist.2, Segregated - ABS Cylinders / Polybeads System)	194
10.19	Effect of aspect ratio (Ra) on the conc. profile. @ Ra = 1.6 (Dist.2, Segregated - ABS Cylinders / Polybeads System)	195
10.20.	Effect of aspect ratio (Ra) on the conc. profile. @ Ra =2.1 (Dist.2, Segregated - ABS Cylinders / Polybeads System)	195
10.21.	Physical appearance of the bed @ Ra = 2.1	196
10.22.	Physical appearance of the bed as observed @ Ra = 3.0	198

10.23.	Effect of aspect ratio (Ra) on the conc. profile. @ Ra = 3.0 (Dist.2, Segregated - ABS Cylinders/ Polybeads System)	199
10.24.	Effect of five different Ra values on the conc. profile	199
10.25.	Effect of aspect ratio (Ra) on the conc. profiles. (Dist.3, Segregated - ABS Cylinders / Polybeads System)	200
10.26	Effect of aspect ratio (Ra) and distributor configuration on the conc. profiles. (Dist.2, Segregated - ABS Cylinders / Polybeads System)	200
10.27.	Effect of the jetsam concentration on the conc. profile (Dist.9,;Segregated - ABS Cylinders / Polybeads System)	202
10.28	A typical concentration profile Ballotini 1090 / Ballotini 550)	204
10.29.	Effect of distributor configuration on the conc. profiles (Segregated - Ballotini 1090 / Ballotini 550 System)	204
10.30.	Effect of central orifice size on the conc. profile (Segregated - Ballotini 1090 / Ballotini 550 System)	205
10.31.	Effect of initial condition on the conc. profile (Dist. 3 - Ballotini 1090 / Ballotini 550 System)	207
10.32.	Effect of distributor configuration on the conc. profile (Well mixed - Ballotini 1090 / Ballotini 550 System)	207
10.33.	Simulation of the solids movement in the bed based on visual observation	208
10.34.	Surface appearance of the particles at different bed heights.	209
10.35.	Photograph showing Ballotini 1090 / Polybeads 1850 mixture in operation with Dist. 8 (6/18 x 1.5)	212

10.36.	Effect of the central orifice diameter on the conc. profile (Segregated - Ballotini 1090 / Polybeads 1850 System)	213
10.37.	Variation of Ballotini peak band height with central orifice diameter (Segregated - Ballotini 1090 / Polybeads 1850 System)	214
10.38	Effect of the peripheral orifice variation on the conc. profile (Segregated - Ballotini 1090 / Polybeads 1850 System)	215
10.39.	Physical appearance of the three locations of jetsam before and after spout-fluidisation experiment (Segregated - Ballotini 1090 / Polybeads 1850 System)	216
10.40.	Effect of the initial jetsam position on the conc. profiles (Segregated - Ballotini 1090 / Polybeads 1850 System)	216
10.41.	Effect of the initial condition on the conc. profile (Dist. 2 - Ballotini 1090 / Polybeads 1850 System)	217
10.42.	Effect of the superficial air velocity on the conc. profile (Dist 2; Segregated - Ballotini 1090 / Polybeads 1850 System)	218
10.43.	Effect of the superficial air velocity on the conc. profiles (Dist.8; Segregated - Ballotini 1090 / Polybeads 1850 System)	219
10.44.	Photograph showing the spout produced with ABS Cylinders / Polycylinders system with Dist. 7	221
10.45.	Effect of the central orifice diameter on the conc. profile (Segregated - ABS Cylinders / Polycylinders System)	222
10.46.	Effect of the peripheral orifice on conc. profile (Segregated - ABS Cylinders / Polycylinders System)	222

10.47.	Effect of the initial condition on conc. profile (Dist. 2 - ABS Cylinders / Polycylinders System)	224
10.48.	Effect of initial condition on conc. profile (Dist. 7 - ABS Cylinders / Polycylinders System)	225
10.49.	Effect of the superficial velocity on the conc. profile (Dist. 2; Segregated - ABS Cylinders / Polycylinders System)	226
10.50.	Effect of the superficial velocity on the conc. profile (Dist. 8; Segregated - ABS Cylinders / Polycylinders System)	226
10.51.	Effect of aspect ratio (Ra) on the conc. profile (Segregated - ABS Cylinders / Polycylinders System)	227
10.52.	Physical appearance of the bed at three different aspect ratios (Segregated - ABS Cylinders / Polycylinders System)	228
10.53.	Concentration profile showing no mixing @ $U_o = 0.59$ m/s (Segregated - Polybeads 1550 / Polybeads 925 system)	229
10.54.	Physical appearance of the experimental stages at different superficial velocities. (Segregated - Polybeads 1550 / Polybeads 925 system)	230
10.55.	Effect of the peripheral orifice configuration on conc. profile (Segregated - Polybeads 1550 / Polybeads 925 system)	231
10.56.	Physical appearance of the bed before and after the experiment (Dist. 2; Segregated - Polybeads 1550 / Polybeads 925 system)	231
10.57.	Effect of the peripheral orifice design on conc. profile (Segregated - Polybeads 1550 / Polybeads 925 system)	232

10.58.	Effect of the central orifice diameter on conc. profile (Segregated - Polybeads 1550 / Polybeads 925 system)	234
10.59.	Flotsam concentration band height vs central orifice diameter (Segregated - Polybeads 1550 / Polybeads 925 system)	234
10.60.	Effect of initial condition on conc. profile (Dist. 2 - Polybeads 1550 / Polybeads 925 system)	236
10.61.	Effect of initial condition on conc. profile (Dist. 4 - Polybeads 1550 / Polybeads 925 system)	236
10.62.	Photograph showing the position of the flotsam band (Segregated - Polybeads 1550 / Polybeads 925 system)	237
10.63.	Photograph showing position of flotsam band (Well mixed - Polybeads 1550 / Polybeads 925 system)	237
10.64.	Photograph showing position of flotsam band @ $U_O = 0.59$ m/s , Dist. 6 (6/18 x 1.5) (Segregated - Polybeads 1550 / Polybeads 925 system)	238
10.65.	Photograph showing position of flotsam band @ $U_O = 0.75$ m/s , Dist. 6 (6/18 x 1.5) (Segregated - Polybeads 1550 / Polybeads 925 system)	238
APPENDIX 1	Detail of Standpipes used for Standpipe distributor	262
APPENDIX 2	Detail of distributors for spout-fluid bed .	263
APPENDIX 2	Detail of Dist. 3 & 4 for spout-fluid bed	264.

NOTATIONS

A	value at the point of intersection at initial jetsam concentration line on the DAP scale, section 10.4.1
A_C	cross section of the fluidised bed, (L^2)
A_S	projected bubble cross section in Burgess et al. model, (L^2)
A_W	cross section of wake solids phase, (L^2)
B	average jetsam concentration in the developed zone
C_j	jetsam concentration
d	mean particle diameter, (μm)
d_p	particle diameter, (mm)
D	bed diameter, (mm)
D_B	bubble diameter, (mm)
D_i	inlet orifice diameter, (mm)
d_{ER}	shape corrected diameter ratio, $(\phi_H \cdot d_H) / (\phi_L \cdot d_L)$
dv	diameter of a sphere having the same volume as the particles, (μm)
DAP	dimensionless axial scale
E_{mf}	voidage at minimum fluidising velocity, (-)
f_m	the fraction of the bubble wake which is assumed completely mixed in the Burgess et al model, section 2.6.2.
F	dimensionless velocity in eq. 2.9
g	gravitational constant, (cm / s^2)
H	bed height, (mm)
H^*	reduced aspect ratio, $1 - \exp(-H/D)$
i	index referring to each sample in eq 3.1
L_S	characteristic particle descent distance in Burgess et al model, (L)
L_W	characteristic vertical wake length in Burgess et al. model, (L)
M	mixing index defined by eq. 2.9 in section 2.6.1 (-)
$M_{Geldart}$	mixing index defined by eq. 2.13
M_{Daw}	mixing index defined by eq. 2.14

M_{Feng}	mixing index defined by eq. 2.19
MI	mixing index as defined by eq. 3.1
n	total number of the sample taken in eq. 3.
ΔP	pressure drop, cm H ₂ O
S	mixing number, (-)
u_o	superficial gas velocity, (m/s)
u_{br}	single bubble rise velocity, (m/s)
U_b	rise velocity of bubble swarm, (m/s)
U	superficial gas velocity in eq. 2.10, (m/s)
U_o	superficial gas velocity, (m/s)
U_{io}	spouting velocity at the orifice, (m/s)
U_{bmss}	minimum spouting velocity of the binary mixture obtained by slow despouting, (m/s)
U_{bmsq}	minimum spouting velocity of the binary mixture obtained by spouting, (m/s)
U_{bmsav}	average minimum spouting velocity of the binary mixture, (m/s)
U_c	minimum fluidising velocity of binary mixture, (m/s)
U_{cq}	minimum fluidising velocity of the binary mixture, (m/s) obtained by fast defluidisation, (m/s)
U_{cs}	minimum fluidising velocity of the binary mixture, (m/s) obtained by slow defluidisation, (m/s)
U_F	the U_{mf} of the component with the lower U_{mf} (fluid), (m/s)
U_P	the U_{mf} of the component with the higher U_{mf} (packed), (m/s)
U_{ms}	minimum spouting velocity, (m/s)
U_{To}	velocity above which mixing takes as defined by after eq. 2.10 (m/s)
U_s	spouting velocity, (m/s)
U_{sf}	minimum spout-fluidising velocity of mono components, (m/s)
U_{sfs}	minimum spout-fluidising velocity of binary mixture obtained by slow despout-fluidisation, (m/s)

U_{sfq}	minimum spout-fluidising velocity of binary mixture obtained by spout-fluidisation, (m/s)
U_{sav}	average minimum spout-fluidising velocity of binary mixture, (m/s)
U_{ds}	descending velocity of solids. (m/s)
u_{mf}	minimum fluidising velocity, (m/s)
V_B	bubble volume, (m^3)
v_d	downward velocity of jetsam particles relative to flotsam particles in the upper bed, (m/s)
v_u	mean upward velocity of jetsam particles across interface between upper and lower beds, (m/s)
V_W	fraction of bubble assumed to be wake solids in Burgess et al. model, (-)
v_{si}	the volume fraction of the total bed contained in a chosen sample in eq 3.1
v_{ji}	the volume fraction of jetsam in the sample in eq. 3.1, (-)
\bar{v}_J	total volume fraction of jetsam in the bed, (-)
Q	total volumetric flow rate in eq. 2.2, (m^3 / s)
Q_{mf}	volumetric flow rate required at minimum fluidising velocity, (m^3 / s)
Q_B	total volumetric flow rate , (m^3 / s)
Ra	aspect ratio (-)
x	mass fraction of the jetsam in the upper uniform part of the bed in section 2.6.1,(-)
\bar{x}	the overall mass fraction of jetsam in the bed in section 2.6.1, (-)
ρ_f, ρ_g	fluid density and gas density, (g / cm^3)
ρ_p	particle density, (g / cm^3)
ρ_R	density ratio of heavy to light particles, ρ_H / ρ_L
ϕ	shape factor

INTRODUCTION
CHAPTER 1

CHAPTER 1

INTRODUCTION

Gas-solid reactors are key components in many chemical and energy conversion processes, including oil refining, coal gasification, coal combustion and mineral processing. The most prominent of these are gas-fluidised beds. However, when the fluidised particles are of different size and density, there is a tendency for the lighter particles to go to the top of the bed, i.e. to segregate.

One special variation of the fluidised bed is the *spouted bed* where gas is introduced through a single orifice. As the gas travels upward, it flares out into the annulus. The overall bed thereby becomes a composite of a dilute phase central core with upward moving solids entrained by a cocurrent flow of gas and a dense phase annular region with countercurrent percolation of gas. Spouted beds are particularly suited for large particles (Geldart type D; $d_p > 500 \mu\text{m}$). Once again differences in particles size and density create a tendency towards segregation.

A most recent introduction to this family is known as the *spout-fluid bed*, where some features of the fluidised bed and some features of the spouted bed are married together. Here again, if the physical properties of the solids differ, segregation can occur. Depending on the particular process application, segregation may either enhance or reduce the overall efficiency. For example, minerals beneficiation is a case in which segregation can be helpful: the separation of as much of the inert material as possible before processing ores in expensive or energy intensive operations is often desirable. Fluidised bed segregation offers a means of accomplishing this separation when other methods are undesirable and/or too expensive. By way of contrast, high sulfur coal combustion in a fluidised bed is an example where segregation can be deleterious: the object in this case is to burn coal in a fluidised bed of calcined limestone so that the sulfur dioxide by-product can be "captured" by reacting it with the calcium oxide. Therefore, it is ideal to have the coal and calcium oxide well-mixed so that the sulfur dioxide coming from the coal has good exposure to the sorbent. Segregation reduces this exposure because the coal particles being less dense, tend to migrate to the top of the bed.

The thesis is divided into three main sections and eleven chapters. **Section I** includes chapters 2 to 5 and deals with *Gas Fluidised Beds*. For convenience, a description of the equipment, material and experimental methods is

presented in this section as chapter 3. The literature review, experimental results/ discussion and conclusion/ recommendations are given in Chapters 2, 4 and 5 respectively.

Section II deals with *Spouted Beds*. The effect of variations in the gas inlet orifice diameter on the mixing and segregation profiles is examined, along with the effect of a number of other parameters. The literature review, experimental results/ discussion and conclusions/ recommendations are given in Chapters 6, 7 and 8 respectively.

Section III deals with *Spout-Fluid Beds*. The spout-fluid bed used in this study is somewhat different from the one generally referred from in the literature, in that the gas for the spout and for the fluidised bed section was supplied from a common plenum chamber whereas, in the conventional spout-fluid bed the fluid for the spout and fluidisation are supplied separately. The literature review and description of our version of the spout-fluid bed, experimental results/ discussions and conclusions / recommendations are presented in Chapters 9, 10 and 11 respectively.

SECTION 1

THE FLUIDISED BED

CONTAINING

CHAPTERS 2, 3, 4 & 5.

CHAPTER 2

THE FLUIDISED BED

A fluidised bed is formed by passing a fluid, usually a gas, upwards through a bed of particles supported on a distributor. The method of passing fluid and fluid solids contacting have a number of unusual characteristics leading to various fluidising states.

2.1 The Phenomenon of Fluidisation

Kunii and Levenspiel (1969) have given an illustration of the various categories which are commonly referred to in the literature. Figure 2.1 shows six basic flow patterns which occur in gas-solid contact. When gas is slowly passed upward through a bed of solids, it merely percolates through the voids and causes the bed to expand slightly: this is a fixed bed. As the flow increases, particles move apart and a restricted particle movement is established: this is now the expanded form. If the flow rate is then increased still further, the individual particles separate from one and another and become freely supported in the fluid. At this point the frictional force between a particle and fluid counterbalances the weight of the particle. The bed is considered to be just fluidised and is referred to as a bed at *minimum fluidisation*; this flow rate is referred to as the *minimum fluidisation gas velocity* (U_{mf}).

Increasing the gas flow rate above the minimum fluidisation velocity leads to large instabilities which take the form of gas voids and bubbles. A further increase in gas flow rate causes more solid agitation and *slugging* begins to occur, a severe form of bubbling in which the bubbles fill the entire section of the bed. These gas bubbles coalesce and grow as they rise, and in a deep bed they may eventually become large enough to spread across the full cross-section of the vessel forcing slugs of solid upwards. Slugging is usually accompanied by violent pressure and flow oscillations.

On further increasing the gas velocity, the heterogeneous, two-phase character of the bed first peaks, then gradually gives way to a condition of increasing uniformity culminating in the *turbulent* state virtually free from large bubbles and voids. In the turbulent fluidised bed, there is an upper bed surface, though it

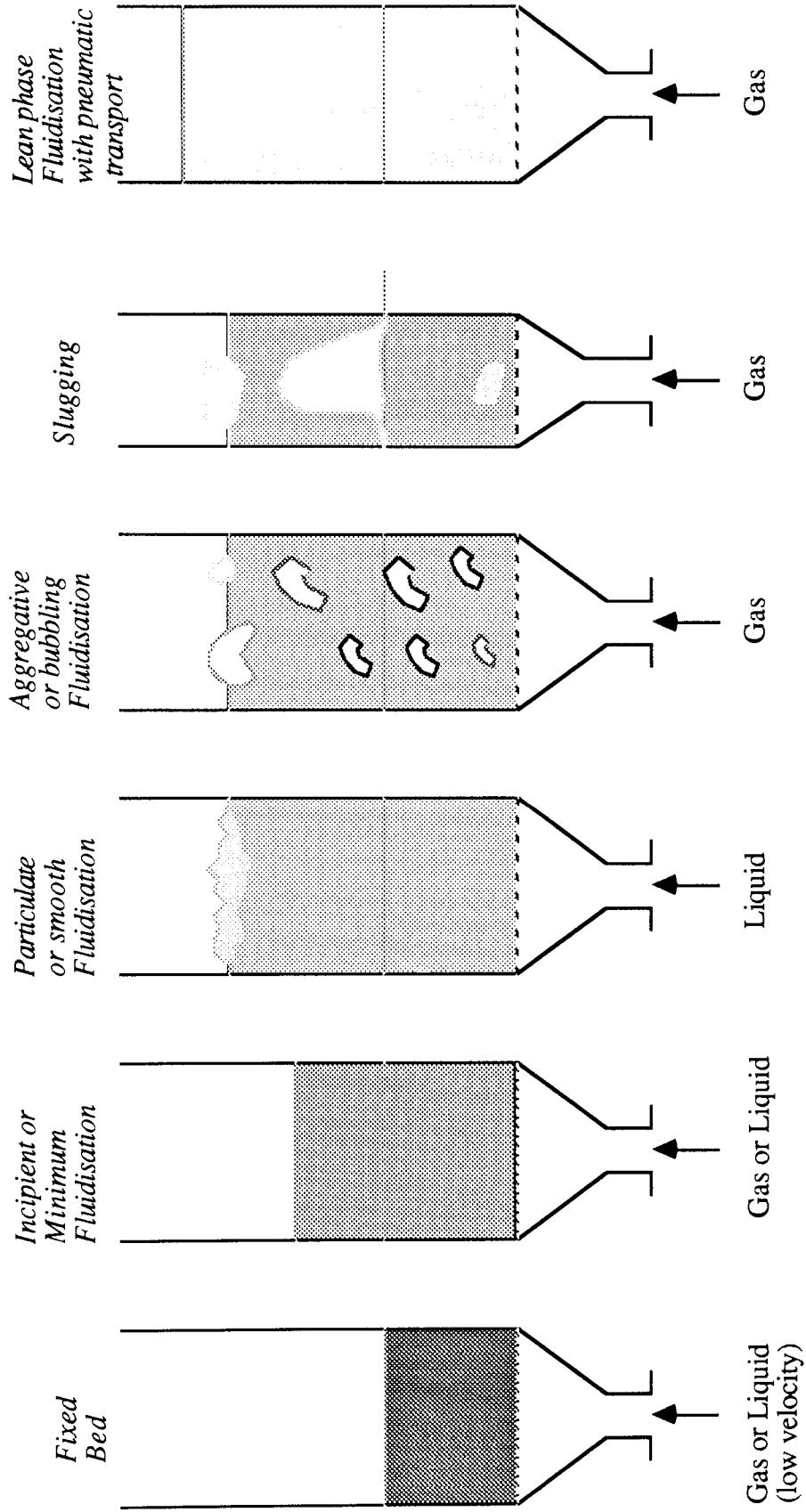


Fig.2.1: Six basic flow patterns in Gas-Solid systems
(adapted from Kunii and Levenspiel, 1969)

is considerably more diffuse than in a bubbling fluidising bed because of the greater freeboard activity attending operation at higher gas velocities. Continuing to increase the gas flow ultimately leads to solids elutriation when the particle terminal velocities are exceeded. This is the pneumatic conveying limit.

Throughout this increase of gas flowrate the volume occupied by the bed increases as is illustrated in Fig. 2.1. Thus local properties such as solids density, gas velocity and solids velocity can fluctuate widely with respect to both space and time, when the fluid velocity is above the minimum fluidising velocity. It is impossible to precisely describe the state of any variable at any particular location in the bed at any particular instant. Therefore, it is common to use the averaged properties for the bed as a whole, such as the overall average bubble size, the mean superficial velocity, and the overall bed solids composition.

Bubble size and velocity are generally used to indicate the *state of fluidisation*. Bubbles are also classified by how fast they move relative to the gas percolation through the interstitial voids. This will be described in the later sections.

2.2. Minimum Fluidisation Velocity

The minimum fluidising velocity may be found by measuring the pressure drop across the bed as a function of gas velocity. It is normal to work from the higher velocities at which the bed is vigorously fluidised down to the lower velocities. The shape of these pressure drop-velocity curves varies slightly with various parameters. Figure 2.2 shows various types of fluidisation along with their minimum fluidisation velocity curves.

A number of research workers have formulated various correlations to predict the minimum fluidisation velocity but the Wen and Yu (1966) correlation seems to give the best results. They correlated many data in the following form:

$$Ar = 1.650 Re_{mf} + 24.5 Re_{mf}^2 \quad (2.1)$$

where

Ar = Archimedes number and is

$$\rho_g \cdot d_v^3 \cdot (\rho_p - \rho_g) \cdot g / \mu^2$$

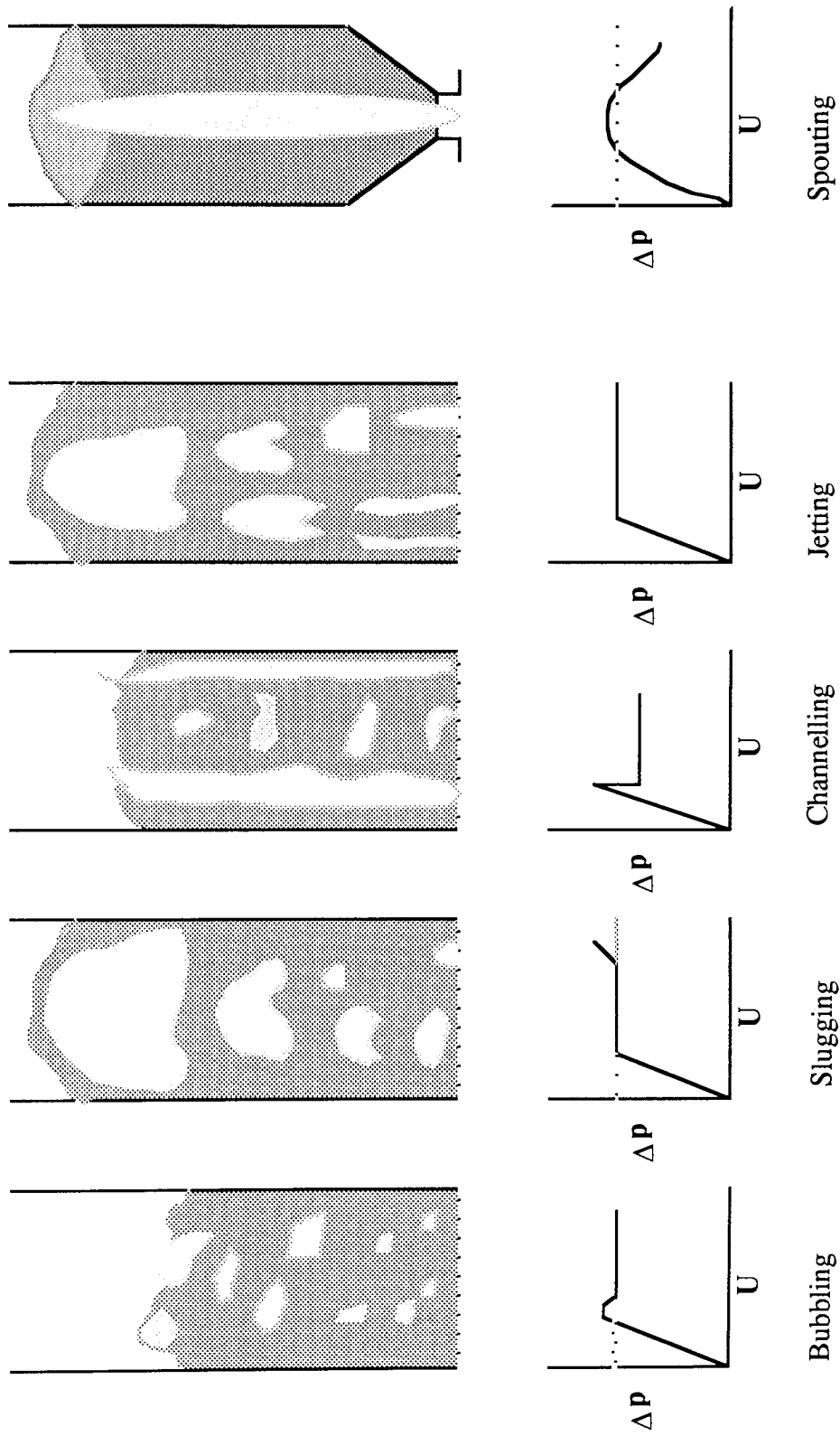


Fig.2.2: Pressure drop versus velocity curves representing various types of fluidisation
(adapted from Geldart 1986)

- Re_{mf} = Reynolds number at minimum fluidising velocity and is defined as $(d_v \cdot U_{mf} \cdot \rho_g) / \mu$
 U_{mf} = is the minimum fluidising velocity
 d_v = diameter of the sphere having the same volume as the particle
 ρ_g, ρ_p = fluid density and particle density
 μ = fluid viscosity

2.3 *The Two-Phase Theory*

Toomey and Johnstone (1952) were the original proposers of the two-phase theory which states that all the gas in excess of the minimum fluidisation velocity passes through the bed in the form of bubbles and can be written ,

$$Q = Q_{mf} + Q_B \quad (2.2)$$

- where Q is the total volumetric flow rate
 Q_{mf} is the volumetric flow rate required for minimum fluidisation
 Q_B is the total bubble volumetric flow rate

Basic features of the above theory are taken from Kunii and Levenspiel and illustrated in Figure 2.3. The detail of the symbols used in the illustration is list below:

- where U_o = superficial gas velocity
 U_b = bubble velocity
 U_s = solid velocity
 E_{mf} = Voidage at minimum fluidising velocity

The fluidised bed can be separated into two regions; an emulsion phase containing the bulk of the solids and the interstitial gas, and a bubble phase which consists of the bubbles and solids in their wake. It is also assumed that the emulsion phase

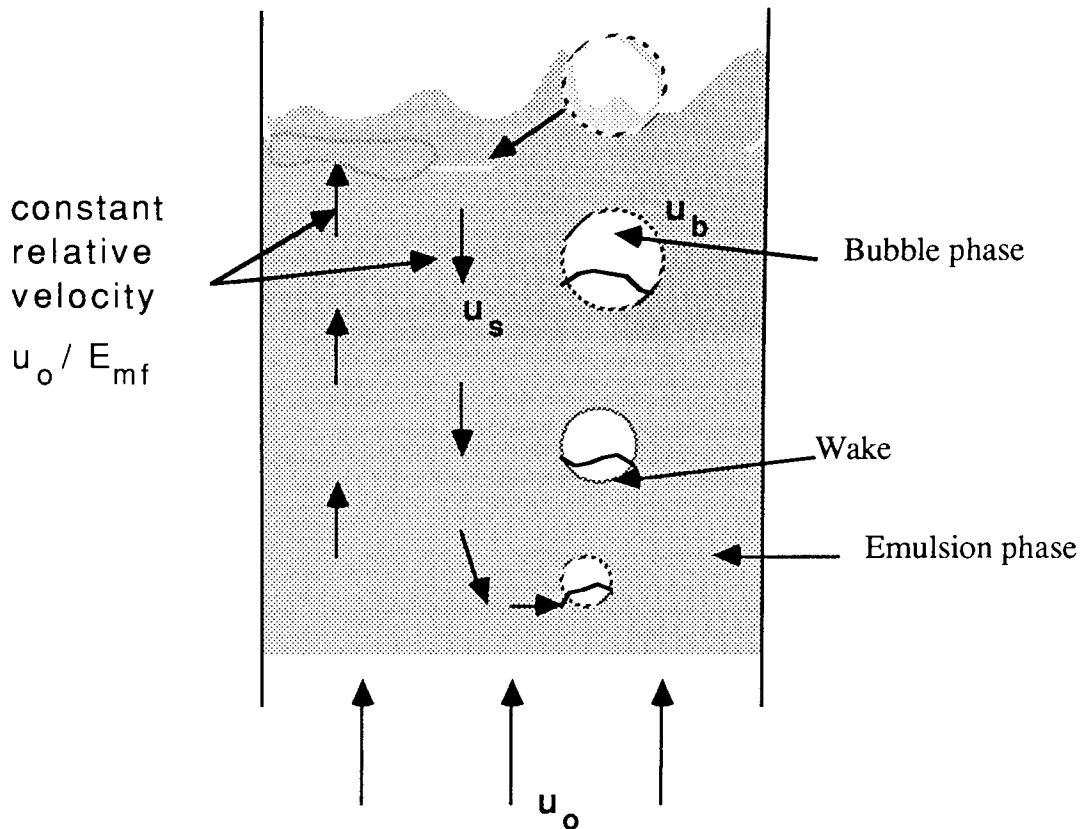


Figure 2.3 : The basic features of the two-phase theory for gas fluidised beds. (adapted from Kunii and Levenspiel, 1969)

emulsion phase remains at the minimum fluidisation state.

2.4. Bubble Dynamics

The motion of the bubbles and their interaction with the surrounding solids and interstitial gas is essential to an understanding of the two-phase theory. Davidson (1961) was the first to analyse the fluid and particle motion near rising bubbles. He assumed that the emulsion phase follows potential flow whereas the interstitial gas flow relative to the particles follows Darcy's Law. One of the most important contributions was that the rising velocity of a single bubble depends only on the square root of the bubble diameter, as listed below:

$$u_{br} = 0.711 (g \cdot D_B)^{0.5} \quad (2.3)$$

where

- u_{br} is the bubble rise velocity, m/s
- g is the acceleration due to gravity, m/s²
- D_B is the bubble diameter, m

Pyle and Rose (1965) extended Davidson's work by developing a theory describing flow within the rising bubble. A concept of "slow moving (or small)" and "fast (or large)" bubbles was also developed. Figure 2.4 illustrates the gas flow pattern around the bubbles. The bubble shown in the lower part of this figure represent fast bubbles, where the bubble rise velocity is greater than the interstitial gas velocity (u_e).

Slow moving (or small) bubbles, as shown in the upper row of Figure 2.4, occur when the bubble rise velocity is less than the interstitial gas velocity. These bubbles do not contain any recirculated gas cloud and the gas uses these bubbles as a shortcut on its way through the bed. Cranfield (1978), McGarth and Streatfield (1971), Canada et al. (1978) and Jovanovic (1979) have studied and confirmed the behaviour of such bubbles.

A distinct form of slow bubble occurs when the bubble growth rate is of the same magnitude as the bubble rise velocity: i.e.

$$\frac{d(D_B)}{dt} \approx u_b \quad (2.4)$$

The bubbles shown in the lower row of Figure 2.4 represent fast (or large) bubbles, where the bubble rise velocity is greater than the interstitial gas velocity. In this case, gas enters the bottom of the bubble, flows upward through it, and leaves at the top into a circulating stream which returns to the bottom. This effect is to create a captive gas cloud which moves up through the bed "attached" to the bubble. A number of fluidised-bed reactor models have been developed for this type of bubble. The recirculating gas cloud is a key assumption of these models, and mass transfer coefficients between the bubble and emulsion gas are defined accordingly.

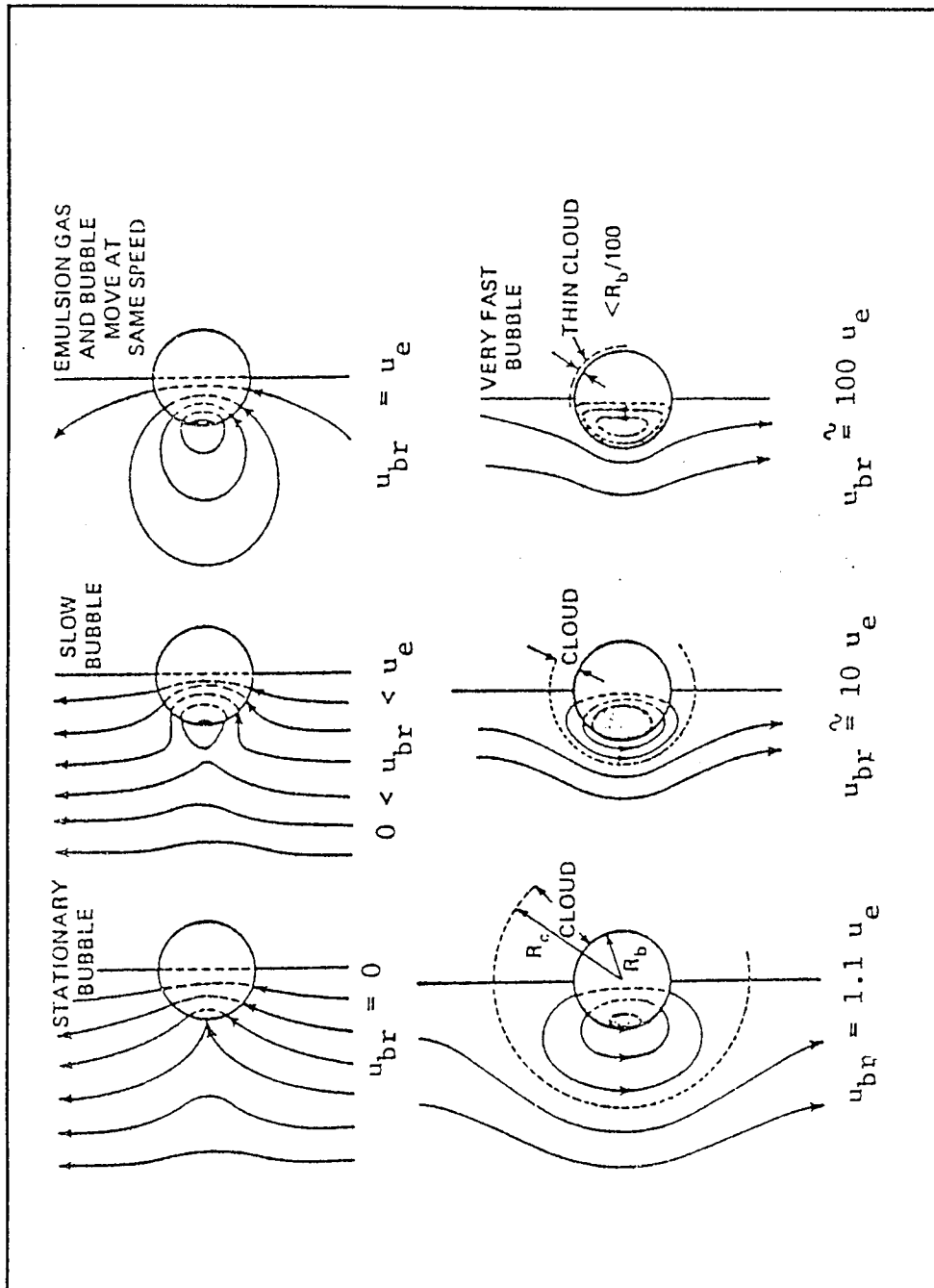


Fig.2.4: The gas flow patterns around bubbles as described by the theories of Davidson (1961) and Pyle and Rose (1965) (adapted from Kunii and Levenspiel, (1969))

In general, the recirculating gas cloud tends to reduce the interphase mass transfer. The most notable of these models are by Rowe(1964), Partridge and Rowe (1966), Latham et al. (1968), Kunii and Levenspiel (1969), Kato and Wen (1969) and Fryer and Potter (1972).

Bubbles play an extremely important role in solid mixing and segregation as the solids are transported in bubble wakes. Therefore, their frequency, speed and size have a significant effect on the mixing/segregation mechanisms.

Bubble dynamics in beds of large particles are somewhat different from those found in fluid-bed systems of relatively small particles because the minimum fluidisation velocities of large particles tend to be high, the velocity of emulsion phase gas is also high and generally exceeds the bubble rise velocity. Under these conditions no cloud is formed round the bubble; gas simply flows through the void from bottom to top under the influence of the prevailing pressure gradient.

Cranfield and Geldart (1972) studied the fluidisation characteristics of large particles in both two- and three- dimensional beds. They found both U_{mf} and E_{mf} to vary with bed height in the 2-D bed but to be practically constant in the 3-D bed. However, in both beds the minimum bubbling velocity remained constant as bed height was changed. Furthermore the visible bubble flow was greater in the 3-D bed than in the 2-D bed at corresponding values of $U-U_{mb}$ but was only some 55% of the excess gas flow. They also found that bubble growth appeared to occur by horizontal rather than vertical coalescence.

2.5. *Solids Motion*

Solids motion is a key concern in gas fluidised-bed mixing and segregation and this is mainly controlled by bubble movement. An other factor which affects the fluidisation behaviour is the physical characteristics of the solid. Some solids undergo considerable bed expansion before the onset of bubbling at U_{mb} at which point the bed collapses to the normal value. There are other powders that are extremely difficult to fluidise at all, the gas merely channelling its way through the bed which remains practically static at all velocities up to the very highest. Geldart (1973) has suggested an excellent classification in which various solids are arranged in four groups. The solids in each group have broadly similar fluidisation

characteristics in air at atmospheric temperature and pressure. Figure 2.5 shows the solids classification diagram for fluidisation under ambient air conditions: this figure is taken from Geldart (1973).

Solids motion is a main factor in gas-fluidised-bed segregation and is generally controlled by bubble motion. Thus it can be sluggish or rapid depending on the bubble size and frequency. The detailed behaviour of solids near a single rising bubble has been described by Rowe et al. (1965) for small particles and Cranfield (1978) for large particles. Rowe et al. concluded that for particles $> 100 \mu\text{m}$, bubbles are the main agents causing particles to move through large distances, and identified two mechanisms for their action. First there is a drift mechanism whereby a bubble draws up behind it a finger of underlying material rather in the manner of the displacement of an inviscid fluid by a rising sphere. Secondly a wake transport mechanism where solids in the bubble wake are carried to the surface and replace the solids moving downward in the emulsion phase. Rowe (1984) has recently indicated that the amount of solids spilled from the wake is probably a small fraction of the total solids in the wake. Cranfield (1978) studied a bed with large (Geldart Group 'D') particles and found that here the finger is also drawn up behind the bubble, but that captive wake formation and shedding did not occur. His results also indicated that the solids finger stopped somewhat short of the bed surface.

2.6. Literature Review - Solid Mixing and Segregation

In the past three decades there has been a number of studies related to solids segregation in gas fluidised beds. A full analysis of each of these studies is beyond the scope of this work. However, a list of the key papers is included in the reference. Most of these studies have been carried out with small diameter particles and mainly using a perforated plate. Only six studies, those of Rowe and Neinow et al. (1972-1982), Fan and Chang (1979), Geldart et al. (1981), Cooke et al. (1982) and Daw (1985), have looked at beds comprising some large particles. A noticeable feature of all these studies was that differences and similarities were highlighted without regard to consideration of the type of distributor used and its effect on the segregation phenomena. Only three studies so far have been carried out which examine the effect of the distributor, those by Naimer (1982), Whitehead et al. (1983) and Feng et al. (1984).

A detailed literature review of five studies regarding solids segregation is

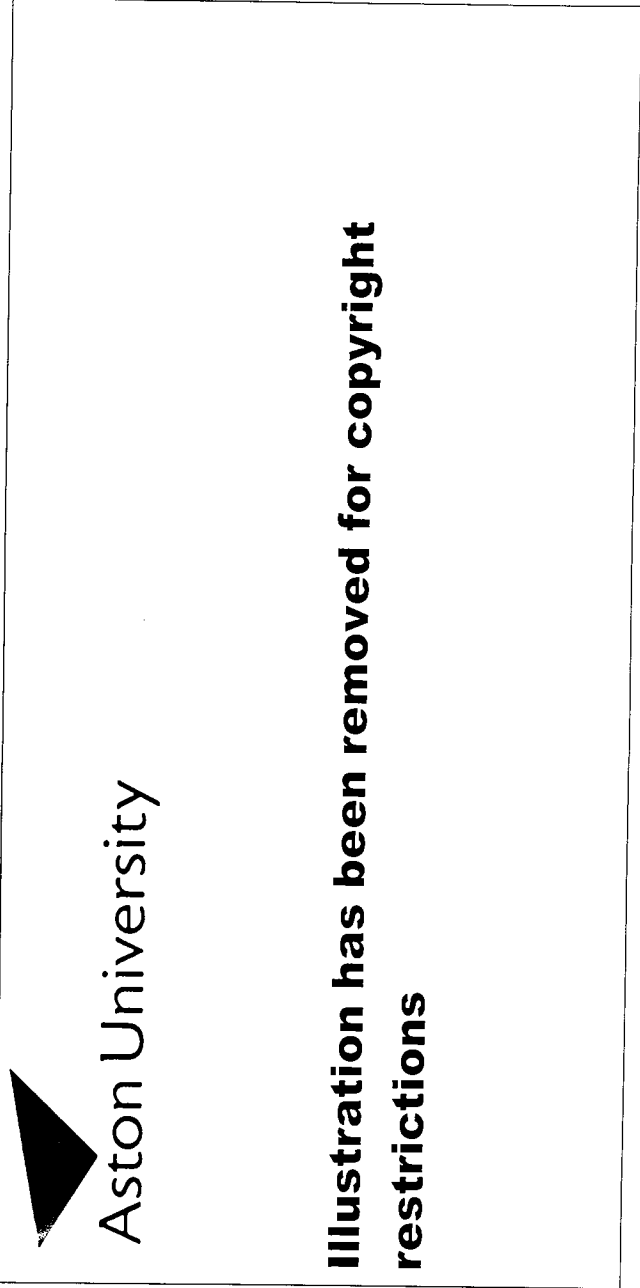


Fig.2.5 Solid classification as described by Geldart (1973)

made below to provide further back ground, along with the three studies which specifically deal with the effect of the distributor design on the solids segregation.

2.6.1. *Rowe and Nienow et al.*

Any review in the field of solids mixing or segregation in gas fluidised beds will be incomplete without special tribute and reference to the extensive investigations carried out by Rowe and Nienow with a number of co workers at University College, London.

Initial work carried out by Rowe et al.. (1972a,b) outlined the mechanisms by which particles in a gas fluidised bed behave using binary systems of near-spherical particles. The work was carried out in a two-dimensional bed using six binary combinations offering a variety of physical characteristics. Rowe et al. consistently observed a uniform composition over a wide middle region of the fluidised bed height, even when appreciable segregation occurred elsewhere. They concluded that the degree of mixing depends very strongly on the gas velocity, and even strongly segregating systems can be either separated or well mixed by controlling this parameter. In segregating conditions, only the bottom region approached a pure composition of jetsam, while at the top the flotsam was always contaminated with jetsam. Typical illustrations of these patterns are shown in Figure 2.6.

They observed three distinctly different mechanisms by which relative particle movement occurred; all were associated with bubbles. The most important mechanism was the lifting of particles in the enclosed wake of a rising bubble. This mechanism tends to reduce segregation and increase mixing because it is the only way particles can move to the top of the bed. The second mechanism involves the falling of particles through bubbles allowing large, heavy particles to fall faster than small and lighter ones. The third mechanism involves the falling of particles through voids induced by the passage of bubbles; this will again help the big heavy particles to settle down. Another phenomenon was noted which, although it was never observed to cause segregation, was responsible for preserving it. This is a quasi-hydrostatic effect that caused particles to "float" on a fluidised bed of denser ones. This effect only appeared to prevent low density particles from moving down, it did not appear to cause them to move up.

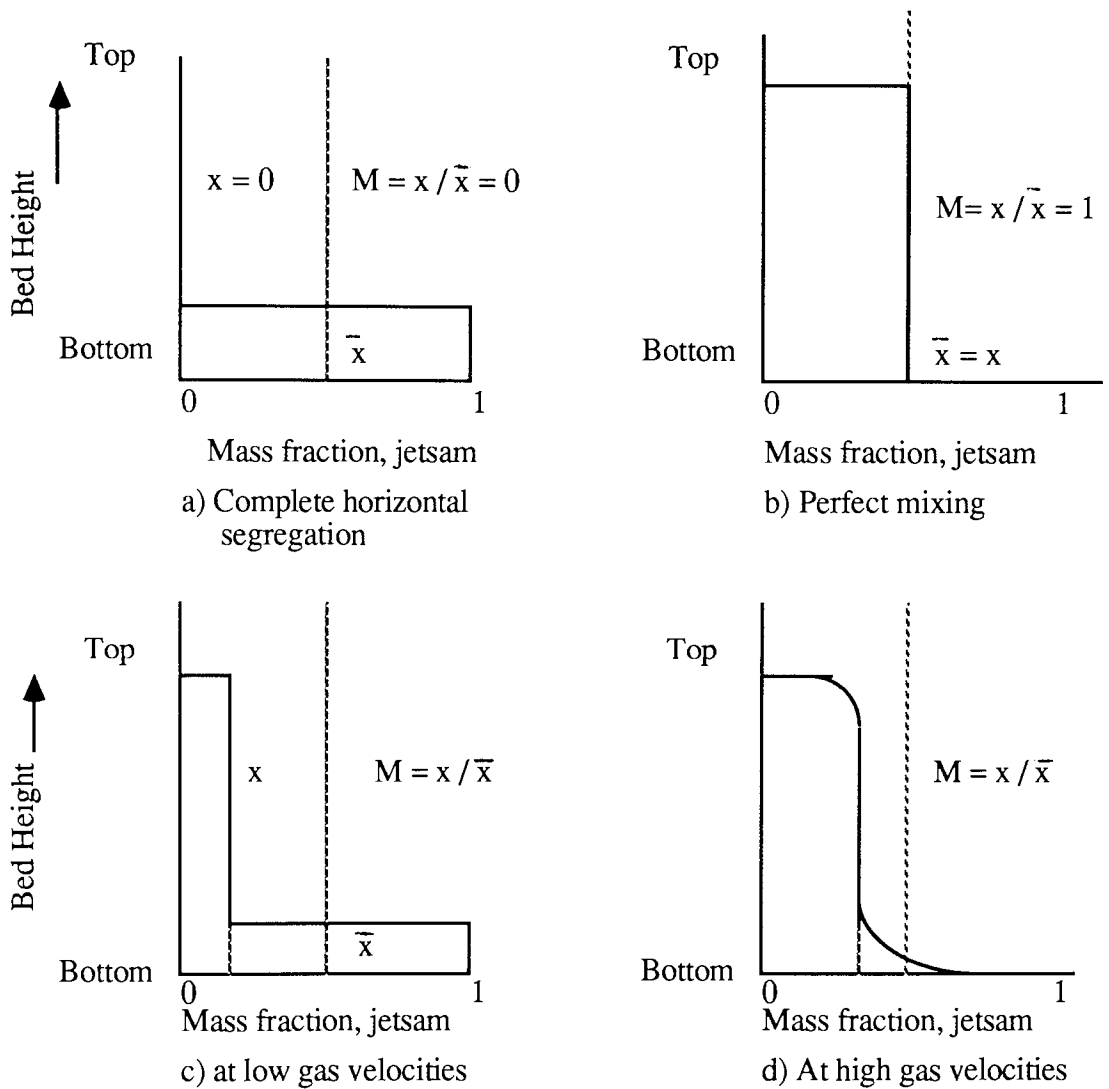


Fig.2.6: Segregation patterns and mixing index for close-sieved binary mixtures
 (adapted from Rowe et al..(1972b))

A mathematical model to describe steady state segregation in a gas fluidised bed containing small particles based upon this work was later developed by Gibilaro and Rowe in 1974. The model was derived in terms of a solids volume balance.

Figure 2.7 illustrates the basic assumptions made by Gibilaro and Rowe in developing this model. Four basic parameters were used to describe the three modes of mixing and the one of segregation.

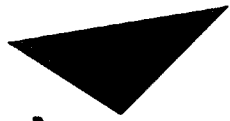
1- **Circulation** : Solids are picked up from the bottom of the bed in the wake of bubbles and are carried to the top. They then leave the wake phase to join the bulk phase of material flowing downward. The volumetric flow rate of solids, w , is proportional to the bubble flow and so is approximately constant across all horizontal planes through the bed.

2- **Exchange** : Since solids are fed continuously into the wake and shed periodically as concluded by Rowe(1973), there can be exchange of solids between the bulk and wake phase. The rate of exchange, q , is defined in terms of the total volumetric rate (of solids) per unit height of bed. This is assumed to be constant over the length of the bed.

3- **Axial Mixing** : Apart from wake circulation, bubbles cause some axial displacement of solids by a 'drift' mechanism which can be described by pseudo-diffusivity. In the model a parameter, r , is defined which is equivalent to the product of a notional diffusion coefficient and the bed cross sectional area.
in their steady-state segregation model.

4- **Segregation** : Jetsam settles to the bottom of the bed more rapidly than flotsam and this tendency to segregate (k) depends strongly on density difference. At each point the downward flow of segregating jetsam is compensated by an equal upflow of flotsam from below. The rate of this transition at any level is proportional to the product of the jetsam concentration at that level and flotsam concentration in the level immediately below.

Gibilaro and Rowe (1974) summarised the formulation of the model in the form of Figure 2.7, which shows the jetsam balance on a typical bed element of height dz . Using the four parameters w , q , r and k , they described the movement



Aston University

Illustration has been removed for copyright restrictions

Fig.2.7: Illustration of the assumptions made by Gibilaro and Rowe (1974) in their steady-state segregation model.

of jetsam in the bulk and wake phase according to the following differential equation:

$$\frac{r}{H} \frac{d^2 C_B}{dz^2} + (w + k - 2k C_B) \frac{d C_B}{dz} + q H (C_w - C_B) = 0 \quad (2.5)$$

$$w \frac{d C_w}{dz} + q H (C_B - C_w) = 0 \quad (2.6)$$

where

r = an axial mixing coefficient (L^4/T)

H = total bed height (L)

z = normalised axial position = y/H

C_B = volume fraction of solids in bulk phase
which are acting as jetsam

C_w = volume fraction of solids in wake phase
which are acting as jetsam

w, q and k are solids circulation, exchange and segregation coefficients.

Gibilaro and Rowe further assumed that the transport parameters r, w, k and q were constant over the bed height. Rather than attempting to integrate the coupled equations directly, they then considered the circumstances under which one or more of the constituent mechanisms may be neglected and obtained analytical solutions for a number of cases. The special cases analysed were:

- 1) strongly segregating systems where axial mixing and phase exchange are negligible.
- 2) systems with exchange between the wake and bulk phases but no axial mixing and
- 3) systems with axial mixing and wake circulation but no exchange between phases.

Gibilaro and Rowe then compared their analytical solutions with the earlier experimental results (Rowe et al. (1972a,b)) with the solutions for cases 1) and 3).

The two results matched closely. They further concluded that phase interchange is usually a very small effect and can generally be neglected. Axial spreading was seen to be important at high gas velocities or in weakly segregating systems.

Although Gibilaro and Rowe's mathematical model was a bold advancement in modelling the segregation phenomenon, the parameters used in this model are still confined to a conceptual description.

Nienow, Rowe and Chiba (1978) studied the mixing and segregation of a small proportion of large particles in gas fluidised beds of considerably smaller ones. They found that large particles behave as flotsam when their density is less than the bulk density of the small particles. Otherwise, mixing and segregation appear to be insensitive to density and particle shape over a wide range unless this is extreme. Particles move downward by being trapped in sinking regions of dense phase and rise by being caught in the wakes of passing bubbles. Nienow et al. used anthracite, char and shale as large particles in the bed of sand or ballotini particles to illustrate their point. They computed two separate correlations relating the average rise velocity and average depth of penetration of flotsam particles as functions of gas velocity. These relationships were:

$$U_R = 1.9 (U - U_{mf})^{0.5} \quad (2.7)$$

$$\text{and } X/H = 0.12 (U - U_{mf})^{0.5} \quad (2.8)$$

where

$$U_R = \text{average rise velocity of a large flotsam particles} \quad (\text{cm/s})$$

$$U = \text{superficial gas velocity} \quad (\text{cm/s})$$

$$U_{mf} = \text{minimum fluidising velocity of the main bed jetsam material} \quad (\text{cm/s})$$

$$X = \text{average depth of penetration of large particles} \quad (\text{cm}), \text{ and}$$

$$H = \text{bed height} \quad (\text{cm})$$

They, further, observed that large flotsam particles rise through a gas fluidised bed at velocities an order of magnitude less than the bubbles. The relationship between rise velocity and penetration depth did depend on the size and

density of flotsam; so that if two kinds are present they are likely to remain in constant proportion throughout the bed.

Cheung (1978) carried out a quantitative analysis of the mixing of two segregating powders of different density in a gas fluidised bed. He used 40 binary mixtures containing solids ranging in size and density from 70µm to 928µm and 1.05 to 8.86 g/cc respectively. For all flotsam rich binary systems, he found that the variation of the mixing index (M) with gas velocity was in accordance with the following equation:

$$M = 1 / (1 + e^{-F}) \quad (2.9)$$

where

F is a dimensionless velocity defined by

$$F = ((U - U_{T0}) / (U - U_F)) \exp(U/U_{T0}) \quad (2.10)$$

Physically, U_{T0} is the gas velocity at which mixing takes over or predominates relative to segregation. Measurement of the mixing index, M, over a range of gas velocities showed it to vary in a logistic manner as shown in Figure 2.8, which illustrates that $U=U_{T0}$ when $M=0.5$. When $U=U_F$, there are no bubbles and therefore, no particle movement and mixing. U_{T0} was correlated with the system parameters - minimum fluidisation velocity, size (and shape), density, proportion of jetsam and aspect ratio - according to the following relationship:

$$\frac{U_{T0}}{U_F} = (U_p / U_F)^{1.2} + 0.9(\rho_R - 1)^{1.1} (d_{ER})^{0.7} - 2.2(x_J)^{0.5} (H^*)^{1.4} \quad \dots\dots\dots(2.11)$$

where

- d_{ER} = shape corrected particle diameter ratio = $\phi_J \cdot d_{PJ} / \phi_F \cdot d_{PF}$
- ρ_R = particle density ratio = ρ_J / ρ_F
- H^* = reduced aspect ratio = $1 - \exp(-H/D)$, and
- D = bed diameter

This correlation fits their experimental data with a standard deviation of 10%. Generally, great caution is recommended in using the correlation for conditions outside the experimental ranges.

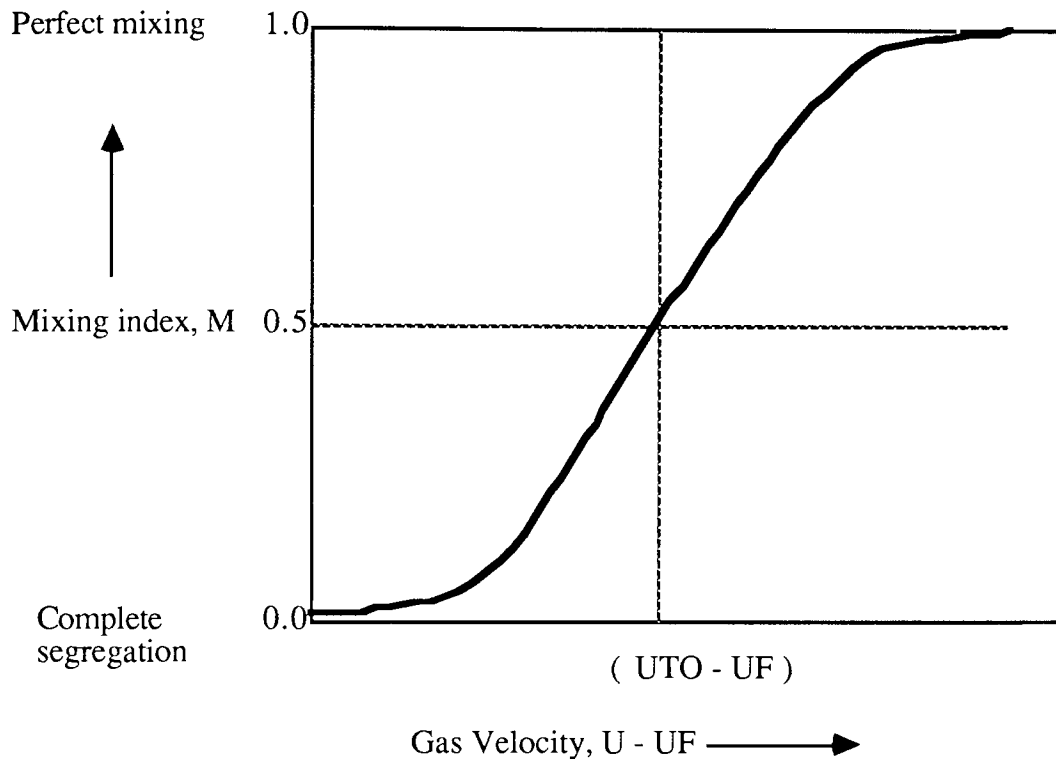


Fig.2.8: Variation of mixing index with excess gas velocity (adapted from Nienow et al.. (1978))

Naimer, Chiba and Nienow (1982) estimated the parameters required for the Gibilaro and Rowe model for gas fluidised beds and linked them to the physics of the bubbling bed predicted. Comparison of experimental and predicted segregation patterns and mixing indices shows good agreement for low jetsam concentration systems and for changes in the gas velocity. However, the analysis breaks down in the case of high jetsam concentrations. The reason offered for this failure was that the high jetsam concentration system offers an additional overlying mechanism which is not included in the Gibilaro and Rowe model.

An important study from an industrial viewpoint is to see what happens in a

continuously operated bed where the mean residence time of each of the two components is considerably greater than the mixing time. Neinow and Naimer (1980) showed and confirmed that the shape of the segregation pattern during continuous operation is the same as that obtained in the batch case, except possibly when the discharge is taken from within the segregated jetsam region at the base of the bed. Thus, if the feed concentration of jetsam is set equal to that in the middle region of the bed as found in batch experiments and also if the analysis is carried out from that region, the mixing index should be identical. A summary of their experimental findings for solids withdrawal from the constant composition region is shown in Figure 2.9. During the unsteady-state period, the outlet composition X_{Out} is a function of the initial composition of the bed X_{initial} . However, after operating for > 5 mean residence times, the initial composition has no effect, and a steady state composition X_{SS} is reached.

2.6.2. Burgess et al. (1977)

Burgess, Fane and Fell (1977) investigated segregation of particles in a gas fluidised bed containing binary mixtures, using a 150mm diameter glass column of height 600mm mounted above a gas distributor with 21 tuyeres each having 8x2.4mm holes. The solids used were sand (143-512 μm), ballotini (143-900 μm), iron powder (143-215 μm) and steel shot (340 μm) with an absolute density of 2.7, 2.9, 6.3 and 7.5g/cc respectively.

Burgess et al. found that for initially segregated beds of binary mixtures of solids of different size and of the same density, the mixing commences at gas velocities just above the u_{mf} of flotsam. For these systems mixing takes place by the gathering of jetsam material in bubble wakes at the interface between the bubbling flotsam layer and the non-bubbling jetsam layer. However, mixtures of particles having different sizes and densities did not begin mixing until the gas velocity exceeded the minimum fluidisation velocity of the jetsam. For such systems the jetsam was the denser component, even if it had a similar or lower minimum fluidisation velocity than the flotsam.

A bubbling bed transport model was used to simulate the complex

behaviour of segregation, based on simple assumptions and minimal parameter adjustment. The wake was assumed to be composed of a well-mixed region and unmixed region as shown in Figure 2.9 and 2.10. The well mixed region was supposed to account for the combined effect of periodic wake shedding and axial drift produced by bubble motion in the bed. The stagnant region accounts for axial movement of solids in the vertical direction of the bulk flow mechanism. This is a somewhat new concept as other workers have always considered the wake as one section.

Burgess et al. followed the approach of Gibilaro and Rowe by dividing the bed into finite sized increments in the axial direction and assuming that each slice was composed of a bulk phase and a wake phase. The minimum fluidisation velocity was calculated at each level based on the local composition, whereas the rate of bubbling was assumed to be given by the two phase theory (i.e. all the gas in excess of the minimum fluidisation requirement is used to produce bubbles). The simulation of the segregation phenomenon was conducted by allowing jetsam to fall down through the bubbles as they passed upwards. Each time a bubble moves from one slice to another, jetsam particles fall an average distance of L_S . Burgess adapted a numerically computed approach to establish the mass balance in finite difference form. A transient mass balance on each slice of the bed gives the concentration assumed to be given by the two phase theory (i.e. all the gas in excess of the minimum fluidisation requirement is used to produce bubbles).

In order to evaluate the various effects of wake mixing, segregation and phase exchange, the following parameters are required:

- V_W , the fraction of the bubble which is wake,
- L_W , the wake length, represents a characteristics vertical wake mixing length,
- L_S , the segregation distance, represents the distance a jetsam particle falls during passage of a bubble,
- A_S , the projected bubble area as the bubble moves upward, and
- f_m , the fraction of wake which is completely mixed.

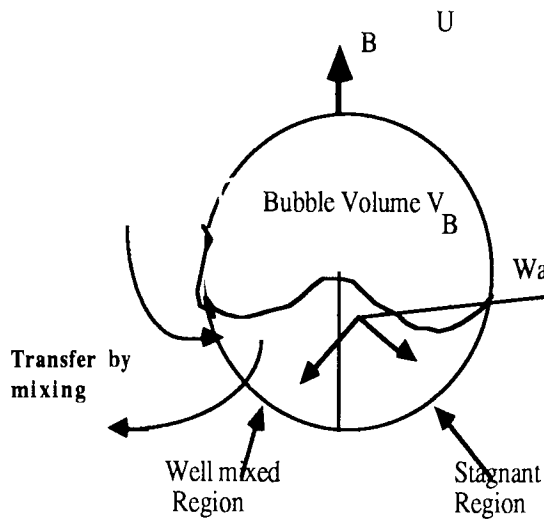


Fig.2.9: Wake mixing model with component

(adapted from Burgess et al. (1977))

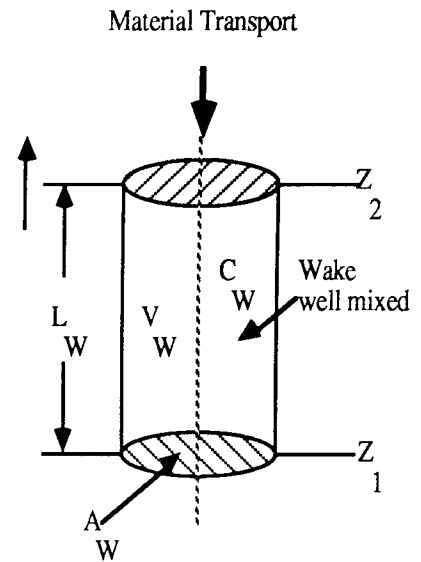


Fig.2.10: Well mixed wake bulk flow representation

The model makes use of the following assumptions and correlations to get these parameters:

- the bubble size is estimated by the correlation of Mori and Wen (1975) using the local U_{mf} and the centre height of the bubbling zone.
- using Rowe's (1971) data, the volume of the wake (V_w) is assumed to be 30% of the volume of the bubble void plus wake; the wake length $L_w = 0.575 * D_B$ and $A_s = (\pi * D_B^2 / 4)$.
- the U_{mf} of the local mixture is predicted using a modified Ergun equation, combined with a correlation of voidage for the mixture developed by Burgess.
- bubble velocity is calculated according to Nicklin (1962)
- the mixing fraction of the wake, f_m , is assumed to be 0.5
- L_s is an adjustable parameter.

This model makes it possible to predict the segregation pattern to some extent. But the procedure is complicated to understand and the concept of a stagnant region existing in the bubble wake is hard to imagine from a physical point of view. In addition, the segregation distance and the fraction of complete and incomplete mixing regions within a wake are still left as adjustable parameters which must be chosen so that the predicted result gives a good fit to that observed.

Also Burgess et al. do not explain the variety of experimental profiles seen in terms of these parameters. It is not clear that the assumption of a well mixed region and a stagnant region in the bubble wake are supported by experimental evidence. The typical values used for V_W , L_W and f_m may or may not be applicable to other systems, especially for systems containing large particles. These quantities would be expected to change with the fluidisation regime.

2.6.3. Fan and Chang (1979)

The first ever study of large particle segregation in gas fluidised beds containing only large particles was carried out by Fan and Chang in 1979. But the work was carried out only in a two-dimensional bed; they used table tennis balls weighing 2.42 and 2.50g. This slight weight difference was created by putting sand in some balls which increased their minimum fluidisation velocity from 2.0483 m/s to 2.0726 m/s. Interestingly this tiny difference in weight produced noticeable segregation at air velocities up to 3.4 m/s.

They noticed that each ball oscillated slightly around a fixed position in the bed prior to the onset of bubbling. Transition from the bubbling bed condition to the slugging bed condition was almost immediate as the gas velocity was increased above the bubbling point. The mixing mechanism was mainly due to the bubble or slug-induced drift and gross circulation, whereas segregation seemed to result from preferential upward drift of lighter balls in the vicinity of rising bubbles and preferential downward movement of heavier balls in the disturbed regions behind bubbles.

Transient experiments revealed that axial mixing was more rapid for the process where the lighter particles were initially placed at the bottom and the denser

particles were placed at the top than for the process when the initial conditions were reversed. However, both initial conditions led to a unique equilibrium concentration distribution, with lighter balls always on top. They further noticed that at low or moderate air flow rates the concentration gradient existed only near the distributor. Also, radial mixing was more rapid than axial mixing but no appreciable segregation occurred in the radial direction.

Fan and Chang also developed a non-stationary numerical random walk model to represent the axial concentration distribution as a function of the operating time. This model predicts the concentration profile as a function of time and ultimately predicts the steady state profile as time approaches infinity. Their model is also applicable to the representation of radial mixing data. They stated that the rates of both axial and radial solids mixing can be generally correlated as a function of the excess air rate which contributes to the creation of air bubbles.

The model appears to fit Fan and Chang's experimental data reasonably well and also gives concentration profiles of the same form as those reported by Rowe et al. (1972). The model appears to be more practical than that of Burgess et al..

2.6.4. Geldart (1981), Geldart, Baeyens, Pope and Van de Wijer (1981)

A number of research workers under the supervision of D. Geldart have also investigated segregation in beds of large particles at high velocities at the University of Bradford, U.K. The segregation work was an off-shoot of their main stream project concerned with the study of particle entrainment.

They used mixtures of large and small particles of sand, metal shot and alumina sized between 45 and 500 μm and fluidised it in both two- and three-dimensional beds. Most of the work was carried out in a three-dimensional bed of 0.29m diameter and 5m high with gas velocities up to 5m/s with and without internal tubes. These internal tubes appeared to have a profound effect on the density distribution. In some cases, three separate zones were produced; a high density section below the internals, a low density section surrounding the internals and another low density section above the internals. When experiments were conducted with tubes, the fines were re-injected below the tubes and no significant affect due to

the tubes was seen. Segregation appeared to increase as the size of the fines decreased along with the increased size of large particles and as the superficial gas velocity approached u_{mf} .

The two useful indices used by Geldart et al. were a coefficient of segregation, C_s , and a mixing index, $M_{Geldart et al.}$. These are defined as

$$C_s = [(x_B - x_T) / (x_B + x_T)] \times 100 \quad (2.12)$$

$$M_{Geldart et al.} = [x / \bar{x}] \quad (2.13)$$

Where x_B and x_T = are concentrations of material of interest in the bottom and top halves of the bed.
 x = is the concentration of material under scrutiny in the top of the bed.
 \bar{x} = mean concentration

They also observed that when the gas velocity is well above the incipient fluidisation velocity, e.g. $(u_o - u_{mf}) > 1\text{m/s}$, segregation was relatively insensitive to gas velocity up to 5m/s. In segregation by size difference. They found that the concentration of fine/coarse material appeared to vary consistently. Also the region near the distributor was particularly rich in jetsam, whilst the remainder of the bed had a fairly constant concentration in beds containing only a small amount of dense particles.

2.6.5. Daw (1985)

Daw (1985) was the first research worker to investigate particle segregation in a gas fluidised bed exclusively using large particles (Geldart type 'D') in a three dimensional bed.

Segregation experiments were conducted with binary systems in a 10.2cm diameter cylindrical bed with air at ambient temperature and pressure. He carried out some 196 experiments with particles ranging from 1750 μm to 6270 μm in diameter

and absolute density ranging from 0.905 to 7.5g/cc. Various operating parameters e.g. air velocity, particle properties, bed height, relative amounts of jetsam and flotsam and bed internals were varied to determine their influence on the steady state segregation pattern. Other features studied were transient segregation and steady-state bed expansion.

Daw developed a mixing index which was used as an indicator of the degree of segregation and provided him with a convenient means of quantifying the effect of parameter changes on segregation. The mixing index (M_{Daw}) was:

$$M_{Daw} = \left[\sum_{n=i} V_{si} \left(v_{Ji} - \bar{v}_J \right)^2 \right] / \left\{ \bar{v}_J \cdot (1 - \bar{v}_J) \right\} \quad (2.14)$$

where :

- i = mixing index referring to each sample
- n = total number of samples taken
- v_{si} = the volume fraction of the total bed contained in sample i
- v_{Ji} = the volume fraction of Jetsam in sample i
- \bar{v}_J = the volume fraction of jetsam in the bed.

The mixing index represents the variance of the jetsam composition along the bed height and was found to be more accurate than the mixing/segregation indices used for small particles by other research workers. The index (I) showed a generally downward trend with increasing gas velocity until it reached a minimum at some velocity between the u_{mf} of jetsam and flotsam. Daw also observed that prominent local maxima and minima appear to occur in the index at velocities where there are abrupt flow transitions; e.g., at the velocity where there is a change from channeling to large-scale bubbling.

At various superficial velocities different segregation behaviours were observed. He designated them as Region 1 and 2. Region 1 segregation was observed when the superficial velocity was less than the jetsam minimum fluidisation velocity but greater than the flotsam minimum fluidising velocity. The bed usually consisted of a jetsam-rich unfluidised zone and a flotsam-rich fluidised zone. The relative sizes of these two zones and their compositions depended on the gas

velocity, the particle densities and sizes, the overall bed composition and initial condition. The second type, designated as Region 2 segregation, occurred when the gas velocity was greater than the minimum fluidising velocity of jetsam. He found that a variety of axial composition profiles can occur depending upon the gas velocity, particle densities and sizes, the type of bed internals, the bed height and overall bed composition. The bed here, was considered to consist of combinations of three zones; 1) a lower, high jetsam zone, 2) a well-mixed zone and 3) a high flotsam zone. When the jetsam percentage was low, the upper zone tended to be much less distinct and the lower and middle zones dominated the bed. With the bed composed of roughly equal amounts of jetsam and flotsam, all three zones were frequently visible. However, a jetsam-rich bed exhibited a predominantly upper zone and generally decreasing flotsam concentration with depth.

Daw also established a segregation model based on the Gibilaro and Rowe (1974) approach. This model had two key dimensionless parameters - D and w , which represent the importance of axial dispersion and large-scale circulation relative to segregation, respectively. A third parameter, V_w , used by Gibilaro and Rowe, representing the fraction of the bed included in the wake phase, was found to be effectively zero. The modified model (with $V_w = 0$) is given by:

$$v_J = 0.5 [\lambda_w + 1 + P \{ (1 + B_2 e^A) / (1 - B_2 e^A) \}] \quad (2.15)$$

where

$$A = z \cdot P / \lambda_D$$

$$P = ((\lambda_w + 1)^2 - 4 \cdot \lambda_w \cdot v_{J0})^{0.5} \text{ and}$$

$$B_2 = (\lambda_w + 1 - 2 \cdot v_{J0} + P) / (\lambda_w + 1 - 2 \cdot v_{J0} - P)$$

$$v_J = \text{average volume fraction of jetsam in the solids at given axial position, (-)}$$

$$v_{J0} = \text{volume fraction of jetsam in the solids at the bottom of the bed, (-)}$$

$$\lambda_w = \text{dimensionless ratio to circulation to segregation parameters,} \\ = w / k, (-)$$

λ_D = dimensionless ratio of axial dispersion to segregation parameters,
= $r. / (k \cdot H)$

z = noremalised height , (= h/H)

h = height above the distributor, (L)

H = total bed height, (L)

Observed range $\lambda_D = 0 - 12.4$

$\lambda_w = 0 - 1.47$

Daw observed similar variations in λ_w as reported by Gibilaro and Rowe, but the values of λ_D were much greater. This shows that the bulk phase dispersion is more important in large-particle beds than in small-particle beds.

Daw's transient segregation phenomena appeared to be simulated reasonably well by a transient form of the Gibilaro-Rowe model. He also combined the gas-species mass balance with the Gibilaro-Rowe segregation model to predict fluidised bed reactor performance. The result developed for first order reaction with one active solid component appeared to be reasonable.

2.6.6. Rice and Brainvich (1986)

Rice and Brainvich have studied the mixing and segregation in two- and three dimensional fluidised beds using a 3D cylindrical bed with an inside diameter of 273 mm and a 2D bed with a 280 x 25 mm rectangular cross section. In both cases a high density porous polyethylene distributor was used. The solids used were equi-density ballotini particles with size range of 105 - 149 μm , 210 - 297 μm and 354 - 590 μm . Their work was basically an extension of Nienow et al.'s work concentrating on binary systems of equidensity spherical particles. The work was carried out both with completely mixed and totally segregated mixtures. In the case, of segregated mixtures, the jetsam was always placed at the bottom and flotsam on the top. They found that at low superficial velocities, the jetsam-rich bottom layer served as a type of extended distributor. But as gas velocity increases, bubble coalescence occurs nearer the flotsam/jetsam boundary, bubble rise velocity increases, and the amount of jetsam lifted in the growing wakes increases

proportionately. They found a marked increase in the rate of transportation of solids in the bubble wake relative to the rate of segregation via circulation through or around bubbles as the velocity approaches U_{TO} . A little effect of aspect ratio (Ra) was noticed, reflecting the role of bubbles in jetsam movement and the increase of average bubble size with bed height. The results obtained from two- and three-dimensional beds were compatible except that the 2D bed data strongly exhibited wall effects. This effect is clearly reflected in the two different correlations for U_{TO} :

for three-dimensional beds:

$$U_{TO} = (U_{FB} \cdot U_{JB})^{0.5} \cdot (2Ra)^{-0.2} \quad (2.16)$$

and for two-dimensional beds:

$$U_{TO} = (U_{FB} \cdot U_{JB})^{0.62} \quad (2.17)$$

Where

U_{FB} = Minimum bubbling velocity of flotsam (cm/s)

U_{JB} = Minimum bubbling velocity of jetsam (cm/s)

2.6.7. Beeckmans and Stahl (1987)

The mixing and segregation kinetics in a strongly segregated gas fluidised bed was investigated by these workers. The work was carried out with two (I.D. 137 mm and 263 mm) cylindrical beds. Both these beds were fitted with perforated plates. They used spherical particles of iron and glass with particle size ranges of 0.25 - 0.60 mm and 0.25 - 0.425 mm respectively. The densities were 2.8 and 7.86 g/cc respectively, giving an effective density ratio of 2.87. Both these particles had the same minimum fluidising velocity of 93 mm/s. In the case of a segregated start, the iron particles were placed at the bottom. They analysed their data in terms of v_d and v_u and its relationship with absolute velocity ($(u / u_{mf}) - 1$); where v_d is the downward velocity of jetsam particles relative to flotsam particles in the upper portion of bed and v_u is the mean upward velocity of jetsam particles across the interface between upper and lower parts of bed. They established a model based on

a pure jetsam stratum underlying a uniform stratum of mixed composition. The model allowed calculation of the average upward velocity of jetsam particles across the interface between the strata, and of the average downward velocity of jetsam particles in the upper stratum. The high fluidising velocity appears to be the main factor in achieving good mixing and this velocity corresponds to a value of 1.38 for u / u_{mf} .

2.7. The Effect of the Gas Distributor Type on the Mixing and Segregation Phenomena in Gas Fluidised Beds

The gas distributor in a fluidised bed system has to perform three important functions, viz. it must initiate movement throughout the entire solids inventory at start up, maintain overall fluidisation and prevent the formation of stagnant zones and produce effective gas-solid contact. These functions are fulfilled by the distributor by providing a uniform flow of small bubbles to enhance mixing. Many investigators, as stated earlier, have indicated that gas-solid contacting is more efficient in the neighborhood of the distributor than higher in the bed and that the distributor design greatly affects both the physical and chemical performance of the bed.

One of the most important phenomena affecting chemical reaction in the bubbling zone of the fluidised bed is the exchange of material between bubbles and emulsion phase. The gas flow and solid motion surrounding any bubble are greatly affected by the motion of other bubbles, especially at the time of bubble coalescence.

The distributor region is believed to play a key role in determining the contacting efficiency of gas fluidised beds. In the literature there is no clear answer to the question of how different types of distributors will influence the performance of a gas fluidised bed reactor. Porous plate distributor for example are known to disperse the gas in the form of small bubbles in the fluidised bed thus yielding good gas/solid mixing. On the other hand, a high coefficient of mass transfer between distributor jets and surrounding suspension can yield even better gas solid mixing for perforated plates.

Cooke et al. (1968) found that changing the distributor could result in major changes in chemical conversion. Chavarie and Grace (1975) discovered that

the concentration of a reacting species fell much more quickly immediately above the distributor than predicted by bubbling bed reactor models. Bahie and Kehoe (1973) showed that reactor performance could be controlled by the distributor region for fast reactions. Grace and de Lasa (1978) confirmed the importance of the grid region and noted that the dilute-phase-to-dense-phase mass transfer rate in the grid region may be rate-controlling under many conditions. Ho et al. (1987) studied the effect of distributor pitch distance on heat transfer in a gas-solid fluidised bed and concluded that the distributor design has little effect on the bubbling zone heat transfer; however, it strongly affects the grid zone heat transfer.

Merry and Davidson (1973) and Agarwal et al. (1980) proposed that even bubble gas distribution in a fluidised bed system can be achieved with a relatively high pressure drop, uniform resistance gas distributor. On the other hand, Werther (1977), Geldart and Kelsey (1968) and Whitehead et al. (1979) have shown that the uniformity of gas flow across the distributor does not necessarily ensure uniformity of gas bubble distribution in the bed. Whitehead and Dent (1982) achieved greater uniformity within the bed with a non-uniform flow, low resistance gas distributor under conditions where bed aspect ratio and fluidising velocities are such that bubbles at the bed surface are small relative to bed width. Wen and Chen (1982) have also observed the bubble shifts and solid circulation caused by non-uniform gas flow. The dynamics of particles around a bubble has significant effects on the bubble shape, which is affected by neighbouring bubbles and the flow pattern of the distributor.

Another serious problem in the design and operation of some fluidised bed reactors, e.g. combustors, is the formation of a dead zone near the distributor. The presence of the dead zones or indeed the formation of totally defluidised layers is enhanced when the bed material contains particles of different size and/or density.

2.8. *Quality of Fluidisation*

Kunii and Levenspiel (1969) have discussed in detail the influence of the distributor on the quality of the fluidisation. Reporting the work of various researchers such as Groshe, they diagrammatically explained this influence. Their findings are summarised in Figure 2.11.

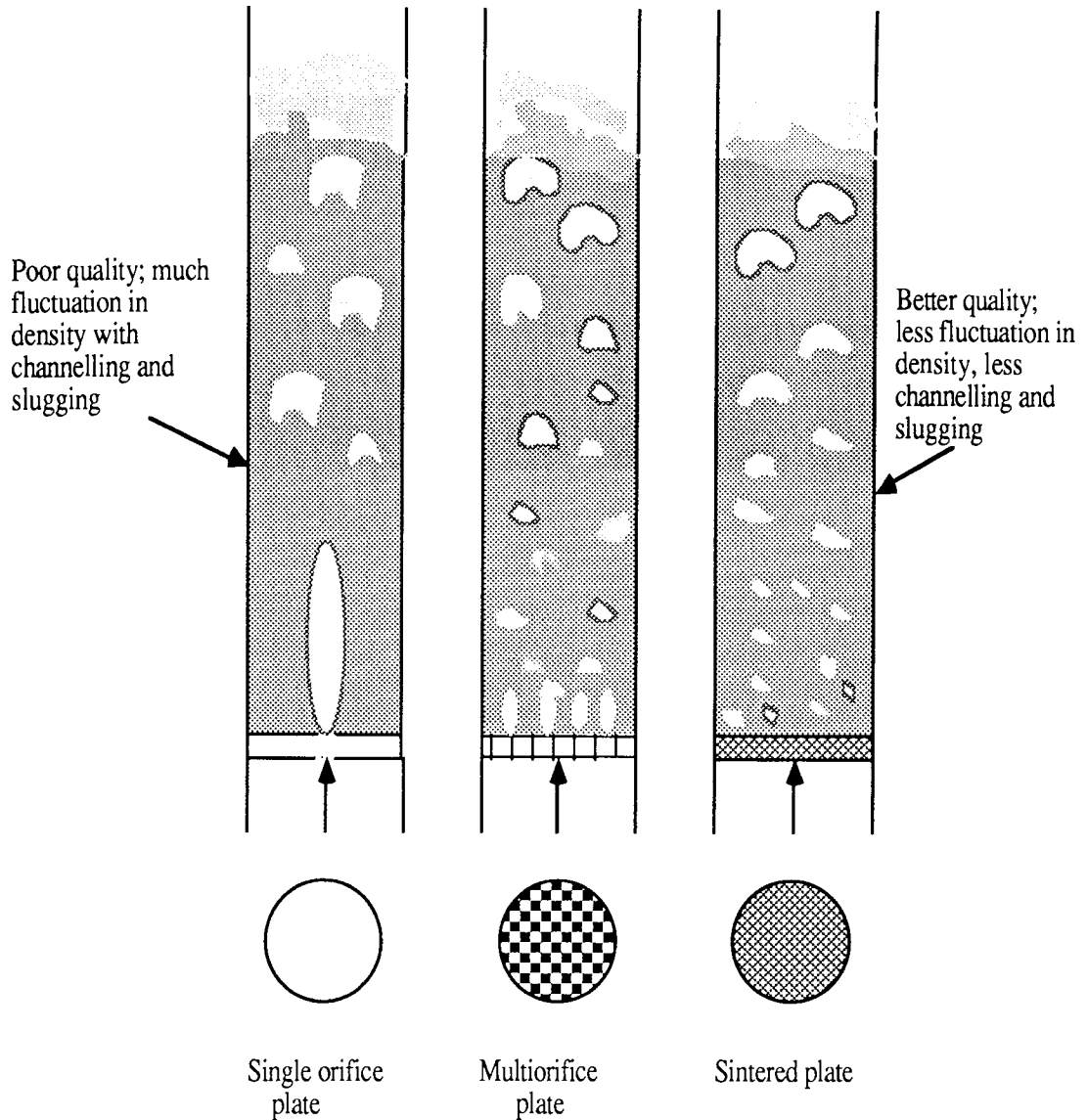


*Fig.2.11: Effect of the type of Distributor on the quality of fluidisation
(adapted from Kunii and Levenspiel (1969))*

With only a few gas inlets the bed density fluctuates appreciably at all flow rates (20-50% of mean value), and more severely at high flowrates: the bed density varies with height and gas channelling may be severe. For many gas inlets the fluctuation in bed density is negligible at low air flow rates but again becomes appreciable at high flow rates: bed density is more uniform throughout, bubbles are smaller, and gas-solid contacting is more intimate with less channelling gas.

Although the gas-solid contact is superior with porous plates, their use is

often not considered in industrial operations due to the danger of blockage, the high "pressure drop" cost and erratic bubbling encountered in such plates. Thus, by using a multi-orifice distributor these problems are overcome while still achieving good initial gas distribution, providing there is a sufficient pressure drop across the plate.

Geldart (1972) has shown that a drilled plate with more than 1000 holes/sq. meter will behave in a similar manner to a porous plate. However, the cost of drilling so many holes can be exorbitant.

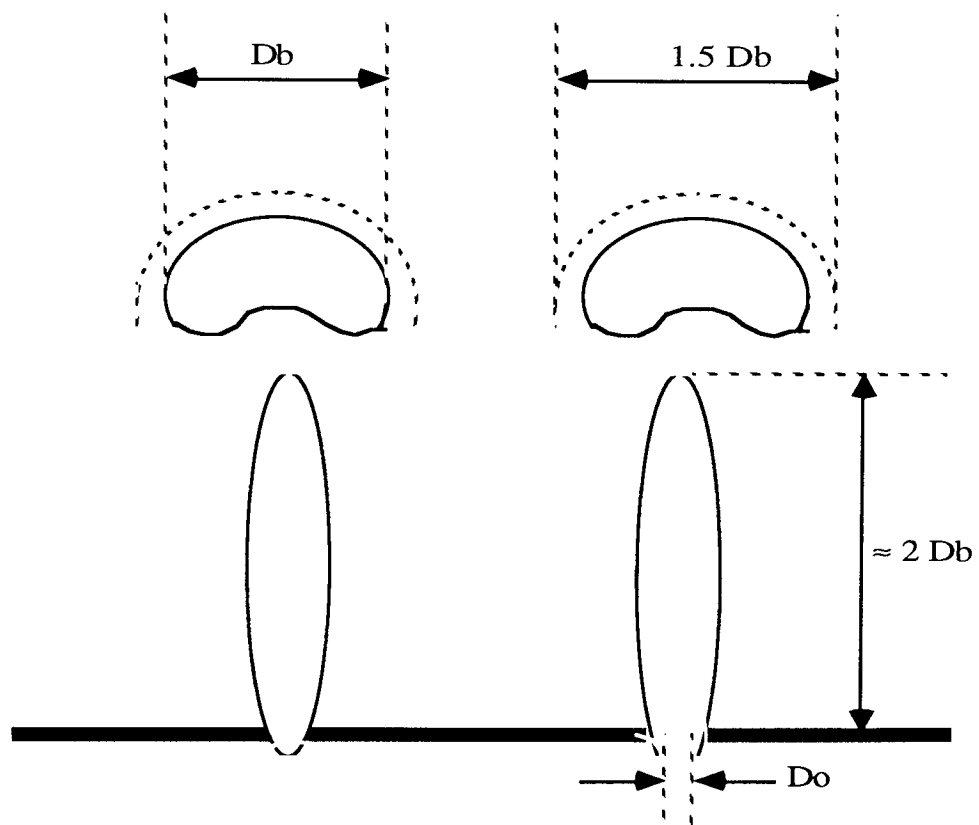


Fig.2.12: Zenz's idealised jet-to-bubble emergence pattern.

(adapted from Zenz (1968))

The grid zone height is an important parameter above which one can apply a classical bubbling bed model. The grid zone height can be defined as the effective jet height, this being the height at which the initial bubble takes off from the jet. Zenz (1968) photographed a large 2-D bed and gave a qualitative description of the

penetration of gas into a bed of particles. The gas was described as taking on an elongated appearance similar to that of a flame before solids inflow separated it from the orifice and pushed it upward in the form of a bubble before being succeeded by another. Figure 2.12 illustrates Zenz's idealised jet-to-bubble emergence pattern.

The width of the jet increases after leaving the nozzle and then decreases toward its end. Botterill et al. (1963) and Zenz (1968) suggested that the transition from a jet to a chain of bubbles occurs only when the gas is entering the bed. Zenz (1968) has also presented the results of his tests along with the results of other research workers relating the penetration depth to orifice diameter ratio, the product of the orifice gas velocity and the square root of gas density.

Massimilla (1985) has reviewed the findings of various workers describing the formation of a jet on the orifice and then breaking away as bubbles; a summary of his review is presented here.

Morkherka et al. (1971) observed elongated cavities, periodically forming above the orifice and leaving it as bubbles as shown in Figure 2.13a. Yang and Kearin (1974), Knowlton and Hirsan (1980) and Kececiogun et al. (1981) have found that the gas enters in the form of a jet plume, developing periodic "necks" and dividing into a series of cavities which grow into embryonic bubbles as shown in Figure 2.13b. Kozin and Baskakor (1967) and Zenz (1968) found that the gas takes on an elongated appearance similar to that of a flame penetrating into the bed before solids inflow separates it from the orifice and displaces it upward in the form of a bubble before being succeeded by another. The idealised jet-to-bubble emergence pattern is shown in Figure 2.13c. Early theories suggested that the transition from a jet to a chain of bubbles is related to the energy of the gas stream entering the bed. Rowe et al. (1979) suggested that gas can enter a gas-fluidised bed in two ways; either as a jet, when a permanent cavity stands at the orifice, or as a chain of bubbles, when volumes of relatively clear gas form and detach periodically from the orifice, which is covered by fluidised particles between successive events as shown in Figure 2.13d. Their work showed that jets are not typical of gas entering into a fluidised bed of particles except when the bed is inadequately fluidised or surfaces are present to hinder the flow of particles towards the orifice.

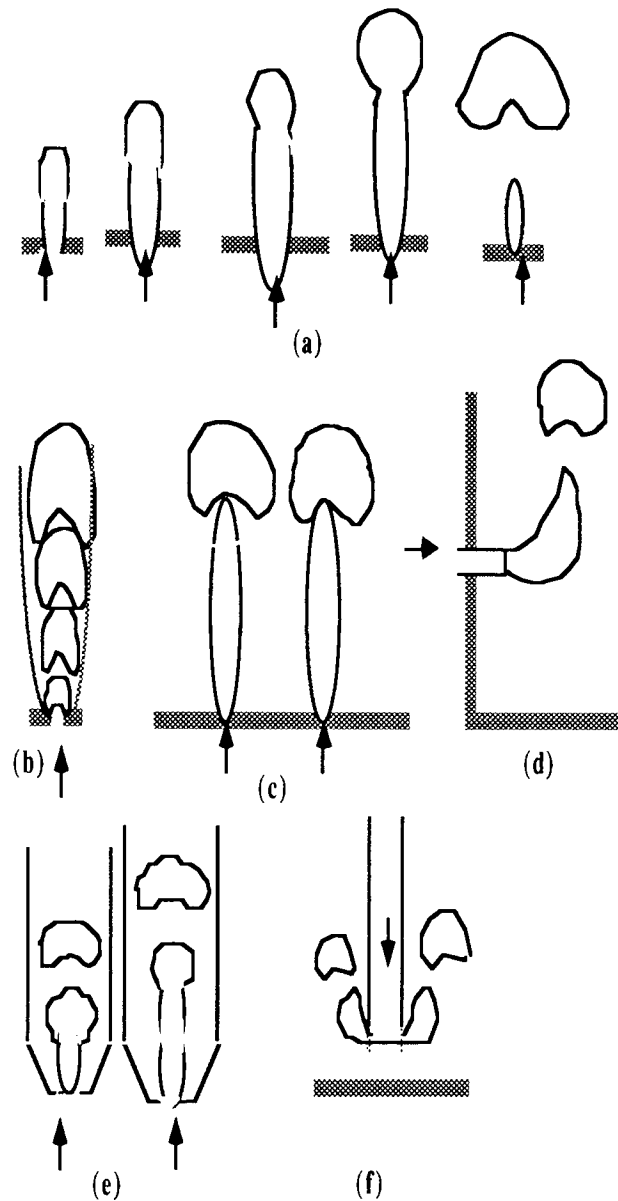


Fig.2.13: Modes of gas discharge in a gas-solid fluidised bed:

- a) Development of jet and formation of bubbles in fluidised bed (Markhevka et al., 1971);
- b) Chain of bubbles and bubble plume (Davidson, 1981);
- c) Jet and bubble formation at the orifices of a distributor plate (Wen 1981);
- d) Jet plume in horizontal discharge (Shakhova and Minaev, 1972);
- e) Jet plume breaking into bubbles at minimum and maximum jet penetration configuration (Kececioglu et al, 1971)
- f) Chain of bubbles from lateral orifices in vertical downward discharge with a slotted pipe (Clift et al., 1976).

(Adapted from Massimilla in 'Fluidisation' by Davidson, Harrison and Clift; 1985)

Other factors besides the degree of bed fluidisation and the presence of walls appear to affect the development of jets. High speed motion pictures of gas injection have shown that, for a given inlet gas velocity at the orifice, the mode of gas discharge gradually changes from the chain of bubbles to the jet type, as bed particle size increase from fine powders (Geldart- Group 'A') to coarse beads (Geldart- Group 'D').

2.9. Literature Review- Effect of the Distributor Design

The following three papers deserve particular mention.

2.9.1. Naimer (1982)

Naimer (1982) devoted a Chapter of his thesis to investigating the effect of the distributor on segregation using binary and tertiary mixtures. Experiments were carried out with solids having mean particle sizes up to about 925 μm , densities up to 7.44g/cc and gas velocities up to 0.36 m/s. A cylindrical bed of 14.7cm diameter as well as a bed of 10cm x 10cm square section were used. Five different distributors comprising a porous plate, a standpipe distributor and three perforated plates of different configurations were used. He also visually studied the jet-to-bubble formation and dead zone formation at the distributors.

Naimer concluded that the quality of mixing is significantly influenced by the type of distributor plate employed. Good mixing is primarily achieved by increasing the initial bubble diameter, but at the same time the 'disturbing' effect caused by the jets also improves the mixing in the bed. In equal density systems, segregation of the size fraction occurs around the jets. The phenomenon is more pronounced in system which have a large mean particle diameter and is similar to the segregation found in spouted beds. The size of the dead zones which form between the jets is mainly influenced by the pitch, superficial gas velocity and the distributor design.

A computer simulation was carried out to predict particle behaviour in the vicinity of the various distributor plates and so determine the segregation profiles; this also showed that the quality of mixing can differ appreciably depending on the choice of the distributor plate.

The work lacked any conclusive evidence as to which mechanism governed the formation of dead zones. Further, it was noted that for the binary and tertiary systems tested there was no significant difference in the segregation patterns obtained when the experiments were performed in either the circular or square bed.

2.9.2. Whitehead, Dent and Close (1983)

Whitehead et al. studied the effect of distributor design on particle segregation in a 0.54m internal diameter steel cylinder surmounted by a 1.14m internal diameter freeboard section for disentrainment. They used two types of distributors which are described as follows:

- a) Multipore, formed by clamping a layer of uniform weave cotton cloth between two sheets of perforated plates arranged with the perforations in alignment, the perforations being 12.7mm diameter set on a 18mm triangular pitch.
- b) Multituyere, containing seven bubble cap tuyeres having variable slit width so that the gas efflux velocity could be changed. Extra flow resistance was also created by inserting a 60 mm diameter orifice in the 76 mm diameter riser pipe.

A wide-size-range of iron ore up to 6.7 mm in diameter having a minimum fluidising velocity of 0.5 m/s, was used for segregation experiments. Two types of experiments were conducted in the apparatus: a) a well mixed sample of bed material was fluidised for a known period, then fluidisation was abruptly terminated; b) other experiments were conducted, sometimes simultaneously with 'a', to determine the behaviour of small amounts of oversize material; monolayers of these particles were placed on either half or on a quarter of the distributor, and bed material was then added and fluidised for a known period. When the bed was sectioned, the amount of close sized range material remaining on the distributor base was recorded. Samples were taken from the upper and lower levels of comparable beds fitted with multipore and multituyere distributors. The results showed that whilst the multi-tuyere system gave no size segregation at a superficial velocity of 1.7 m/s, the multi-pore system showed definite size stratification at 3.7 m/s.

It is generally accepted that the segregation is accentuated by operation at low superficial velocities; therefore, the distributor design has a material influence

on bed behaviour of a wide size range material.

Despite the segregation of coarse material in the multi-pore system, it still remained mobile. Interaction between the bed and distributor in such a system is very complex as the upper layers of the bed have a lower incipient fluidising velocity than the base.

2.9.3. *Feng, Chen and Whiting (1985)*

The effect of the distributor was investigated for the purpose of design and scale up of large fluidised bed combustors. Four orifice plates with different configurations were used to study the effect of distributor design on bubble formation and solids mixing. The experiments were carried out in a three-dimensional fluidised bed of 27.94 cm diameter and a two-dimensional bed with dimensions of 30.48 cm x 1.27 cm. The material used were 600-841 μm sand and 841-1200 μm limestone. The static bed height in both beds was 15 cm.

Four orifice plates with different configurations, but each with the same total free area, were made. Two distributors (I & II) had uni-sized orifices either 7.14 mm or 3.57 mm in diameter at 42.5 mm and 22.2 mm triangular pitches. The other two distributors (III & IV) had two-sized orifices and a circular demarcation line. The distributors were divided into two zones- a centre zone and a side zone. Distributor III had smaller diameter orifices ($d_1 = 2.38$ mm) in the centre zone and larger diameter orifices ($d_2 = 3.95$ mm) on the side zone whereas the configuration was reversed for distributor IV. In each case, the open area of the centre zone was one third of the total, which in turn was 2.27% of the total cross-sectional area of the bed.

Motion pictures were used to study bubble formation and coalescence. Pressure profiles inside the three-dimensional bed were measured for all the distributors to study bubble flow patterns, and tracer particles were used to study mixing patterns at various superficial velocities and particle sizes. These tracer particles were larger and less dense than the bed particles and these were added to the top of the bed after the bed had been running and reached steady state. The bed was divided into five, 3 mm thick, layers to sample the particles. The results were analysed using a concentration ratio which is expressed as follows:

$$C_i = (T_i / T) / (S_i / S) \quad (2.18)$$

where

- C_i = concentration ratio
- T_i = weight of tracer in a layer
- S_i = weight of bed particles in a layer
- T = total weight of tracer
- S = total weight of bed particles

In the case of perfect mixing inside the bed, the concentration ratio is unity. The following mixing index ($M_{\text{Fen at el.}}$) was used to indicate the degree of mixing:

$$M_{\text{Fen at el.}} = \sum (C_i - C)^2 \cdot W_i \quad (2.19)$$

Where

- M = mixing index
- C_i = concentration ratio in layer i
- C = concentration ratio at perfect mixing (=1)
- W_i = weight fraction of bed particles in layer i

For the case of perfect mixing, the mixing index is zero.

They found that distributor III performed better than the rest and distributor IV was the worse. The best mixing for distributor III was reached when the ratio of superficial velocity to minimum fluidising velocity (U_o / U_{mf}) equalled 1.4. As the ratio U_o / U_{mf} was increased further, the difference in mixing between I, II and III decreases. When U_o / U_{mf} was larger than 1.65, or the superficial velocity was greater than 50 cm/s, the flow regime of the bed was changed from bubbling fluidisation to slugging fluidization and the configuration of the distributor become irrelevant.

CHAPTER 3

EXPERIMENTAL EQUIPMENT

3.1 Experimental Equipment

The equipment used in the experimental work is shown schematically in Figure 3.1. The air-solid reactor column is 500mm long and 138mm in diameter. This column was used for all the three reactor systems namely the fluidised, spouted, spout-fluid bed.

Dry, air at essentially room temperature, was the fluidising/spouting medium. The air was taken from an 80p.s.i.g. main, passed through an oil/water filter and stored in a pressure vessel. The air was then passed to a dry gas meter, which indicated the volumetric air flow rate at 80p.s.i.g. The dry gas meter was supplied by Imac Systems Ltd., Fleet, Hants; the meter was of centrifugal type and the operation of the meter was based on the principle of speed measurement within an accuracy of (+/-)0.5%. The air from the dry gas meter was reduced in pressure to 40p.s.i.g., filtered and was fed into an inlet manifold which was connected to a bank of variable area flow meters. The air supply to each flow meter was controlled by an individual needle valve. The outlet of each meter was further connected to a gate valve so that the air supply could be terminated at any point without disturbing the other meters. The outlets of the flow meters were then connected to a common manifold, fitted with a pressure gauge to indicate the system pressure. The outlet of the manifold was fitted with a needle and a gate valve and was, then, connected to the plenum chamber of the reactor column. Another ball valve was fitted close to the plenum chamber and this was frequently used to isolate the bed. Figure 3.1 shows the general arrangement of the equipment.

The flow meters were metric type rotameters, two of which were suitable for small air flows and two for large air flows. With this arrangement, it was possible to meter air flows corresponding to linear reactor velocities between 0.01m/s to 4.0m/s. The flow to each meter was finely controlled by a needle valve; this also enabled the meter to be operated under pressure if so desired in order to increase the range and to reduce the float oscillation. Additional error in the reading of the rotameter was estimated to be (+/-)2.0%. All the air flows quoted are, therefore, accurate to within (+/-)2.5%. The vessel was constructed of clear perspex pipe with 138mm inner and 150mm outer diameter; thus giving a 6mm thick wall.

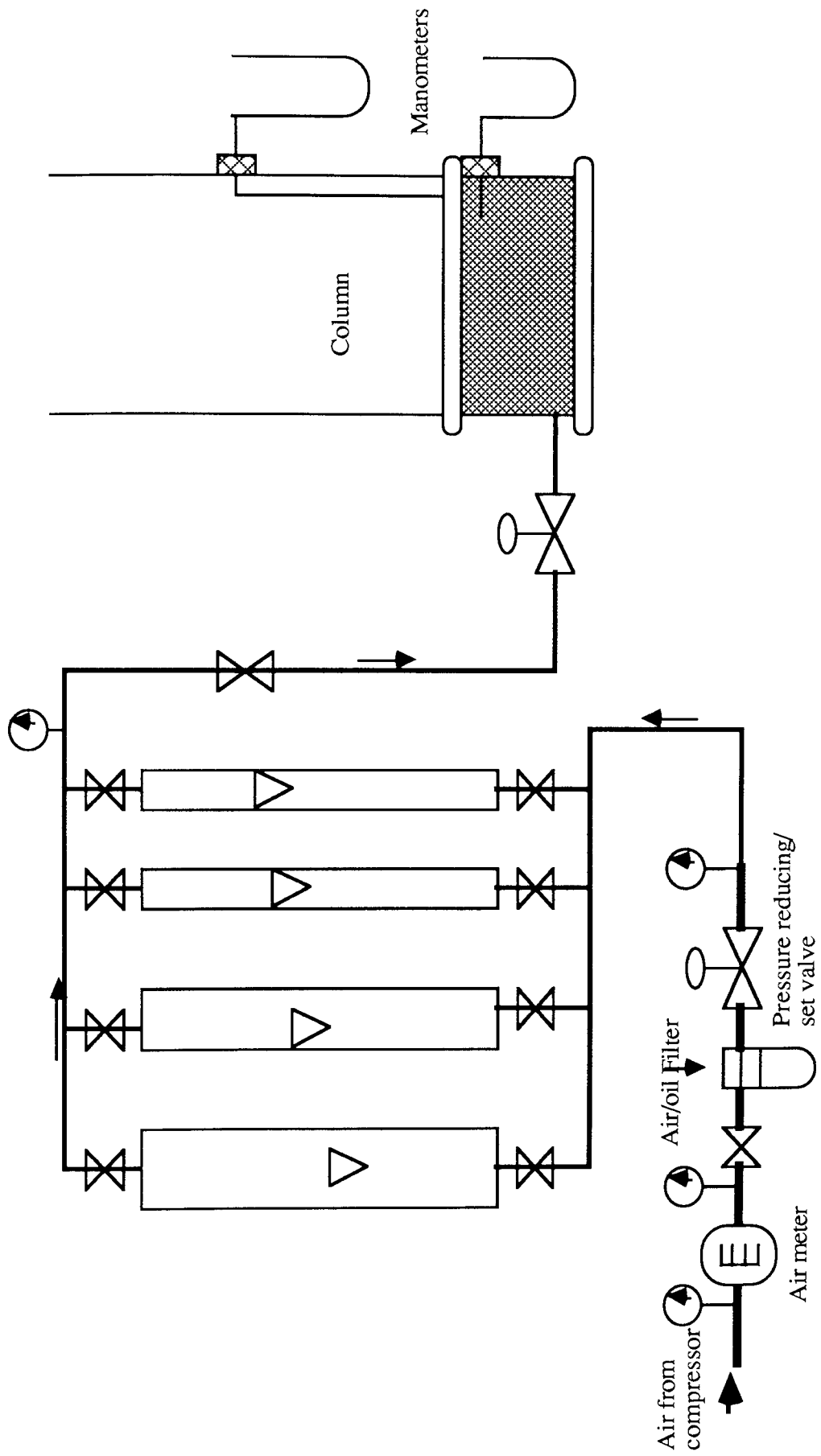


Figure 3.1: Schematic arrangement of the experimental apparatus

Water manometers were connected with pressure taps at various axial positions below and above the distributor. In addition, an adjustable pressure probe was used to measure pressures at arbitrary levels in the bed. This pressure probe was inserted from the column wall above the surface of the bed while the sensing element could be located anywhere in the bed. The sensing side of the probe had an opening of 1.6mm and a piece of 325mesh stainless steel was placed at its open end in order to prevent its blockage by fine particles. Details of the pressure probe are shown in Figure 3.2. A photograph of the column and pressure probe is shown in Figure 3.3.

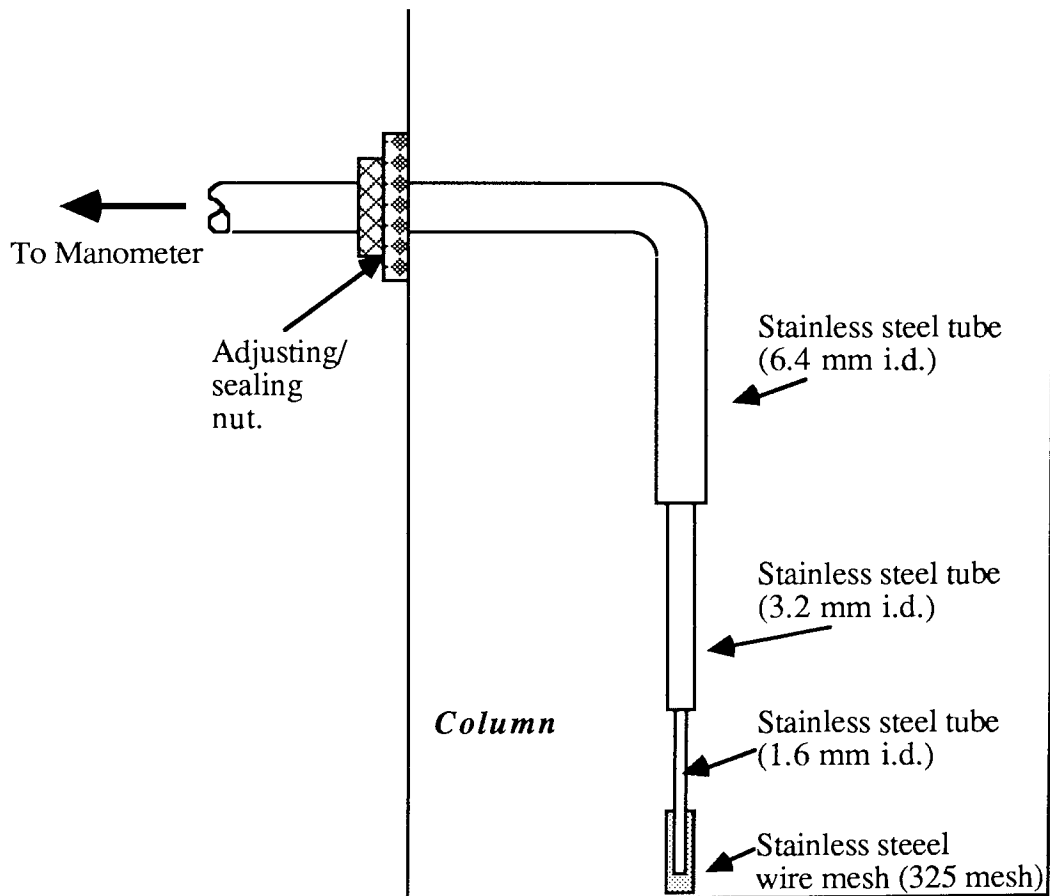


Fig.3.2: Adjustable pressure probe for measuring pressure at arbitrary radial positions in the fluidised bed.

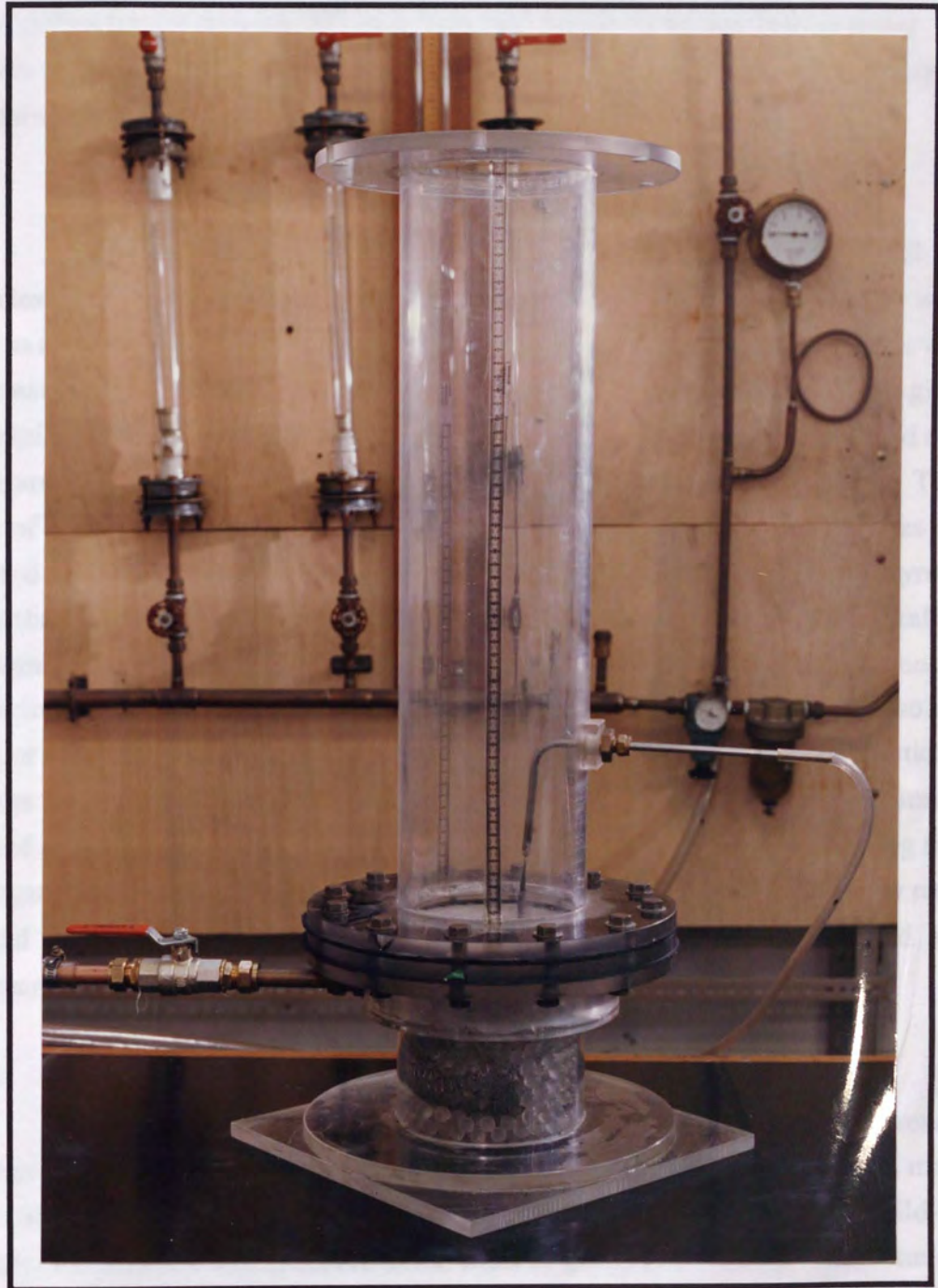


Fig.3.3: Photograph of the Column and Pressure Probe used.

The plenum chamber of the bed was also constructed from clear perspex and packed with knitmesh packing and large ballotini particles. The air was supplied by a 15mm diameter copper pipe which entered the chamber from the upper end and then turned through 90° to deliver the air just above the bottom end of the plenum chamber: in this way, the air passed through the packing in the chamber, thus minimising the effects of pressure fluctuation and flow irregularities.

3.2 *The Solids*

Particular attention was given to the selection of solids so that all the particles were well within the Geldart class 'D'. Spherical and cylindrical solids were used to assess the effect of particle shape. The effect of the density difference was demonstrated by selecting particles manufactured from polystyrene and glass ballotini. White spherical polystyrene particles of various size ranges were used and these are referred to as *Polybeads* followed by the mean particle diameter. Two sizes of cylindrical particles were used. Red cylindrical polystyrene particles are referred to as *Polycylinders* and black cylindrical particles from the polystyrene masterbatch, are referred to as *ABS Cylinders*. Glass ballotini particles are called *Ballotini* followed by their mean particle size. A great deal of time was spent in preparing particles of narrow size band; this was achieved by screening the solids three or four times. A slight difference in density between the polystyrene particles and the masterbatch compound was noticed but as this difference was quite small, both of these particles were regarded as equal density particles. In the mixing and segregation experiments, the size ratio ranged from 1.7 to 4.0 while the density ratio ranged from 1.0 to 2.6. The physical properties of the solids studied are summarised in Table 3.1.

3.3 *Electrostatic Effects*

It was anticipated that the perspex pipe and solids would readily retain electrostatic charge. Preliminary experiments indicated that this was the case, most noticeably at moderate to high velocities. The main evidence for charge build-up was that the particles would adhere to the walls or group into clusters. One solution to the problem that was investigated was to humidify the inlet air by spraying a small stream of water into the inlet lines. This certainly reduced the static charge but the process was difficult to control and frequently resulted in a film of water forming on the particles. This water film in turn altered particle behaviour due to surface tension effects.

Table 3.1: Physical properties of the experimental solids

Solids	Particle		Minimum Fluidising Velocity (m / s)
	Shape	Size (μm)	
Polybeads 1850	Spherical	1700 - 2000	0.58
Polybeads 1550	Spherical	1400 - 1700	0.46
Polybeads 1090	Spherical	1000 - 1180	0.31
Polybeads 925	Spherical	850 - 1000	0.25
Ballotini 1090	Spherical	1000 - 1180	0.63
Ballotini 550	Spherical	500 - 600	0.29
ABS Cylinder	Cylindrical	Dia. : 2400	
		Len.: 3000	0.72
Red Polycylinder	Cylindrical	Dia. : 750	
		Len.: 3000	0.34

An anti-static spray supplied by RS Components Limited was then tried. The spray was applied to both the solids and the column walls and proved to be extremely effective in eliminating electrostatic charges. The anti-static effect was noticeably reduced after 2/3 runs. However, this proved to be no problem and the column walls were thoroughly sprayed and air dried before every run. This frequent and generous use of spray on the walls not only eliminated the static charge but also eliminated the need to spray the solid after 2/3 runs.

3.4 The Sampling Procedure

Rowe et al (1972), Nienow et al (1978), Geldart (1981) and Cooke et al (1982) have all developed a sampling technique based on vacuum removal of sequential layers from a slumped bed. This method of sampling was employed throughout the author's work to assess the axial solids concentration profiles. Whilst the radial concentration profiles were not measured quantitatively, visual observations were always recorded.

It was found that maintaining an arbitrary but constant sample size over the entire bed could lead to confusion in the data analysis, particularly where there were rapidly changing gradients. Therefore, smaller sized samples were taken in sections of the bed which obviously had high concentration gradients. Usually 14 to 18 samples were collected from each bed. The vacuum sampler is illustrated in Figure 3.4.

This device consisted of a 6 mm i.d. stainless steel, graduated sampling tube which was fitted with an adjustable boss: this was used to determine the exact depth of the sample in the bed. In the case of samples thicker than 0.5 cm, the sampling probe was lowered gradually in small steps to avoid disturbance of the remaining bed. The samples were passed into a cyclone which separated the solids from air; solids were then collected in a 'sample collecting vessel'. Various vacuum sources were tried and it was found that a vacuum cleaner was best suited for the purpose.

3.5 Sample Analysis

The bed samples were analysed mainly by screening using 'Endicott' hand sieves. After separation, each component was weighed and the composition, based on weight and volume fractions, was calculated.

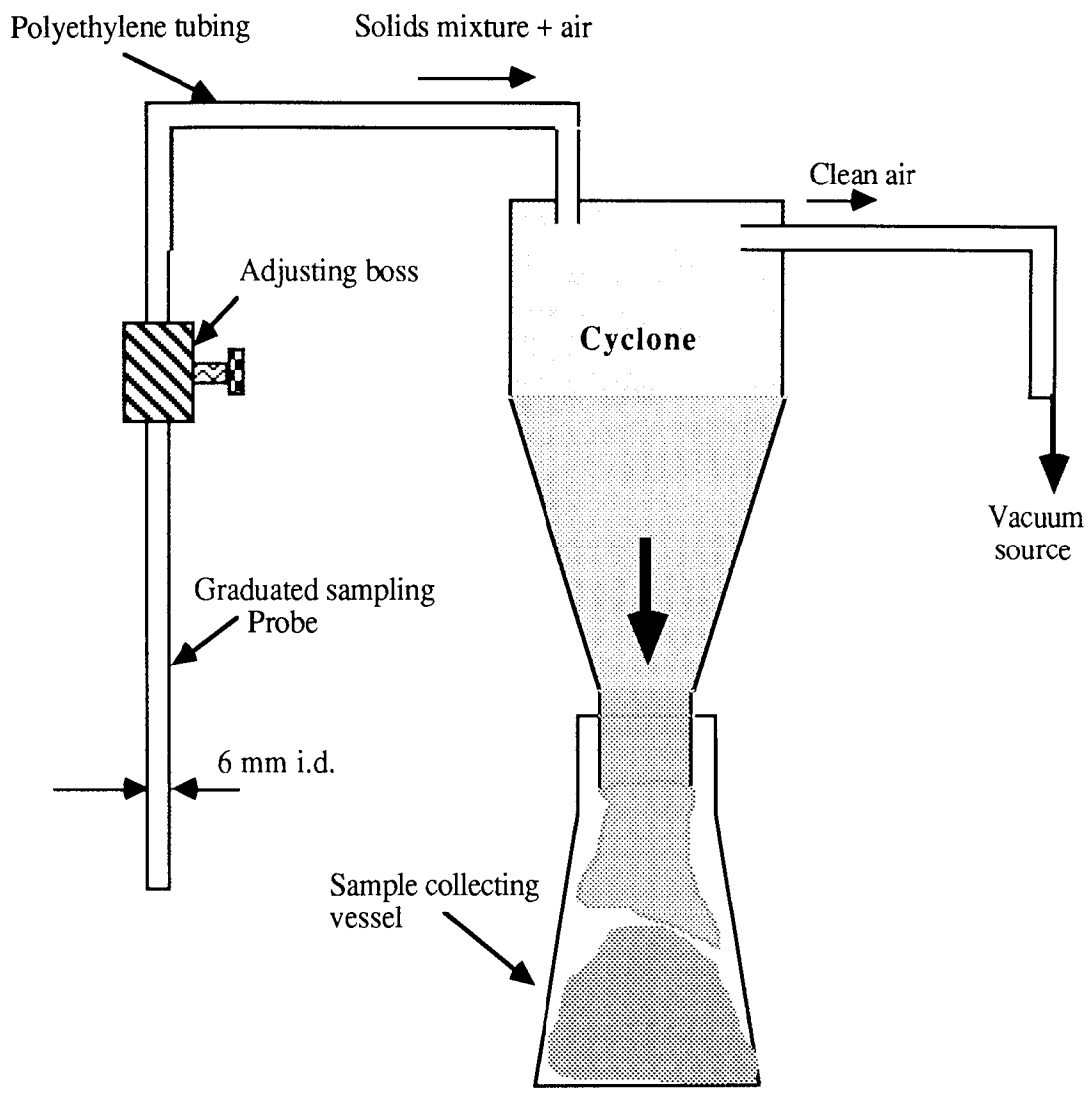


Fig.3.4 : Vacuum sampling device used to remove samples from the slumped bed.

3.6 *Mixing Index (MI)*

The mixing index correlation developed by Daw (1985) was used as an indicator of the degree of mixing/segregation. This provided a convenient means of quantifying the effect of parameter changes on mixing/segregation. The mixing index used was:

$$MI = \left[\sum_{n=i} V_{si} (v_{Ji} - \bar{v}_J)^2 \right] / \{ \bar{v}_J \cdot (1 - \bar{v}_J) \} \quad (3.1)$$

for perfect mixing $MI = 0.00$

for complete segregation $MI = 1.00$

where

i = index referring to each sample

n = total number of samples taken

v_{si} = the volume fraction of the total bed contained in sample i

v_{Ji} = the volume fraction of Jetsam in sample i

\bar{v}_J = the total volume fraction of jetsam in the bed

This mixing index was mainly used to compare rather than assess the effect of distributor design on the particle mixing/segregation.

CHAPTER 4

FLUIDISED BED - EXPERIMENTAL RESULTS

4.1. Measurement of the Minimum Fluidising Velocity - Procedure

The experiments to determine the minimum fluidising velocity were carried out in the 138 mm i.d. perspex bed described in Chapter 3. The bed was fitted with a bronze porous distributor plate and the fluidising air was metered by various rotameters forming part of the air rig, as shown in Figure 3.1. The total bed pressure drop was measured by a 1.6 mm i.d. tube placed in the bed directly above the distributor plate.

Initially, the minimum fluidising velocity of each component to be studied was measured followed by the minimum fluidising velocity of the binary mixture. For single components the solids were fluidised for 3 to 4 minutes at a relatively high air flow rate before conducting the experiments; the bed pressure drop was noted as the air flow was steadily decreased. The second set of results was obtained while slowly increasing the air flow rate until the solids were violently fluidising.

For binary mixtures, each system was tested using two defluidisation procedures to assess U_{CQ} , the composite minimum fluidising velocity corresponding to fast defluidisation and U_{CS} , composite defluidisation velocity obtained by slow defluidisation. In both cases the bed was fluidised at a superficial air velocity of $U_o > 2.U_{mfj}$ for approximately 5 minutes. The two composite fluidising velocities were measured following the procedure shown in Figure 4.1.

The method was adapted from the work of Cheung (1976). For the slow defluidisation valves, U_{CS} , the air flow rate was reduced steadily to 0 over a period of approximately 20 minutes (well above the time needed for the bed to reach its maximum segregation) while noting ΔP_{bed} . For the fast defluidisation value, U_{CQ} , the air supply was abruptly cut off after the initial fluidisation, and then starting from $U_o = 0$ the superficial air velocity was increased slowly while measuring the pressure drop ΔP_{bed} . From the plots of ΔP_{bed} vs U_o , both U_{CQ} and U_{CS} were found.

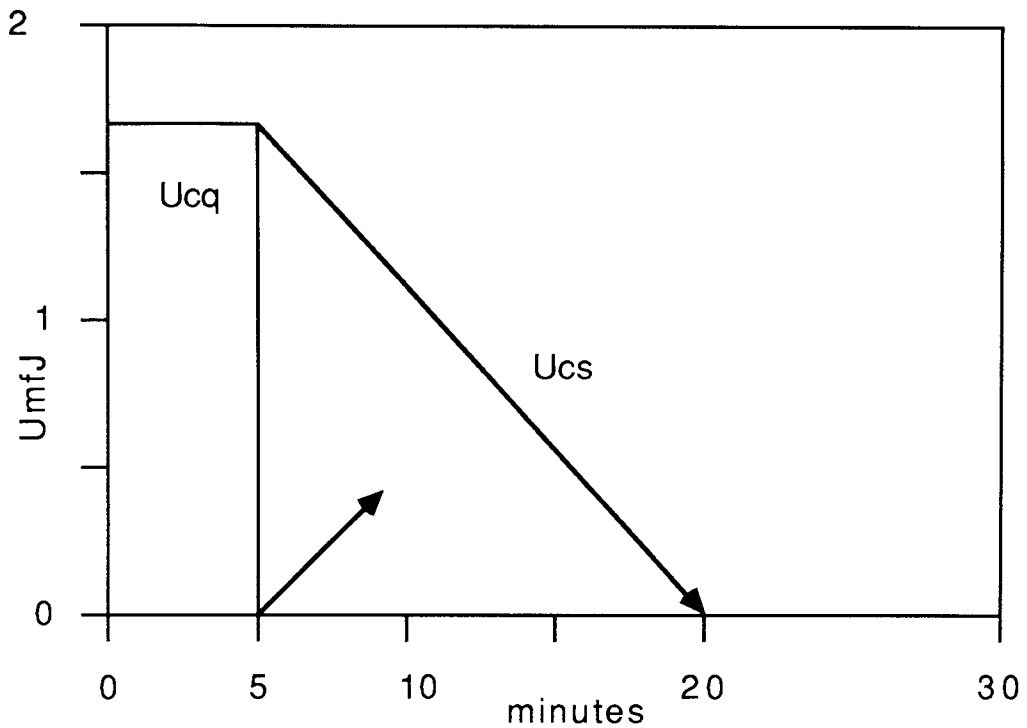


Fig.4.1: The Two Defluidisation Procedures (adapted from Cheung, 1976)

Minimum Fluidising Velocity - Experimental Results

The minimum fluidising velocity was obtained by plotting ΔP_{bed} vs air velocity and then establishing the point of incipient fluidisation. A typical plot for U_{mf} Polybeads 1550 is shown in Figure 4.2, giving two slightly different minimum fluidising velocities with increasing and decreasing air flow rates. The average of these two values is taken to be the minimum fluidising velocity of the solid. The minimum fluidisation curve for a binary system (Polybeads 1550 / Olive green Polybeads 925 90% / 10%) is illustrated in Figure 4.3. The two U_{mf} curves for the same system were taken following the procedure shown in Figure 4.1; two slightly different U_{mf} values were recorded. The composite minimum fluidising velocities for all the mixtures under consideration were calculated and are shown in Table 4.1.

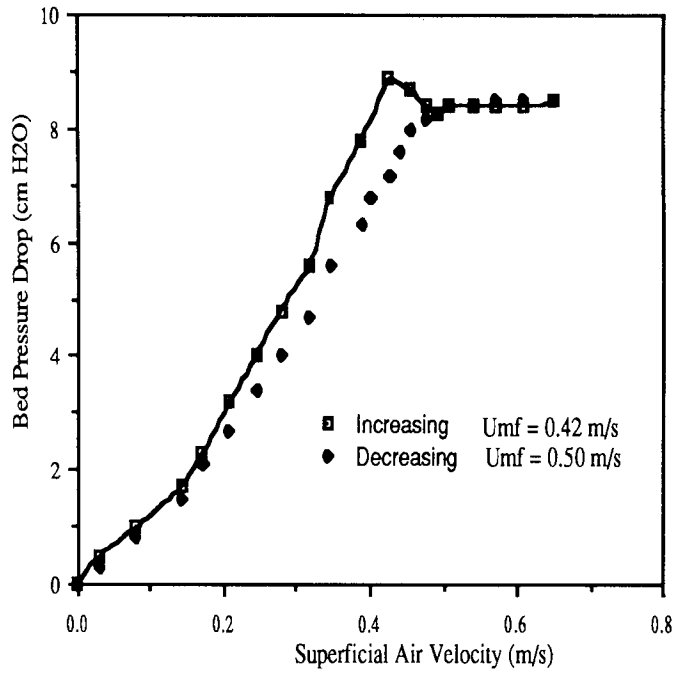


Fig.4.2: *Umf* curve - Polybeads 1550 (Size range: 1.40 -1.70 mm)

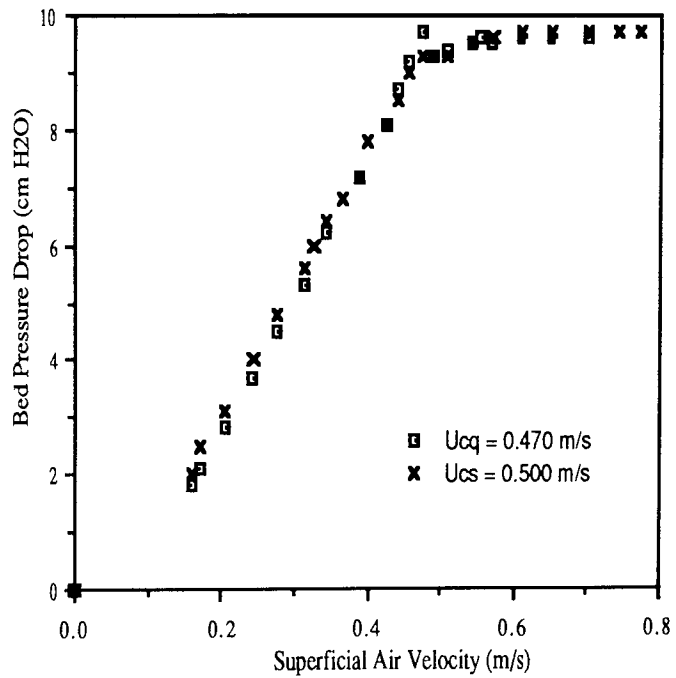


Fig.4.3: *Umf* curve - Polybeads 1550 / Olive green Polybeads 925 (90% / 10% w/w)

Table 4.1: Summary of the minimum fluidising velocities - for the binary systems used

Solids	System d μm	wt. %	Measured m/s		$\frac{U_{cq}}{U_{cs}}$	Average U_c (m/s)
			U_{cq}	U_{cs}		
Polybeads	1090	90				
ABS Cylinder	2400	10	0.35	0.39	0.90	0.37
Ballotini	550	80				
Ballotini	1090	20	0.35	0.37	0.95	0.36
Polybeads	1850	80				
Ballotini	1090	20	0.62	0.72	0.89	0.67
Poly-cylinder	750	90				
ABS cylinder	2400	10	0.40	0.48	0.83	0.44
Polybeads	925	10				
Polybeads	1550	90	0.46	0.50	0.94	0.48

4.2. The Procedure for Mixing/Segregation Experiments

All the mixing/segregation data were collected under steady state conditions. The steady state experiments for binary systems were always preceded by exploratory runs to determine the rapidity with which the steady state was reached. This usually consisted of repeated measurements of the top composition of the bed as a function of time.

In all experiments, the air flow was always adjusted so that the same experimental conditions were achieved. It was found that the time required to reach steady state was usually less than 5 minutes. Therefore, in all cases, the bed was operated for 10 minutes before sampling.

Almost all steady state experiments were carried out with one of two initial conditions- segregated or well mixed. In the former case the solids were carefully placed on the bed in layers, usually with flotsam on the bottom, although some experiments were carried out with flotsam on the top. In the latter case, a well mixed bed was created either by fluidising the column at much high superficial velocities or by dividing the solids into 10 equal, well mixed portions and then placing them very carefully, one at a time, in the bed.

Different types of fluidisation behaviour were observed depending upon the superficial gas velocity. When the superficial gas velocity was between the minimum fluidisation velocity of the two components, the bed usually separated into two distinct layers- a fluidised, flotsam-rich upper layer and an unfluidised, jetsam lower layer. However, when the superficial gas velocity was above the minimum fluidising velocity of the jetsam, visually there was no proof of any formation of an unfluidised layer. Daw (1985) noticed these regions and referred to them as Region 1 segregation, where $u_{mfF} < u_o < u_{mfJ}$, and Region 2 segregation, where $u_o > u_{mfJ}$.

4.3. Distributor Plates

The design of the gas distributors has been shown to affect both the physical and chemical performance of a fluidised bed (Whitehead and Dent 1967; Geldart. and Kelsey 1968; Qureshi and Creasy 1979). The distributor has a strong influence on the size and frequency of the bubbles in a fluidised bed. This, in turn, affects directly the performance of the fluidised bed.

One of the most important requirements of an effective gas distributor is that it must ensure uniform gas distribution throughout the bed. Maldistribution or channelling of flow will lead to excessive gas bypassing in parts of the bed and poor gas-solid contacting in other parts. The ratio of the pressure drop cross the distributor to that across the bed has frequently been used as an approximate design criterion to ensure even gas distribution through the bed.

There are many types of distributor. Of these, the perforated plate is the most common and simplest type of distributor. The holes are drilled directly in the plate supporting the bed material. The holes can be either straight, divergent or convergent. Zenz (1968) suggests that upward diverging holes will help eliminate

dead zones. The size and configuration of these holes can be varied for specific applications. In the author's study, three perforated plates having different hole configuration and size were used.

Another relatively new distributor, but popular especially in the combustion industry, is the standpipe distributor. This is simpler to fabricate and similar in performance to a perforated plate. A diagram of this type of distributor is shown in Appendix 1; pipes are welded on to the perforated plate and sealed at the top and generally four holes are drilled near the top end. These holes are some distance away from the surface of the distributor, thus providing a stagnant layer of solid on top of the distributor which can act as a heat insulator. In the author's work a modified version of the standpipe distributor was constructed by reducing the length of the pipe so that the holes were very near to the distributor surface: this eliminated the stagnant layer near the distributor due to the standpipe length which could give misleading results in solid segregation work. The dimensions of the standpipe used are also given in Appendix 1.

Another distributor which is regularly used in universities and research laboratories is the porous plate. This type is too expensive and too brittle for industrial use. In the author's research, a porous plate was used to obtain comparative data. The plate was 3 mm thick and constructed from bronze particles and supplied by Accumatic Engineering Ltd, Wrexham, North Wales: as Grade 'Fine D', retaining all particles $> 30\text{-}40\ \mu\text{m}$. Details of the various distributors are given in Table 4.2.

All the perforated and standpipe distributors were constructed from 13mm thick sheets of clear perspex. Each plate was carefully marked and drilled to achieve the exact configuration. To prevent the weeping of particles and blockage of the orifices, all the perforated plates were covered with 325 mesh stainless steel screen. The standpipe and porous distributors were used without covering. The pressure drop across the different distributors was also measured and the characteristic curves are presented in Figure 4.4.

The effect of the different distributor plates on the minimum fluidising velocities was also investigated. It was expected that the value of U_{CS} would be affected by the distributor. However, it was found that the different types of

distributor had no significant influence on the minimum fluidising velocities (U_{CS} and U_{CQ}) for a given system. Photographs of the five distributors used are given in Figure 4.5.

Table:4.2. The Distributor Plates (Bed Diameter = 138 mm)

Plate	Porous	Standpipe	Perforated	
			2	3
Pitch (cm) PD		3	2	1.4
Hole dia. (mm)		1	1	2.4
No. of holes		19 standpipes, each with 4 holes	37	57
Free Area (%)		0.4	0.19	1.7

All the perforated plates used had a triangular pitch.

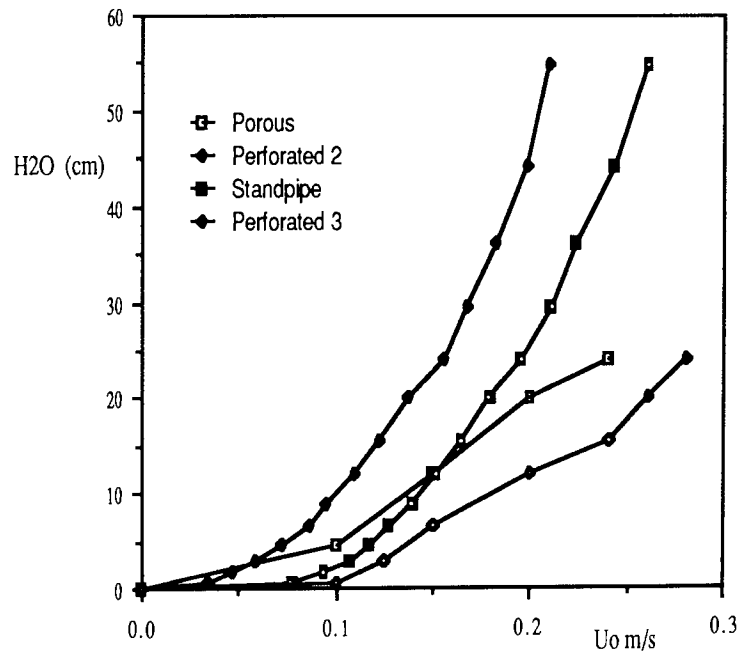


Fig.4.4: Pressure drop across the various distributors used



Fig. 4.5: Photograph showing the distributors used in the fluidised bed systems

4.4. Review of the Experimental Programme

The objective of the work was to study the effect of the distributor on the solids concentration profile. Obviously there are a number of other parameters which influence the concentration profile e.g. particle size ratio, particle density ratio, initial starting condition, aspect ratio, shape factor and superficial gas velocity. As there is only a limited amount of published work on the effect of distributor design on solids segregation in gas fluidised beds, experiments were performed with binary mixtures.

Experiments were conducted with a range of solid binary and tertiary mixtures but only the work carried out with five binary mixtures is reported here - four were flotsam-rich and one jetsam-rich. These were selected to cover a spectrum of experimental parameters and physical characteristics. In all experiments starting from the segregated mode, the minor component was neatly placed on top of the major component. Generally the superficial velocity was 15 to 20% greater than the minimum fluidisation velocity of the mixture. Details of the mixtures used and their physical characteristics are given in Table 4.3. The selection of two systems, no. 3 and 4, possibly needs further explanation.

The binary System no.3 (Ballotini 1090 / Polybeads 1850) was selected to study the combined effect of the solid density and size variation. The Ballotini particles were only 60% of the size of the Polybeads but these were 2.5 times denser than the polybeads. The governing factor was the similarities in minimum fluidising velocity of these two solids.

The System 4 (ABS Cylinders / Polycylinders) was chosen to highlight the special problems associated with the mixing/segregation of cylindrical particles. The density ratio was kept close to unity.

4.5. Experimental Results

4.5.1. The ABS- Polybeads System

This is an equi-density, flotsam-rich system having particles of different size and shape. The flotsam was spherical and the jetsam was cylindrical in shape. The equivalent mean diameter ratio was 3.9. The overall jetsam weight fraction was kept constant at 10% and the static bed height at 21.6 cm. The experiments were carried out with all four distributors.

Table 4.3. Mixtures Used

Systems	Solids	d (μm)	ρ_s (kg/m^3)	U_{mf} (m/s)	wt. %	U_c (m/s)	Shape
1	Polybeads	1090	1000	0.31	90	0.37	Spherical
	ABS Cylinder	2400	1050	0.86	10		Cylindrical
2	Ballotini	550	2950	0.30	80	0.36	Spherical
	Ballotini	1090	2950	0.80	20		Spherical
3	Polybeads	1850	1000	0.64	80	0.67	Spherical
	Ballotini	1090	2450	0.69	20		Spherical
4	Polycylinder	750	1000	0.34	90	0.44	Cylindrical
	ABS Cylinder	2400	1050	0.86	10		Cylindrical
5	Polybeads	1550	1000	0.50	90	0.48	Spherical
	Polybeads	925	1000	0.25	10		Spherical

System nos. 1, 2, 3 and 4 were *flotsam rich* and no.5 was *jetsam rich*.

Effect of the Distributor Design

Figure 4.6 illustrates some typical concentration profiles for this system using four different distributors. All the experiments were carried out from the initial segregated mode and at a superficial air velocity of 0.46 m/s. In all cases, the bed was gently bubbling with little solid entrainment. The solids visually appeared to be well mixed without significant radial concentration. This was subsequently confirmed on sectioning the bed which showed that the radial jetsam concentration was fairly uniform throughout the bed. Examination of the profiles shows that the standpipe distributor was somewhat better than any other plate, followed closely by perforated distributor 2, especially when compared with the performance of the porous plate distributor.

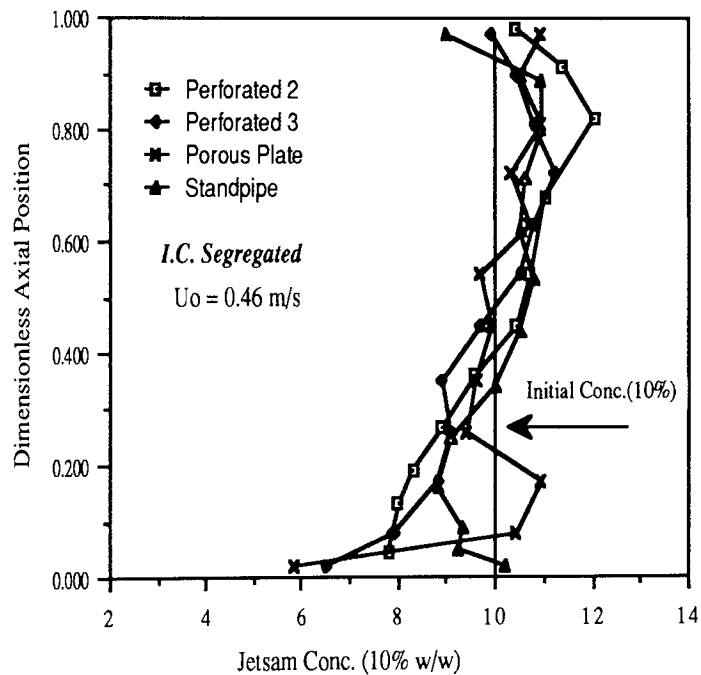


Fig.4.6: *Effect of four distributors on the concentration profile*

The concentration profiles obtained with the same four distributors but with a different initial condition, i.e. from the well mixed mode, are shown in Figure 4.7. Once again the standpipe and perforated plate 2 distributors performed better than the others with perforated plate 3 following closely the same pattern. The perforated plate 2 led to a lower jetsam concentration near the surface, although there was no evidence of violent bubbling / entrainment. These observations are in line

with the findings of Naimer (1985) who has attributed these to two possible mechanisms, i.e.

- 1) the high local linear velocity which has a greater tendency to set stagnant particles into motion
- 2) the discrete apertures which create larger initial bubbles that can pick up larger amounts of jetsam from the bottom of the bed.

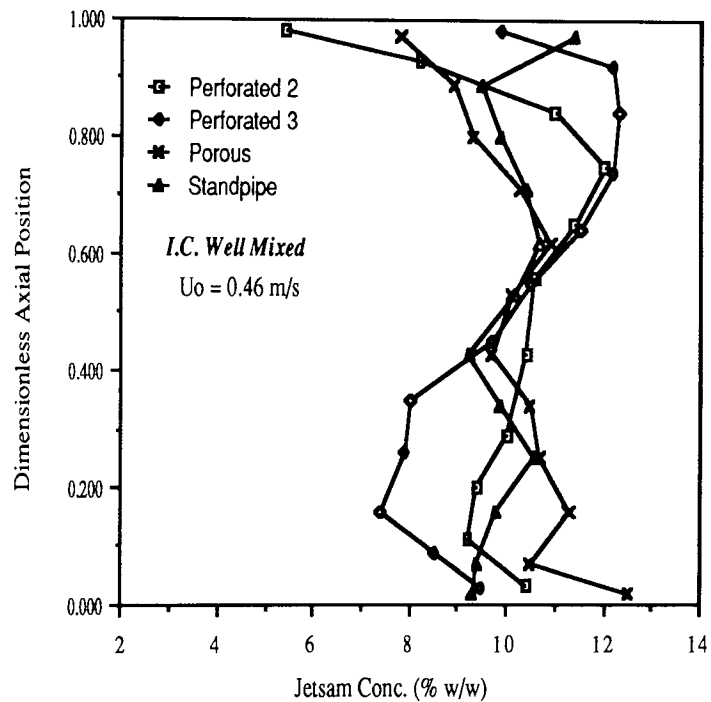


Fig.4.7: Effect of four distributors design on the conc. profiles

Effect of the Initial Condition

The effect of the initial condition (i.e. how the solids were placed in the fluidising bed) was investigated using perforated distributors nos.2 and 3. The experiments were carried out with completely segregated solids and with well mixed solids. The concentration profiles thus obtained are shown in Figures 4.8a and 4.8b respectively.

For distributor no.2, both the concentration profiles follow a similar

pattern but having different jetsam concentration in each layer. Interestingly the crossing point from high to low concentration in the well mixed case and vice versa in the segregated case lies in the middle of the bed. In the case of the well mixed bed, the jetsam concentration reduces sharply from the middle to the top of the bed; becoming < 5% on the surface. One reason for this lean mixture could be attributed to the entrainment and elutriation, but most importantly it tells us about the solid movement. Initially all the jetsam particles are equally distributed in the bed; after the experiment most of the jetsam is shifted towards the bottom creating a more segregated bed.

In the case of the segregated start, all the jetsam particles are placed on the top and after the experiment these jetsam particles are rather more uniformly distributed in the bed. The entrainment and elutriation effects are far less in this case, containing nearly average (i.e.10%) of jetsam on the surface.

The effect of the initial condition with perforated plate 3 shows a somewhat different picture especially at the surface, where the jetsam concentration is the same. However, slightly below the surface the two curves behave differently giving a jetsam concentration difference of nearly 2%, which again diminishes at the middle of the bed and then switches over. In the lower half of the bed, the jetsam concentration in both cases is less than the initial concentration (i.e. 10%). Once again near the distributor the curves switch over giving a jetsam concentration of nearly 6% with the 'segregated mode'.

Effect of the Superficial Velocity

The effect of varying the superficial velocity on the segregation profiles was investigated using perforated distributor no.2 and the standpipe distributor, as shown in Figures 4.9 and 4.10 respectively. Figure 4.9 illustrates the changes in the profiles when U_0 was varied from 0.34 m/s to 0.52 m/s, while the column was fitted with perforated plate no.2; the solids were well mixed before experimenting.

Figure 4.9 shows that the profiles generally follow the same pattern. The bed becomes relatively more segregated at the two ends when U_0 is increased from 0.34 m/s to 0.44 m/s.

Now, on further increasing U_0 to 0.52 m/s, the bed is approaching well

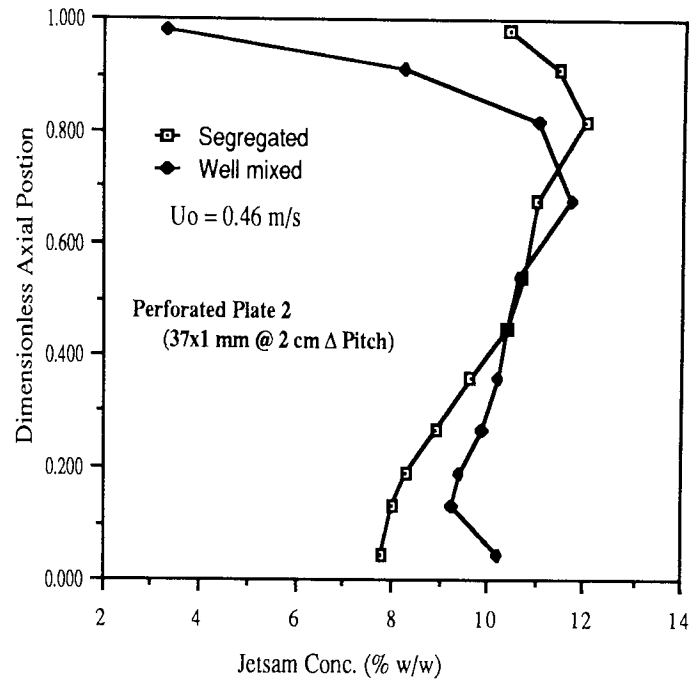


Fig.4.8a: Effect of the Initial Condition

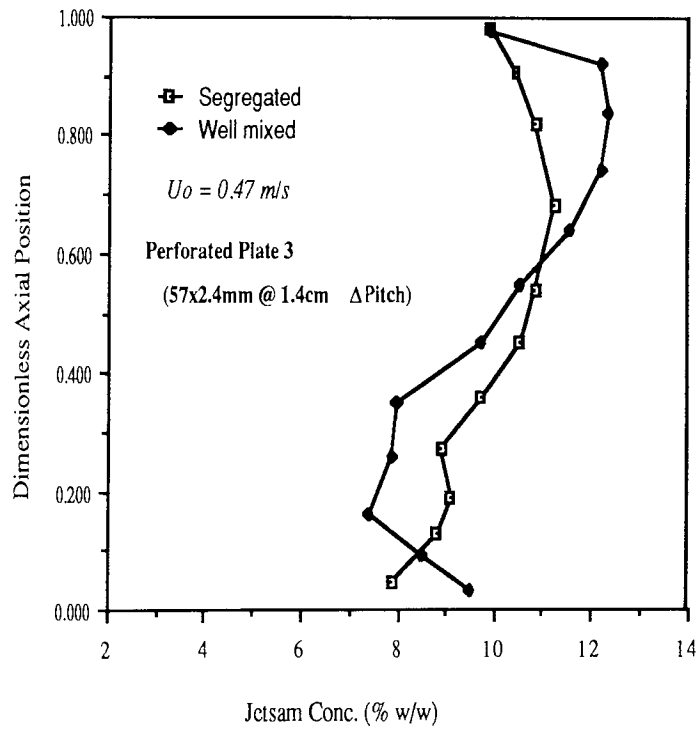


Fig.4.8b: Effect of the Initial Condition on conc. profile

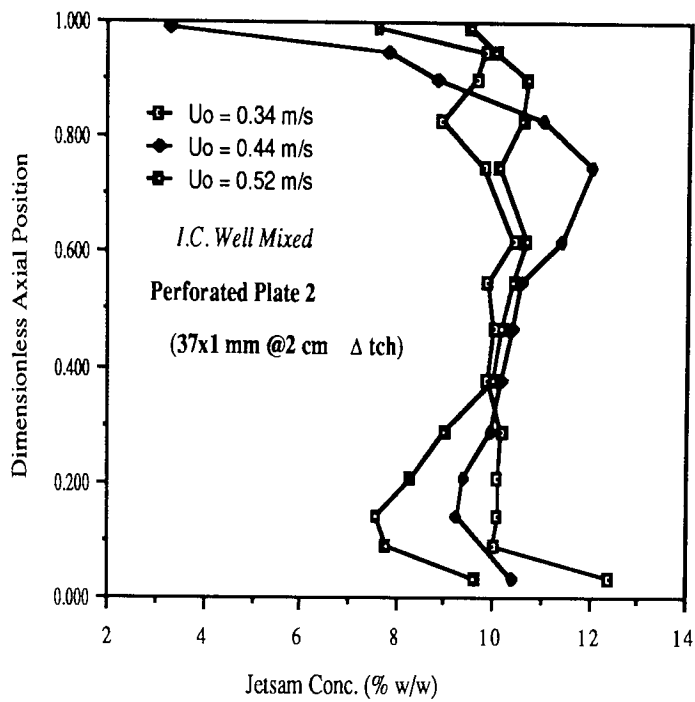


Fig.4.9: Effect of U_o on the concentration profile

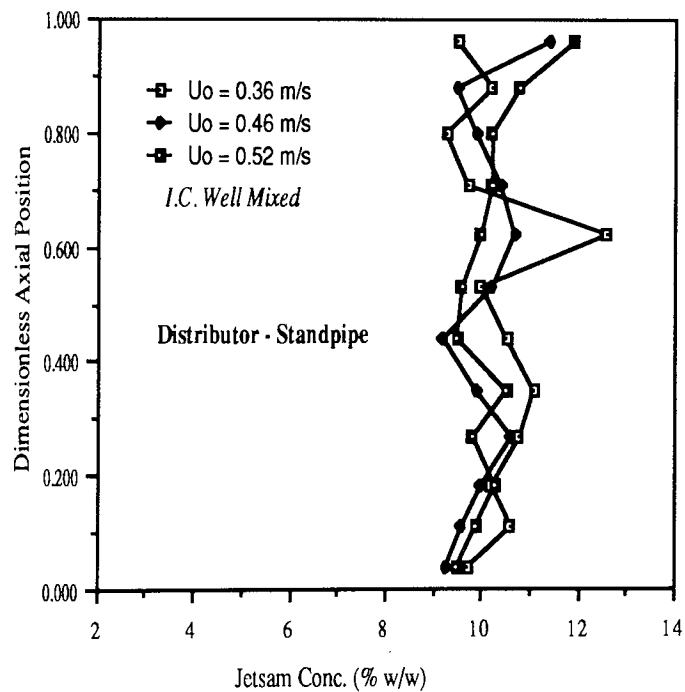


Fig.4.10: Effect of U_o on the concentration profile

mixed except near the distributor where the jetsam concentration is less than average. The effect of the changes in superficial velocity were more pronounced with the standpipe distributor when U_O was increased from 0.34 m/s to 0.52 m/s, starting from well mixed solids. The jetsam concentration was quite erratic when the bed was fluidised at 0.34 m/s. This behaviour seemed to be damped down a little when U_O was increased to 0.44 m/s. A further increase in the superficial velocity tended to create a more uniform concentration profile except at the ends. This contrasts with the observations made with other distributors when the entrainment of flotsam dominates the top layer.

Rowe et al (1972) have established that particle movement in a fluidised bed is solely caused by bubbles. One could therefore attribute the difference in the concentration profile obtained with different distributors solely to the bubble growth. The difference in the concentration profiles shown in Figures 4.9 and 4.10 illustrates two different bubble growth rates associated with their respective distributors. Bubble growth rate/size offered by the standpipe type distributor appears to be more suited for mixing systems of the ABS Cylinder / Polybeads type.

4.5.2. The Ballotini 1090 / Ballotini 1550 System

This is a flotsam-rich system containing equidensity spherical particles with a size ratio of 2:1. The bed consisted of 80% of the flotsam particles ($d_p = 500-600 \mu\text{m}$) and 20% of the brown jetsam particles ($d_p = 1000-1180 \mu\text{m}$). The static bed height was kept constant at 14.3 cm.

Effect of the Distributor Design

Figure 4.11 illustrates the concentration profiles for this system obtained with four distributors. Experiments were conducted from an initial well mixed mode at a superficial velocity of 0.48 m/s. The superficial air velocity was $\approx 30\%$ greater than the minimum fluidisation velocity of the mixture. The bed was gently fluidising without any excessive particle entrainment. The radial distribution of the jetsam was fairly uniform.

The two distributors which clearly performed above the rest were the standpipe distributor and perforated distributor no. 2; careful examination of these two profiles further reveals that the perforated distributor no. 2 has performed even better than the standpipe distributor. This is in contrast with observations

experienced with System 1, where the standpipe type distributor has performed better than the perforated distributor 2.

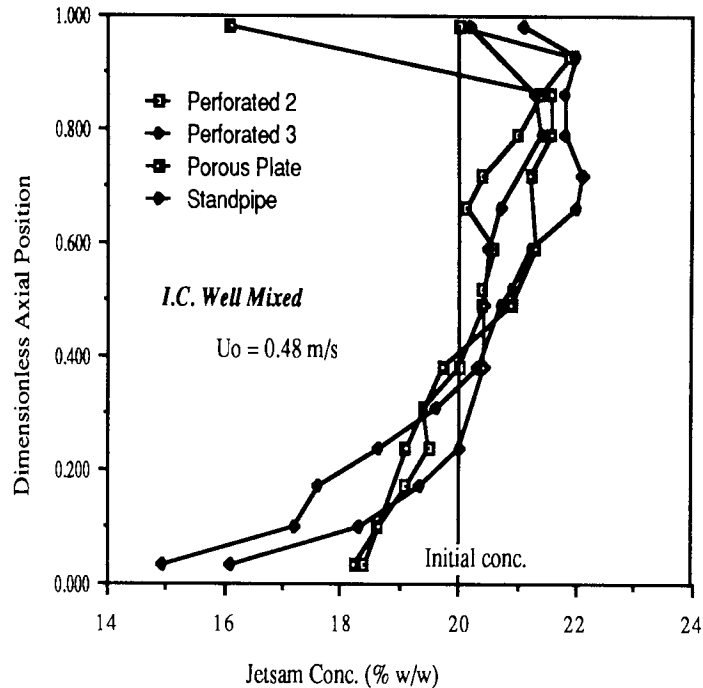


Fig.4.11: Concentration profiles obtained with four distributors

Perforated distributor no.3, containing a number of relatively big orifices, caused segregation especially in the lower half of the bed, whereas the porous plate distributor exhibited poor performance particularly in the top layers. Once again the results showed that distributors producing a number of small bubbles, like the porous plate, and ones producing a number of large bubbles, like perforated distributor no. 3, exhibit poor performance in their own way.

Effect of the Initial Condition

The effect of the initial condition on the concentration profiles is illustrated in Figure 4.12. Both these profiles were obtained with perforated distributor no. 2, starting with well mixed and completely segregated mixtures. The superficial velocity was 0.48 m/s, which is well above the u_{mf} of the flotsam but less than the u_{mf} of the jetsam. This velocity produced a nicely bubbling bed.

The figure shows that both the profiles are similar in shape. The indication

is that the initial condition has no effect on the pattern of the concentration profile and only a slight effect on the concentration of any solids.

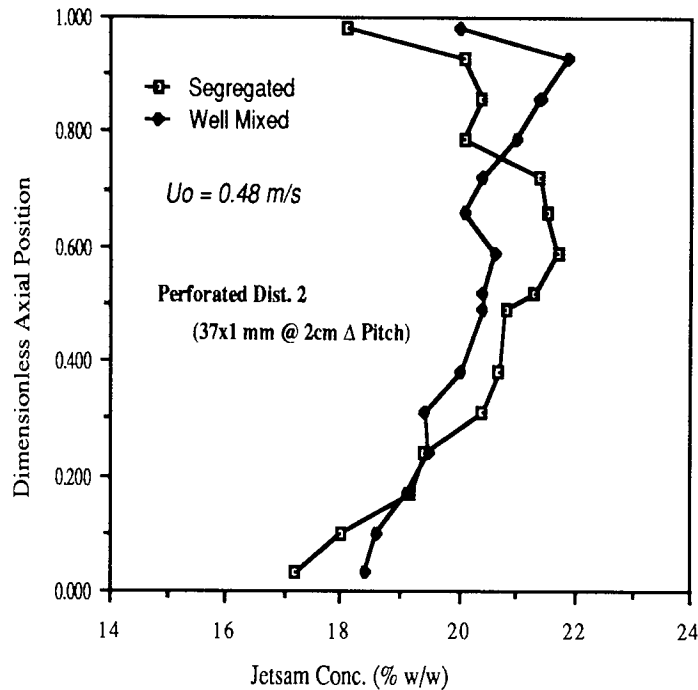


Fig.4.12: Effect of the initial condition (Ballotini550 / Ballotini1090)

4.5.3. The Ballotini 1090 / Polybeads 1850 System

This is a binary system containing spherical particles of dissimilar size and density. The role of jetsam was played by the yellow, soda glass ballotini particles having a size range of 1.00-1.18 mm and that of flotsam by the white polybeads having a size range of 1.7-2.0 mm, giving a size difference ratio of 1.7. The density ratio was 2.95. The overall jetsam concentration was 20% w/w. Both these solids have similar minimum fluidising velocities i.e. 0.64 m/s for polybeads1850 and 0.69 m/s for ballotini1090.

Effect of the Distributor Design

The effect of the distributor design was studied with three distributors namely, perforated plate no.2, standpipe and porous plate distributors. All the experiments were conducted from the 'well mixed' mode. The experiments were conducted at a superficial air velocity of 0.79 m/s, which $\approx 18\%$ greater than the mixture's fluidisation velocity. The bed was gently bubbling but it was observed that most of the air was escaping without being transformed into bubbles, thus

increasing the porosity. The concentration profiles are shown in Figure 4.13.

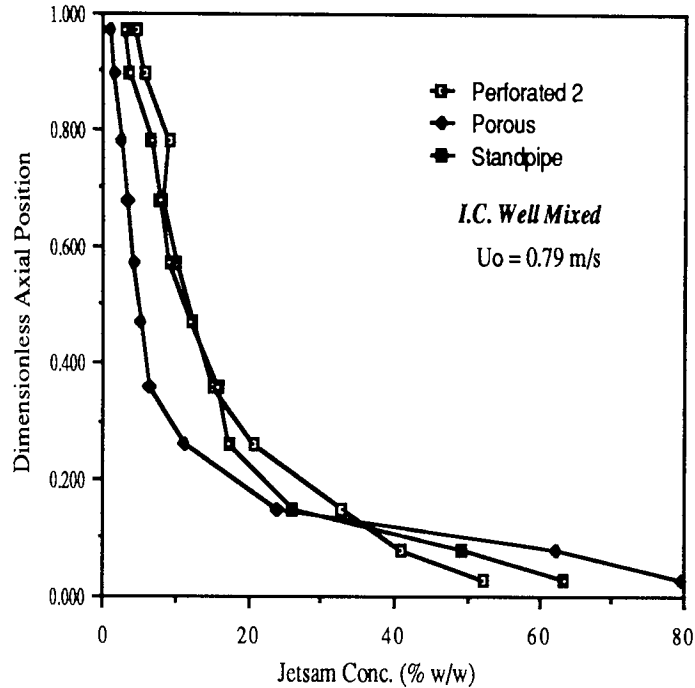


Fig.4.13: Concentration profile with three distributors (Ballotini1090 / Polybeads1850)

The profile due to the porous plate shows that most of the ballotini were transferred to the bottom suggesting that the small bubbles produced by the porous plate were unable to carry the heavy particles to the top. The profiles due to the other two distributors, namely perforated plate no.2 and the standpipe distributor are very similar to each other and are somewhat better than that for the porous plate: the jetsam concentration at the distributor is $\approx 53\%$ and $\approx 63\%$ respectively compared with $\approx 80\%$ with the porous plate distributor.

Effect of the Superficial Air Velocity

A series of experiments was carried out using the porous plate distributor to ascertain the effect of the superficial air velocity when starting from the fully mixed state. The static height of the bed was constant in all the experiments. The particles were initially mixed at high superficial velocity in the fluidising column to obtain a well mixed system; the bed was sectioned and analysed and found to be completely mixed. The experiments were carried out at six different superficial velocities

starting from 0.5 m/s and finishing at 1.4 m/s.

It was observed that at a superficial velocity < 0.5 m/s, there was no movement of the particles and, therefore, segregation did not take place. However, when the superficial velocity was increased to 0.5 m/s, a gentle particle movement was noticed allowing the heavier particles to travel down. This was further confirmed upon sectioning the bed, a larger portion of the jetsam lying on the distributor. This is contrary to the findings of Cheung et al (1978) and Naimer (1982), who reported that segregation takes place even at a low superficial velocity.

Figure 4.14 shows the concentration profiles obtained at three superficial velocities- 0.5, 0.68 and 0.79 m/s. For $U_o = 0.5$ m/s, there was slight segregation near the distributor and at the surface, but when U_o was increased to 0.68 m/s, the mixture was virtually totally segregated and nearly all the jetsam particles were gathered near the distributor. A similar profile was obtained when U_o was increased to 0.79m/s, indicating the maximum segregation that can be achieved at these superficial air velocities.

Three further profiles obtained at the superficial air velocities of 1.0, 1.2 and 1.4 m/s are shown in Figure 4.15. These confirm the initial finding that as U_o is increased beyond 0.79 m/s, the segregation of the mixture was decreasing and solids were approaching the well mixed state. All three profiles are very similar; the mixing improved when the superficial air velocity was increased from 1.0 m/s to 1.2 m/s but no improvement was observed with further increase from 1.2 to 1.4 m/s. In all three cases, a small quantity of jetsam stayed at the bottom illustrating that a superficial velocity higher than twice the minimum fluidising velocity of the mixture was required to achieve a totally mixed bed.

It was interesting to find that by gradually increasing U_o , a profile similar to the one obtained at 0.5 m/s was established. This is clearly shown in Figure 4.16, which compares the profiles obtained at two superficial velocities, i.e. $U_o = 0.5$ m/s and 1.4 m/s respectively. These two velocities can be described as U_{TO} , 'take over velocity', where the mixing mechanism takes over from the segregation mechanism and vice versa. Cheung et al (1978) have studied this in greater detail.

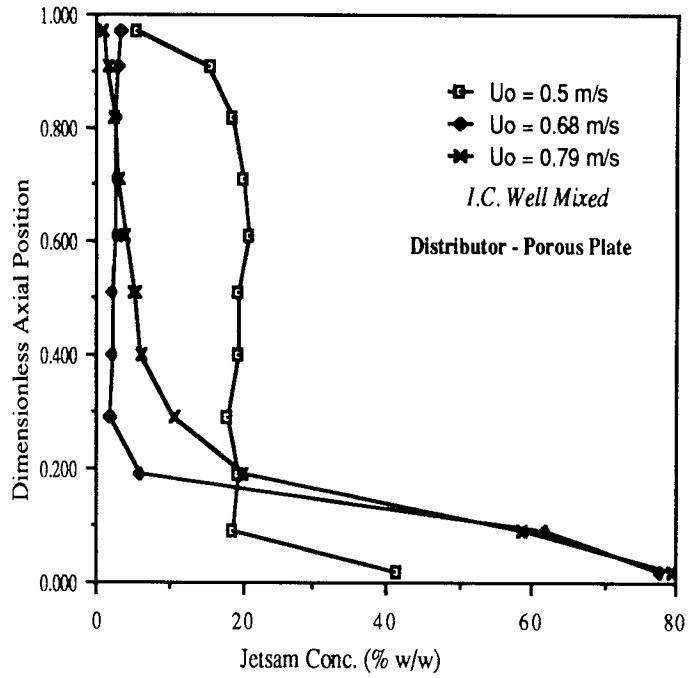


Fig.4.14: Effect of U_o on the concentration profile

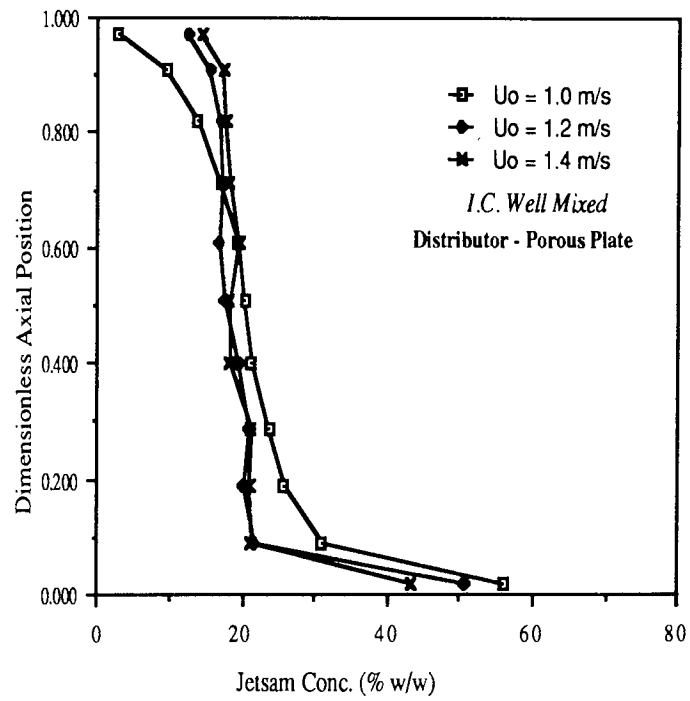


Fig.4.15: Effect of U_o on the concentration profiles

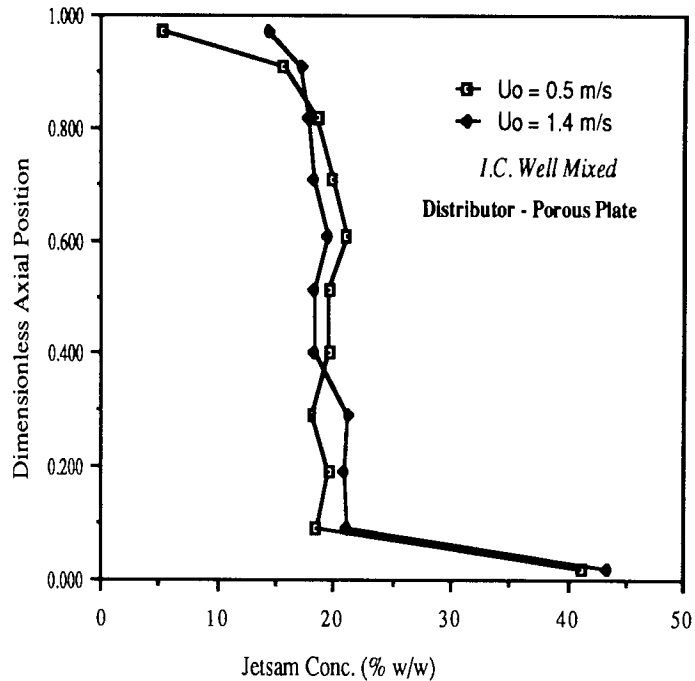


Fig.4.16: Similarity in concentration profiles at two different U_o values

Effect of the Aspect Ratio (R_a)

Three experiments were carried out to study the effect of the bed aspect ratio. Again the porous plate distributor was used. All the experiments were carried out at a fixed superficial air velocity of 0.87 m/s starting with an initially well mixed bed. A superficial air velocity of 0.79 m/s gave almost complete segregation; therefore, a slightly higher air velocity was selected. The aspect ratios investigated were 0.8, 1.1 and 2.75 respectively. Figure 4.17 illustrates the concentration profiles obtained for these three experiments.

The weight percentage jetsam concentration was plotted against the axial position. The effect of the aspect ratio is obvious. The work clearly shows that with higher aspect ratio, segregation is far less and the particles stay uniformly mixed in the main body of the bed except at the two ends. This shows that the effect of distributor design is less noticeable with deeper beds. The present work illustrates that the selection of the aspect ratio to nullify the effect of the distributor design is dependant on the particle physical characteristics. A deeper bed with aspect ratio of 2.5 or even higher may be required for more segregating type mixtures.

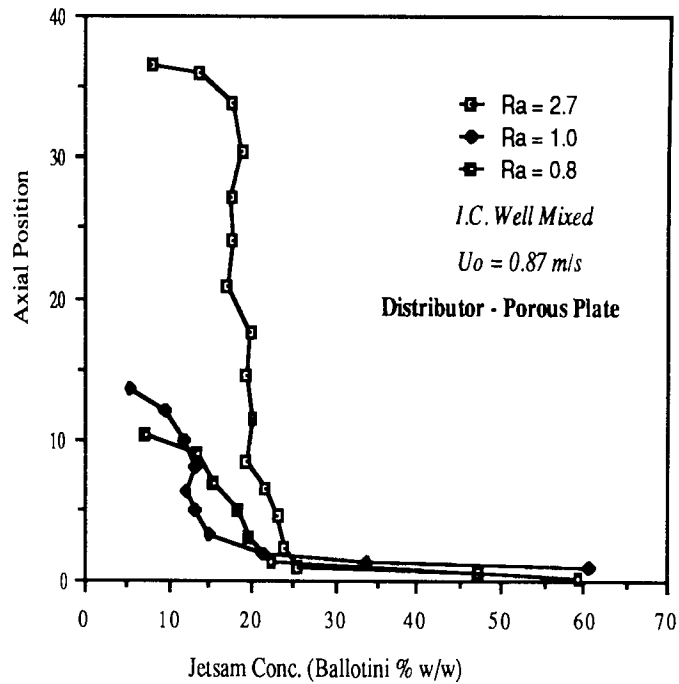


Fig.4.17: Effect of the Aspect Ratio on the concentration profiles

4.5.4. The ABS Cylinders / Polycylinders System

This is an equidensity non-spherical binary system containing cylindrical particles of similar length but of different diameter. The Polycylinders, which were 3 mm long and 0.75 mm in diameter, played the role of flotsam occupying 90% of the bed, while the ABS Cylinders, which were 3 mm long and 2.4 mm in diameter, performed as jetsam. The comparison with these two cylindrical particles was made in the form of "the equivalent mean spherical diameter" and this shows that the ABS Cylinders are 2.3 times larger than the Polycylinders. The static bed height was maintained at 18.5 cm while the jetsam was always placed on the top.

Effect of the Distributor Design

The concentration profiles obtained with five distributors are shown in Figure 4.18. The worst concentration profile was obtained with perforated distributor no. 3, while the standpipe distributor followed closely behind. This is an interesting observation because in all the other solids systems investigated, the standpipe distributor performed well. Once again the best performance was obtained from distributor no.2 having 37x1 mm holes at 2 cm triangular pitch. The porous distributor and perforated distributor no. 1 performed identically, as was expected. These experiments clearly show that the effect of the distributor design

on the mixing and segregation phenomena is more pronounced in the case of non spherical particles.

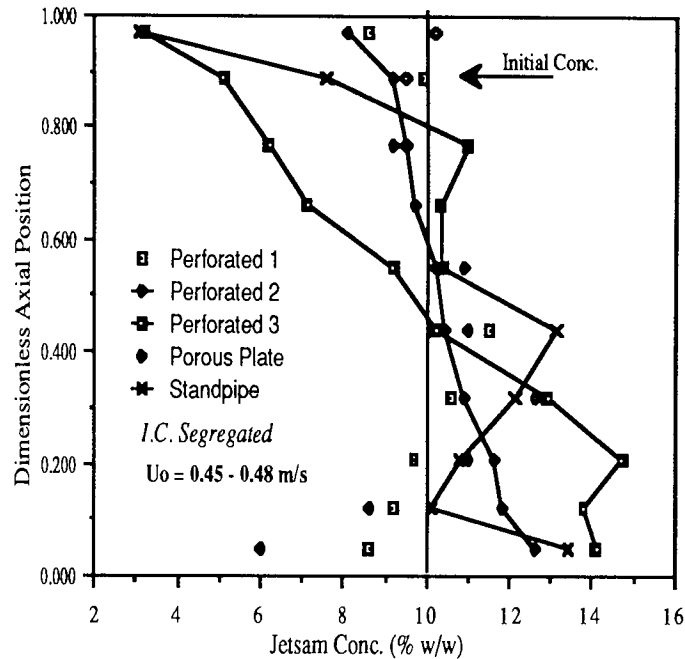


Fig.4.18: Concentration profiles with five distributors.

Effect of the Superficial Velocity.

In order to examine the effect of the superficial air velocity on the segregation pattern, the distributor giving the worst performance i.e. perforated distributor no. 3, was selected and the superficial velocity was initially increased from 0.47 m/s to 0.54 m/s, while all the other conditions were kept constant. The concentration profiles thus obtained are shown in Figure 4.19, illustrating that a slight increase in the superficial gas velocity has worsened the mixing performance, producing two regions- an upper region containing a very small percentage of the jetsam and a lower region containing a high percentage of the jetsam. It was anticipated that a near uniform mixture could only be obtained with a superficial velocity approaching close to the u_{mf} of the jetsam. This, again shows the important effect of distributor design when handling non spherical particles.

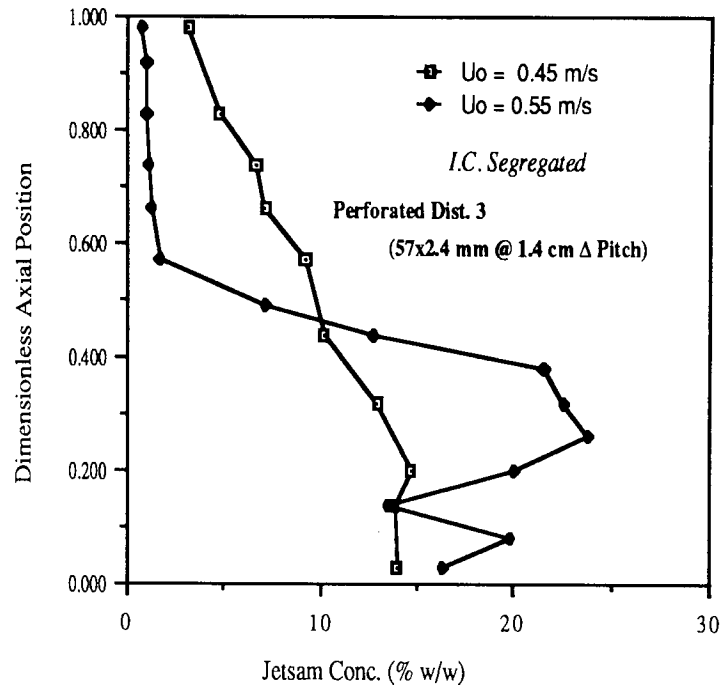


Fig.4.19: Effect of U_o on the concentration profile

Effect of the Initial Condition

Perforated plate distributor no.2 was used to highlight the effect of the initial condition on the concentration profile. Two experiments were carried out- one with the segregated initial condition and the other with the well mixed system. Both these experiments were conducted at an air superficial velocity of 0.48 m/s. The bed achieved steady state within 2 minutes of start-up regardless of the initial condition, but the experiments were conducted for ten minutes. The concentration profiles thus obtained are shown in Figure 4.20. The profiles are similar in both cases, although with the well mixed start the jetsam concentration in the upper half of the bed gradually decreased towards the surface: this highlights the fact that the entrainment and elutriation effects are more pronounced with the well mixed start. It is anticipated that, if the segregated mode experiment were carried out with jetsam sandwiched in the middle of flotsam bed, the final concentration profile would follow the well mixed profile even more closely.

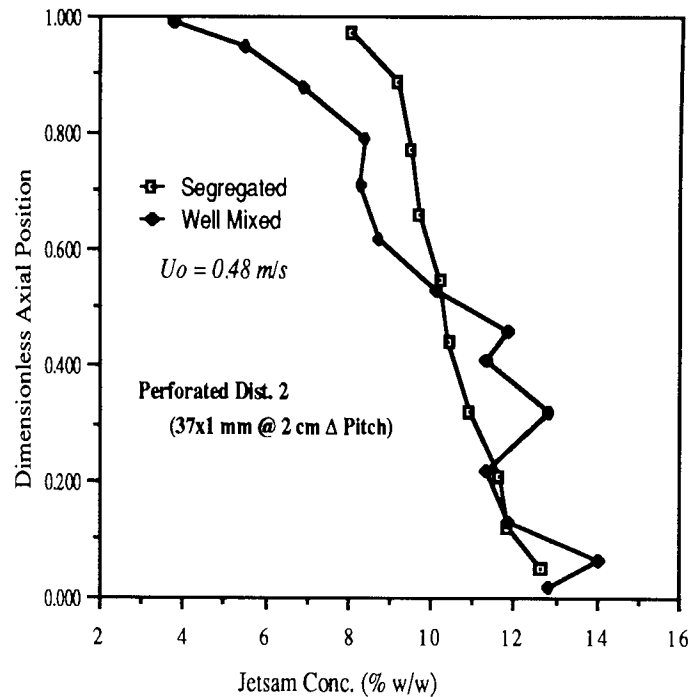


Fig.4.20: Effect of the initial condition on the concentration profile

4.5.5. The Polybeads1550 / Polybeads925 System

This is an equi-density jetsam rich system containing 90% of jetsam, Polybeads 1550 ($d_p = 1.4-1.7$ mm) and 10% of flotsam, Polybeads ($d_p = 850-1000\mu\text{m}$). The particle size ratio was 1.68. The static height of the bed was kept constant at 22.6 cm, while flotsam was always placed at the top.

Effect of the Distributor Design

Figure 4.21 illustrates the concentration profiles of this system using five distributors. All experiments were carried out from the initial segregated mode and at a superficial velocity of 0.58 m/s. Examination of these profiles shows that the perforated distributor no. 2 and the standpipe distributor performed in a similar way to each other and were marginally better than the other distributors. The porous plate seems to exhibit the worst performance with a kink in jetsam concentration of 85.7% just above the distributor.

The perforated distributor no. 3, containing 57x2.4mm holes at 1.4 cm triangular pitch, performed extremely well except in the top layer, where the elutriation and entrainment effects seemed to outweigh the mixing mechanism. This

illustrates that creating a number of larger initial bubbles achieved better mixing and has decreased the dead space volume at the bottom of the bed. However, this introduces a new feature to the complex mixing mechanisms in the form of excessive flotsam entrainment.

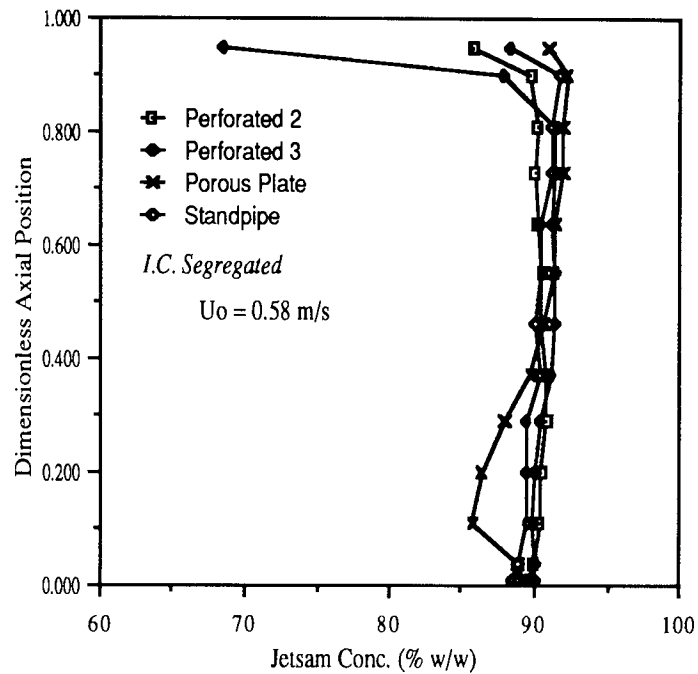


Fig.4.21: Effect of distributor design on the concentration profiles

Effect of the Superficial Air Velocity

The effect of varying the superficial air velocity on the segregation was investigated with only one distributor, namely perforated plate no.2. All the experiments were carried out from the segregation mode with the flotsam lying on top of jetsam. The superficial air velocity was slowly increased while observing the state of the bed. It was noted the bed stayed in a packed state until $U_0 = 0.29\text{m/s}$; and at this velocity the flotsam (olive green polybeads) showed some movement. A further increase in the velocity initiated fluidisation of these flotsam particles independently from the white jetsam particles: the jetsam appeared to act as an extended distributor. This situation continued until $U_0 = 0.40\text{m/s}$ when a few white jetsam particles started moving into the flotsam region. A further increase to 0.48m/s showed some noticeable changes and a record of this was made. Figure 4.22

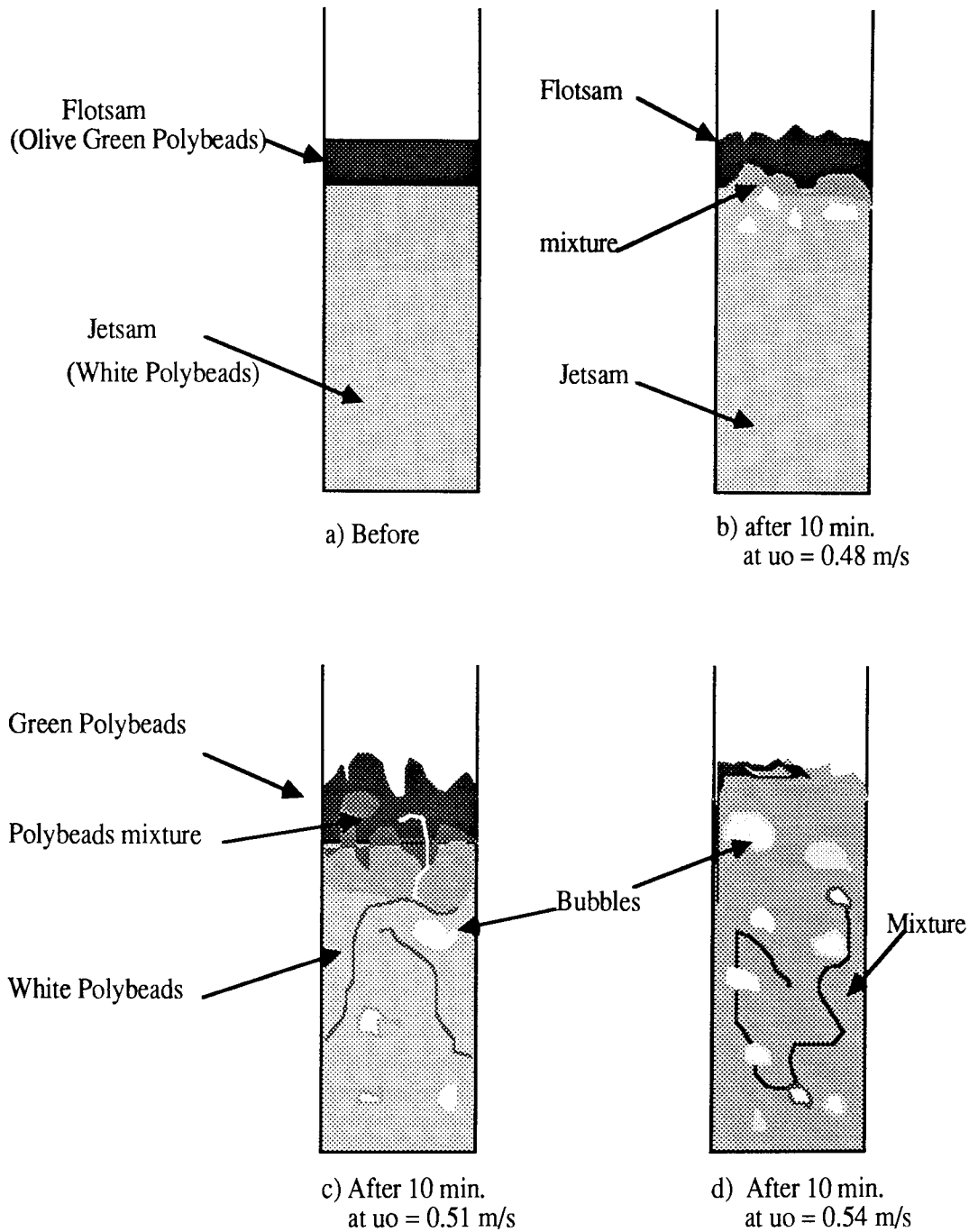


Fig.4.22: Physical appearance of the bed as observed at different velocities.

shows the physical appearance of this system as recorded after conducting the experiments at different superficial velocities. Figure 4.22a shows the positions of the particles before conducting any experiments. Figure 4.22b shows the changes in particles state after operating for 10 minutes at $U_o = 0.48\text{m/s}$. The velocity was then further increased to 0.51 m/s ; although only a very small increment in the velocity, it catalysed a great deal of jetsam movement. On further increasing the velocity to 0.54 m/s the bed completely fluidised with only a very small portion of jetsam staying at the top.

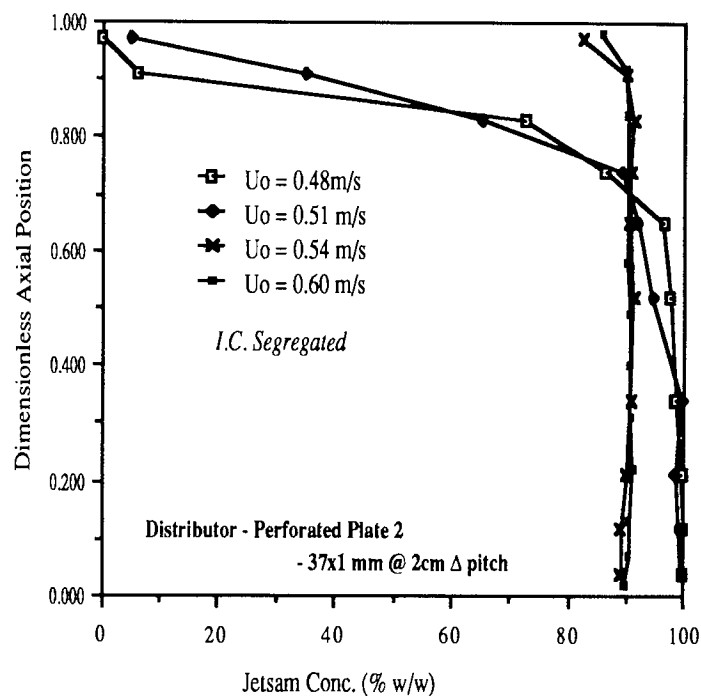


Fig.4.23: Effect of the superficial air velocity on conc. profiles

The velocity was further increased to 0.58 m/s when it was completely fluidising without any stagnant flotsam layer at the top. The beds were sectioned after each run, as previously described, to ascertain the jetsam concentration throughout the bed and these concentration profiles are shown in Figure 4.23. It can be seen that the bed remained in a segregated state until the superficial velocity was higher than the minimum fluidisation velocity of the mixture. The two profiles obtained at 0.54 m/s and at 0.58 m/s exhibit little difference giving a well mixed bed except at the top where, once again, the entrainment and elutriation effects are significant.

Effect of the Initial Condition

This effect was investigated with perforated plate no.2 (37x1mm). The experiments were conducted from two initial conditions i.e. segregated and well mixed. In both cases the superficial velocity was 0.58 m/s and the static bed height was kept constant at 22.5 cm. The concentration profiles thus obtained are shown in Figure 4.24, illustrating the strong influence of the initial flotsam position on the final solids concentration profile. A well mixed bed containing uniformly distributed flotsam particles was obtained when starting with the segregated mode. However, when starting with the well mixed mode, the flotsam particles tended to segregate and were concentrated mainly near the surface. 84% of the flotsam was present in the top 1 cm slice of the bed; the second and third 1 cm slice contained 77% and 28% respectively but only 3.3% flotsam was present near the distributor. The general appearance of the bed was similar in both cases; both beds behaved in the bubbling mode with little or no splashing. However, in the case of the well mixed start, the bed started segregating from the very start of the experiment with a substantial portion of the flotsam staying near the surface of the bed.

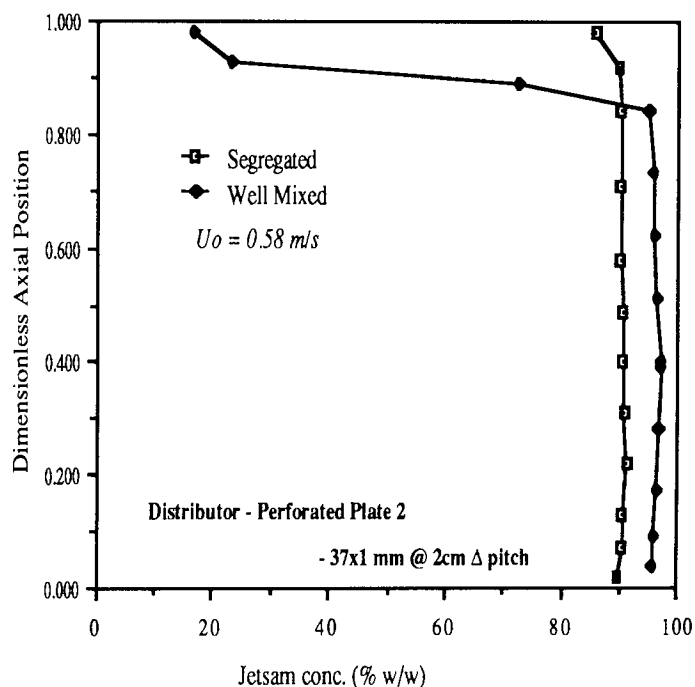


Fig.4.24: Effect of the initial condition on conc. profile

CHAPTER 5

DISCUSSION, CONCLUSIONS AND RECOMMENDATIONS

5.1 Discussion

The effect of the distributor design on the concentration profile is well illustrated in the preceding chapter with the results obtained from five sets of binary mixtures using four distributor plates. As it is well established that particle movement in a fluidised bed is solely caused by bubbles and these are initiated by a small jet according to Zenz (1968); the formation of these jets and bubbles was visually observed from the column wall and a brief account of this is given below:

Generally a similar transition from jet-to-bubble gas flow was observed from the column wall with perforated plates and with all the mixtures containing a large proportion of spherical particles. This is shown diagrammatically in Figure 5.1. The length of these jets varied between 1 to 3 cm and then these jets were converted into bubbles. Figure 5.2 illustrates the formation of bubbles as observed with the porous plate - no formation of jet at the distributor surface was observed. However, the author believes that very small jets were formed with the porous plate which were quickly converted into bubbles and were, therefore, invisible from the column wall. The length of these jets was considerably increased with mixtures containing a large proportion of cylindrical particles and jets of up to 6 -7 cm height were noticed.

In the case of the standpipe four horizontal jets were visible from beneath the plate. These jets extended a small distance horizontally and then bent upwards and were converted into bubbles. This is shown diagrammatically in Figure 5.3. Naimer (1982) has found that the bubble generated from each jet of a given standpipe immediately coalesces with bubbles rising from the other jets of the same standpipe before continuing upward. The author found no evidence of this mechanism as the coalescence of bubbles was extremely unclear visually.

The performance of these distributors was analysed and compared by calculating the Mixing Indices of the concentration profiles. These Mixing Indices were calculated using Daw's (1985) Mixing Index formula as described in section 3.6 and are tabulated in Table 5.1. Although some of the indices are quite small, they nevertheless provide a good comparison for different distributors.

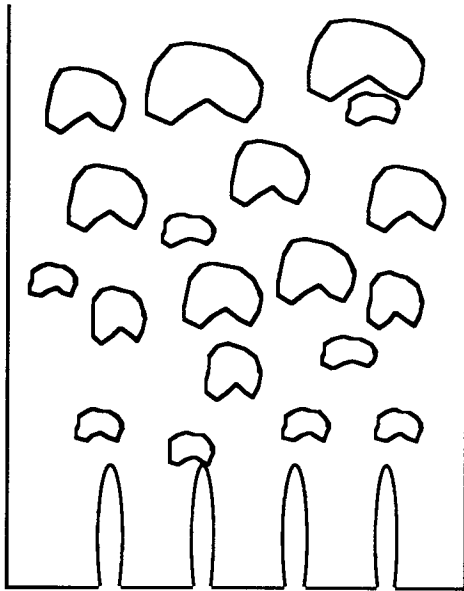


Fig. 5.1: Transition from Jet-to-Bubble as visible at the Bed Wall using Perforated Plates.

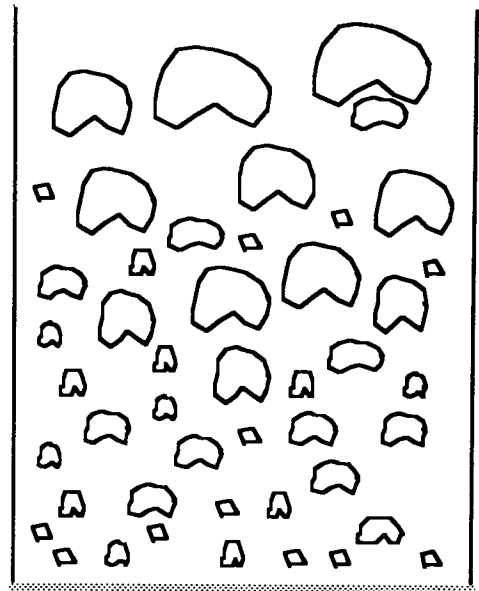


Fig.5.2: Formation of Bubbles with Porous Plate as visible from Column Wall.

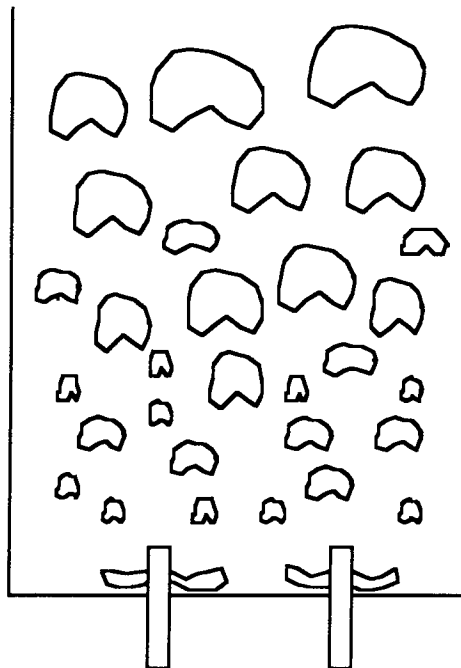


Fig.5.3: Jets emerging from Standpipes visible from below the Distributor.

Table 5.1: Mixing Indices for the binary systems tested

Initial Condition	Uo m/s	Mixing Indices			
		Porous	2	3	Standpipe
System - ABS / Polybeads 1090 (90% / 10%)					
Segregated	0.46	0.0011	0.0019	0.002	0.0007
Well Mixed	0.46	0.005	0.002	0.0034	0.00042
Well Mixed	0.36		0.00069		0.00033
Well Mixed	0.52		0.001		0.0008
System - Ballotini 1090 / Ballotini 550 (80 % / 20 %)					
Well Mixed	0.48	0.0023	0.0006	0.0028	0.00091
Segregated	0.48		0.0011		
System - Ballotini 1090 / Polybeads 1850 (80 % / 20 %)					
Well Mixed	0.79	0.522	0.25	0.30	0.19
Well Mixed	0.50	0.002			
Well Mixed	0.68	0.734			
Well Mixed	1.00	0.009			
Well Mixed	1.20	0.0013			
Well Mixed	1.40	0.0007			
System - Polycylinder / ABS (90 % / 10 %)					
Segregated	0.48	0.0032	0.00011	0.009	0.0077
Segregated	0.55			0.090	
Well Mixed	0.48		0.007		
System - Polybeads 925 / Polybeads 1550 (90% / 10 %)					
Segregated	0.58	0.00063	0.00118	0.012	0.0006
Segregated	0.48		0.57		
Segregated	0.51		0.44		
Segregated	0.54		0.0011		
Segregated	0.60		0.0009		

The standpipe type distributor stands out clearly as the best with the ABS / Polybeads system, regardless of the initial conditions, and this must be attributed to the availability of the local points of high linear gas velocity. Closer visual inspection of the pattern reveals that, in the case of the standpipe, the mixing around the jets was so pronounced that the polybeads (the smaller particles) behaved like jetsam. Naimer (1985) has also observed this behaviour when using standpipe type distributors. There could be a number of reasons for this phenomenon:

- a- due to the radial injection of the gas, jets of high local linear velocity are created, leading to intense localised mixing zones in which stagnant particles are set in motion.
- b- the discrete apertures create larger initial bubbles which consequently can pick up large amounts of jetsam from the bottom of the bed.

The perforated distributors 2 and 3 produced similar mixing indices when starting from the segregated mode, but in the case of the well mixed start, distributor 2 showed improvement on 3. Since distributor 3 had a free area nearly 10 times that of distributor 2, it was thought that it would substantially reduce the dead zone on the distributor. The results showed that the initial bubble diameter and high linear gas velocity played an important role in achieving good mixing.

It is important to note that decreasing the number of holes in the bed will increase the dead zone volume on the distributor. This can be a significant disadvantage which must be taken into account during the design of a distributor.

The initial condition did not have any impact on the concentration profile with distributor 2 giving exactly the same mixing index, 0.002, although the profiles obtained were significantly different from each other. This again emphasizes the pitfall of relying only on one performance indicator. Distributor 3, on the other hand displays clearly the effect of the initial condition both in the mixing indices and in the concentration profiles.

The standpipe type distributor scored the best with the ballotini 1090 / ballotini 550 system, followed by perforated distributor 2. The porous plate was the worst along with perforated distributor 3. This effect could only be attributed to the initial bubble diameter and the local linear velocity. The effect of U_0 on the

concentration profile using the porous plate confirms that the mixture stayed reasonably well mixed upto 0.5 m/s but as the superficial velocity approached the minimum fluidising velocity the particles started to segregate but reverted to the well mixed state at the higher velocity of 1.0 m/s; further increase in the value of U_0 did not make any difference.

All three distributors, namely standpipe, perforated distributor 2 and porous plate had completely segregated the different density well mixed mixture (Polybeads 1850 / Ballotini 1090) when operated at a slightly higher velocity than the minimum fluidising velocity. The highest degree of segregation was achieved by the porous plate followed by the standpipe and perforated distributor 2.

The porous plate performed well when handling the non spherical particle system - Polycylinder / ABS. Although the perforated distributor 2 achieved the lowest Mixing Index, thus exhibiting the best mixing, the porous plate scored better than the standpipe and perforated distributor 3: this was observed qualitatively and was further confirmed by the mixing indices. This is an interesting observation and would require considerably more work to understand: it is also clear that the particle shape cannot be ignored in mixing and segregation mechanisms. Perforated distributor 3 produced the worst mixing index and even a further increase in the superficial gas velocity did not improve the results.

The porous plate also produced a very good mixing index when operated with the jetsam rich system - Polybeads 925 / Polybeads 1550. Both perforated distributors performed worse than the porous plate and standpipe distributor with perforated distributor 3 showing the poorest mixing index. The increase in U_0 with perforated distributor 2 improved the mixing index.

5.2 Conclusions

The work clearly demonstrates that the quality of mixing is significantly influenced by the type of distributor used. Different criteria need to be emphasised in selecting a suitable distributor to achieve either maximum mixing or segregation. The distributor performing the best mixing will not produce the best segregation, if required, for the same system. Good mixing is mainly achieved by

- a) increasing the initial bubble diameter
- b) the disturbing effect caused by the jets.

Segregation patterns observed in these relatively large particle systems appeared to be similar to those observed by other workers in the case of small particle systems. However, the extent of particle segregation can be appreciable in large particle systems.

In equal density systems, good mixing occurred when the superficial gas velocity was less than the jetsam minimum fluidising velocity but greater than the flotsam minimum fluidising velocity and slightly higher than the composite minimum fluidising velocity (U_c).

In differing density systems, the superficial gas velocity needed to be substantially higher than the jetsam minimum fluidising velocity in order to achieve good mixing. A superficial gas velocity equal to or even slightly higher than the jetsam minimum fluidising velocity will promote severe segregation.

Particle shape only seems to have an effect when all the components are non spherical. The system containing one spherical and one non spherical component seemed to behave in a similar way to spherical particle systems.

The jetsam and flotsam rich systems also effected the concentration profile and could substantially influence the selection of distributor.

The standpipe type distributor generally displayed good mixing potential regardless of the system.

5.3 Recommendations for Future Work

Futher studies should be focused on the following aspects to clearly understand the effect of distributor design on the mixing and segregation mechanisms.

- 1- Standpipe type distributors produced significantly better mixing and further work needs to be carried out to fully appreciate the advantages of this type of distributor. Areas suggested for future study include:

- a) the effect of the standpipe configuration
 - b) the effect of number, size and position of holes on the standpipe
 - c) the effect of the length of the standpipe on the dead zone.
-
- 2- Although most of the mixing and segregation studies have been carried out with small particles, very limited data are available with large particles. Further work is recommended to study the mechanisms which govern the motion of a range of large diameter particles in gas fluidised beds. Experiments should also include large and irregular shape particles.
 - 3- The work should be repeated in large diameter beds. As most of the experiments were obtained in a small diameter bed, the effect of scale up needs to be determined for industrial purposes.
 - 4- The electrostatic forces and humidity have been shown to greatly influence the mixing and segregation mechanisms. A systematic investigation of these effects needs to be carried out: this may provide an explanation for the conflicting experimental results described in the literature.
 - 5- A mathematical model needs to be developed to include the effect of the distributor on the mixing and segregation mechanisms.

SECTION 11

THE SPOUTED BED

CONTAINING

CHAPTERS 6, 7 & 8.

CHAPTER 6

THE SPOUTED BED

6.1 Introduction

The spouted bed is a fluid-solids contacting device that has industrial potential for gas-solids systems in which the solid particle size exceeds 0.5 mm. With such particles, spouting often holds advantages over fluidisation since

- a) the pressure drop is only half to two-thirds of that for fluidisation,
- b) the gas contacting is superior because bypassing associated with large bubbles in fluidisation of such large particles is much reduced, and
- c) the device is structurally simple with no distributor.

The spouted bed may be used for heating/cooling, drying, coating, granulation, adsorption/desorption, solids mixing, chemical reaction and many other processing operations.

The essential features of the spouted bed are shown in Figure 6.1. The particle movement is determined by the interaction of the upward moving fluid stream, the gravitational forces and the random collision of the particles. The gas is introduced into the bed through an entry nozzle or orifice plate and forms an open cylindrical cavity that penetrates to the bed surface, this region being termed the "spout". Some of the gas seeps out into the annular bed of solids surrounding the spout. The pattern of particle movement is different in the two characteristic zones of the annulus (see Figure 6.1). Gravitational force and interparticle collision tend to reduce the ascending velocity of the particles in the spout. In the annular zone, the action of the upward flow of gas is considerably diminished on account of a smaller portion of the gas passing through this zone and its larger flow area compared with that of the spout. The interparticle collision has a smaller influence on particle movement and, therefore, they are moving along nearly parallel trajectories. In this zone it is the gravitational force that is prevailing and effecting a downward particle flow.

Spouting remains stable at different scales and both small and large beds may be operated, provided the gas inlet is properly designed. Berquin (1964) has

reported the operation of a bed 2.5 m in diameter and there is no upper limit to the diameter yet detected.

Most studies on spouted beds have been concerned with closely-sized particles, for example seeds, and a general feeling emerged that particles in mixtures or size-distributed materials are uniformly distributed both radially and vertically in the annular region. However, recent evidence has shown that this belief is incorrect. Sometimes an uneven distribution may pose problems; in other cases, an uneven distribution may be advantageous since certain particles, requiring either longer processing or more frequent contact with the inlet gas, may be arranged to have a longer residence time or a circulation path that more often brings them near to the gas inlet.

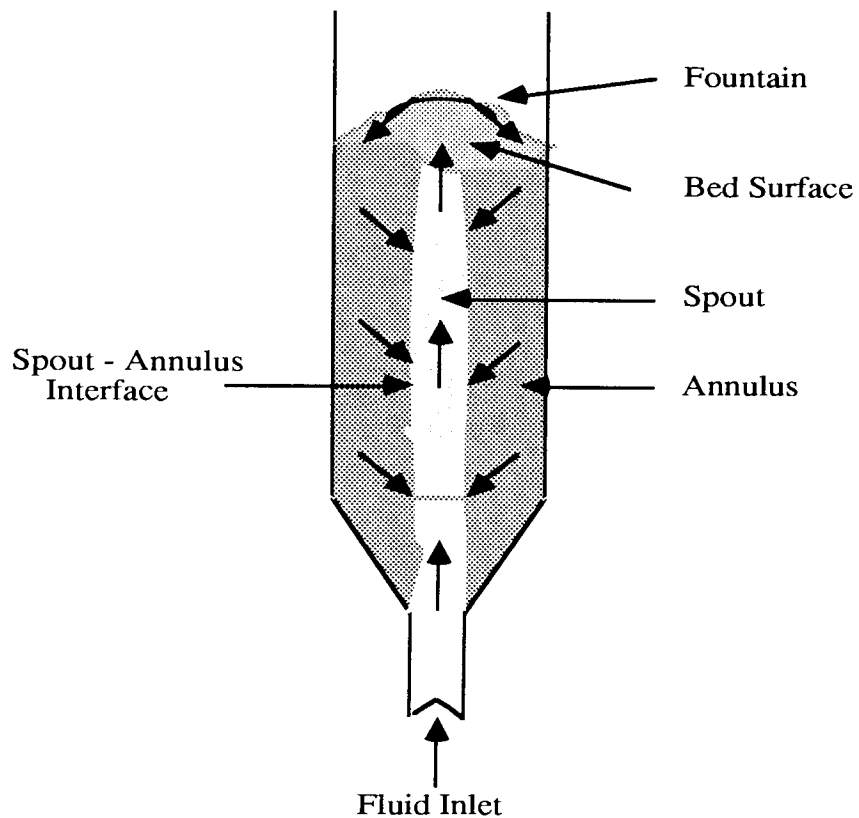


Fig.6.1: Schematic diagram of a spouted bed; arrows indicate direction of solids movement. (adapted from Mathur and Epstein, 1974)

The literature review for this chapter is presented in the form of extended summaries of key papers followed by an overview of the current state of the art. Emphasis is placed on contributions made to the subject of segregation in the spouted bed.

6.2. Literature Review

6.2.1 Berquin (1964)

Berquin (1964) patented a "Method and apparatus for granulating materials and hardenable fluid products" using a spouted bed granulation system. He found that large granules segregated out in the upper part of the annulus near its periphery but the mechanism was not elucidated. He concluded that the proportion of undersize particles could be minimised by "judicious location of the overflow pipe".

6.2.2 Mathur (1972)

Mathur (1972) studied comminution of solids by hard balls in a spouted bed. In some experiments, a large difference in density between the two solids gave rise to segregation, although segregation was absent for similarly sized solids if the density ratio did not exceed 3.

6.2.3 Piccinini, Bernhard, Campagna and Vallane (1977) & Piccinini (1980)

Piccinini et al. (1977) gave the first mechanistic account based on studies with 0.5 to 1.0 mm diameter glass ballotini binary mixtures. The experiments were conducted in an 80 mm diameter column. The experimental beds were generally shallow and operated continuously. They found that under steady state condition the proportion of coarse particles in the bed was up to twice that in the feed and this led to a discharge of mixtures richer in fine particles. Their work also showed that at low gas velocities, larger particles have a tendency to circulate in the upper and inner portion of the annulus because of the segregation phenomenon taking place inside the fountain, whilst at high gas velocities maldistribution was eliminated. Piccinini (1980) extended his previous work in a continuously operated spouted bed with different discharge pipes in various spouting regimes. He discovered a critical gas velocity which resulted in reversal of the segregation so that mixture richer in the coarse particles could be discharged. This result is consistent with that obtained by McNab and Bridgwater (1979), who studied the mixing and segregation properties

of the fountain.

6.2.4 *Robinson and Waldie (1978)*

Robinson and Waldie investigated particle cycle times in a spouted bed of polydisperse particles. The experiments were carried out in a half-section perspex column with conical base. The internal column diameter was 145 mm and granular sodium chloride particles (diameter ranged from 1.4 to 5.0 mm, density 2050 kg/m³) were used. They also carried out some supporting experiments in a full three-dimensional glass column of 150 mm internal diameter. They concluded that there was evidence for segregation of particles due to size. Once a particle developed a short cycle time in the bed, this tended to continue.

6.2.5 *Cook and Bridgwater (1979)*

Cook and Bridgwater extended Piccinini's work further to provide information on the mechanisms that arise and demonstrated the importance of the positioning of solids outlet pipes for continuous spouted beds. Their work was carried out in a 0.193 m diameter bed using two species materials differing in both density and size, which were mustard seed (mean diameter 2.2 mm, true density 1170 kg/m³) and glass beads (mean diameter 3.0 mm, true density 2970 kg/m³). They found that the dense, coarse fraction accumulated in the upper inner annulus and small particles accumulated at the outer edge of the free surface by percolating upwards through the interstices of larger particles. They concluded that the consequences of segregation were considerable, and that it was an oversimplification to assert that the more massive component always congregated at the upper part of the annulus.

6.2.6 *McNab and Bridgwater (1979)*

McNab et al. (1979) studied the particle segregation in a spouted bed by building a half-bed of semi-circular cross-section. Particular attention was focused on new data concerning the behaviour of a closely-sized material in the fountain and free surface regions. They observed that there are three types of fountain present in a spouted bed:

- a) a partial fountain where the material falls on only part of the annular surface;
- b) a full fountain where the material falls over the entire surface;

- c) an overdeveloped fountain where some material bounces off the vessel walls above the annulus before falling onto the bed.

Their work mainly concentrated on the partial and full fountains. They found that, in the spout, there was good radial mixing and that the radial position on leaving the spout was related to the radial position on landing on the top free surface. Close to the top free surface there will generally be radial flow, inwards or outwards, of particles since the principal part of the annulus was approximately in plug flow. Partial fountains exhibited principally radial outflow, whereas overdeveloped fountains showed radial inflow. However, in the case of full fountains the downward flux onto the surface will probably vary with radial position and the behaviour was less certain.

Another feature studied was the segregation at the free surface region due to interparticle percolation as particles cascaded down the sloping surface of the annulus. They concluded that interparticles percolation must also exist in the annulus since that region is also subject to shear strain. These phenomena will affect the circulation time in the bed and the residence time distribution for a continuously operated bed.

6.2.7 Kutluoglu et al.. (1983)

Kutluoglu et al.. (1983) investigated particle segregation in spouted beds in a 152 mm i.d. "half column" of semi-circular cross-section, with a conical plexiglas lower section having a 60° angle and 12.7mm diameter inlet orifice which was covered by 100 mesh screen to prevent dumping of particles. The objective was to study the spout behaviour of a single species bed and segregation and desegregation mechanisms of three sets of binary mixture. The particles used for the study were polystyrene beads ($d_p=1.1\text{mm}$), mustard seeds ($d_p=2.2\text{mm}$), glass beads ($d_p=1.1\text{mm}$) and urea ($d_p=1.5\text{mm}$). The data were collected by frame-by-frame analysis of cine-film.

Their study showed that the particle trajectories in the fountain region are strongly influenced by collisions and crowding. The outermost particles gain radial velocities which range from about 17% to 45% of the centreline vertical particle velocity at the level of the annulus surface. Also, there is a strong correlation between the radial position at which particles leave the spout and the radial landing

position on the annulus surface.

With binary particle systems, they found that heavier particles tend to follow tighter circuits through the fountain, annulus and spout. The major factor promoting segregation is that the heavier particles are scattered much less in the radial collisions which occur in the fountain region. However, if the gas velocity is increased so that the fountain is overdeveloped causing particles to bounce inwards from the outerwall, then there is a decrease in the segregation. Segregation is also less severe for the low spouted bed heights where fountains are so dilute that there are few particle-particle collisions.

They concluded that the fountain collision-induced segregation appears to be primarily a function of the relative particle mass of the two species, in addition to the operating variables mentioned above. Therefore, two species with the same particle mass but different size and density showed no tendency to segregate. On the contrary, some segregation can be caused by particles rolling along the free surface and by mixing processes in the spout. The influence of interparticle percolation in the annulus appeared to be small.

6.2.8 Uemaki et al. (1983)

Uemaki et al. (1983) studied particle segregation in a 20 cm diameter column with a 60 degree conical base. The experiments were performed with binary mixtures of silica sand in narrow fractions having a mean diameter of 0.655, 0.961, 1.52 and 2.23mm. Data were obtained by analysing 0.2kg samples which were withdrawn through a 1.2cm i.d. sampling tube rising through the conical base of the column. The sampling tube was designed to extract particles from any radial position at any level in the bed. In particular, they studied the effects of particle size difference, superficial gas velocity and composition of components on segregation.

They concluded that considerable radial segregation as well as axial segregation occur in beds of large particle size difference, even for high gas velocity. The degree of segregation increases with increasing particle size difference and that considerable segregation occurs in spouted beds even with higher gas velocities. They did not observe any significant effect of composition of components on segregation behaviour. Although they used three different inlet nozzle diameters, the effect on segregation was not mentioned.

6.3 Summary of Previous Segregation Studied

Berquin (1964) was the first to observe particle segregation in spouted beds. Piccinni et al. (1977) gave the first mechanistic account based on studies with mixtures of glass beads. Their work showed that heavier particles have a tendency to circulate in the upper and inner portion of the annulus because of the segregation phenomenon taking place inside the fountain, especially at low gas flows. They extended their work to continuous systems (1980) and found that continuous operation led to a discharge of mixture richer in fine particles. Also, they established that the weight fraction of one component in the discharge system was in equilibrium with the weight fraction of the component in the bed of solids. They also operated continuous spouted beds with different discharge pipes in various spouting regimes. A critical gas velocity was found which resulted in reversal of the segregation so that mixtures richer in the coarse component could be discharged. This result is consistent with that drawn by McNab and Bridgwater (1977), who studied the mixing and segregation properties of the fountain.

Cook and Bridgwater (1978) detected radial and angular segregation of the heavier component in a half-sectional spouted bed. Their study in a full bed provided further information on the mechanics and the positioning of solids outlet pipes.

Robinson and Waldie (1978) and Cook and Bridgwater (1978), while recognising the probable importance of the fountain, also provided evidence of differences in particle trajectories due to percolation of finer particles through the coarser ones. Robinson and Waldie (1978) even allow for possible segregation in the spout region, whereas McNab and Bridgwater (1978) state that there is good radial mixing in the spout.

Kutluoglu et al. (1983) have studied the fountain region in detail and concluded that particle trajectories in the fountain region are strongly influenced by collisions and crowding. This collision-induced segregation appeared to be primarily a function of the relative particle mass of the two species, whereas species with the same particle mass but different size and density showed no tendency to segregate. They also found that segregation is less severe if the gas velocity is increased so that the fountain is overdeveloped, causing particles to bounce inwards from the outer wall, a trend already reported by Piccinni et al. (1977) and

Cook and Bridgwater (1978).

Uemaki et al.. (1983) found that considerable radial segregation as well as axial segregation occurred in beds of large particle size difference. The degree of segregation increased with increasing particle size difference and considerable segregation persisted even at high gas velocities.

It is clear that there is a need for fundamental work to identify the primary mechanisms by which segregation occurs. So far, the fountain region has been shown to play a strong role and received some attention. Regretably the other end of the spouted bed, namely the "gas inlet", has received little attention. The author believes that in every gas-solid system the end effects play a vital role and, therefore, effort has been made here to highlight some of the many features which are influenced by the gas inlet region.

CHAPTER 7

THE SPOUTED BED - EXPERIMENTAL RESULTS

7.1 The Procedure for Minimum Spouting Velocity Experiments

The minimum spouting velocity experiments were carried out in the 138 mm i.d. cylindrical perspex bed described in Chapter 3. The bed was fitted with a perspex plate having a 14 mm diameter central orifice. The spouting air was metered by the flow rig shown in Figure 3.1. The total bed pressure drop was measured by a 1.6 mm i.d. tube placed in the bed directly above the distributor plate. All the experiments were conducted with only one type of distributor. Initially the minimum spouting velocities (U_{ms}) of all the mono components were measured followed by the binary mixtures experiments. In the case of the binary mixtures the solids were hand mixed in ten small portions and were carefully placed in the bed one after the other.

7.1.1. Minimum Spouting Velocity - Experimental Results

The pressure drop versus flow relationship for spherical Polybeads 1550 (particle diameter 1400 - 1700 μm) and for cylindrical Polycylinders are illustrated in Figures 7.1 & 7.2 respectively; these types of plot were obtained for all the components to ascertain the minimum spouting velocity.

The minimum spouting velocity curves for various binary systems were also obtained following the procedure outlined in section 4.1. The binary mixtures were mixed at a higher spouting velocity and then the pressure drop / velocity data was collected by fast and slow despouting of the bed. A typical illustration is shown below in Figure 7.3 and results are summarised in Table 7.1.

The minimum spouting velocity for both mono particles and binary mixtures is found to be less than the minimum fluidising velocity (U_o) observed as described in Chapter 4. This difference is more pronounced with larger particles, e.g. the minimum fluidising velocity observed for ABS Cylinders (equivalent particle diameter 2.4 mm) is 0.86 m/s whereas minimum spouting velocity for these particles is 0.75 m/s. This finding is quite in line with previous research workers. Lefroy and Davidson (1969) have found that the relative velocity between gas and particles is less than U_o in the annulus and much more than U_o in the spout. The overall spouting velocity is usually less than U_g .

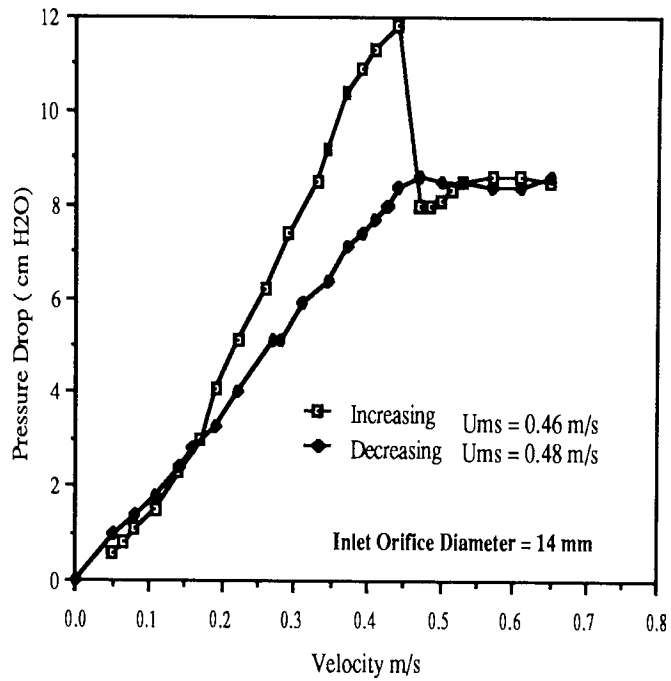


Fig.7.1: *Ums* plot for Polybeads 1400 - 1700 μ m

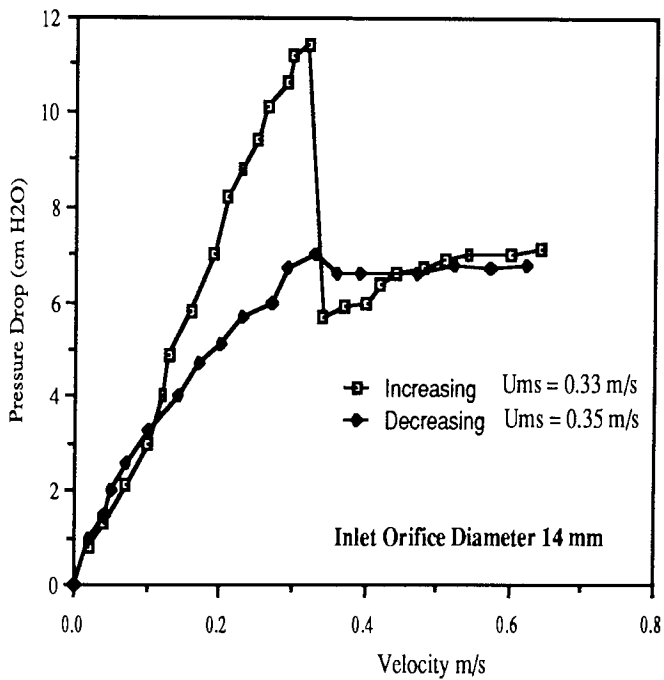


Fig.7.2: *Ums* plot for Red Polycylinders

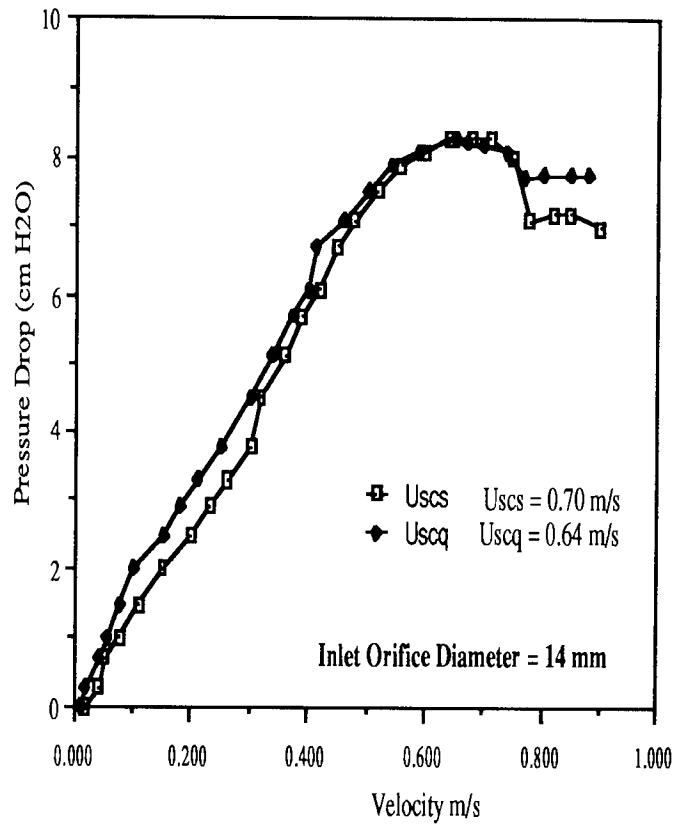


Fig.7.3: Minimum spouting velocity of ABS Cylinder / Polybeads (90% / 10%)

Table 7.1: Summary of the Minimum Spouting Velocities
- Binary mixtures used
(using a 14mm Orifice Diameter)

Systems	Solids	d (μm)	wt. %	U_{ms} (m/s)	U_{scs} (m/s)	U_{scq} (m/s)	U_{sav} (m/s)																																																																																
1	Polybeads	1090	90	0.30	0.37	0.35	0.36																																																																																
	ABS Cylinders	2400	10	0.75				2	Polybeads	1850	80	0.59	0.67	0.57	0.62	Ballotini	1090	20	0.65	3	Polycylinders	750	90	0.34	0.44	0.42	0.43	ABS Cylinders	2400	10	0.75	4	Polybeads	1550	90	0.47	0.44	0.48	0.46	Polybeads	925	10	0.24	5	Polybeads	1090	75	0.30	0.40	0.39	0.395	ABS Cylinders	2400	25	0.75	6	Polybeads	1090	50	0.30	0.46	0.42	0.44	ABS Cylinders	2400	50	0.75	7	Polybeads	1090	25	0.30	0.59	0.56	0.575	ABS Cylinders	2400	75	0.75	8	Polybeads	1090	10	0.30	0.70	0.64	0.67
2	Polybeads	1850	80	0.59	0.67	0.57	0.62																																																																																
	Ballotini	1090	20	0.65				3	Polycylinders	750	90	0.34	0.44	0.42	0.43	ABS Cylinders	2400	10	0.75	4	Polybeads	1550	90	0.47	0.44	0.48	0.46	Polybeads	925	10	0.24	5	Polybeads	1090	75	0.30	0.40	0.39	0.395	ABS Cylinders	2400	25	0.75	6	Polybeads	1090	50	0.30	0.46	0.42	0.44	ABS Cylinders	2400	50	0.75	7	Polybeads	1090	25	0.30	0.59	0.56	0.575	ABS Cylinders	2400	75	0.75	8	Polybeads	1090	10	0.30	0.70	0.64	0.67	ABS Cylinders	2400	90	0.75								
3	Polycylinders	750	90	0.34	0.44	0.42	0.43																																																																																
	ABS Cylinders	2400	10	0.75				4	Polybeads	1550	90	0.47	0.44	0.48	0.46	Polybeads	925	10	0.24	5	Polybeads	1090	75	0.30	0.40	0.39	0.395	ABS Cylinders	2400	25	0.75	6	Polybeads	1090	50	0.30	0.46	0.42	0.44	ABS Cylinders	2400	50	0.75	7	Polybeads	1090	25	0.30	0.59	0.56	0.575	ABS Cylinders	2400	75	0.75	8	Polybeads	1090	10	0.30	0.70	0.64	0.67	ABS Cylinders	2400	90	0.75																				
4	Polybeads	1550	90	0.47	0.44	0.48	0.46																																																																																
	Polybeads	925	10	0.24				5	Polybeads	1090	75	0.30	0.40	0.39	0.395	ABS Cylinders	2400	25	0.75	6	Polybeads	1090	50	0.30	0.46	0.42	0.44	ABS Cylinders	2400	50	0.75	7	Polybeads	1090	25	0.30	0.59	0.56	0.575	ABS Cylinders	2400	75	0.75	8	Polybeads	1090	10	0.30	0.70	0.64	0.67	ABS Cylinders	2400	90	0.75																																
5	Polybeads	1090	75	0.30	0.40	0.39	0.395																																																																																
	ABS Cylinders	2400	25	0.75				6	Polybeads	1090	50	0.30	0.46	0.42	0.44	ABS Cylinders	2400	50	0.75	7	Polybeads	1090	25	0.30	0.59	0.56	0.575	ABS Cylinders	2400	75	0.75	8	Polybeads	1090	10	0.30	0.70	0.64	0.67	ABS Cylinders	2400	90	0.75																																												
6	Polybeads	1090	50	0.30	0.46	0.42	0.44																																																																																
	ABS Cylinders	2400	50	0.75				7	Polybeads	1090	25	0.30	0.59	0.56	0.575	ABS Cylinders	2400	75	0.75	8	Polybeads	1090	10	0.30	0.70	0.64	0.67	ABS Cylinders	2400	90	0.75																																																								
7	Polybeads	1090	25	0.30	0.59	0.56	0.575																																																																																
	ABS Cylinders	2400	75	0.75				8	Polybeads	1090	10	0.30	0.70	0.64	0.67	ABS Cylinders	2400	90	0.75																																																																				
8	Polybeads	1090	10	0.30	0.70	0.64	0.67																																																																																
	ABS Cylinders	2400	90	0.75																																																																																			

7.2. The Experimental Strategy

Two main parameters were initially chosen as the central foci for the mixing/segregation experiments: these were gas inlet orifice diameter and the initial condition of the mixture i.e. 'segregated' and 'well mixed'. Five other parameters were explored; these were particle size, particle density, spouting gas velocity, static bed height and overall bed composition .

7.3. Interpretation of the Experimental Data

Generally in this type of study, the samples are collected either axially and/or radially and concentration is plotted against a dimensionless position. This approach was followed by the author in presenting data obtained from samples collected axially.

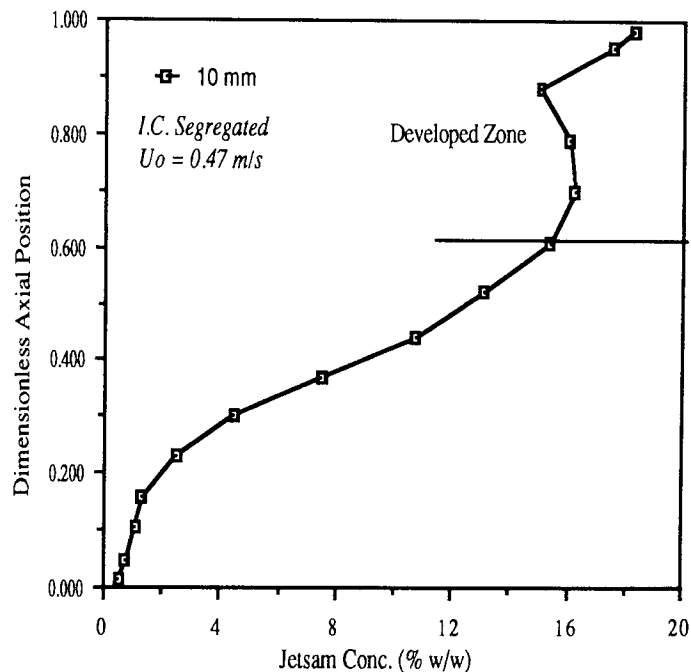


Fig.7.4: A typical Concentration Profile - Polybeads 1090 / ABS Cylinder

Figure 7.4 shows a typical concentration profile with jetsam concentration plotted against the dimensionless axial position (h_i/H). Visual observations show that two distinct zones exist in the bed and that the spout penetration zone expands from the gas inlet orifice to some height where it occupies the complete cross-section. This zone which exists at the lower end of the bed is termed the "undeveloped zone" and it is very much dependent on the

design of the lower section of the bed. The upper section can be described as the "*developed zone*". It is the results from this particular zone that are considered in the analysis: all the calculations, such as concentration ratio and the Mixing Index, refer to this zone only.

7.4 Experimental Results

7.4.1 The ABS Cylinders - Polybeads System

This is an equi-density flotsam-rich system having particles of different size and shape. The flotsam was spherical particles of polystyrene beads with the particle size range of 1.0 to 1.18mm. The jetsam was cylindrical particles of ABS which were 2.4mm in diameter and 3.0 long. The spherical equivalent mean diameter ratio was 3.9. The overall jetsam weight fraction was kept constant at 0.1 and static bed height at 21.6cm.

Effect of Orifice Size

The experiments were carried out with 7 different orifice diameters. In all cases, a stable full fountain was established by adjusting the air flow rate to the bed. Table 7.2 provides a summary of the operating conditions. The data show that the volumetric air flow rate increases with inlet diameter up to a value of 10mm; thereafter, it virtually stays constant regardless of the inlet diameter.

An interesting point to emerge from Table 7.2 is that the air velocities required to establish a stable fountain for the 4 and 6mm inlets were less than the minimum fluidising velocity. The relationship between the orifice inlet diameter and the spouting air velocity required to achieve a full fountain is shown in Figure 7.5.

The data can best be described mathematically by the relationship:

$$\log U_{oi} = 2.745 - 0.2236 \cdot D_i \quad (7.1)$$

where

U_{oi} is the superficial air velocity at the orifice (m/s)

and D_i is the inlet orifice diameter (mm)

Table 7.2: Summary of the Operating Variables

Orifice Dia. D_i (mm)	Superficial Air Velocity U_o m/s	Velocity at Orifice U_{oi} m/s	$\log(U_{oi})$
4	0.31	359	2.56
6	0.32	171	2.23
8	0.40	116	2.06
10	0.47	87	1.94
14	0.42	41	1.61
17	0.50	32	1.51
25	0.46	14	1.14

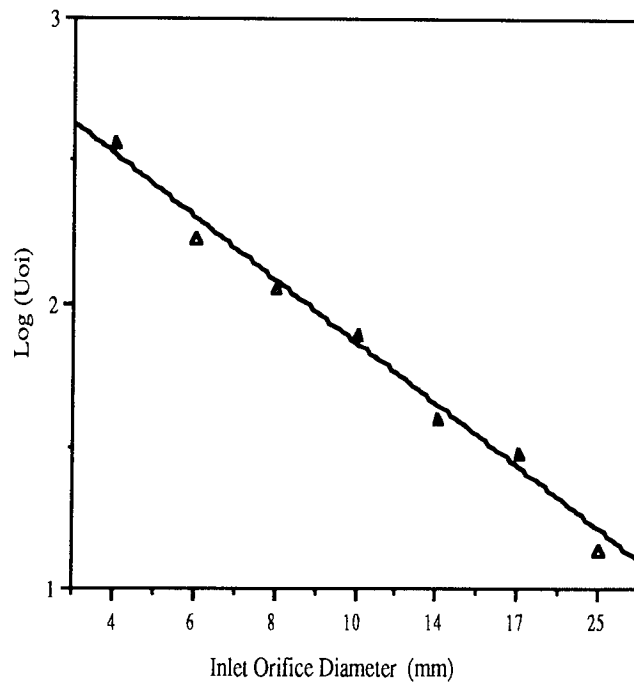


Fig.7.5: Inlet Orifice Diameter vs log of Spouting Velocity

The variation in the concentration profiles with different orifice diameters is shown in Figure 7.6. These profiles were obtained with four orifices 4, 6, 8 and 10 mm in diameter. It can be seen that the air inlet diameter has a profound effect on the concentration profile.

Using the initial jetsam concentration (i.e.10%) as a reference value, the curve which crosses this line at the lowest point on the vertical scale is the one generated with the 6mm orifice; thus, this is the orifice that leads to the largest value of the developed zone. The other curves all cross the 10% line at higher positions, including that for the 4mm orifice diameter, if only marginally so.

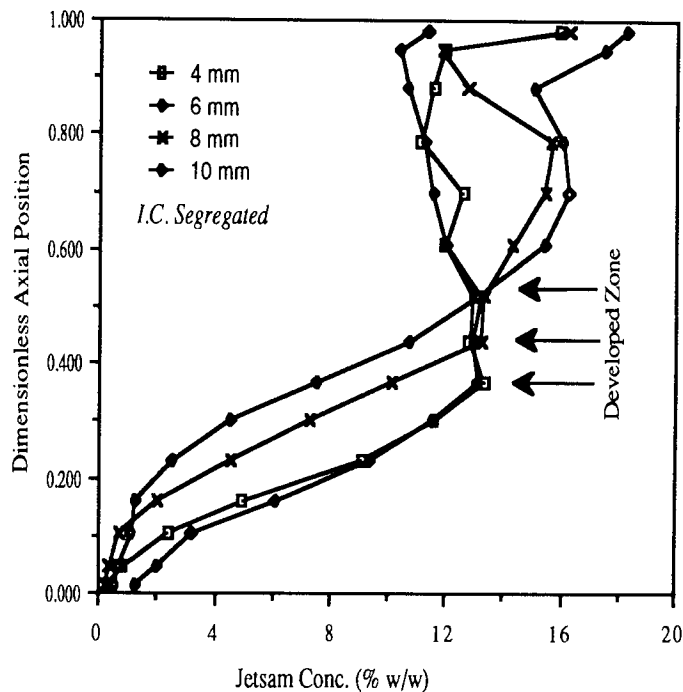


Fig.7.6: Effect of the Inlet Orifice Diameter on the Conc. Profile

By examining the results in the "developed zone", we find that the curves for the 4 and 6mm orifices are almost identical except at the surface of the bed where entrainment effects are much more pronounced in the case of the smallest orifice. The spout for the 4 mm inlet was considerably higher, ≈ 43 cm from the inlet, compared with the 6 mm inlet spout which was 27 cm high. The path of the ABS cylindrical particles travelling downwards along the column wall was visually followed and it was established that in the case of the 6 mm inlet these particles were inwardly disappearing at 9 cm above the distributor whereas with the 4mm

inlet they were disappearing at the 8 cm level. It was anticipated from these experimental observations that these two concentration profiles would be considerably different from each other but the sectional analysis produced a somewhat different picture. The greater height of the 4 mm spout obviously resulted in the appearance of relatively more flotsam particles on the bed surface. Generally, both these curves lie close to the 10% line, implying good mixing in the developed zone.

The general behaviour observed with the 8 and 10 mm inlet was similar, the spout height being roughly the same ≈ 28 cm. However, the black ABS cylindrical particles seemed to disappear at ≈ 12 cm above the distributor which was nearly 3 cm higher than for the 6 mm inlet level. The results for the 8 and 10mm inlets show a lot of scatter even in the developed zone with the jetsam concentration varying from 10% to 18%.

Figure 7.7 shows the concentration profiles when using 6,10,14 and 17mm diameter air inlet orifices. The profiles below the 10% jetsam concentration line are virtually the same for three of the orifices namely 10, 14 and 17 mm diameter inlets and, even in the developed zone, the behaviour is similar. Therefore, it can be said that changing the air inlet diameter from 10mm to 17mm has hardly any effect on the concentration profile. However, when these profiles are compared with the curve for the 6mm inlet, significant differences are revealed. The 6 mm diameter inlet produced a larger developed zone with an average jetsam concentration of 11.7%.

The general system behaviour with the 10, 14 and 17 mm diameter inlets was very similar. The spout height was ≈ 28 cm and the black ABS cylinders travelling downwards were disappearing inwardly at about the same vertical level in all three cases.

Figure 7.8 compares the concentration profiles obtained with 6, 8 and 10 mm diameter inlets. An additional concentration profile for a 25 mm inlet is also shown in Figure 7.8. This profile lies close to that for the 8mm inlet and in between those for the 6 and 10mm inlets. The visual observations confirmed the similarity between the 8 mm and 25mm cases. Another rather unusual observation with the 25 mm inlet showed that occasionally the spout converted into a bubble near the bed

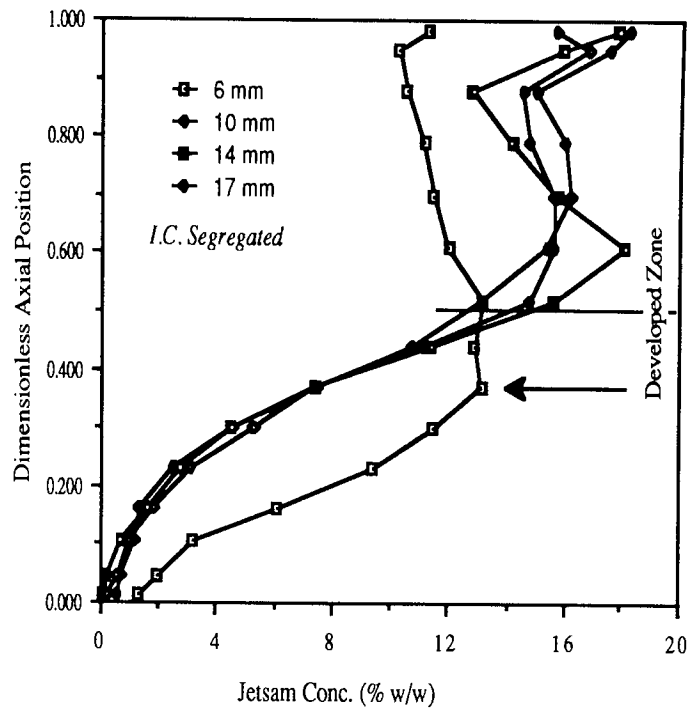


Fig.7.7: Effect of the Inlet Orifice Diameter on the Conc. Profile

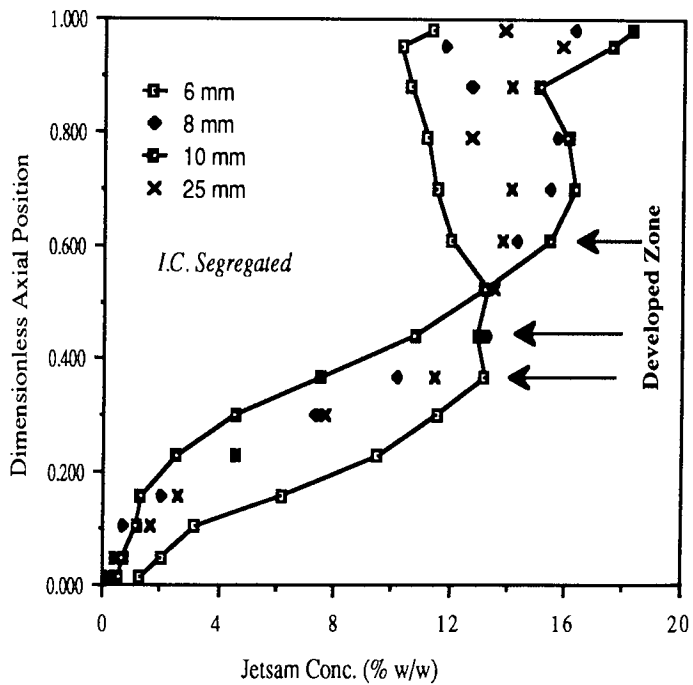


Fig.7.8: Effect of the Inlet Orifice Diameter on the Conc. Profiles

surface. This is in line with previous studies where it was concluded that there is a

critical limit to bed and fluid inlet cross sectional area and beyond this limit the bed tends to behave like a fluidised bed.

Quantative analysis of the data was carried out by calculating the Mixing Index (MI) using equations 2.14 with respect to the developed zone only. A plot of Mixing Index (MI) and inlet orifice diameter is presented in Figure 7.9. This shows that the segregation increases initially with increase in orifice diameter and then levels off followed by a sharp decline. It further tells us that the inlet orifice of diameter 6 mm gives the best mixing; increasing the diameter to 10 mm decreases the mixing and particles start to segregate. This behaviour persists until the inlet diameter is increased to 25 mm which produces somewhat better mixing. However, with a 25 mm diameter orifice inlet the spouting behaviour begins to recede and fluidisation appears to take over. Another interesting point which can be seen is that a similar value of the Mixing Index was achieved with 10 mm and 17 mm diameter orifices.

A practical limit is set at about 4mm orifice diameter. Below this value, there is not sufficient air flow to establish a spout and, additionally, there is a build up of pressure below the distributor.

In a three dimensional bed it is difficult to viusalise the exact spout penetration; generally two dimensional or semi cylindrical beds are used for this study. However, there has been some doubt expressed about the validity of results because of the wall effects with 2-D or semi cylindrical beds. During the author's mixing/segregation experimental programme the bed was sectioned for analysis and this provided some information about spout penetration inside the 3-D bed. There are in fact radial concentration changes along the depth of the bed. The size of these contours was physically measured and used to construct the spout penetration inside a 3-D bed. Figure 7.10 shows a section of the bed fitted with a 10 mm diameter orifice inlet and spouted at 0.47 m/s for 10 minutes starting from the segregated state. It shows that the spout has taken nearly two thirds of the bed height to activate the full circumference of the bed. The variation in inlet orifice diameter has only a slight effect on this penetration zone. This zone also appears to be independent of the aspect ratio of the bed.

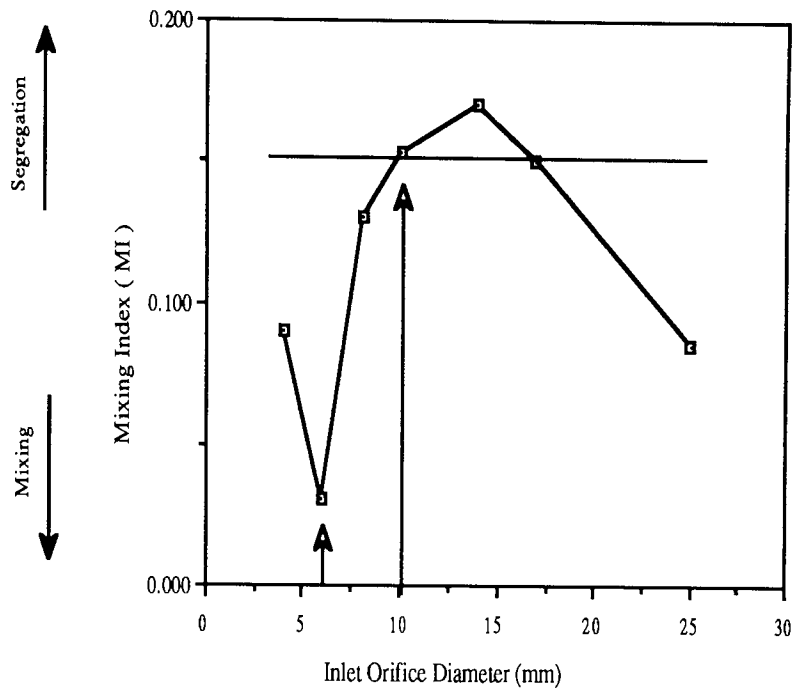


Fig.7.9: Relationship between Inlet Orifice Diameter vs MI

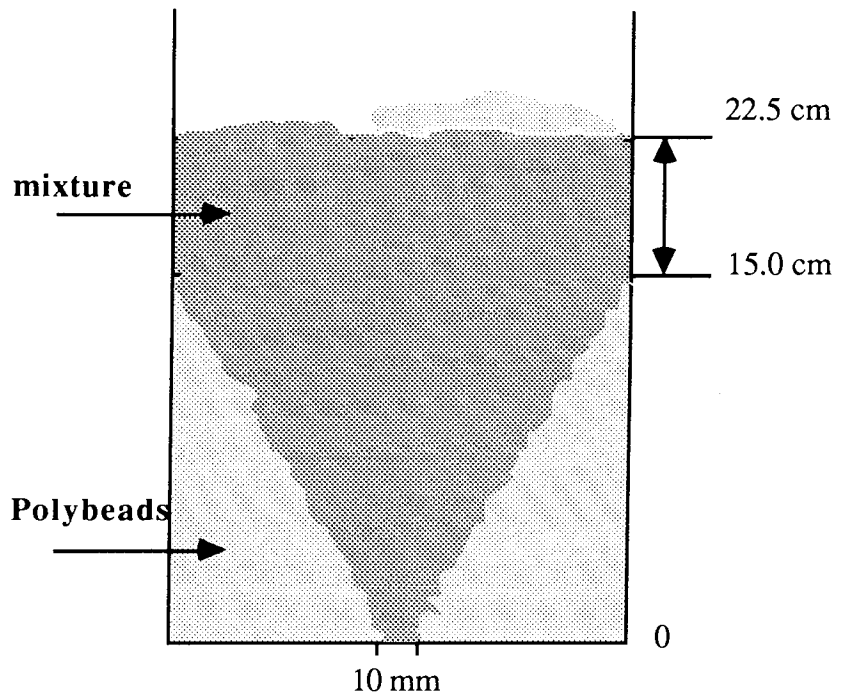


Fig.7.10: A sectional view of the Spouted Bed

Effect of the Spouting Velocity

A study into the effect of the spouting velocity on the concentration profile was carried out to determine whether the penetration height could be substantially altered. The work was carried out with the 14 mm diameter orifice inlet. Three different air velocities ranging from 0.47 m/s to 0.85 m/s were used. The first experiment was carried out with the minimum spouting velocity required to produce a stable spout and this gave a spout height of 27 cm. The velocity was then increased to 0.61 m/s which in turn increased the spout height to 38 cm and a further increase to 0.85 m/s produced a 44 cm tall spout. At the higher spouting velocity, an intense particle movement was noticed but again this intensity was restricted to the upper one third of the bed.

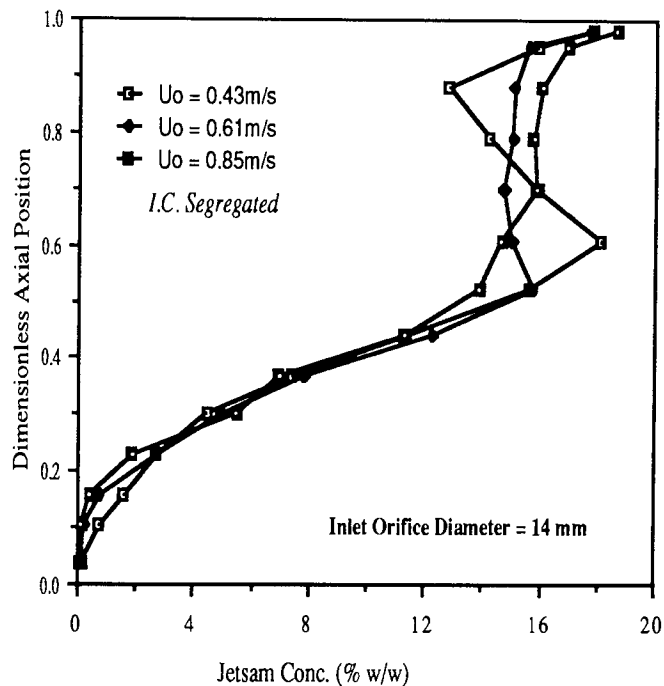


Fig.7.11: Effect of the Superficial Air Velocity on the Conc. Profile

Figure 7.11 shows the concentration profiles obtained at these three spouting velocities and they confirm the visual observations that changes over the lower section are small with more significant variation at the top of the bed, thus creating a deep cone at the lower section. The limiting cone angle appears to be dependant on the internal friction characteristics of the solids and for ABS Cylinders / Polybeads system it was calculated to be 57° .

Effect of the Initial Condition

The effect of initial conditions on the concentration profiles was studied by conducting the experiments with segregated and well mixed beds. The well mixed system was hand mixed in ten equal portions and then these were placed on top of each other. The operating conditions for both these experiments were kept constant. Figure 7.12 illustrates the concentration profiles. Although the jetsam concentration is different, the shape of the curves, until they intersect each other, is similar. The curves intersect at the 8 cm level in the bed with an average jetsam concentration of 7.1%. Below this intersection the profiles are very different; $\approx 8\%$ at the distributor for the well mixed case and only 0.13% for the segregated case. The spout appearance and height were similar in both case.

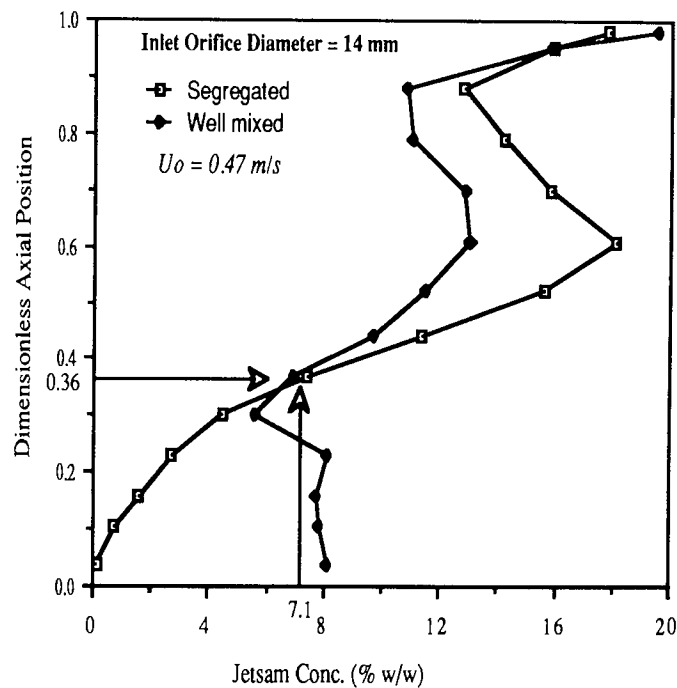


Fig.7.12: *Effect of the Initial Condition on the Conc. Profile*

Effect of the Aspect Ratio (Ra)

The effect of aspect ratio (Ra) on the concentration profile was examined at two different bed heights, i.e. at 22.2 cm and 35.0 cm with an aspect ratio of 1.6 and 2.5 respectively. The inlet orifice diameter was 10 mm and the experiments were conducted from the segregated state. The concentration profiles are shown in

Figure 7.13. A slightly higher spouting velocity was required for the deeper bed. Both the profiles show similar behaviour. The deeper bed gives better mixing in the main section of the bed with an average jetsam concentration of 12.8% compared with 16.2% with the shallower bed. The size of the undeveloped zone remained constant with similar jetsam concentrations in both cases. The spout was not very pronounced in the deeper bed and occasionally converted into bubbles which illustrates that the maximum spoutable height was slightly less than that of the deeper bed used.

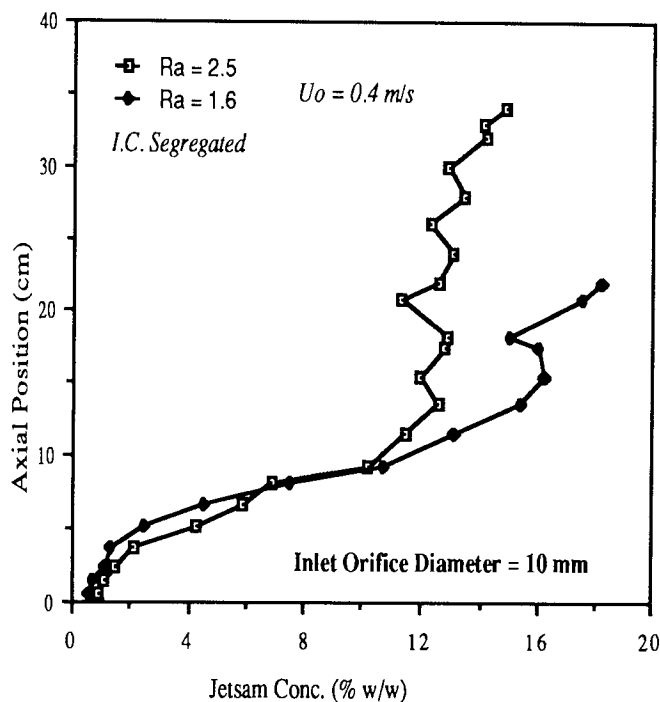


Fig.7.13: Effect of the Aspect Ratio (Ra)

7.4.2 The Ballotini1090 / Polybead1850 System

This system was composed of the yellow glass ballotini with a particle diameter range of 1.00-1.18 mm and white Polybeads having a particle diameter range of 1.7-2.0 mm. Apart from the size difference ($dp_b/dp_p=1.7$), there was also a density difference of 2.45 times. The main reason for selecting these materials was the close similarity in the minimum fluidising velocity. The static bed height ranged from approximately 15.0 to 30.0cm. The overall ballotini weight fraction was kept constant at 0.2, the ballotini playing the role of jetsam in the mixture.

Most of the experiments were carried out from the segregated mode in which the ballotini was placed on top of the polybeads. It was noticed that when the mixed bed reached a steady state condition, and this generally took 2 minutes, a band of yellow ballotini was formed a few centimeters above the distributor. Also, the fountain was much taller and pronounced as compared to that for the Polybeads/ABS system described above.

A typical concentration profile for this system using the 10mm diameter orifice and operating at the lowest possible spouting velocity to maintain a stable full fountain is shown in Figure 7.14.

The bed divides itself into two regions; one containing nicely mixed particles and the other with segregated particles. The profile exhibits a point of the highest jetsam concentration and this point is referred as the 'Peak Point'. This peak point on the concentration curve corresponds to the vertical position of the ballotini band in the bed. Above the band, a little radial segregation was observed but below the band the radial segregation was quite severe.

The effect of the spout penetration was studied by gradually sectioning the bed and physically measuring the penetration in the radial direction. This information was then used to construct the spout penetration zone inside the bed. The experiment was conducted from the completely segregated mode with the minor component (jetsam) on the top while the bed was fitted with a 10 mm diameter inlet orifice. Figure 7.15 shows a picture of the sectioned bed. This picture is very different from the penetration picture obtained for the Polybeads 1090 / ABS system. Much of the jetsam has been transferred to the bottom half of the bed and the characteristic cone of Figure 7.10 has almost disappeared. The cone angle calculated from this reconstructed cone was 25° .

Effect of Orifice Size

The effect of the inlet orifice diameter was studied with three different inlets namely of 10, 14 and 17 mm diameter and the concentration profiles are shown in Figure 7.16. The general behaviour of the bed was very similar and in all cases the spout height was ≈ 18.5 cm. The mixing improved when using the 14 and 17 mm diameter orifices and there was little difference in the jetsam concentration. The spouting velocity required to establish a stable spout ranged from 0.69 - 0.77 m/s for the three orifices.

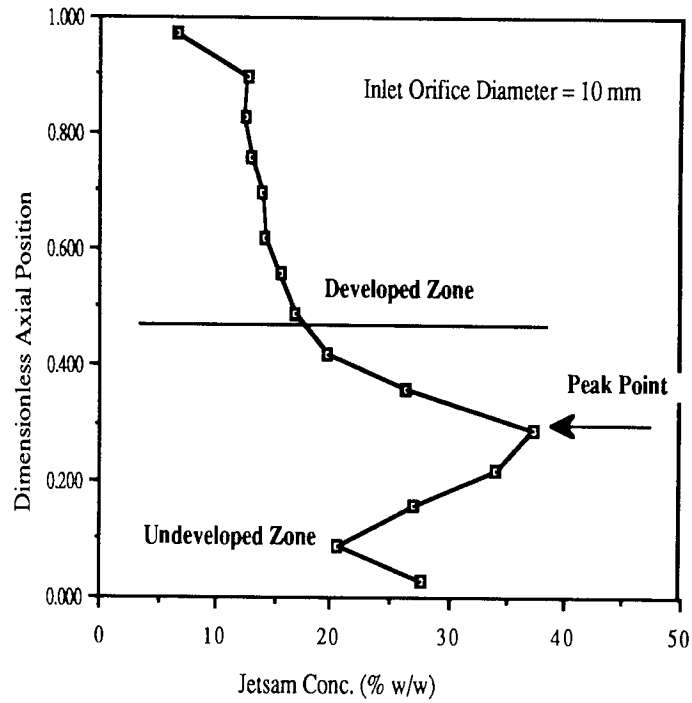


Fig.7.14: A typical Concentration Profile - (Polybeads 1850 / Ballotini 1090)

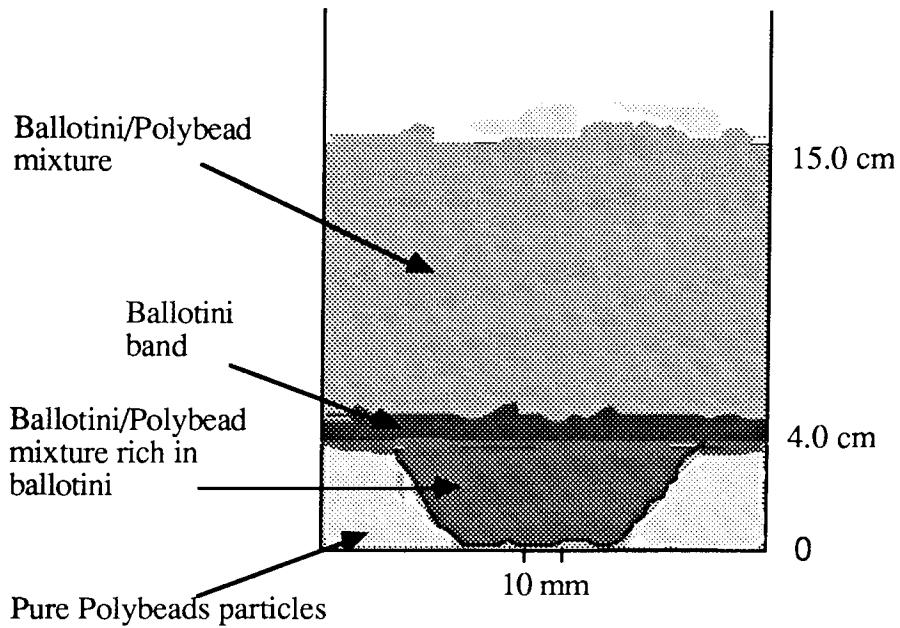


Fig.7.15: Spout penetration with 10 mm diameter orifice inlet

The peak points for the 14 and 17 mm inlets were exactly at the same position of 6 cm whereas with the 10 mm inlet it was at the 4 cm level. The jetsam concentration at the peak point was also different; 27% with the 14 and 17 mm inlets and 35% with the 10 mm inlet. Below the peak point there is another kink in the curve caused by the higher proportion of ballotini particles settling near to the air inlet. This behaviour is completely different from that observed with the equi-density system and can be attributed to the density difference.

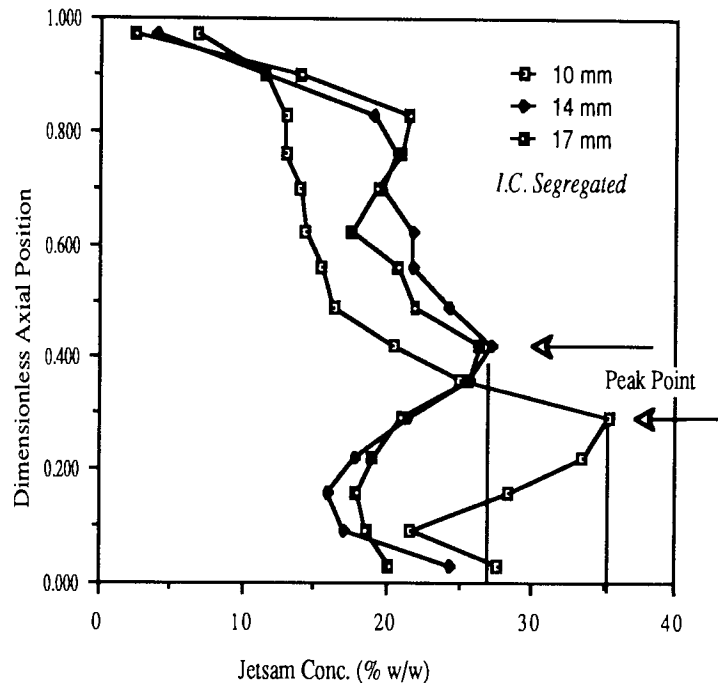


Fig.7.16: Effect of Inlet Orifice Diameter on the Conc. Profile

The top layer near the surface also shows a high level of segregation which is due to the preferential entrainment of polybeads in the spout: it is well established that segregation will be severe when different density particles are allowed to fall freely.

The general bed behaviour and the position of ballotini band were similar with 14 mm and 17 mm diameter orifices. The spout appearance and ballotini band position for the 10 mm and 14 mm diameter inlets are reconstructed in Figure 7.17 and 7.18 respectively.

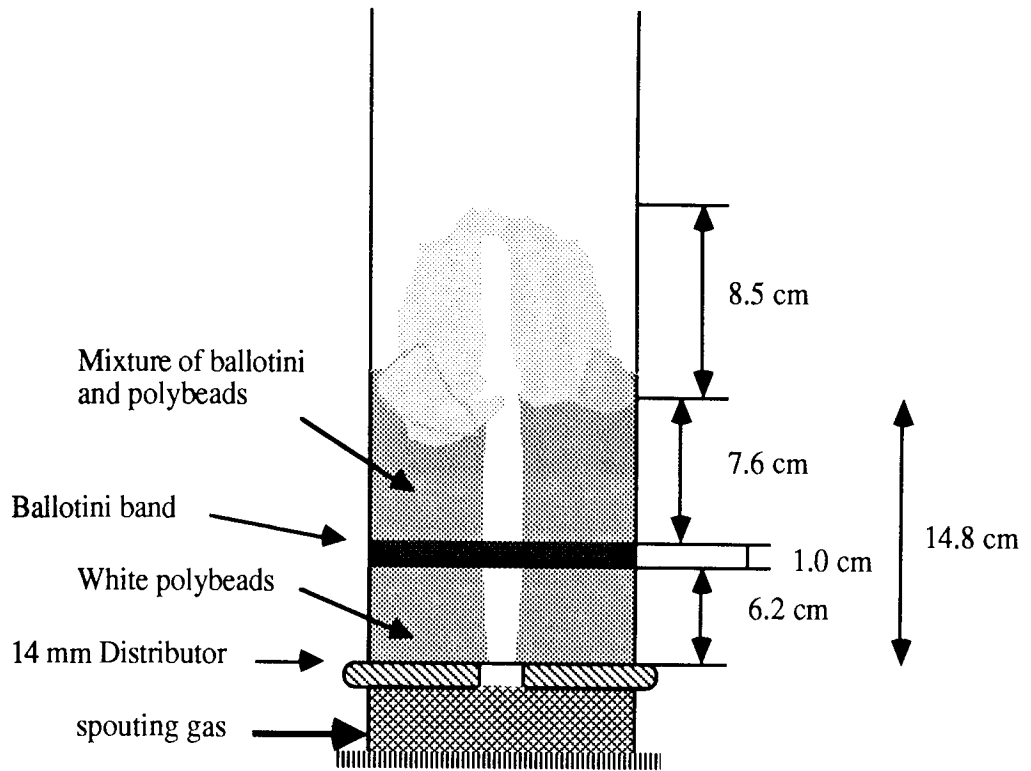


Fig.7.17: Physical appearance of the spouted bed with 14 mm diameter gas inlet orifice.

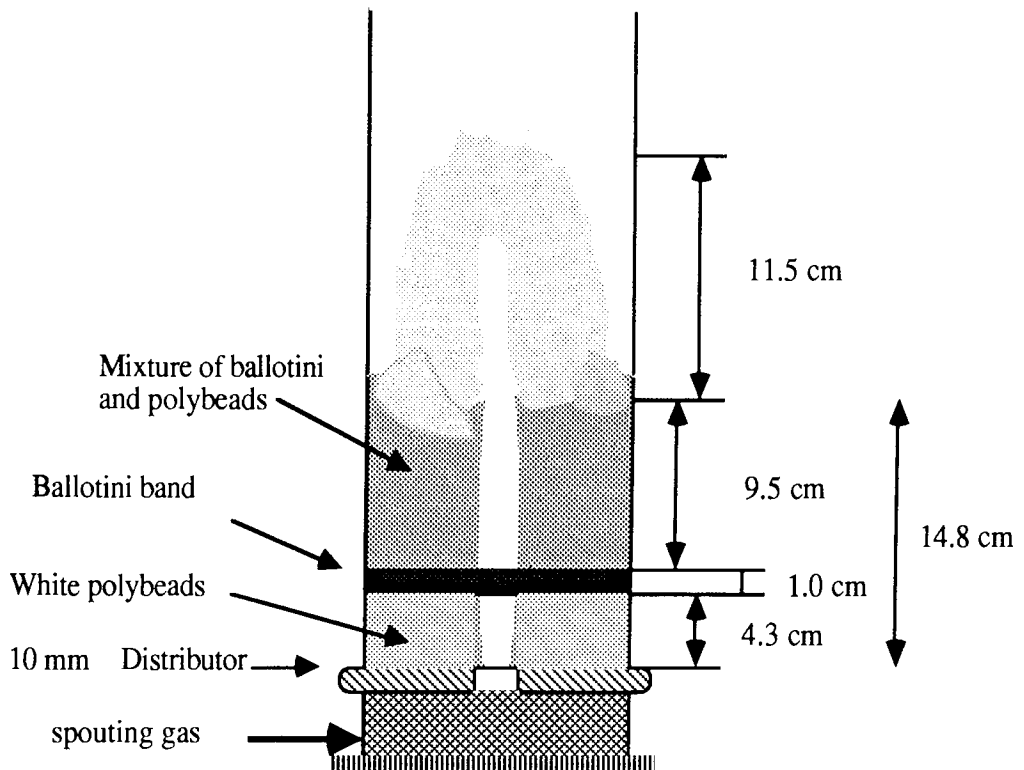


Fig.7.18: Physical appearance of the spouted bed with 10 mm diameter gas inlet orifice.

Effect of the Spouting Velocity

In order to explore the mixing further, experiments were carried out at higher spouting velocities and the profiles thus obtained are shown in Figure 7.19. This indicates that with highly segregating mixtures, such as ballotini / polybeads, increases in the spouting velocity can promote segregation.

An increase from 0.65 m/s to 0.77 m/s in the spouting velocity did not have a marked effect on the concentration profile. A further increase in the air velocity aggravated mixing. The changes in the superficial velocity resulted in different spout heights e.g. 27.0 cm for 0.65 m/s, 40.0 cm for 0.77 m/s and 47.0 cm for 1.14 m/s. The increase in the velocity had a direct effect on the concentrated ballotini band which lowered gradually with the increase in the velocity and a higher percentage of ballotini was found on the distributor. A further experiment was carried out to visually ascertain the effect of superficial velocity and it was found that, at 1.6 m/s, the ballotini band nearly disappeared, the bed became very violent and slightly better mixing was achieved.

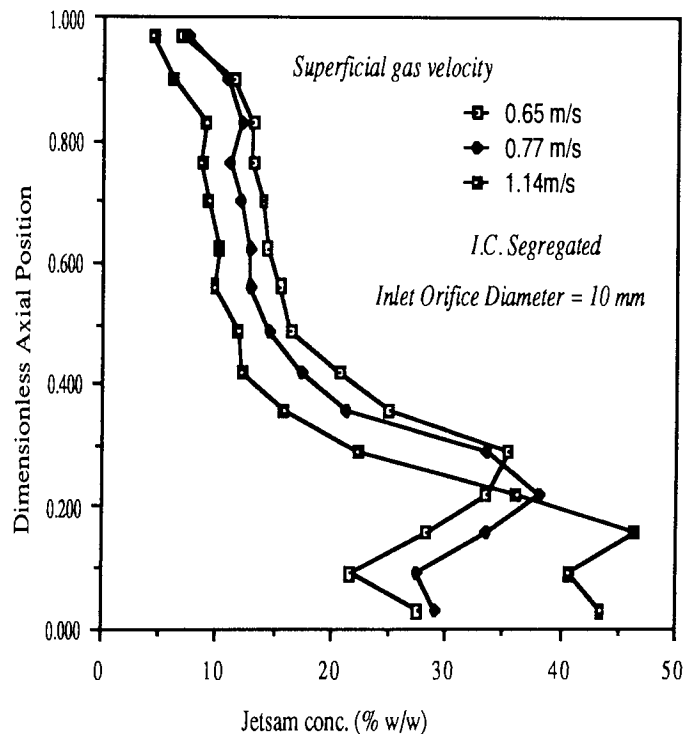


Fig.7.19: Effect of Superficial Air velocity on the Conc. Profiles

Effect of the Initial Condition

Experiments were also conducted to establish the effect of the initial bed condition on the final concentration profile under the same operating conditions. All experiments were carried out with the solids totally segregated but the position of the jetsam within the bed was altered. Three cases were studied with jetsam placed at the top, bottom and in the centre. The static bed height was kept constant at 15.0cm and in all cases, the 10mm diameter orifice inlet was used. The spouting velocity was 0.65 m/s and this produced a 28.0 cm tall spout; the expanded bed height was 15.9 cm. The concentration profiles obtained from the three experiment are shown in Figure 7.20 which illustrates that the profiles obtained when the jetsam was placed at the top and in the centre are remarkably similar; whereas the third profile, obtained with jetsam placed at the bottom, is different in concentration but identical in shape.

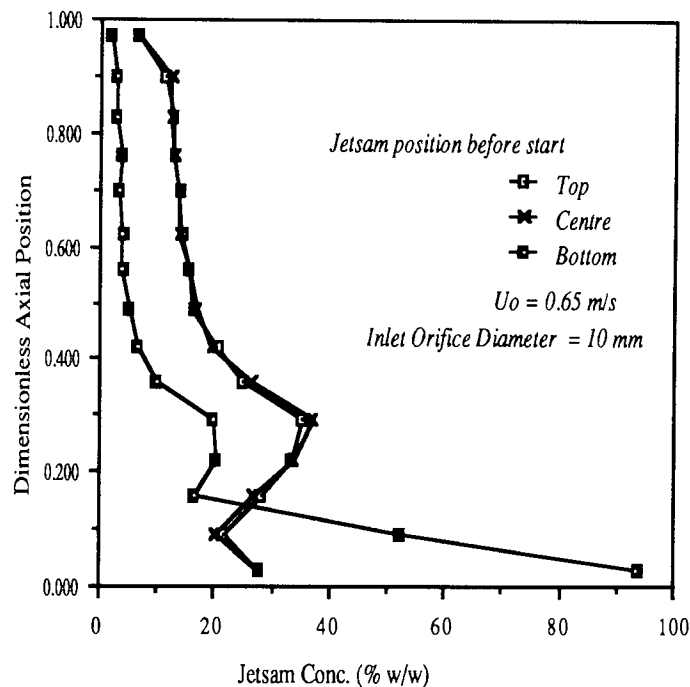


Fig.7.20: Effect of the Initial Jetsam position on the Conc. Profiles

One can conclude that the mixing pattern and concentration profile is independent of jetsam location, in a segregated mode, provided it is placed somewhere above the peak point. However, if the jetsam is placed below the peak point, then only a fraction of this is circulated which will effect the overall jetsam concentration but not the shape of the profile.

Effect of the Aspect Ratio (Ra)

The effect of aspect ratio on the concentration profile was explored using the 10mm diameter air orifice inlet. Two sets of experiments were conducted- one with an aspect ratio of 1.07 ($H_s=14.8\text{cm}$) and the other with an aspect ratio of 2.14 ($H_s=29.6\text{cm}$). The ballotini/polybeads content was kept constant at 20%/80% w/w. It was found that a slightly higher superficial velocity was required with a deeper bed to establish similar spouting conditions. The concentration profiles of ballotini under these conditions are shown in Figure 7.21. Both of these profiles exhibit similar behaviour. The peak point is at about the same position and below this the bed is unaffected by the change in the aspect ratio. Above the peak point, the deeper bed shows much better mixing, with the upper half of the bed except the top layer containing an average of 20% w/w of jetsam. Both the profiles have a similar jetsam concentration at the surface suggesting comparable entrainment effects.

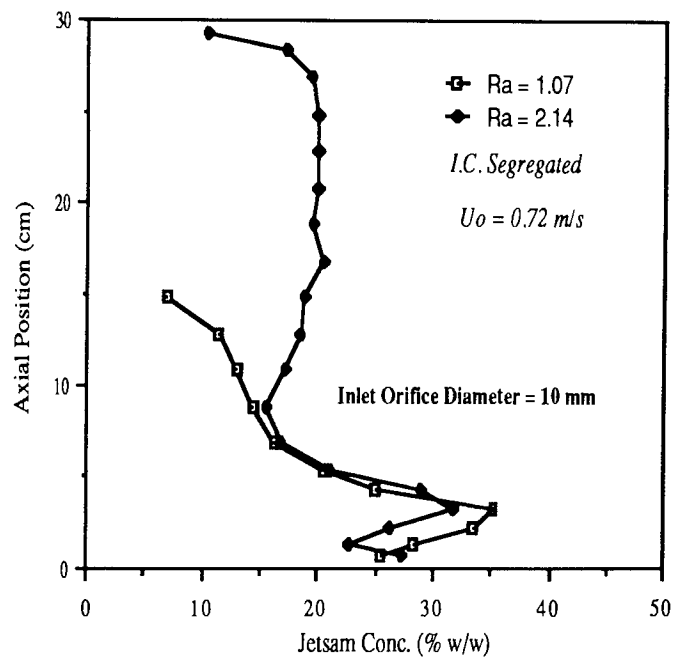


Fig.7.21: Effect of the Aspect Ratio (Ra) on the Conc. Profile

The spout showed some signs of deterioration in the deeper bed although air bubbles were not detected near the surface. The spout height above the expanded bed surface was also reduced; 12 cm with the shallower bed and only 7 cm with the deeper bed.

7.4.3 The Polycylinder / ABS Cylinder System

This system is different from the other systems tested because of the shape factor. Both the solids were cylindrical, approximately similar in length but of different diameter. There are various parameters used to characterise cylindrical particles; the author has used the 'equivalent mean spherical diameter' to aid comparison with spherical particles. The term 'equivalent mean spherical diameter' is the diameter of a sphere having the same surface area as the cylindrical particle. The equivalent mean spherical diameter ratio of the cylindrical solids was 2.3. The role of jetsam was played by the ABS cylinders at a constant weight fraction of 0.1, while the static bed height was kept constant at 18.5cm.

Effect of Orifice Size

The experiments were carried out with 3 different orifice diameters, namely 10, 14 and 17 mm. Again, in all cases, a stable full fountain was established by adjusting the air flow rate to the bed. Figure 7.22 illustrates the concentration profiles obtained for this system. All the experiments were carried out at a spouting velocity of 0.45 m/s and, in all cases, a very tall and somewhat tilted spout was observed; the average height of the spout recorded varied from 30 to 40 cm above the spout bed height. A number of interesting features emerged from this work and these are listed below:

- a) The diameter of the air inlet does not seem to have any effect on the concentration profile.
- b) All the bed remains in what can be described as the undeveloped zone with poor mixing in both axial and radial directions. This observation is in complete contrast with those made in studies of other systems.
- c) The spout was elevated well above the bed surface (≈ 37 cm tall; expanded bed height at 19.3 cm)
- d) The particle movement was very sluggish

Effect of the Spouting Velocity

In an attempt to improve the mixing, a further experiment was conducted at a higher superficial velocity while using the 10mm diameter air orifice inlet. The spouting velocity was increased from 0.48 m/s to 0.63 m/s. The minimum spouting velocity of this mixture as measured was 0.44 m/s. The two profiles obtained at these spouting velocities are compared in Figure 7.23.

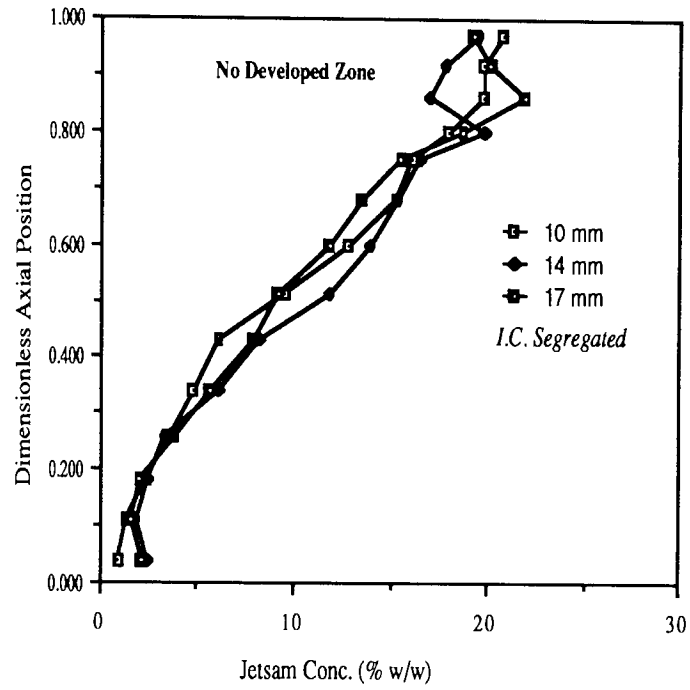


Fig.7.22: Effect of the Inlet Orifice diameter on the Conc. Profile

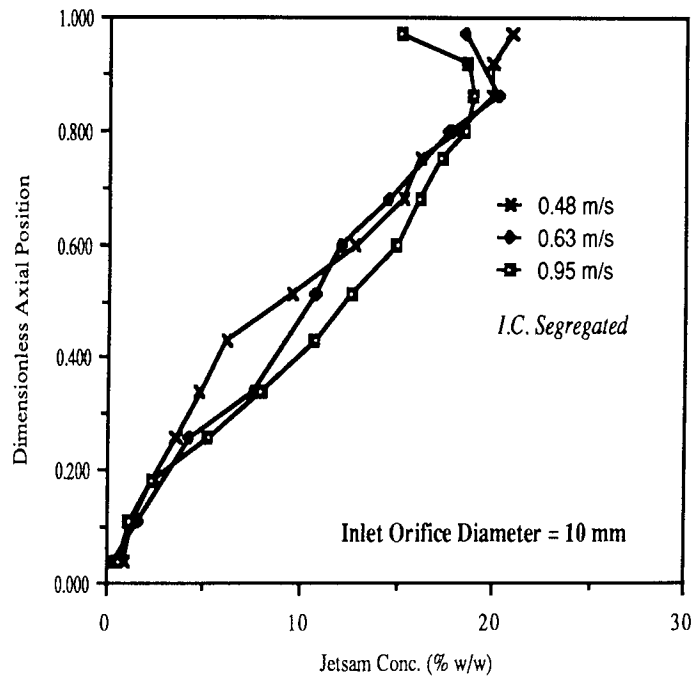


Fig.7.23: Effect of the Spouting Velocity

The concentration profiles illustrate that even the higher spouting velocity fails to improve the mixing. The concentration profile obtained at $U_0 = 0.63$ m/s was very similar to the one obtained at $U_0 = 0.48$ m/s. The general spouting and particle mixing behaviour were very similar in both the cases. The increase in the spouting velocity further increased the height of spout to 45.0 cm.

A further experiment was conducted with spouting velocity at 0.95 m/s. This further increases the height of the spout to 60.0 cm with polycylinders getting severely entrained in the air stream. The concentration profile thus obtained is also shown in Figure 7.23. A reduced jetsam concentration at the top section can be noticed which is mainly due to the entrainment effects.

Effect of the Aspect ratio (Ra)

To establish if the developed zone appears somewhat higher in the bed, the static bed height was doubled from 18.2cm to 35.6cm. A slightly higher spouting velocity, 0.5 m/s, was needed to establish a stable spout with this deeper bed. Again a much taller spout was formed extruding nearly 20 cm above the expanded bed surface. The bed appeared to be stagnant up to 25 cm in height and, above this level, some particle movement was noticed. Figure 7.24 compares the concentration profiles obtained at these two bed heights.

Once again, only a slight improvement in mixing was achieved. There appears to be some uniformity of jetsam concentration in the upper one third of the bed and it could be argued that a developed zone is beginning to emerge. But there is no clear indication of the sudden change, e.g. emergence of a developed zone, which has been observed with the other systems studied. However, it can be expected that a developed zone can be established in the bed with aspect ratio higher than 2.6. This illustrates that the formation of the developed zone is firmly related to the physical characteristics and especially to the shape factor of the solids in question.

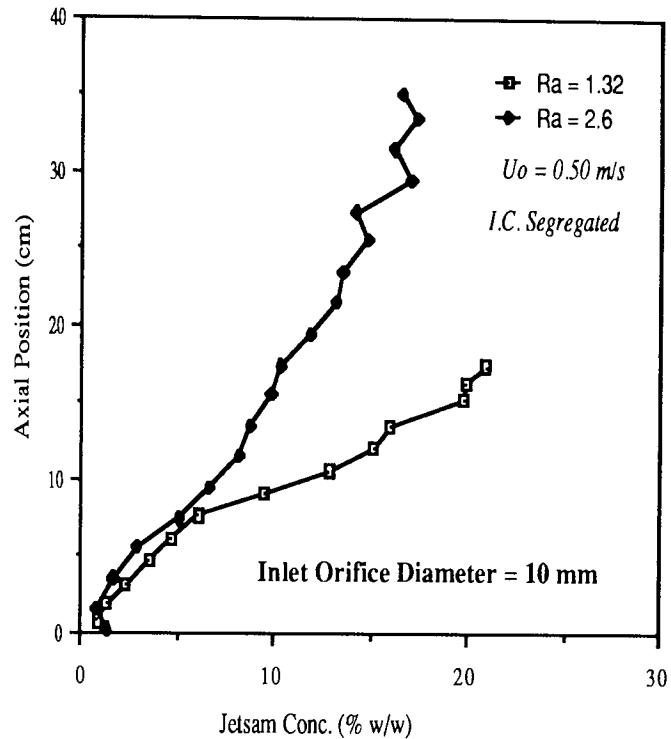


Fig.7.24: Effect of the Aspect Ratio (Ra_0) on the Conc. Profile

7.4.4 The Polybead 1550 / Polybead 925 System

This is a **jetsam-rich** system containing 90% of the larger particles and 10% of the smaller polybead particles. Both the solids are of the same material having the same density but differing in colour and size. The role of jetsam was played by the white Polybeads1550 and the flotsam was olive green Polybeads925. The particle size ratio was 1.68. The static height of the bed was kept constant at 22.6cm, while flotsam was always placed at the top.

Effect of Orifice Size

Six different diameters of air inlet orifice were used. Again, in all cases, a stable fountain was maintained by adjusting the air flow rate to the bed. Table 7.3 shows the air flows required in order to maintain a stable full fountain with each orifice. The data reveal that only a 20% increase in the volumetric air flow rate was required when the orifice diameter was increased by over 4 times.

Table 7.3 Summary of the Operating Variables
The Polybead 1550 / Polybead 925 System

Orifice Dia. D_i (mm)	Superficial Air Velocity U_o m/s	Velocity at Orifice U_{oi} m/s	$\log(U_{oi})$
6	0.47	250	2.40
8	0.49	141	2.15
10	0.53	101	2.00
14	0.54	52	1.70
17	0.55	34	1.54
25	0.57	17	1.23

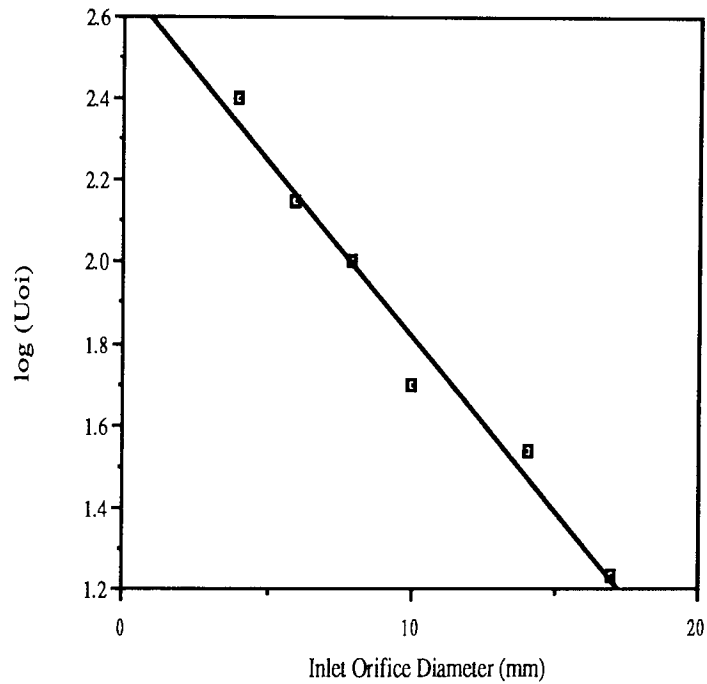


Fig.7.25: Inlet Orifice Diameter vs log (Uoi)

These data are presented graphically in Figure 7.26 which shows that a substantially higher air velocity is required to establish a stable fountain for the smaller orifices. The following mathematical equation best describes the relationship

between the inlet orifice diameter and the superficial velocity at the inlet orifice.

$$\log (U_{oi}) = 2.6825 - 0.086 \cdot D_i \quad (7.2)$$

where

U_{oi} is the superficial air velocity at the orifice (m/s)

and D_i is the inlet orifice diameter (mm)

Two distinct flow regimes were observed. The initial introduction of air created a fluidising condition in the flotsam layer until this upper layer became a bubbling fluidising bed, with the jetsam particles acting as an extended distributor. When the bed was analysed at the end of a run, it was found that virtually no mixing had taken place. This indicates that mixing in a jetsam-rich system will only take place if the air flowrate is higher than the minimum spouting velocity of the mixture.

On further increasing the air flowrate a spout was developed and mixing did take place. The flotsam particles were then swept down by the column wall and instantaneously a concentrated band of flotsam particles was formed a few centimeters above the distributor. This band divided the column into two distinctly separate zones and identical to the ones established with the Ballotini 1090 / polybeads 1850 system (this was a different density system).

Typical concentration profiles for this system are shown in Figure 7.26. It was found that the peak of the curve, i.e. where the concentration of the jetsam is a minimum and that of the flotsam a maximum, corresponds to the centreline of the flotsam concentration band.

The height of this band above the distributor varied with orifice diameter. The jetsam particles appeared to form a packed bed below this band; whereas above, solid mixing took place. In the annulus, flotsam solids underwent "stick-slip" motion near the bed surface where the upward motion of the flotsam particles was constantly being suppressed by the jetsam particles.

Figure 7.27 shows the concentration profiles of this system using 6, 8, 10 and 14mm diameter orifice inlets. The effect of the inlet diameter on the peak point is clear; increasing the inlet diameter elevates this point. The initial increase from 6 mm to 8 mm produced a jump in the band height but then the changes were more gradual. The flotsam concentration at the band also varies with the change in inlet

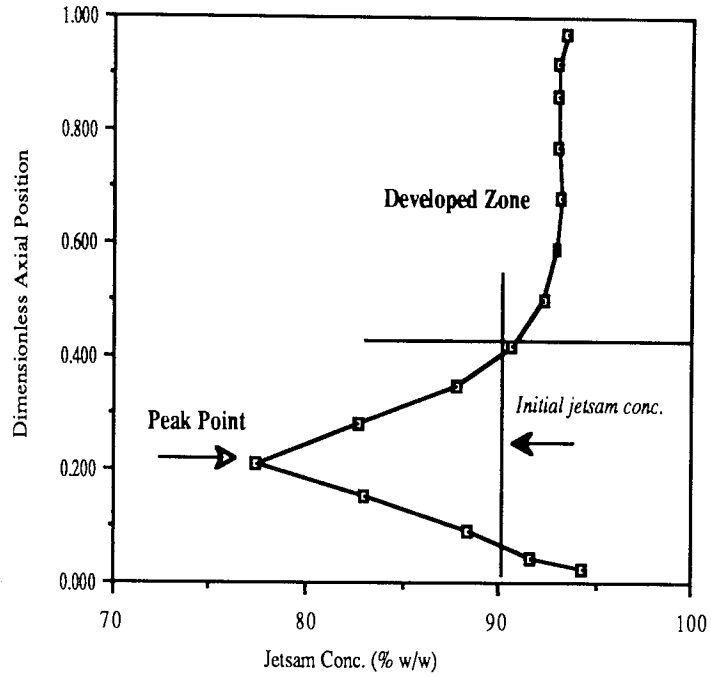


Fig.7.26: Typical concentration profile

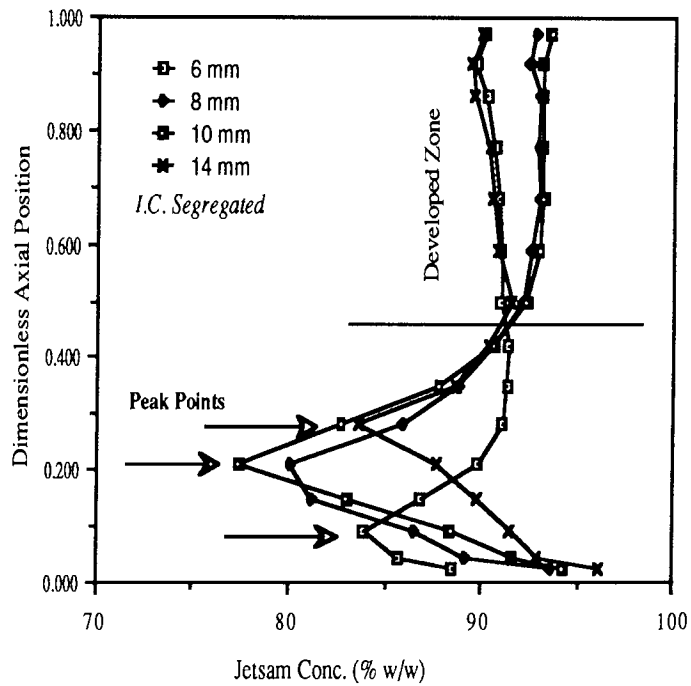


Fig.7.27: Effect of the Inlet Orifice diameter on the Conc. Profile

orifice diameter, but in rather an erratic way. The actual thickness of the bands appeared to be constant and they looked very similar to each other. The spout was very similar as well; ≈ 8 cm above the expanded bed height of 23.2 cm.

The effect of the orifice inlet diameter was further explored with two other inlets namely 17 mm and 25 mm. The profiles obtained are shown in Figure 7.28 which also shows the profiles for the 8, 10 and 14 mm diameter inlet. The figure shows that a systematic pattern is emerging in these concentration profiles with regard to the position of their peak point on the vertical scale. The profiles of the 8 and 10mm inlets have similar peak points except that the latter is sharper than the former. The peak point has shifted higher in the bed with the 14 mm inlet; the 17 mm and 25 mm orifices gave similar results.

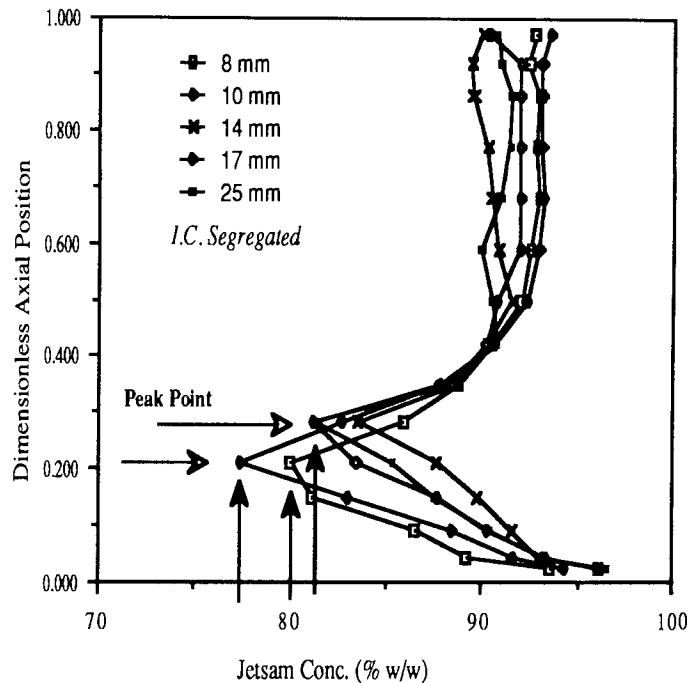


Fig.7.28: Effect of the Inlet Orifice Diameter

The effect of the inlet orifice diameter can best be described by plotting the diameter against the flotsam band concentration, as shown in Figure 7.29. The band height initially increases with the increase in the inlet diameter but then levels off. It can be anticipated that the band height would stay stationary even if the inlet diameter were to be further increased.

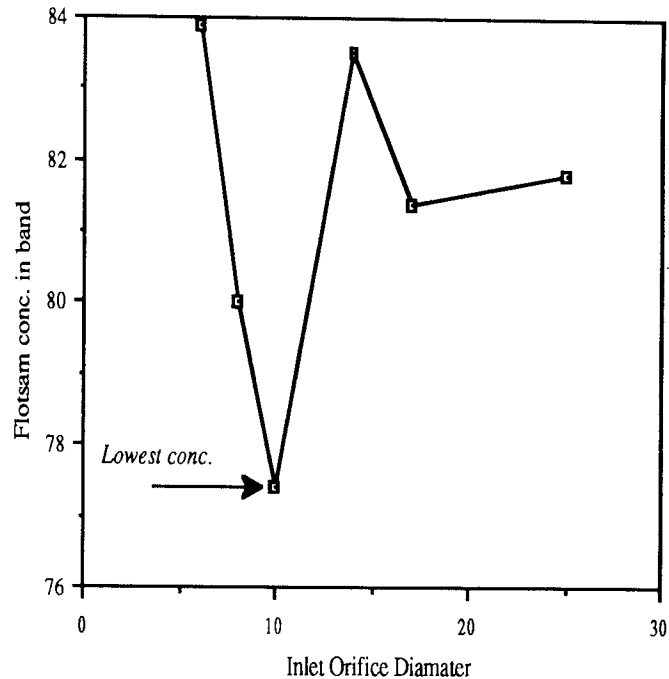


Fig.7.29: Effect of the Inlet Orifice Diameter on the Flotsam Concentration Band

Effect of the Initial Condition

The effect of the initial condition of the solids on the concentration profiles when using the 10mm diameter inlet is shown in Figure 7.30. One profile was obtained when the solids were completely segregated and flotsam was placed on top of the jetsam. The other profile was obtained when the experiment was conducted with a fully mixed bed; ten equi-weight portions of the solid were mixed separately by hand and placed in the bed.

Both the concentration profiles are identical in shape above the peak point, the jetsam concentration being 10% higher in the case of the 'segregated' profile. The spout heights in both cases were similar = 31.0 cm. Below the peak point, the effect of the initial conditions is obviously more marked. An interesting feature emerging from this figure is that the change in the initial condition had no effect on the height of the concentrated flotsam band. However, it once again illustrated the similar mixing trend regardless of the initial starting position. The slight difference in the jetsam concentration level in these two profiles was expected due to the different initial starting conditions.

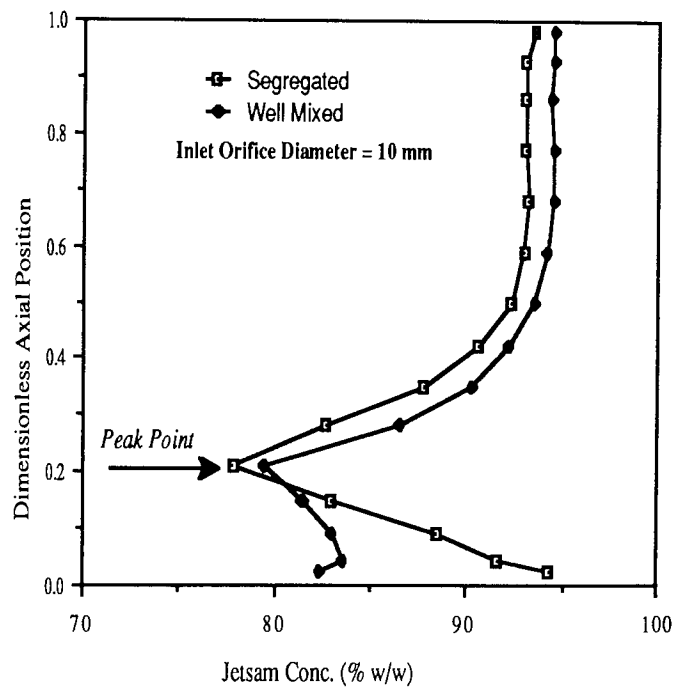


Fig.7.30: Effect of the Initial Condition

CHAPTER 8

DISCUSSION, CONCLUSION AND RECOMMENDATIONS

8.1 Discussion

Mixing and segregation experiments have been carried out in a flat-bottomed spouted bed instead of the conventional form with a conical bottom. The reasons for this were:

- a) the lack of adequate design information for the conical bottom vessel
- b) to aid comparison with experiments with other systems

Mathur and Epstein (1974) state that "the exact design of the gas inlet has an important effect on spouting stability; however, the question of inlet construction has received insufficient attention". The researchers at the National Research Council of Canada have found, by trial and error, that spouting is more stable when the gas inlet orifice is somewhat smaller than the narrow end of the cone. The use of a flat bottom allows the system to develop its own cone. Indeed, the author's work demonstrates that the angle of the cone varies from system to system and with different inlet diameters. An attempt made to reconstruct the cone by successively removing the layers during a mixing experiment using the ABS Cylinder/ Polybead system with a 10 mm diameter orifice inlet is shown in Figure 7.10. A second cone, shown in Figure 7.15, was constructed using contours obtained with the Polybead 1850 / Ballotini 1090 system. A comparison of these cones points to that disadvantage of using one type of conical section for various experimental systems.

In all cases, a partial fountain (spout) was established, where the particles fall on only part of the annular surface and the fountain envelope does not reach the vessel wall. The layer-by-layer analysis of the spouted bed suggests that the bed is made of three distinct regions. Region I in the upper part of the annulus where the particles move uniformly and intense mixing takes place, ignoring some disturbance observed at the top where the flow is perturbed by the fountain. This region is frequently referred to as "*The Developed Zone*" in this present work. Region II is where the solids leave Region I and converge inward to the spout and are finally taken up into the spout. Finally, Region III corresponds to the dead zone formed near the distributor. The size of these three regions is dependent on a number of operating parameters and solid characteristics. A diagrammatic illustration of these regions in a spouted bed is shown in Figure 8.1.

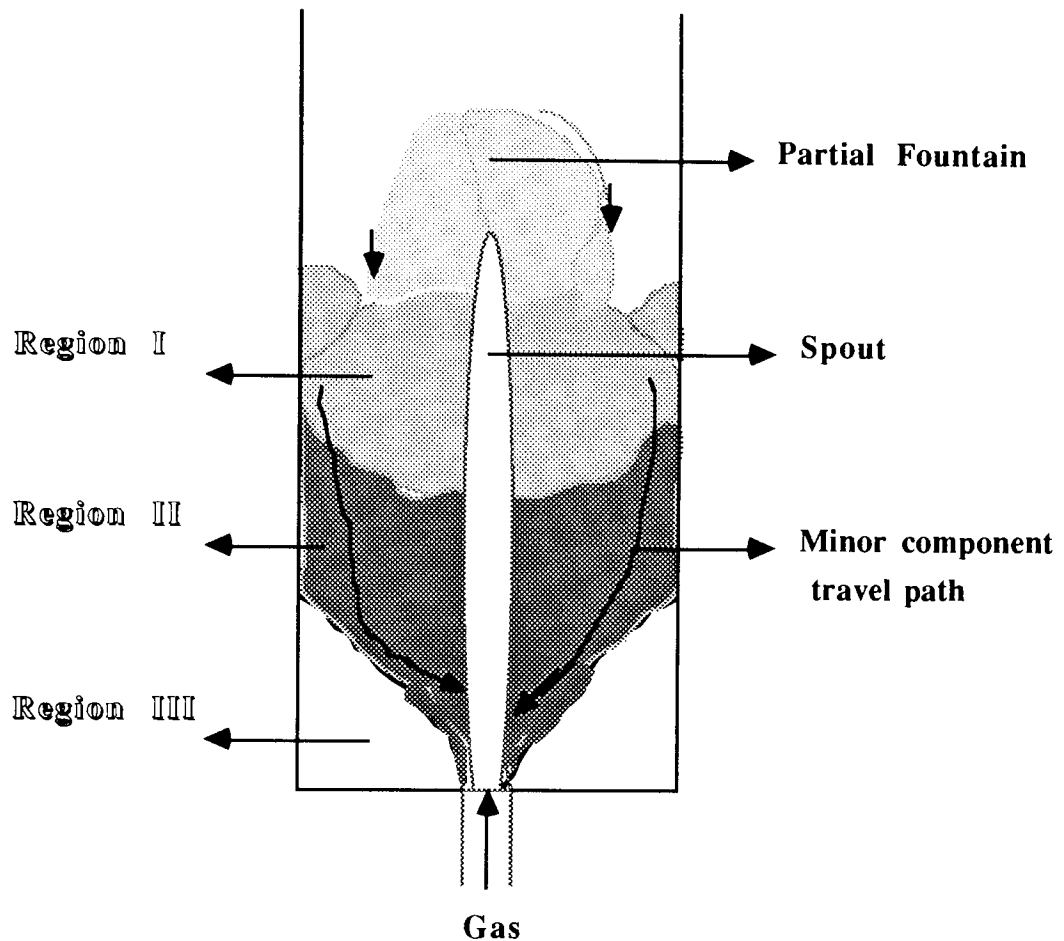


Fig. 8.1: The spouted bed as observed

The work was carried out with four particle systems which cover a wide spectrum of physical characteristics. The other general observations made can be summarised as follows.

For the flotsam-rich equi-density system (i.e. ABS Cylinders / Polybead 1090), the spouted bed led to good mixing just above the minimum fluidising velocity of the mixture. The variation in inlet orifice diameter altered the position of the developed zone; this in turn would have an effect on the design of the conical section of a column. The cone angle appears to depend to some extent on the internal friction characteristics of the solids and was found to be 57° for this system. This finding is in slight disagreement with Hunt et al. (1965) who states that for most materials its value is in the region of 40° .

The findings were more complicated in the case where both the density and size were different (i.e. Ballotini / Polybeads). For moderately shallow beds ($Ra = 1$), the spouted bed served as a good mixer basically due to the density difference. However, when the aspect ratio was ≥ 2.0 , good mixing could occur only if the conical section was quite steep. The cone angle in this case was found to be 27° which is substantially different from the unidensity ABS Cylinders / Polybeads system.

The effect of the shape factor was explored with the ABS Cylinders / Polycylinder system. The experiments were carried out with three different inlet orifice diameters and showed that the concentration profile is virtually independent of this variable and that the resulting mixing of the solids was much more feeble than in true spouting. This finding is in line with Becker's (1961) observation, that, in the case of strongly ellipsoidal particles, such as flexseed and barley, although a channel resembling a spout was formed by the air jet in the bed, the resulting agitation was very feeble. The results show that the 'pseudo-spout' formed was unaffected by the variation in orifice inlet diameter and aspect ratio and behaved like a solids free channel, which probably owed its stability to the interlocking tendency of the particles. Reddy et al. (1968) in their experiments using deep beds of polystyrene observed a similar phenomenon.

The behaviour of particle mixing / segregation in a jetsam-rich, equi-density system was observed with Polybeads 1550 / Polybeads 925, containing 90% jetsam. Using the 90% jetsam concentration line to assess the mixing behaviour (Figures 7.27 & 7.28), it was noted that the upper portions of all the curves on the right hand side of this line are vertical, show little scatter and lie within a relatively narrow band. However, the situation is completely different on the left hand side where the effect of the inlet diameter is more visually pronounced. The work shows that the height of the undeveloped zone is dependent upon the inlet diameter; increasing the diameter increases the height of this zone until the inlet diameter is 17mm where it stabilises.

The general shape of the concentration profile is independent of the initial condition of the bed with the peak point staying at the same level. Only a small increase in the air flowrate is required to establish a stable fountain on increasing the inlet diameter. However, it should be noted that the minimum spouting velocity is much more affected by the inlet diameter; increasing the inlet

diameter from 6mm to 25mm leads to a fifteen-fold decrease in velocity.

8.2 Conclusions

This is probably the first time that the analysis of a spouted bed has been carried out by sectioning the bed layer-by-layer. This method of analysis and the use of a flat-bottomed spout bed provided new insight into the spouted bed system.

- a) The spout bed consists of three regions and the upper region (developed zone) is where the intense mixing takes place.
- b) There is an optimum gas inlet orifice diameter which relates to the physical characteristics of the solids employed. Variation in this diameter can aggravate mixing.
- c) The conical section of the spouted bed varies widely with the type of solids to be treated and needs to be carefully designed for each individual system. The standardisation of this factor could lead to poor performance of the spouted bed system.
- d) In the case of the unidensity jetsam rich system and different density flotsam rich system, a band of concentrated minor component was formed a centimeter above the distributor. The vertical location of this band appeared to be directly related to the gas inlet orifice diameter.
- e) Beds rich in cylindrical particles behaved completely differently from the spherical particle rich beds. The bed stayed completely segregated at the normal operating condition; even the bed with an aspect ratio of 2.6 did not produce any developed zone.

8.2 Recommendations for Future Work

Future gas-spouted bed mixing/segregation studies should focus on five principal areas:

- 1) Development of a set of rules for the design of the conical section of the spouted bed.

- 2) Experiments aimed at developing the relative mixing / segregation behaviour of a large number of different solids systems.
- 3) Experiments aimed at explaining the different behaviour observed with cylindrical particles and at establishing the principles which make them behave differently from spherical particles.
- 4) Development of a correlation to predict mixing and segregation behaviour under prescribed operating conditions.
- 5) Experiments to determine the scale-up effects.

Item 1 should be carried out such that parameter interactions and beds having more than two component solids are included. Formation of dead zones and their relation with the gas inlet orifice and other operating parameters need to be explored.

Items 2, 3 and 4 are closely related and are concerned with the solid system employed. Obviously this study is needed to establish a firm basis for general design methods. It will be difficult to establish a universal correlation to encompass all systems.

Scale-up factors and the transfer of the experimental results on to the industrial scale are of fundamental importance for designers of spouted bed reactors. Mixing and segregation behaviour is likely to be strongly influenced by the size of the spouted bed, especially with regard to large-scale convection parameters. Thus, some large-scale experiments will be essential in establishing the validity of bench scale data.

SECTION III
THE SPOUT-FLUID BED
CONTAINING
CHAPTERS 9, 10 & 11.

CHAPTER 9

THE SPOUT-FLUID BED

9.1 Introduction

Although the fluidised bed has a number of advantages over its competitors, it also has some disadvantages which severely restrict its use in industry, one of these being its limitation to handle large particles. Davidson and Harrison (1962) and Lefroy (1966) have concluded that the effectiveness of the fluidised bed is seriously impaired due to bypassing of gas in the form of large bubbles when handling particles ≥ 1 mm diameter.

The problem of handling large particles in a fluidised bed can be overcome by a special version called the *spouted bed*. Here, a high velocity air jet is injected through an orifice at the bottom of the column. This high velocity jet causes a stream of particles to rise rapidly through the centre of the column: this region is known as the spout. The particles rise above the bed surface and rain down in a fountain onto the outer edge of the bed known as the "annular region". The particles then gradually descend downward and inward until they are drawn into the spouted region and are forced upward again. Mathur (1971) states that the regime of stable spouting is critically dependent on certain conditions and unless these are satisfied, the movement of solids becomes random, leading to a state of aggregative fluidisation, and with increase in fluid flow to slugging. The main parameters involved are particle size and size distribution, gas -inlet diameter, column diameter, cone angle, gas flow rate and bed depth.

A modification of the usual spouted bed is the "*spout-fluid bed*" where gas from the central large orifice is supplemented by auxiliary gas from much smaller orifices spaced in a regular pattern. Kono (1980) has found that the addition of the auxiliary gas further helps to prevent agglomeration and sintering and improved gas-solid contacting. The idea of superimposing a fluidising action on an already spouted bed, or vice versa, has received the attention of several investigators. Chatterjee (1970) was probably the first research worker to investigate the hydrodynamic behaviour of a bed in which spouting and fluidisation occur simultaneously. Chatterjee found that such a system, like an ordinary spouting bed, overcomes the limitations of stratification and slugging inherent in a fluidised bed, but without the restrictions with respect to particle size and bed depth which are

associated with the stability of the usual spout-bed. He further argued that the excess gas flow required for "spout-fluidising" is well spent, since with the annulus fluidised, the effectiveness of gas-solid contact is improved and so is the intermixing of solids. Chatterjee's spout-fluid bed is diagrammatically shown in figure 9.1.

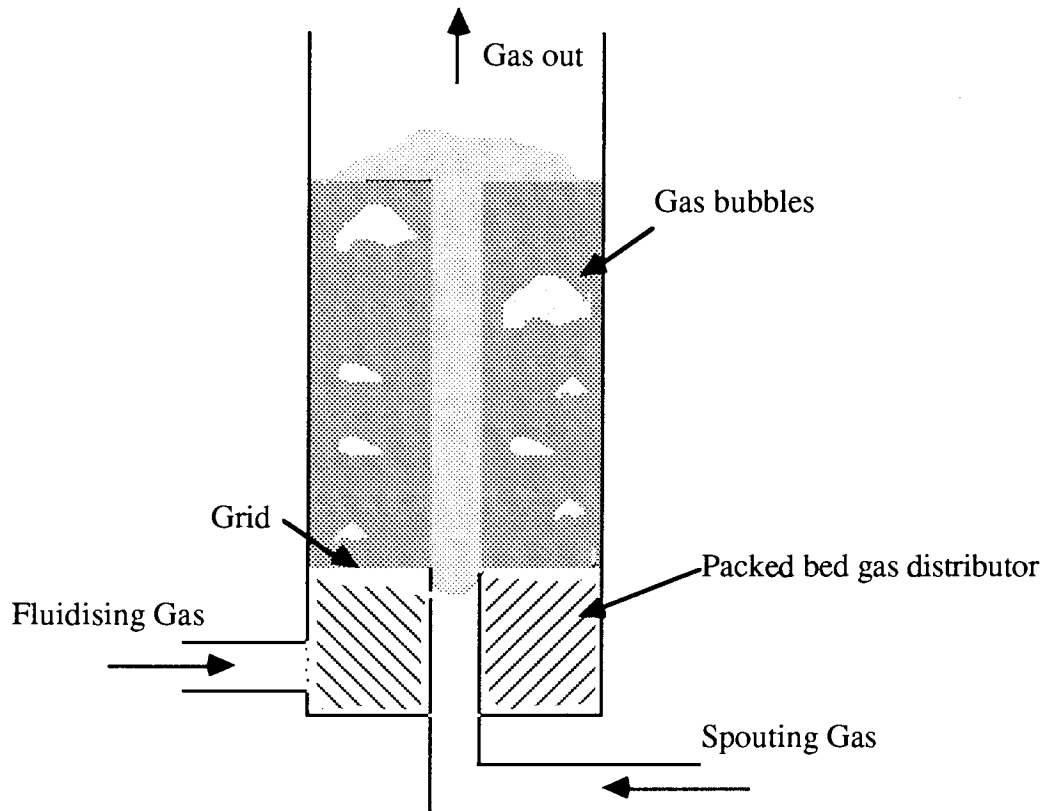


Fig.9.1: Spout-fluidised bed (adapted from Chatterjee (1970))

Nagarkatti and Chatterjee (1974) investigated the bed properties at different values of fluid flow rate, particle diameter, orifice diameter and bed height. They applied the theory of Mamuro and Hattori (1968) to obtain a correlation equation for the minimum spout-fluidisation velocity. The equation of Mathur and Gishler (1955) was used to determine the minimum spouting velocity.

Littman et al. (1974) measured the minimum spout-fluid flow rate as a function of bed height and nozzle diameter for a spout-fluidised bed with water. They used an extension of the theory of Mamuro and Hattori (1968) to explain the

annulus pressure drop.

Hadzisdmajlovic et al.(1983) studied the mechanics of spout-fluid beds at the minimum spout-fluid flowrate. They used various formulae developed mainly for spouted beds to establish a correlation for determining the spout diameter, the maximum spoutable height and annular pressure drop in a spout-fluid bed.

Heil and Tels (1983) published their findings into the pressure distribution in spout-fluid bed reactors. They used a pressure probe to sense the pressure and found that the pressure measurement with a probe near or in the spout channel can influence the entire bed; therefore, the results could be erroneous and not reproducible. They managed to establish a computer model to predict pressure distribution when the bed was in a stable spouted-bed regime.

9.2. Flow Regimes

The flow regime maps built up for spout-fluid beds by various research workers display differences, partly due to variation in distributor geometry and partly due to differences in the terminology. Littman et al.(1976), for example, in using the term spout-fluid bed, refer to a condition in which the normal spouting is accompanied by additional aeration, but not fluidisation, of the annulus, whereas the pioneer Chatterjee (1970), in using the same term, refers to a condition in which the annulus particles surrounding the central spout are actually fluidised.

Recently, an excellent piece of research work has been presented by Sutanto (1983) identifying the various flow regimes in a spout-fluid bed. The experiments were carried out in a cylindrical 'half-column' of diameter 152 mm and height 1.05 m fitted with a 60° conical base perforated distributor. The central spouting air was supplied by either a 19.1 or 25.4 mm diameter semi circular orifice. The fluidising air was supplied through 35x3 mm diameter orifices along the conical base. Each of these auxiliary gas distribution chambers was connected via a separate control valve and orifice plate to the air supply to allow independent control of the fluidising air flow. Polystyrene particles of 2.9 mm diameter were used giving a bed depth of 600 mm. However, he used two variants to determine the flow regimes:

- a) by adjusting the central air flow while holding the auxiliary air flow constant .

- b) by stepwise changing the auxiliary flow while the central air flow was fixed.

Sutanto observed that the visual differences in flow regimes were quite distinct and were accompanied by changes in the bed pressure drop or pressure fluctuations. Sutanto plotted the auxiliary (fluidising) air flow rate (q) against the central (spouting) air flow rate (Q), both normalised with respect to the minimum fluidisation flow rate (q_{mf}). A copy of Sutanto's plot is shown in Figure 9.2.

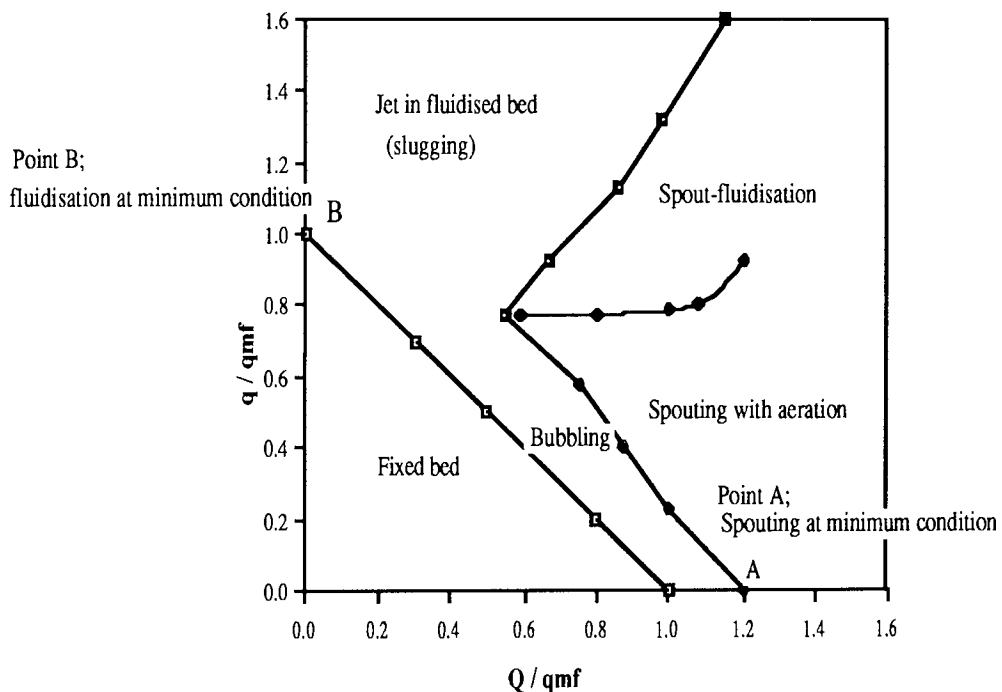


Fig.9.2: Regimes map for polystyrene particle ($d_p = 19.1 \text{ mm}$ & $H_b = 600 \text{ mm}$) (adapted from Sutanto (1983))

Sutanto (1983) rationalised the observations into four main flow regimes. A summary of the four flow regimes supplemented by the diagrams displayed in Figure 9.3 is given below:

- 1) **Fixed bed:** The particles stayed immobilised and formed a fixed bed when the total flow of central air and auxiliary air was less than the minimum fluidisation flow rate. This is shown in Figure 9.3a.

- 2) ***Jet in fluidised bed:*** When the total flow rate was greater than the minimum fluidisation flow rate (q_{mf}), the bed exhibited two fluidisation states. When the auxiliary flow was high, slugging occurred in the upper part of the bed, similar to that in the conventional fluidised beds. At lower auxiliary flow rates, smaller bubbles reached the bed surface. The transition between these two subregimes was gradual: Figures 9.3b and 9.3c shows these two regimes.
- 3) ***Spouting with aeration:*** The bed gives an appearance of a conventional spouted bed when a relatively small auxiliary flow rate is accompanied by a large central flow rate. Figure 9.3d shows a typical bed exhibiting this regime.
- 4) ***Spout-fluidisation:*** Sutanto designated only one regime as true spout-fluidisation and this is shown in Figure 9.3e. He states that, in this regime, stable spouting could not be achieved. Instead, the particles in the upper section were fluidised, while the spout below showed instability, periodically discharging bubbles near the surface. In the case of millet seeds ($d_p=2.3\text{mm}$), he found that bubbles were forming only a few centimeters above the central orifice. He drew attention to the close resemblance of this regime with that of a conventional spouted bed operated at, or just above, the maximum spouting height.

Sutanto also constructed regime maps for two other types of solids, namely millet and polyethylene, at various bed heights. The general behaviour was similar but there were some apparent differences. For example, the more angular polystyrene particles had a more extensive spouting-with-aeration region and were more likely to slug than the polyethylene and millet. A reduction in the spouting with aeration was noticed by increasing the inlet orifice diameter. In all cases, transitions between different regimes were more gradual than implied by the sharp boundaries in Figure 9.2.

Vukovic et al. (1984) also studied the flow regimes for a spout-fluid bed. The experiments were performed in a cylindrical column, 70 mm in diameter and 1 m in length using a spout inlet tube 15 mm in diameter. Calcium carbonate particles, 1.8 mm in diameter with a density of 2600 kg/m^3 were used as the solid phase, air

and water were used as the spout-fluidising fluids. Two separate fluid inlets were used, one for the spout and the other for the annulus. The results were used to create flow regime maps: they identified three flow regimes.

Regime 1: When the total flow rate was above the minimum spout-fluidisation velocity, the bed was very similar in appearance to that of an ordinary spouted bed. The initial bed height was equal to or less than H_{mSF} (the maximum spoutable height at the minimum spout-fluidisation flow rate). This regime is identical to Sutanto's "spouting with aeration" regime.

Regime 2: Further increase in the annular flow rate with a constant spoutable flow rate created some bubbles in the annulus but mainly near the surface. This regime is similar to the initial stages of Sutanto's "spout-fluidisation" regime.

Regime 3: Further increases in the annular flow rate caused fluidisation (i.e. bubbling) at lower and lower levels in the annulus. Finally, when the annular flow rate reached the minimum fluidisation velocity, the bottom of the annulus was just fluidised and bubbles originated there. This, again, resembles a part of Sutanto's spout-fluidisation regime.

9.3. The Author's Spout-Fluid Bed System

The development of spout-fluid beds offers a new approach to the solution of gas-solid handling problems. However, a number of operational features still need to be investigated, one being the careful balance that is required between the spout and annulus fluid flow rate. A limited amount of research has been undertaken as outlined in the previous sections, but there are other options to be explored. Instead of supplying two different flowrates for fluidising and spouting, the author chose to use a common plenum chamber similar to that for a fluidised bed. The distributor was similar to the one commonly used for the spout-fluid bed, i.e. a large diameter orifice in the centre to generate a spout and a number of smaller orifices arranged peripherally to create a fluidising effect. It was anticipated that the large diameter orifice would first become operative and that, at higher flow rates, the smaller orifices would become active.

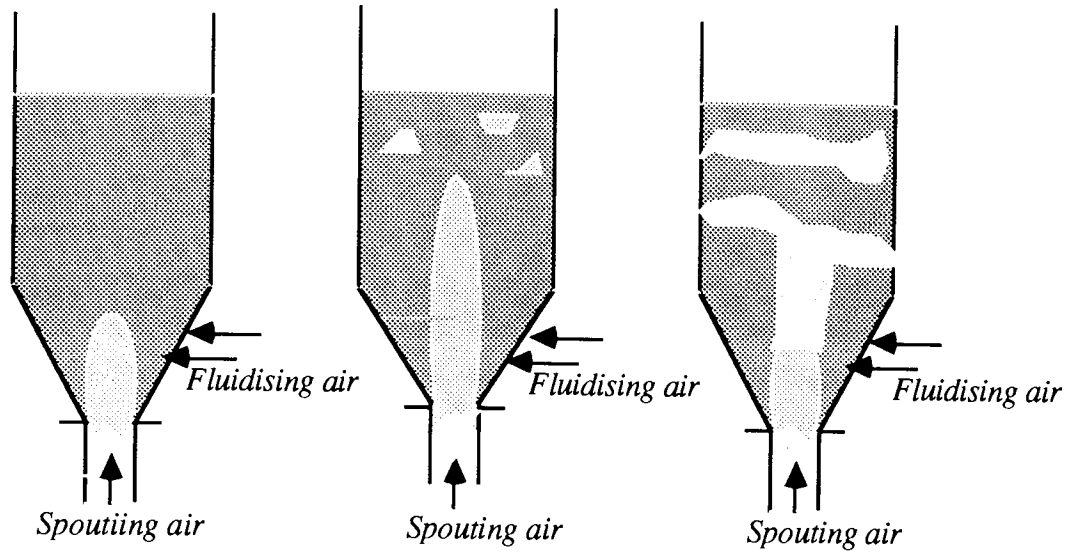


Fig. 9.3a:
Fixed bed

Fig. 9.3b:
Jet in Fluidised bed
(with bubbles)

Fig. 9.3c:
Jet in Fluidised bed
(slugging)

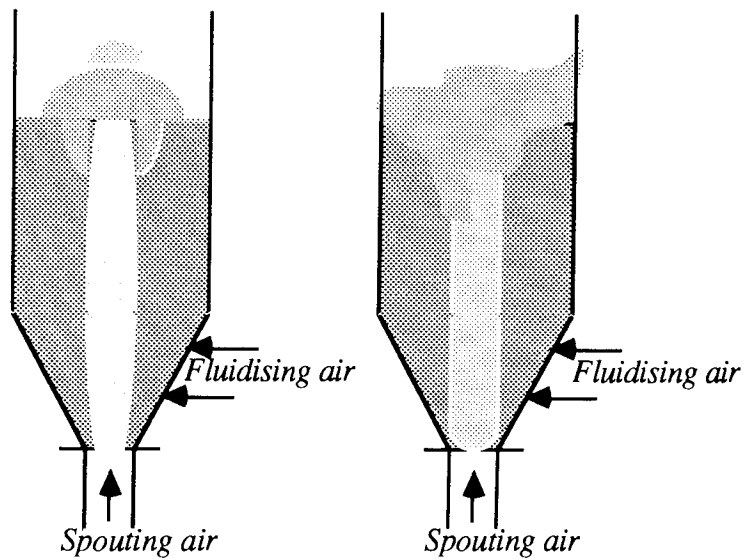


Fig. 9.3d:
Spouting with aeration

Fig. 9.3e:
Spout-fluidisation

Fig.9.3 a-e: Physical appearance of the various flow regimes in spout-fluidisation
(adapted from Sutanto (1983))

The choice of the central orifice diameter was a difficult one. A review of the spouted bed literature revealed that, generally, the central orifice diameter to bed diameter ratio is 0.1. The author, therefore, decided to use various diameters for the central orifice giving a range of 4 to 18% of the bed diameter. The size and configurations of the peripheral orifices were decided after an extensive literature review. The various combinations of the central orifice and peripheral orifices were used to provide eleven different distributors. Complete details of these distributors are given in Table 9.1; Figure 9.4 is a photograph of the distributors. The dimensional drawings of these distributors are given in Appendix 2.

Each distributor has been assigned a number followed by a coded description of the orifices sizes. For example, in the case of Distributor no.6 (10/18x1.5), the first number in the bracket reveals the size of the central orifice, i.e. 10 mm, the second gives the number of the peripheral orifices multiplied by the size of the peripheral orifice diameter in mm. This approach is used for the reader's convenience when discussing different distributors.

All the distributor plates were constructed from 13mm thick clear perspex sheet. Each plate was carefully marked and then drilled. To prevent weeping of particles, a 325 mesh wire gauze was attached to the upper surface of the distributors used.

Table 9.1 : Details of the Central and Peripheral Orifices for Distributors

Bed Diameter - 138 mm

Distributor no.	Central Orifice dia. (mm)	Peripheral dia. (mm)	Peripheral no.	Orifice Pitch* (cm)	Total Free area (%)
1.	6	1	150	1	0.98
2.	6	2	36	2	0.95
3.	6	2	13	-	0.65
4.	6	1	35	-	0.37
5.	6	1.5	54	1.5	0.82
6.	6	1.5	18	3.0	0.40
7.	10	1.5	18	3.0	0.73
8.	14	1.5	18	3.0	1.24
9.	9.5	1.5	18	3.0	0.68
10.	17	1.5	18	3.0	1.73
11.	25	1.5	18	3.0	3.51

* All the peripheral holes were **triangularly** pitched

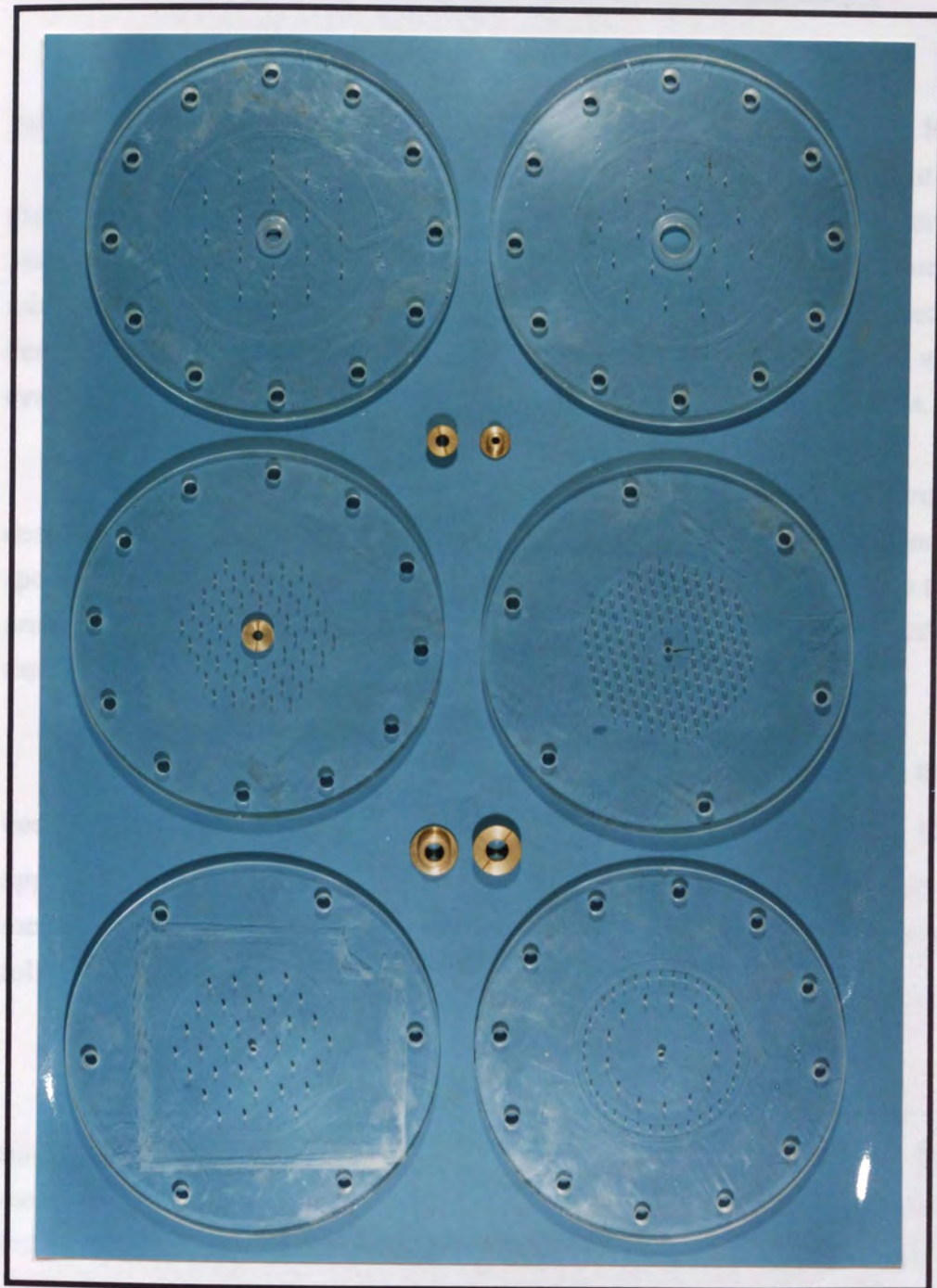


Fig. 9.4 Photograph showing the various distributors used in spout-fluid bed experiments.

CHAPTER 10

SPOUT-FLUID BED- EXPERIMENTAL RESULTS

10.1 Measurement of the Minimum Spout-fluidisation Velocity

It was essential to find out the minimum velocity required to spout-fluidise the bed because of the unique way of introducing the fluid. However, it was anticipated that the value of the spout-fluidisation velocity would be related to the minimum fluidisation velocity. The experimental procedure has been described in detail in Section 4.1. The spout-fluidisation velocity of each solid was first evaluated and then, the minimum spout-fluidisation velocity of the mixtures.

All the experiments were carried out in the 138 mm i.d. perspex bed described in Chapter 3. The bed was fitted with different types of distributor and the spout-fluidising air was metered by the flow rig shown in Figure 3.3. The total bed pressure drop was measured by a 0.15 mm i.d. tube placed in the bed directly above the distributor.

For each binary system both U_{sfq} and U_{sfs} were found. In both cases the bed was spout-fluidised at a superficial air velocity of $U_o > 2.0 U_{sfj}$ for approximately 10 minutes after which the maximum bed pressure drop was measured. Then the two composite spout-fluidisation velocities were measured following the procedure shown in Figure 4.1.

Experimental Results

Experiments were initially conducted with Dist. no. 9 (10/18x1.5) and the minimum spout- fluidisation velocity of all the solids under investigations was measured. Figure 10.1 shows a minimum spout-fluidisation velocity curve for red Polycylinders. The general shape and pattern of the curve is similar to the curves obtained for minimum fluidisation and minimum spouting velocities. When the bed is changed from the static state to an active one, it behaves more like a spouted bed than a fluidised bed. This is evident from the sharp drop observed in the ΔP -velocity curve following the change in bed status from the static / expanded to spout-fluidised. A minimum spout-fluidisation velocity curve for a binary mixture of Polybeads 1550 (90%) and Polybeads 925 (10%) is shown in Figure 10.2: again these curves follow the standard pattern. A central spout was established in

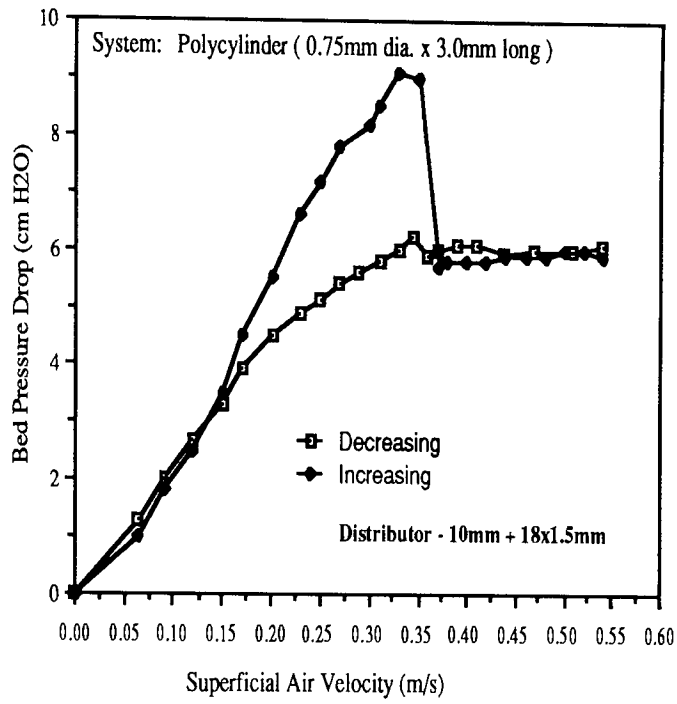


Fig.10.1: Minimum spout-fluid velocity curve

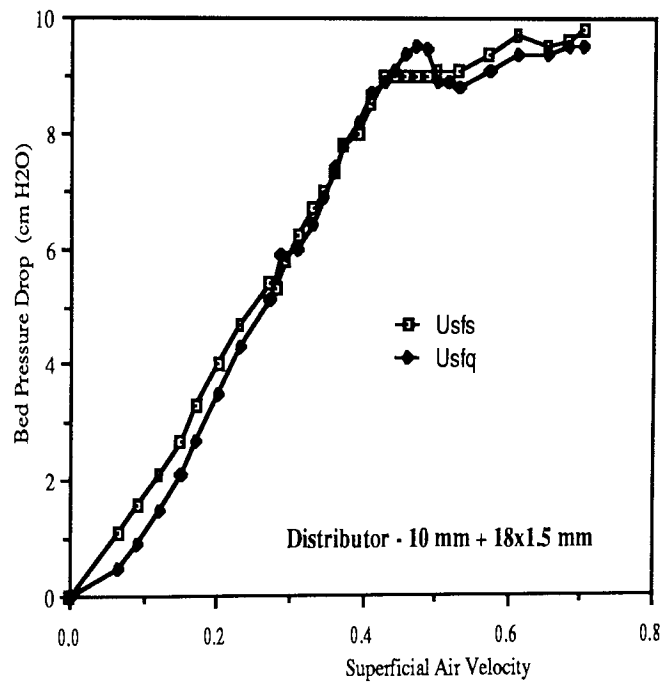


Fig.10.2: Spout-fluid velocity curve - Polybeads 1550 / Polybeads 925 (90% / 10%)

each case at a superficial air velocity slightly greater than the minimum spout-fluidisation velocity. In the case of the unidensity systems containing a majority of spherical particles the spout was short and flimsy, whereas in the case of unidensity, non spherical and different density, spherical particle systems, the spout was tall and very distinguished.

A very marginal effect of the distributor design was noticed and even that could be attributed to the experimental error. The pressure drop-velocity plots for the Polybeads 1850 (80% w/w) and Ballotini 1090 (20% w/w) system obtained with two different distributors are shown in Figure 10.3. Both of these plots give the same minimum spout-fluidisation velocity.

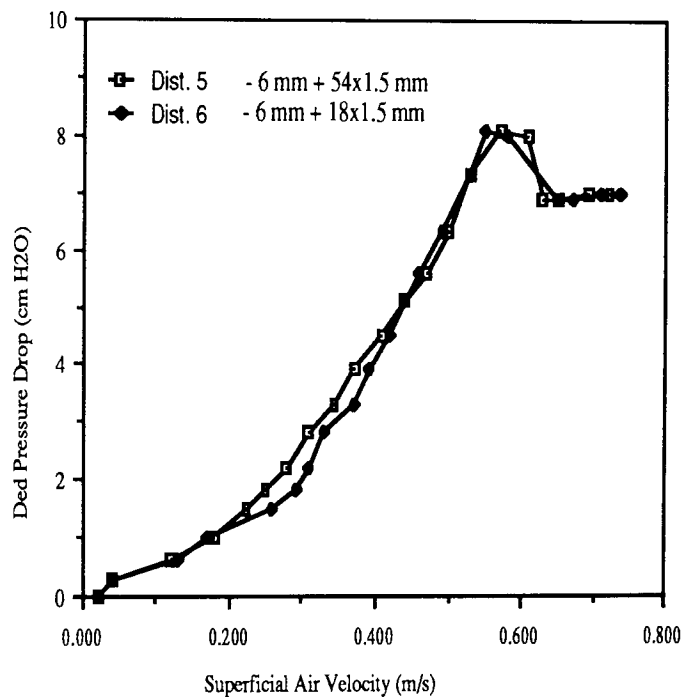


Fig.10.3: Effect of distributor design on the Minimum spout-fluiding velocity

The minimum spout-fluidisation velocity was found to be independent of the aspect ratio. The results obtained from a number of experimental studies confirmed that the value of the minimum spout-fluidisation velocity is unaffected by the changes in the bed height. Two typical plots are shown in Figure 10.4. The bed was composed of 75% w/w of Polybeads1090 and 25% w/w of ABS Cylinders. The aspect ratios were 1.1 and 2.0 respectively. The curves shown were obtained

when the superficial air velocity was steadily increased through the bed. The minimum spout-fluidisation velocity in both the cases was found to be 0.4 m/s.

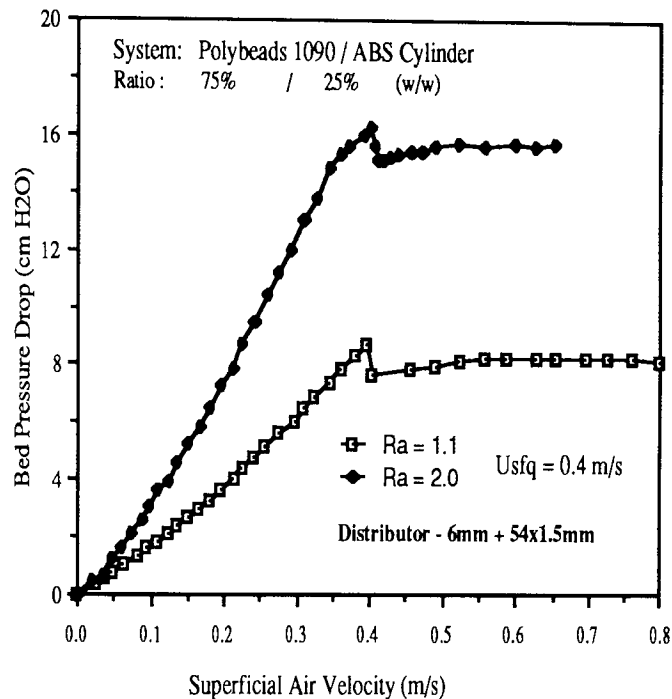


Fig.10.4: Effect of the Aspect Ratio (Ra) on the Minimum spout-fluidising velocity

A summary of the minimum spout-fluidising velocities of various mono- and binary systems is given in Table 10.1. These figures compare very well with the minimum fluidising velocities given in Table 4.3 for the same components. The small difference between the pairs of values can be safely attributed to experimental error. The behaviour of the bed during the experiments resembled closely spouted bed behaviour especially when the superficial air flow rate was increased steadily. In each case, initially a spout developed at the centre of bed surface and on further increasing the superficial air velocity, the bed behaved as a typical spout-fluid bed.

10.2 Flow Regimes

Preliminary experimental work was carried out to establish the various flow regimes that exist in the author's version of the spout-fluid bed. In all cases, the layer of minor component (generally jetsam) was placed at the bottom and then the major component was carefully placed on top. The static bed height was kept constant during every set of experiments. A predetermined air flow was

Table 10.1: Summary of the Minimum Spout-fluidisation Velocities

Systems	Solids	d (μm)	wt. %	U_{sf} (m/s)	U_{sfs} (m/s)	U_{sfq} (m/s)	U_{sfav} (m/s)
1	Polybeads	1090	90	0.32	0.38	0.36	0.37
	ABS Cylinder	2400	10	0.79			
2	Ballotini	550	80	0.29	0.375	0.345	0.36
	Ballotini	1090	20	0.67			
3	Polybeads	1850	80	0.61	0.68	0.60	0.64
	Ballotini	1090	20	0.67			
4	Polycylinder	750	90	0.32	0.44	0.46	0.45
	ABS Cylinder	2400	10	0.79			
5	Polybeads	1550	90	0.50	0.46	0.48	0.47
	Polybeads	925	10	0.29			
6	Polybeads	1090	75	0.32	0.42	0.39	0.405
	ABS Cylinder	2400	25	0.79			
7	Polybeads	1090	50	0.32	0.47	0.43	0.45
	ABS Cylinder	2400	50	0.79			
8	Polybeads	1090	25	0.32	0.63	0.58	0.605
	ABS Cylinder	2400	75	0.79			
9	Polybeads	1090	10	0.32	0.73	0.65	0.68
	ABS Cylinder	2400	90	0.79			

All the systems except no.5 were *flotsam rich*

passed through the bed and then the bed was sectioned to establish the height of spout penetration. In each series of experiment the above procedure was repeated several times after gradually increasing the air flow rate through the bed. After a series of experiments, the static bed height was changed and the series was repeated. At least two bed heights were investigated. The experimental results for one system, operated at two different bed heights, are reported below.

The experiments were carried out in the 138 mm diameter cylindrical column fitted with Distributor No.7 (10/18x1.5). The system employed was Ballotini 1090 / Polybeads 1850 (20% / 80% w/w). The yellow Ballotini particles were placed at the bottom and white Polybeads at the top. Both of these solids have a similar u_{mf} . Eleven experiments were carried out at different air flowrates, but six main stages were noticed. Figure 10.5a-f is a schematic diagram of the physical appearance of the spout-fluid bed at a various flowrates. The bed behaved as a fixed bed at $u_0=0.53$ m/s; the first appearance of a spout at the centre was noticed at $u_0=0.61$ m/s but its appearance was intermittent. A clear spout emerged at $u_0=0.68$ m/s; the spout was in the centre occupying ≈ 6 cm circle in the middle. The total spout height was 22.5 cm whereas the expanded bed height was 20.8 cm. On further increasing the air flowrate to 0.75 m/s, the spout was increased to 25.5 cm covering a 7.5 cm circle in the middle of the bed. At 0.85 m/s, the spout elongated to 28.0 cm and bed expanded to 21.5 cm. At this stage it was anticipated that increasing the air flowrate would increase the length of spout, the bed becoming more and more violent. Figure 10.5f shows at a typical case: the superficial air velocity was 1.4 m/s; this gave a spout height of 35.0 cm, the bed moving towards the transport mode. On increasing the superficial air velocity still further, it was found that the spout always existed. The conclusion to be drawn from these experiments is that the existence of the spout is not totally dependent on the superficial velocity.

The effect of doubling the static bed height to 39.0 cm was also explored. The schematic diagrams of this bed at three different superficial air velocities are shown in Figure 10.6a-c.

The physical appearance showed that a central spout always existed and even when the bed height had been substantially increased but stayed immersed inside the bed. Interestingly in all cases, the spout height stayed virtually constant at 22.0 cm and above this level was converted into small bubbles. Further increase in

System: **Ballotini 1090 / Polybeads 1850**
 20% 80% (w/w)
I.C. **Jetsam (Ballotini 1090) at the bottom**
Distributor 7: **10 mm + 18x1.5 mm**
Bed Height: **19.5 cm**

■ Ballotini 1090 (20% w/w)
 ■ Polybeads 1850 (80% w/w)

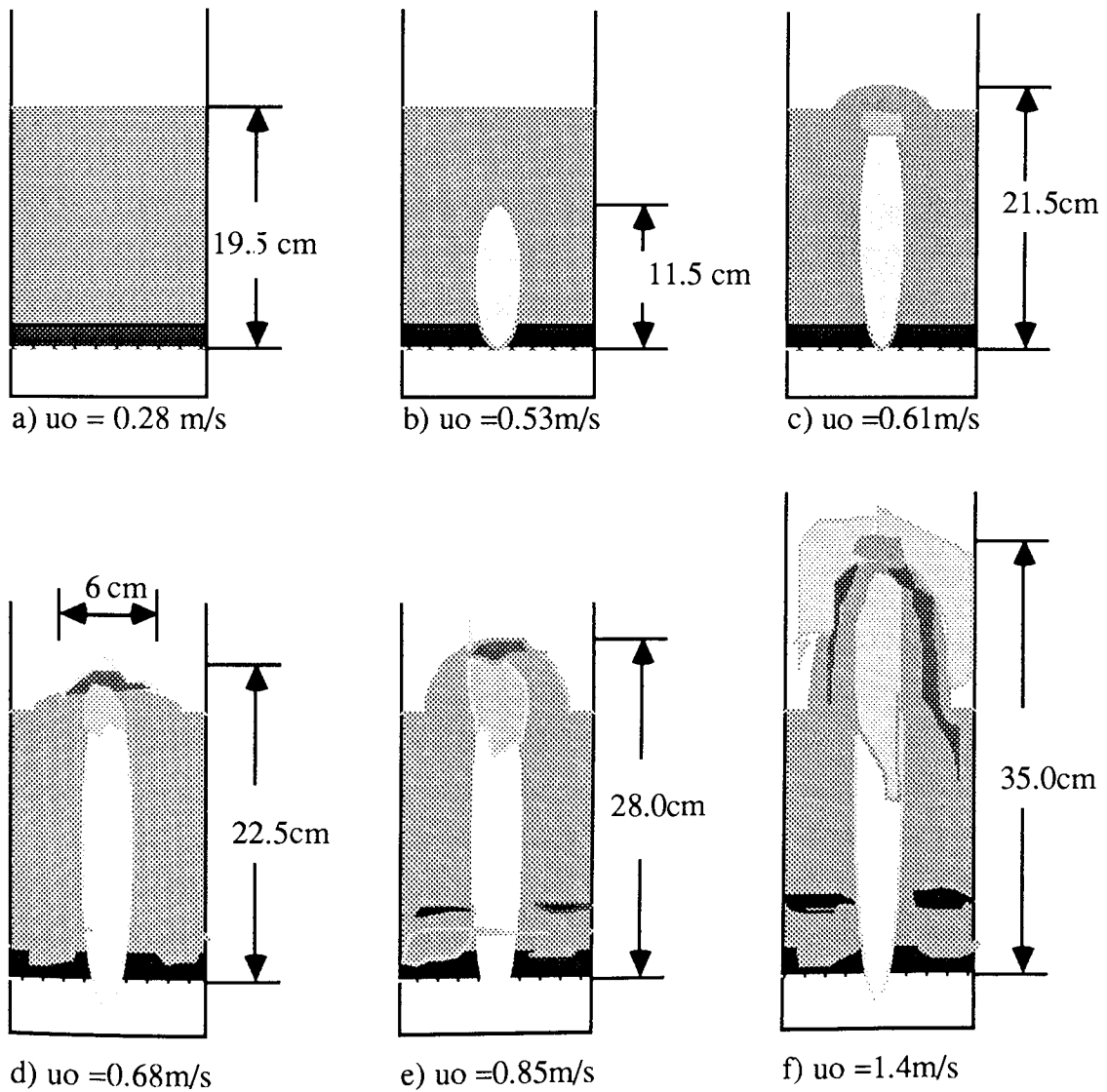


Fig.10.5a-f: Physical appearance of the various flow regimes as observed.

the superficial air velocity created bigger and bigger bubbles which eventually became equal to the bed diameter and led to slugging. This behaviour was always observed at velocities higher than 0.85 m/s, with the slugging becoming stronger.

This brief but effective study confirmed that the author's version of the *spout-fluid bed* performs in a manner similar to that of the conventional spout-fluid bed where fluid is supplied by two separate inlets, one for spouting and the other for fluidising. In both cases, a clear visible spout can be developed provided the bed height is less than the maximum spoutable height - a typical 'spouting with aeration' version as designated by Sutanto (1983). The author's study shows that even at higher superficial velocities a central spout exists, whereas Sutanto in his "spout-fluidisation" regime did not achieve a stable spout: it is believed that the instability of the spout was caused by the semi-circular column wall. A detailed study into the development of these flow regimes is essential but regrettably this is outside the scope of the present study.

10.3. The Experimental Strategy - Solids Mixing / Segregation

Spouting offers advantages when handling large particles and so preference for this mechanism was maintained in all experimental work:

- a) by keeping the static bed height to less than the maximum spoutable height and
- b) by maintaining the superficial air velocity at a higher level than that required for spouting.

Two main parameters were initially chosen as the central foci for the mixing / segregation experiments: these were the effect of the central spout orifice diameter and the diameter and configuration of the peripheral (annular) orifices. Eleven distributors with different size/configuration of central and peripheral orifices were studied but the data obtained from only nine distributors have been reported in this work. Details of which are given in Table 9.1. Six other parameters were explored; these were particle size, particle density, spouting/fluidising air velocity, static bed height, overall bed composition and initial condition. The work was carried out with a number of binary and some tertiary systems but the work with only five binary systems is presented here.

System: **Ballotini 1090 / Polybeads 1850**

20% 80% w/w

I.C. Jetsam (Ballotini) at the bottom

Distributor 7: 10 mm + 18x1.5 mm

Bed Height: 39.0 cm

- Ballotini 1850 (20% w/w)
- ▣ Polybeads 1090 (80% w/w)

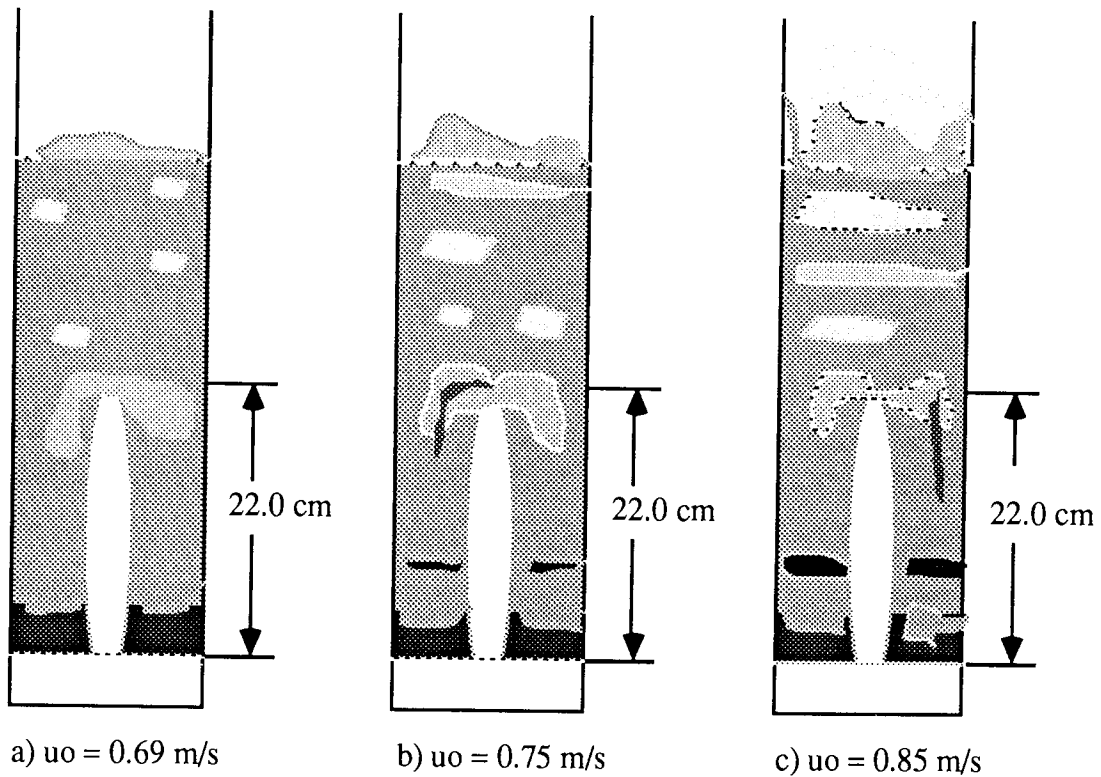


Fig.10.6a-c: Physical appearance of the various flow regimes ($H_b = 39.0$ cm)

It was not feasible to set up a detailed factorial design because of the relatively large number of variables and the considerable time involved in running a single experiment and analysing the samples (usually about 2 hours). Uncertainty as to the appropriate parameter levels to use in the design was yet another problem. Consequently, the approach used was largely heuristic and the search for general patterns of behaviour was emphasised at the expense of mathematical modelling and empirical correlation.

10.4 Experimental Results - Solids Mixing/Segregation

10.4.1 The ABS Cylinders / Polybeads System

This was a binary system of equidensity particles but having a different shape factor. The spherical particles were white expandable polystyrene with a size range of 1000 - 1180 μm , which acted as flotsam occupying 90% of the bed. The black ABS particles were cylindrical in shape, 2.4 mm in diameter and 3.0 mm long, occupying 10% of the bed and acting as jetsam; the equivalent spherical particle diameter, based upon the circumferential area, was 7.2 mm. The static bed height and aspect ratio were kept constant at 21.6 cm and 1.6 respectively. The superficial air velocity ranged from 0.46 m/s to 0.49 m/s.

The experiments were mainly carried out from the completely segregated state when the jetsam was neatly placed on the top of the flotsam, giving an initial Mixing Index of $x = 0.1$. However, some experiments were carried out from the 'well mixed' state, where the particles were initially well mixed by fluidising the mixture vigorously at a superficial velocity higher than the u_{mf} of jetsam for 15 min.

In one series of experiments, the diameter of the centre hole was varied while the spherical holes were kept constant: in a second series, the distributors had a centre hole of fixed size, while the configuration of the peripheral holes was altered.

The results are presented graphically with jetsam concentration plotted against Dimensionless Axial Position (DAP). The general shape of the curves is similar: the jetsam concentration is very low at the bottom of the bed, increasing gradually along the DAP axis until it stabilises. The lower portion is designated the 'undeveloped zone' and the upper portion the 'developed zone'. The author's

experience has shown that this will always be the case with a spout-fluid bed system in a flat bottomed, cylindrical column.

Effect of Distributor Design

The effect of the variation of the centre hole size on the concentration profiles was initially studied with three distributors. The centre hole diameters used were 6, 10 and 14 mm, while the peripheral holes were kept constant at 18x1.5 mm at 3 cm triangular pitch. A distinctly different concentration profile was obtained even with this modest centre hole size variation. The profiles thus obtained are shown in Figure 10.7.

The figure shows that in all three cases the transition from the underdeveloped to the developed zone occurred at exactly the same point. Also there is an optimum centre hole diameter which will give the best mixing; variation from this optimum diameter in any direction promotes segregation; the optimum can vary from system to system. However, for the system in hand the optimum diameter is 10 mm, leading to a steady average jetsam concentration of 12.8% in the developed zone.

Next, an investigation was made of the effect of the variation of the configuration, number and size of the peripheral holes while the central orifice diameter was the same in both cases. Two concentration profiles were obtained and they are shown in Figure 10.8. One distributor had a 6mm diameter central orifice and 18x1.5 mm peripheral orifices on a 3.0 cm triangular pitch, while the second one had a 6 mm central orifice and 54x1.5 mm peripheral orifices on a 1.5 cm triangular pitch. The figure shows that the threefold increase in the number of peripheral orifices led to a slight improvement in particle mixing. The size of the developed zone increased from 55% to 65%: also, there was less variation of jetsam concentration in the developed zone giving an average jetsam concentration of 12.7%. The general pattern of the profiles is the same.

A comparison of this concentration profile with others obtained by changing the central orifice diameter shows that this profile lies close to the one obtained with Dist.7 (10/18x1.5), which contains a 10 mm diameter central orifice but only 18 instead of 54 peripheral orifices. The % free area of Dist.7 is 0.73% compared with 0.82% for the Dist 5 - giving a 9% difference in free area.

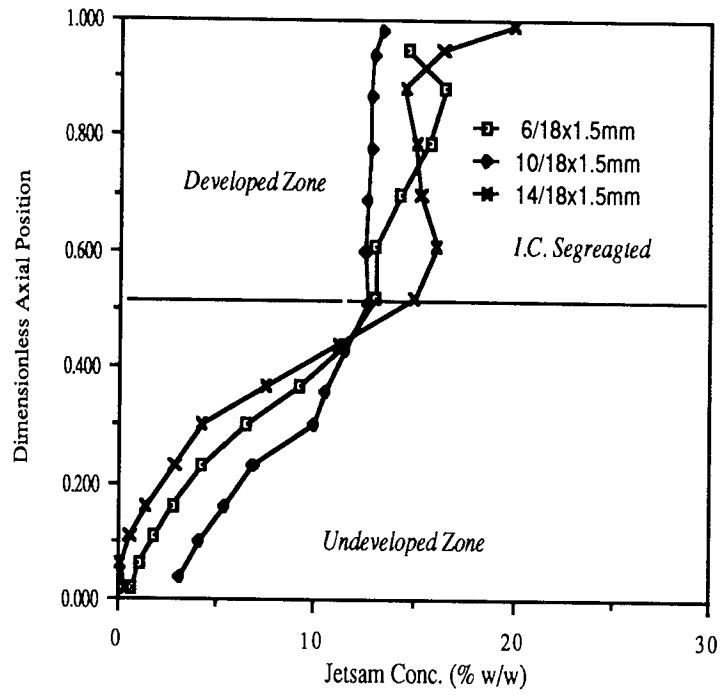


Fig.10.7: Effect of the central orifice diameter variation on the conc. profile

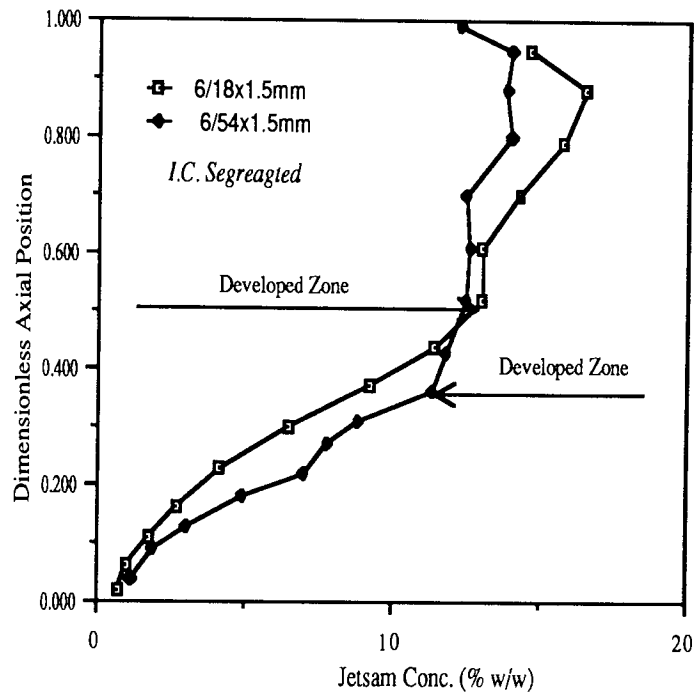


Fig.10.8: Effect of the peripheral orifices on the conc. profile

The superficial air velocity was also different; 0.45 m/s for Dist.5 (6/54x1.5) and 0.51 m/s for Dist.7 (10/18x1.5). The author's experience has shown that a somewhat higher superficial velocity is required to establish a stable spout for the distributors containing a large diameter central orifice, as discussed in Chapter 7. This difference in the superficial air velocity is evident from the spout height; the total spout height for Dist.7 was 35.5 cm and for Dist.5 was 27.0 cm. The similarity in these two profiles is shown in Figure 10.9.

Next, consideration was given to the effect of the position of the peripheral orifices on the jetsam concentration profile, using distributors with a 6 mm central orifice.

Figure 10.10 shows the jetsam concentration obtained with two different distributors. Dist.4 (6/35x1) contained 35 off one mm orifices drilled in the form of a circle 5 mm apart from the column wall and 71 mm radius from the centre. This configuration resulted in a gradual increase in the concentration profile, abolishing the distinction between the developed and undeveloped zones.

Introducing a further 13x2 mm orifices in the form of a circle 40 mm radius from the centre led to the second concentration profile shown in Figure 10.10. The % free area was therefore changed from 0.37% to 0.65%: this resulted in the generation of the two expected zones, the developed zone having an average concentration of 12% and occupying 63% of the bed.

The effect of the variation in peripheral orifices was further explored by conducting experiments with three distributors having a fixed central orifice diameter of 6 mm but different peripheral orifices. These were Distributors no. 1, 2, and 5 containing 150x1 mm, 36x2 mm and 54x1.5 mm orifices respectively. The concentration profiles thus obtained are shown in Figure 10.11. Those obtained with two distributors having 54x1.5 mm and 36x2.0 mm peripheral orifices are similar; the average jetsam concentrations in the developed zone are 12.7% and 13.5% respectively. Increasing the number of the orifices to 150 in Distributor no.1 resulted in a even better jetsam concentration profile, occupying 60% of the bed with an average jetsam concentration of 11.0%.

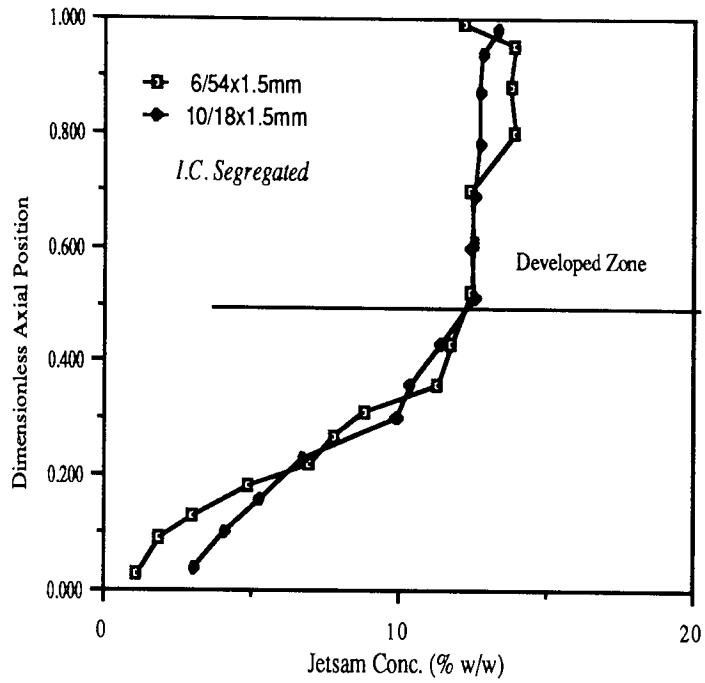


Fig.10.9: Similar conc. profiles obtained from two different distributors

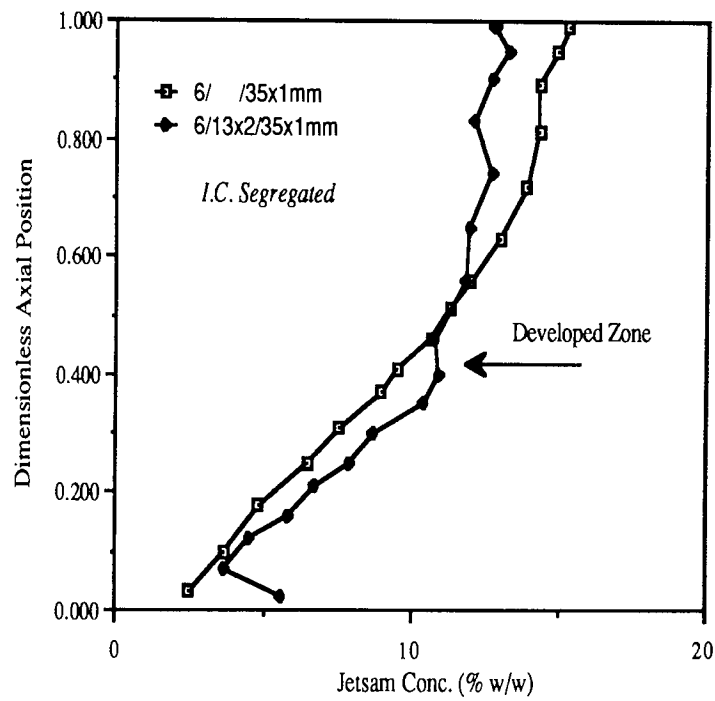


Fig.10.10: Effect of the peripheral orifice configuration on the conc. profile

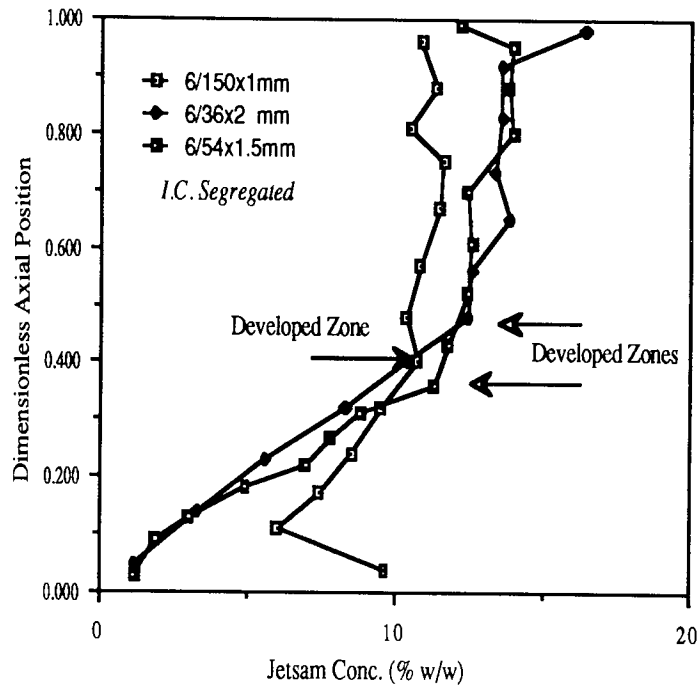


Fig.10.11: Effect of the peripheral orifices on the conc. profile

Analysis of the Data - The Mixing Number, S

In order to achieve the best mixing, one should look for the largest possible developed zone with the jetsam concentration close to that of the initial jetsam concentration. Alternatively, one strives to minimise the size of the developed zone.

To aid data analysis, a mathematical approach has been developed. This approach is tailor-made for analysis of the data obtained from the spout-fluid bed system and is different from the Mixing Index (MI), described in Section 3.6. This uses the area of the developed zone above the point on the DAP scale where the concentration plot intersects the average jetsam concentration to determine a mixing number.

Now, for the ideal case, i.e. for a perfectly mixed bed, the jetsam concentration will be 10% in the entire bed, i.e. over $DAP = 1.0$ and for the totally segregated mixture all the jetsam should stay at the distributor.

Therefore, a Mixing Number, S, can be defined as

$$S = \frac{[(\text{Average jetsam concentration}) - (\text{Initial jetsam concentration})]}{(\text{Size of the developed zone on the DAP scale})} \times$$

In practice, for spout-fluid beds in a flat bottomed cylindrical vessel, this will be impossible to achieve as part of the bed will be occupied by the undeveloped zone with a lower proportion of the jetsam than in the developed zone. Therefore, the distribution having the lowest mixing number, only in the developed zone, will be the best. The mixing numbers, S, for the various experimental runs have been calculated and are listed in performance order in Table 10.2. These figures clearly show that Dist.1 (6/150x1) led to the best mixing. Dist.3 (6/13x2/35x1) and Dist.7 (10/18x1.5), occupied second place with a mixing number of 0.7; this is followed by Dist.5 (6/54x1.5) with a mixing number of 1.0.

There appears to be a sharp difference between Dist.1 and Dist.8 - the two extremes. The point of intersection of these curves at the 10% concentration line is very similar i.e. 0.40 and 0.42; but the average jetsam concentrations in the developed zones are very different i.e. 11.0% and 15.4%. In case of Dist.1, the spout was only 4 cm higher than the bed surface with frequent bubbling by the column wall, whereas, in the case of Dist.8 (14/18x1.5), the spout was 8 cm above the bed surface, without any bubbling. This observation demonstrates that different mechanisms are controlling the particle movement in the bed and these mechanisms are related to the distributor design. It appears that a fluidisation mechanism is controlling the particle movement in the case of Dist.1 (6/150x1) whereas with Dist.8 (14/18 x1.5), the spouting mechanism is predominant. The distributors exhibiting the fluidisation as the controlling mechanism produced the highest mixing number in the Table 10.2.

The concentration profiles obtained with the four best distributors namely, Dist.1, Dist.7, Dist.3 and Dist.5 are shown in Figure10.12. These profiles show close similarity in the developed zone with a little difference in jetsam concentration on the distributor.

Table 10.2: Calculation of the Mixing Number, S

System: The ABS Cylinders / Polybeads 1090
I.C.: Segregated

Distributor numbers	Free area (%)	Point of intersection at 10% conc. line on DAP scale (A)	Average Jetsam % in developed zone (B)	S = A(B-10)
Dist.1 (6/150x1)	0.98	0.40	11.0	0.40
Dist.7 (10/18x1.5)	0.73	0.30	12.1	0.63
Dist.3 (6/13x2/35x1)	0.65	0.33	12.1	0.69
Dist.5 (6/54x1.5)	0.82	0.36	12.7	0.97
Dist.4 (6/35x1)	0.37	0.43	13.3	1.42
Dist.2 (6/36x2)	0.95	0.39	13.7	1.44
Dist.6 (6/18x1.5)	0.40	0.39	14.0	1.56
Dist.8 (14/18x1.5)	1.24	0.42	15.4	2.27

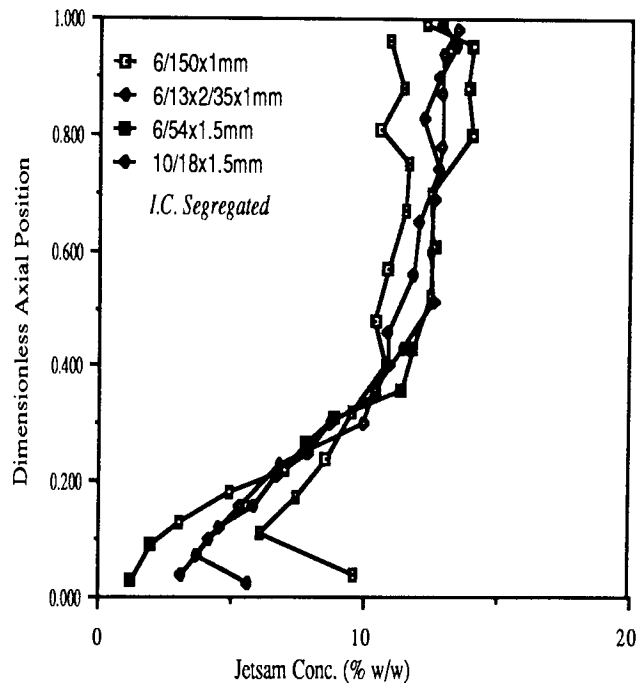


Fig.10.12: Four Conc. profiles with the best distributors

Effect of the Initial Condition

A set of experiments was carried out starting from the completely mixed mode, to examine the effect of the initial condition on the concentration profile. The mixture was prepared by vigorously mixing the particles at a superficial velocity of 2.6 m/s for 15 minutes. The air supply was then abruptly stopped and analysis of the bed confirmed that the particles were fully mixed.

The segregation experiments were conducted with five different distributors. In each case, particles were vigorously mixed and then the air supply was reduced to the desired superficial velocity for 10 minutes. The bed was then analysed, as previously described in Section 3.4. The concentration profiles obtained by using these four distributors are shown in Figure 10.13.

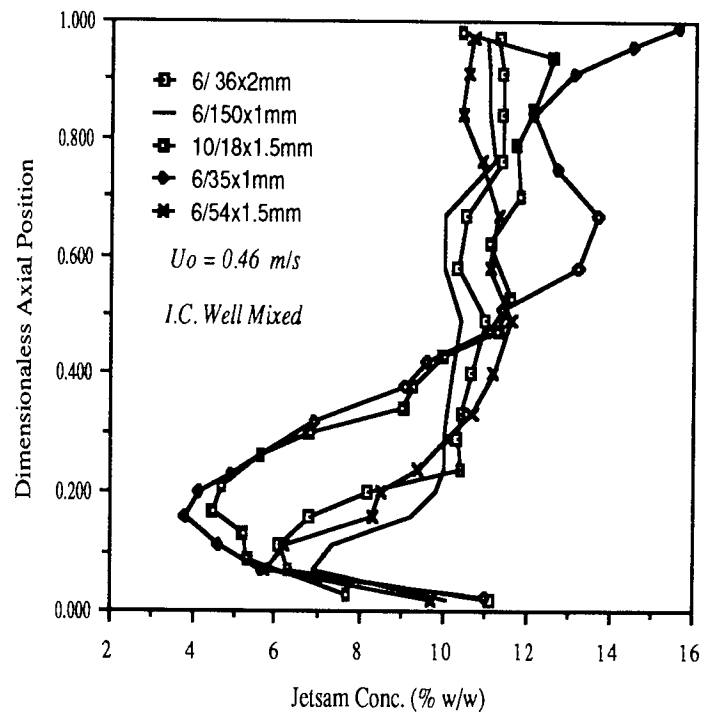


Fig. 10.13: Effect of Initial Condition on the Conc. Profile

The general pattern of the profiles with all the distributors is the same and will be divided into two main zones - the '*Developed Zone*' and the '*Undeveloped Zone*'. The jetsam concentration initially decreases as one travels from the distributor to the surface and it reaches a minimum at some position above the distributor, that will be described as the "*dip value*". This dip

value appears to be directly related to the free area of the distributors. Dist.1 (6/150x1) has 0.98% free area and the dip value of this plate is 7%; whereas Dist.4 (6/35x1) has 0.37% free area and its dip value is 3.7%.

The analysis of the experimental data was carried out in a similar manner to the 'segregated mode', as discussed in section 10.4.2. Once again the analysis was restricted to the developed zone when calculating the mixing number. The calculations are listed in Table 10.3.

Table 10.3 Calculation of the Mixing Number, S

System: The ABS Cylinder / Polybeads 1090
I.C. Segregated

Distributor numbers	Free area (%)	Dip Values	(A)	(B)	S = A(B-10)
Dist.1 (6/150x1)	0.98	7.0	0.20	10.4	0.08
Dist.2 (6/36x2)	0.95	6.2	0.22	10.8	0.18
Dist.5 (6/54x1.5)	0.82	5.5	0.34	11.1	0.38
Dist.7 (10/18x1.5)	0.68	4.6	0.43	11.4	0.60
Dist.4 (6/35x1)	0.37	3.7	0.45	12.9	1.30

where

A = Point of intersection at 10% concentration line on DAP scale

B = Average Jetsam % in developed zone

The best performance was obtained with distributors 1 and 2, both having a 6 mm central orifice and with 150x1 mm and 36x2 mm peripheral orifices, respectively. The worst performance can be attributed to distributor 4 with a mixing number of 1.3. The performance of the distributors in establishing a concentration profile starting with the 'well mixed state' appears to be more influenced by the % free area.

A comparison of the effect of the initial conditions on the concentration

profiles is shown in Figure 10.14. The plot shows two profiles obtained while the column was fitted with Dist.2 (6/36x2). The superficial velocity was kept constant at $U_0 = 0.46$ m/s. Both the profiles reveal a 'developed zone' and 'undeveloped zone' and the effect of the starting condition is also apparent.

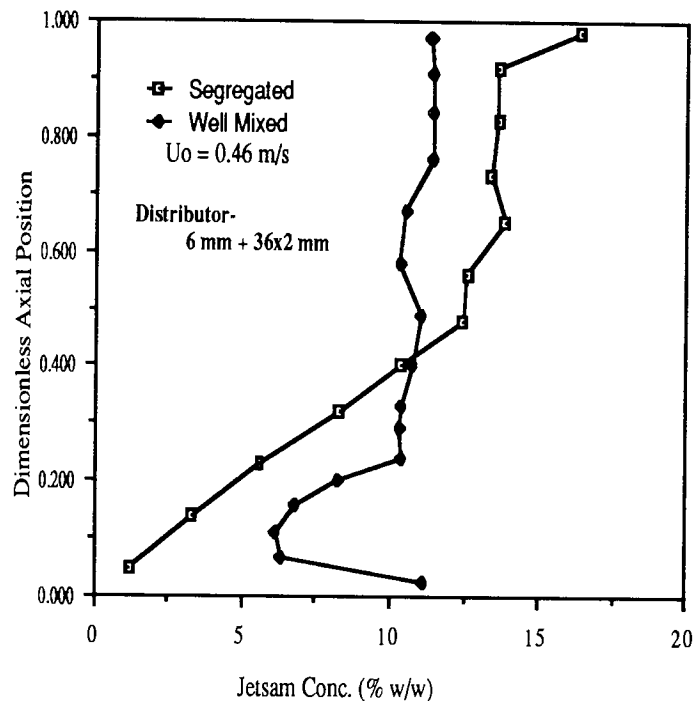


Fig.10.14: Effect of initial condition on the conc. profile

Effect of the Superficial Air Velocity (U_0)

The effect of the superficial velocity on the concentration profile was studied with two distributors namely Dist.5 (6/54x1.5) and Dist.7 (10/18x1.5). In both cases, the experiments were started from the completely segregated mode with jetsam particles (ABS cylinders) being placed on the top.

Figure 10.15 illustrates the concentration profiles obtained with Dist.7 (10/18x1.5). The first experiment was carried out at $U_0 = 0.46$ m/s; this produced a two zoned bed. The upper zone was quite well mixed and lower zone was segregated. The spout height was 27 cm, i.e. ≈ 5 cm above the expanded bed. The path of the black ABS cylinders was visually followed along the column wall and found to disappear inwardly at nearly 9 cm above the distributor. In the second experiment the velocity was increased to 0.55 m/s; this resulted in an increase in the

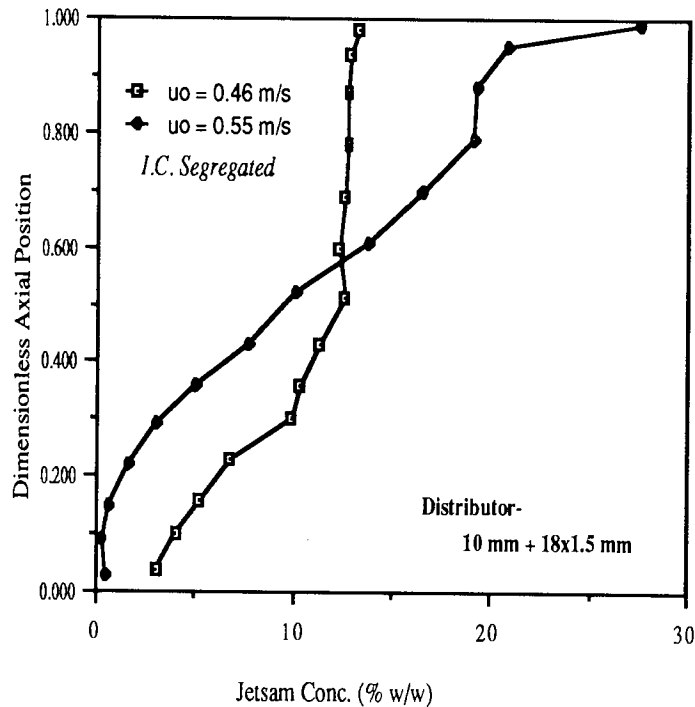


Fig.10.15: Effect of the superficial air velocity on the conc. profile

spout height to 36 cm i.e. ≈ 13.5 cm above the expanded bed. The black ABS particles travelling along the column wall were now found to disappear some 14 cm above the distributor: this gave the impression that the jetsam particles were concentrated at the bed surface. After each experiment, the bed was sectioned and plots were constructed. The concentration profiles obtained with these two experiments are shown in Figure 10.15.

These profiles confirm the visual observations. The increase in the superficial air velocity has promoted segregation rather than mixing. It was difficult to pin point the exact cause for this behaviour in the three-dimensional bed but it is thought to associated with the "shape" of the spout. It appears that at higher superficial velocities the spout becomes thinner, especially at the bottom, and taller. This will reduce the radial penetration of the spout and will push more and more solid upward through the central spout.

The concentration profiles obtained with Dist.5 (6/54x1.5) at two different superficial air velocities are shown in Figure 10.16. The general solids mixing behaviour observed with this distributor was identical to that observed with

Dist.7. However, an improvement in the solids mixing was noticed at higher superficial velocity which was contrary to the previous results. Although the % free area of Dist.5 is slightly greater than the Dist.7 (approximately 11%), this difference can only be attributed to the difference in orifice size and configuration.

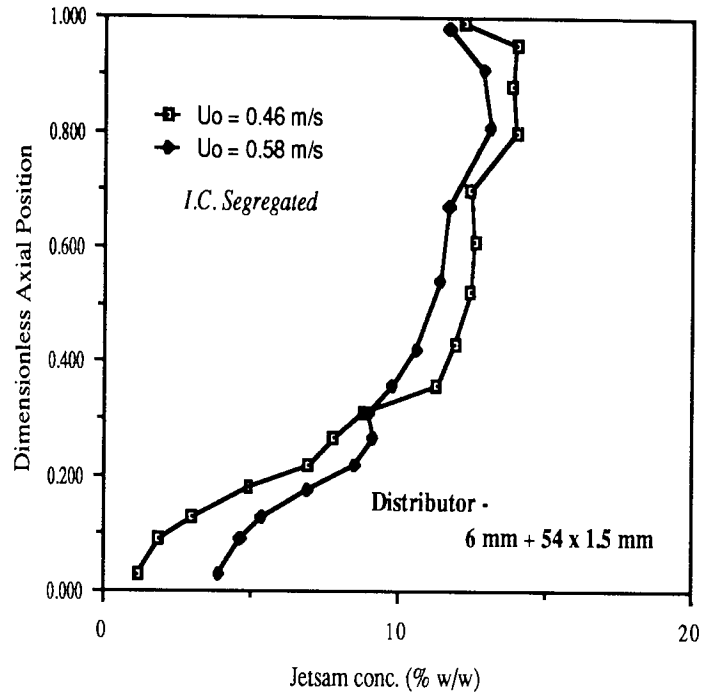


Fig.10.16: Effect of the superficial air velocity on the conc. profile

Effect of Aspect Ratio (Ra) on the Concentration Profile

The effect of aspect ratio has been explored with the ABS Cylinders / Polybeads 1090 system. All the experiments were carried out with Dist.2 having one 6 mm central orifice and 36x2 mm peripheral orifices. The initial condition used in all the experiments was the segregated mode, where jetsam was neatly placed on top of the flotsam giving an average jetsam concentration of 0.1. The superficial air velocity used ranged from 0.4 m/s to 0.46 m/s, but the main criterion was the establishment of a reasonable *central spout*.. Each run was carried out for 10 minutes.

Five experiments were carried out with the aspect ratio ranging from 0.6 to 3.0. The results are presented in the same systematic way as the experimental programme so that the reader can become familiar with the sequential development of patterns which dictated the course of the work.

The concentration profile for a shallow bed, with an aspect ratio of 0.6 and static bed height of 8.2 cm is presented in Figure 10.17. The profile shows that the bed stayed segregated although some of the jetsam shifted downwards. The jetsam concentration in the top layer was reduced from 100% to 19.6% with only 2.2% of jetsam at the distributor. The spout was very pronounced; ≈ 6 cm above the expanded bed surface.

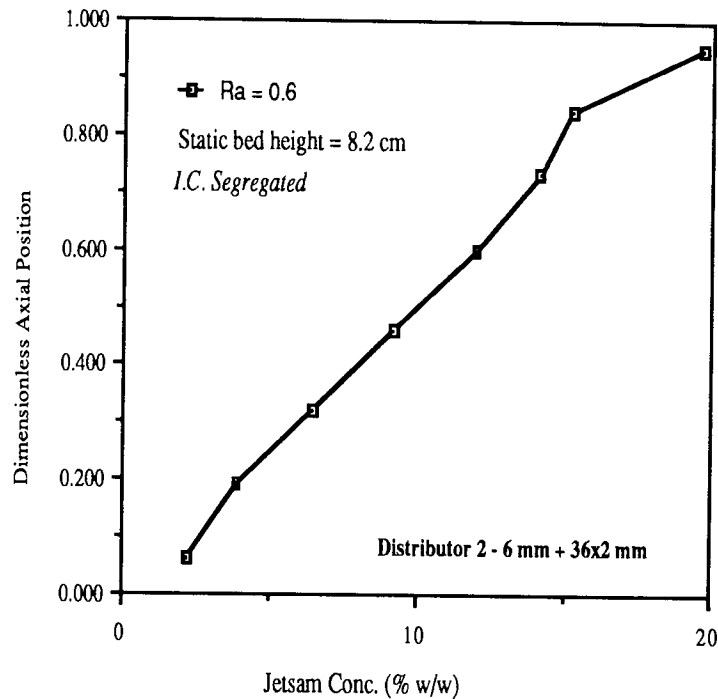


Fig.10.17: Effect of Ra on the conc. profile

The static bed height was then increased to 15.0 cm giving an aspect ratio of 1.1. The concentration profile thus obtained is shown in Figure 10.18. The profile illustrate that the top 20% of the bed appears to be more stable with the jetsam concentration at about 16% to 17%. The spout was quite pronounced; ≈ 5 cm above the expanded bed height. A small developed zone is begining to emerge at the top end of the bed. The remaining 80% of the bed behaved similarly to the one with an aspect ratio of 0.6: the mixing was, however, improved.

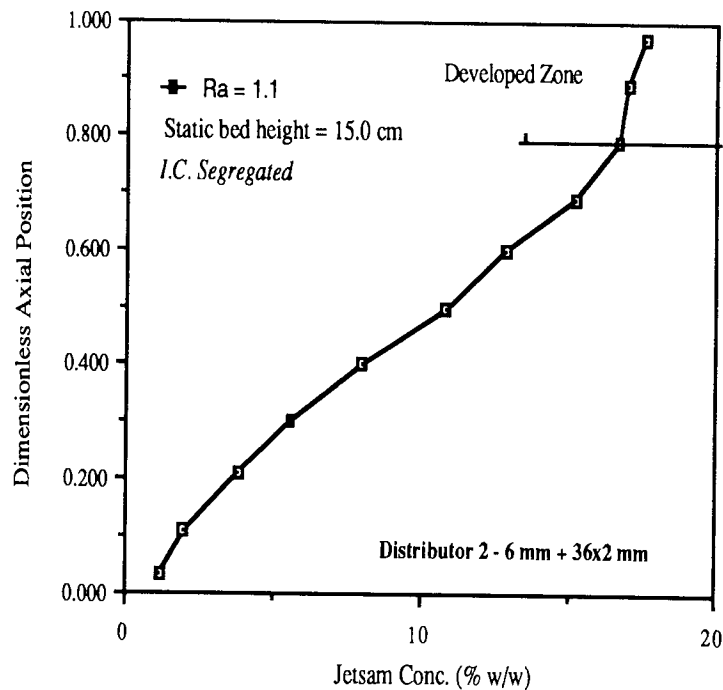


Fig.10.18: Effect of Ra on the conc. profile

The aspect ratio was further increased to 1.6 with a static bed height of 21.8 cm and the concentration profile of this bed is shown in Figure 10.19. The bed divided itself into two zones - 'developed' and 'undeveloped'. The undeveloped zone occupied 40% of the bed from the distributor to a height of 9.0 cm. Above this, the developed zone was formed. The mixing in the developed zone was much improved, although the jetsam concentration was some 30% higher than the initial concentration. The concentration profile in the undeveloped zone is reminiscent of that in the beds with lower aspect ratio. The spout was \approx 4.5 cm above the expanded bed.

Figure 10.20 illustrates the concentration profile when the aspect ratio was increased to 2.1, with a static bed height of 28.8 cm. The bed divided itself into two zones. Interestingly, the undeveloped zone occupied the same vertical section of the bed as in the preceding experiment, i.e. up to 9.0 cm above the distributor. A consequence of this is that the average jetsam concentration in the developed zone approached more closely to the ideal figure of 10%.

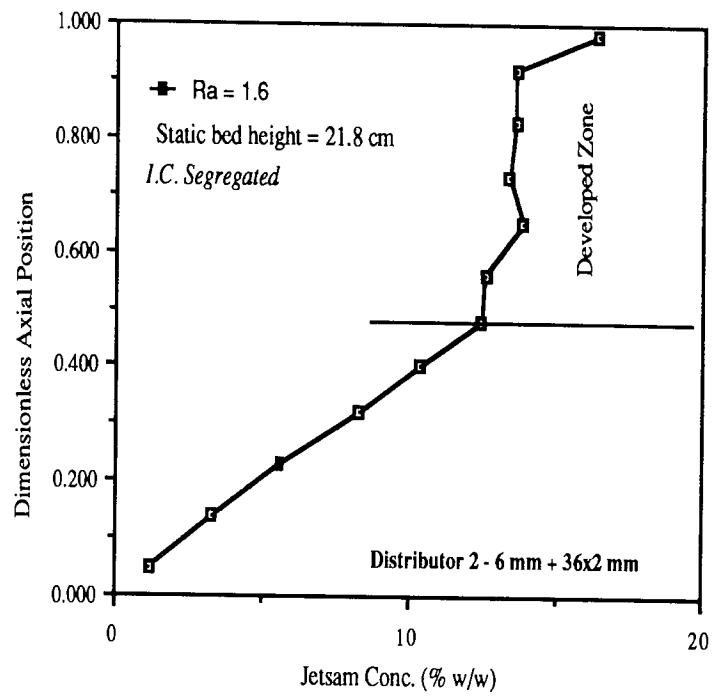


Fig.10.19: Effect of Ra on the conc. profile

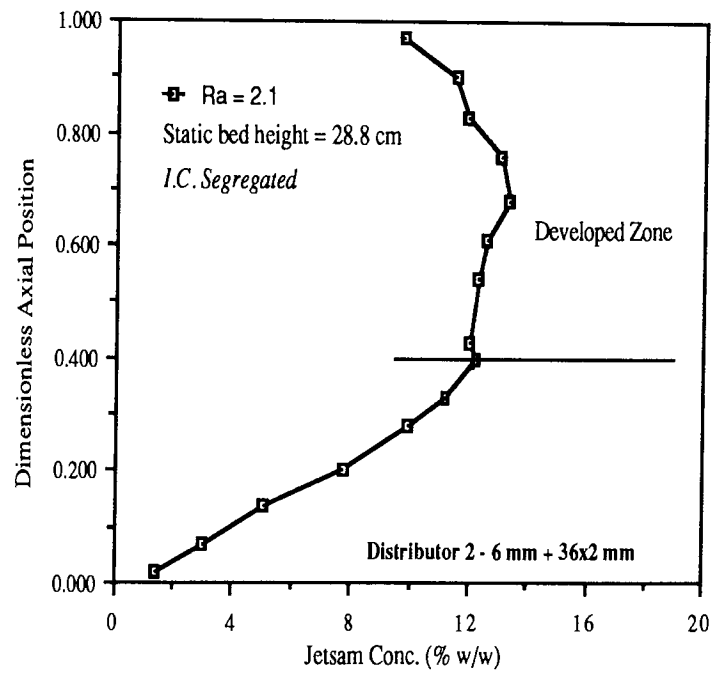


Fig.10.20: Effect of Ra on the conc. profile

The path of a black ABS cylindrical particle travelling downward by the column wall was visually followed and it was found that the particle disappeared inwardly at ≈ 10 cm above the distributor. This observation was made from all sides of the column wall. It was difficult to establish the exact height of the spout, but the top of the spout appeared to come somewhere near the bed surface. It was also observed that black particles tended to move in a circular path adjacent to the central spout, but in the upper half of the bed. Two separate circles were traced on either side of the spout. It was impossible to establish whether these circles were joined with the spout or were completely separate. An attempt has been made to construct a schematic diagram of this behaviour and this is shown in Figure 10.21.

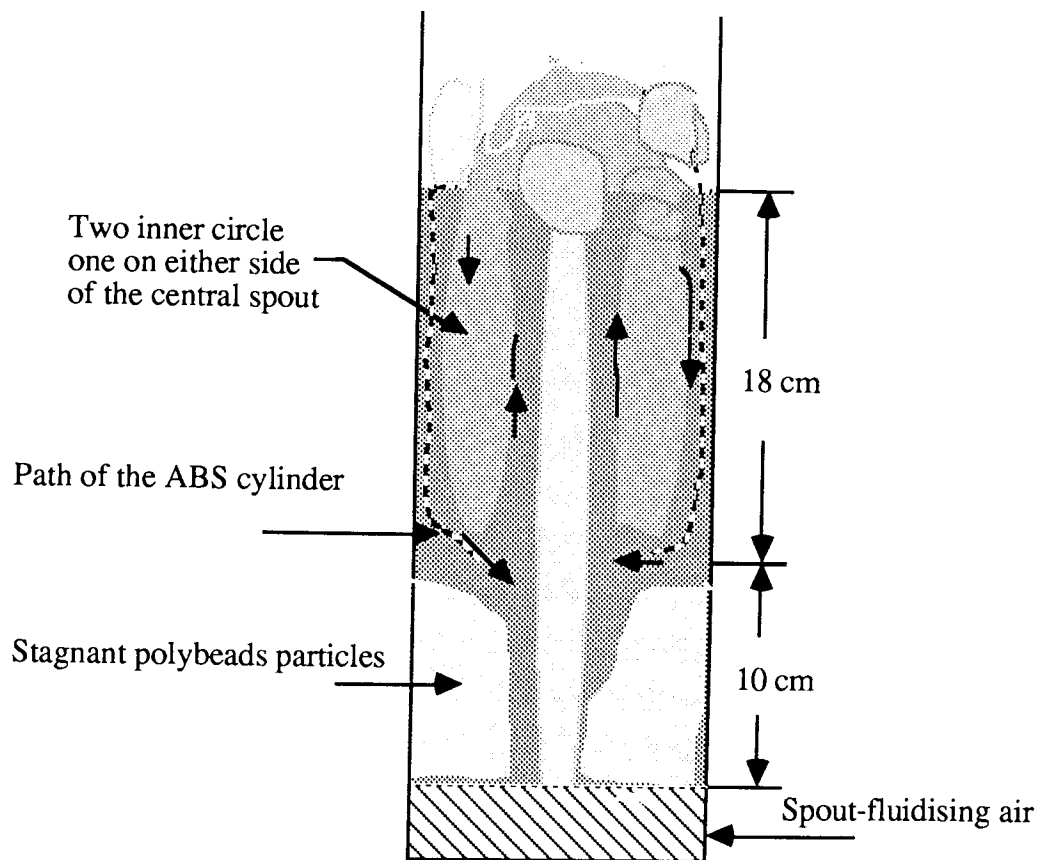


Fig.10.21: Physical appearance of the bed at $Ra = 2.1$

The static bed height was then increased to 3 times the bed diameter to 42.0 cm. The superficial air velocity was kept constant at 0.45 m/s. The spout was completely invisible but the general behaviour of the solids showed that there was a central spout present inside the bed. The upper one third of the bed was behaving as a typical bubbling/slugging bed with bubbles frequently bursting at the surface. The first 9 cm of the bed was completely stagnant containing white Polybead particles. In the middle section, some of the black ABS particles appeared to form a local elongated circle similar to that observed with the 27.8 cm deep bed. Again, two separate circles appeared to be operative in each radial section of the column. The movement of a few black ABS particles was visually followed and they again appeared to move inward at ≈ 10 cm above the distributor. A schematic diagram has been constructed describing the physical appearance and this is shown in Figure 10.22. The circular mixing patterns inside the developed zone were only observed in deep beds with aspect ratios ≥ 2.5 .

The concentration profile is shown in Figure 10.23 and this illustrates that once again the bed has divided itself into two zones. The size of the undeveloped zone tends to remain constant at $\approx 9/10$ cm above the distributor. As expected, the jetsam concentration in the developed zone was even closer to the initial concentration and calculated to be 11.2%.

As a summary of these findings, all five concentration profiles obtained at the various bed heights are plotted against their actual axial position in Figure 10.24. This figure demonstrates how the increase in bed height changes the jetsam concentration in the bed and that there is a minimum and maximum height which produce a central spout and the developed zone. This finding illustrates a typical spouted bed behaviour where a minimum bed height is always required to produce a spout. Therefore, one can conclude that in the spout-fluid bed under consideration, the influence of spouting rather than fluidisation is dominating.

The combined effect of the aspect ratio and distributor design was also briefly studied. The aspect ratio effect on concentration profile was studied using another distributor, namely distributor no.3 (6/13x2/35x1). Three concentration profiles with bed aspect ratios of 1.1, 1.6 and 2.1 respectively are shown in Figure 10.25.

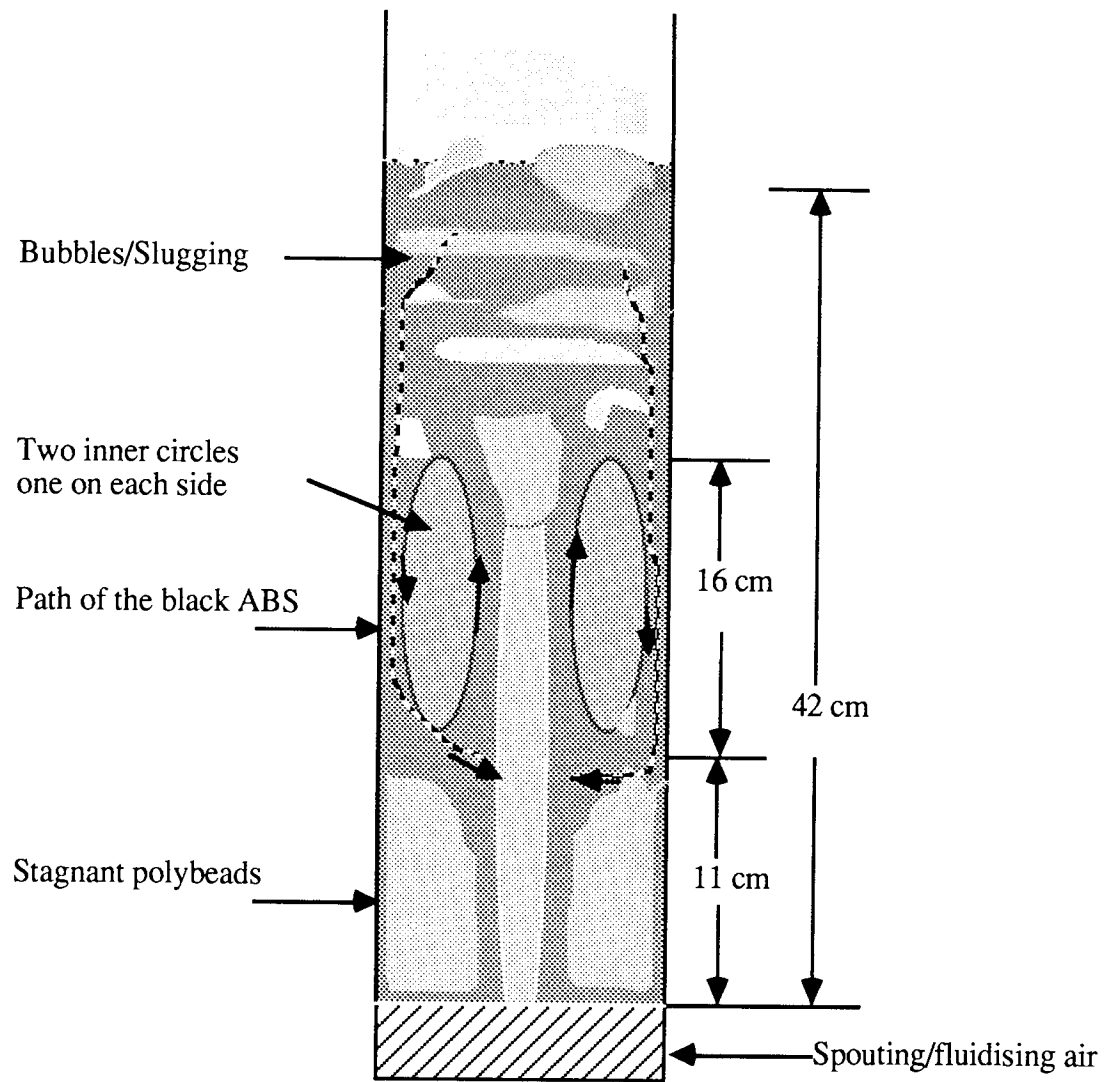


Fig.10.22: Physical appearance of the bed as observed at $Ra = 3.0$

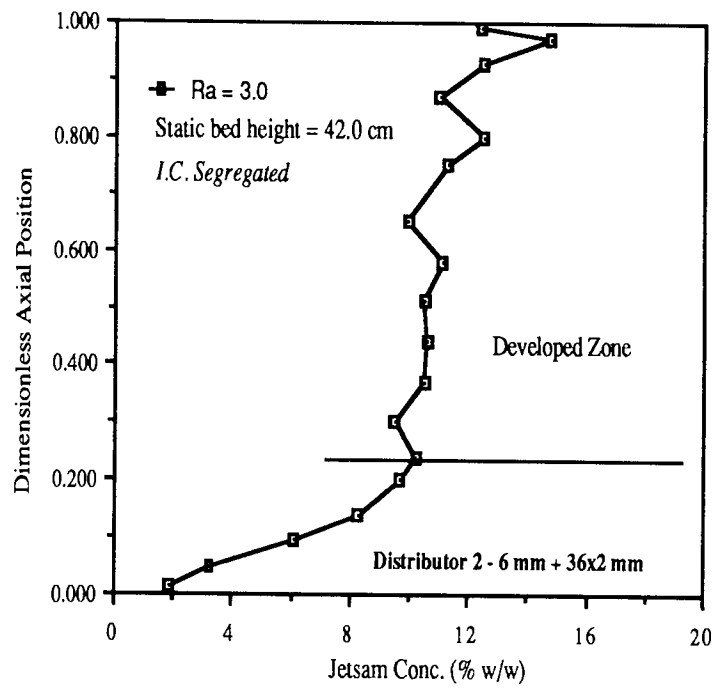


Fig.10.23: Effect of Ra on the conc. profile

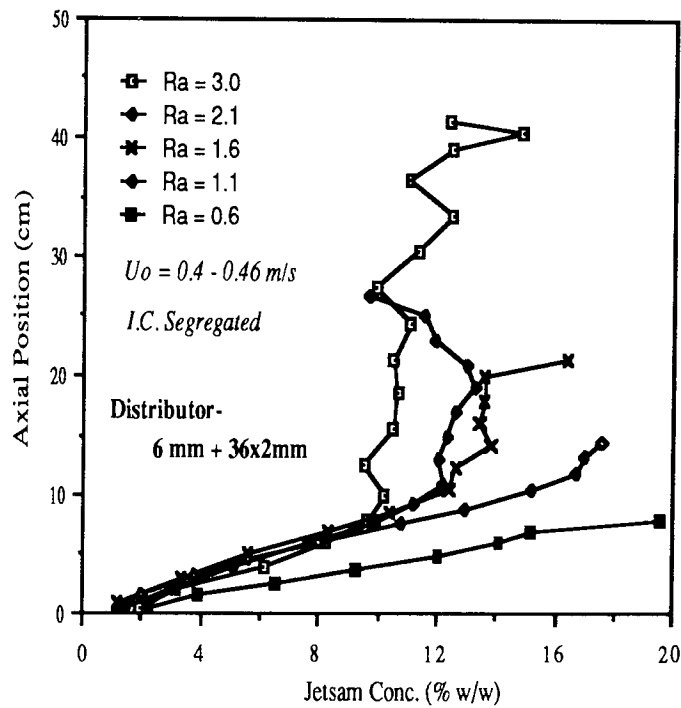


Fig.10.24: Effect of five different Ra values on the conc. profile

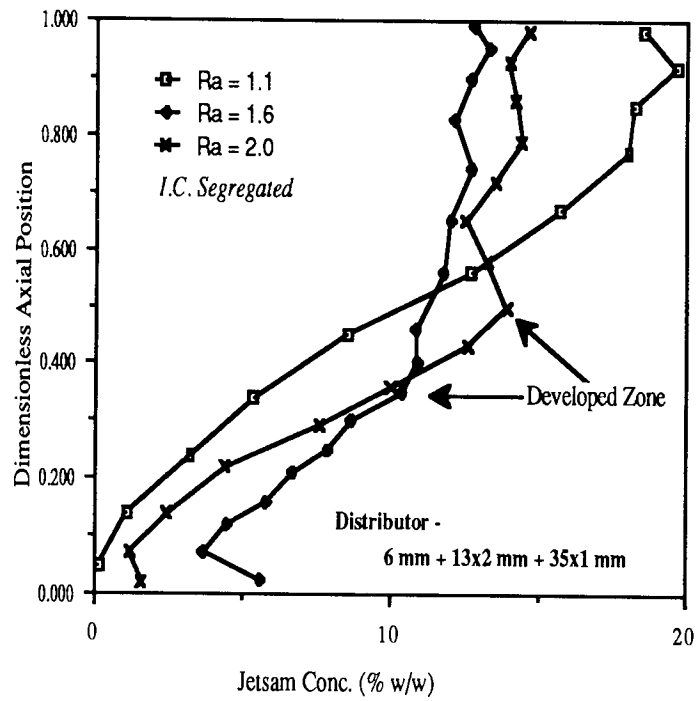


Fig.10.25: Effect of Ra on the conc. profiles

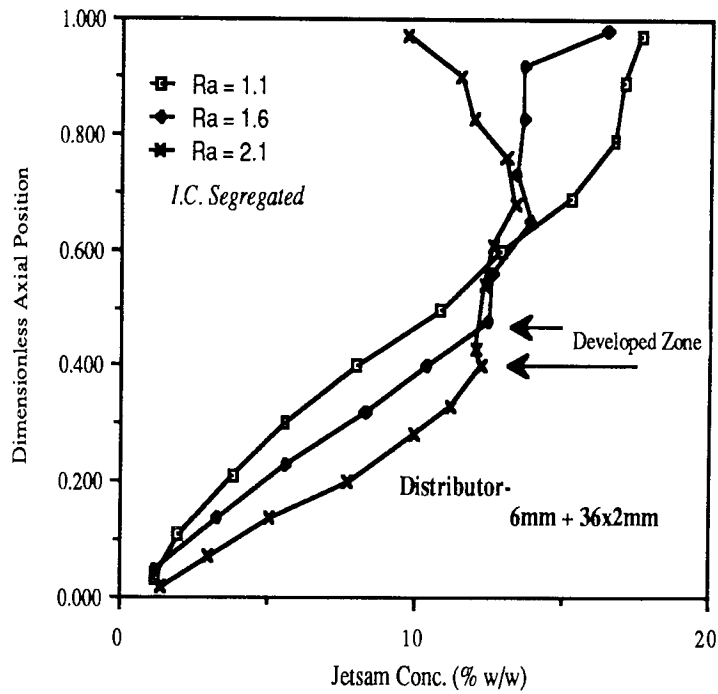


Fig.10.26: Effect of Ra and the distributor configuration

An examination of this figure shows that with an aspect ratio of 1.1, the bed stays segregated. A more balanced concentration profile was achieved when $Ra = 1.6$, the developed zone having an average jetsam concentration of 12% and occupying 63% of the bed. The situation worsened again once the aspect ratio was increased from 1.6 to 2.0: the size of the developed zone was reduced to about 50% of the bed with an average jetsam concentration of 13.8%. This is in contrast to the profiles obtained using distributor no.2 (6/36x2), as shown in Figure 10.26. This shows that when the aspect ratio was increased from 1.6 to 2.0, the height of the undeveloped zone stayed constant and that of the developed zone increased. This comparison suggests that a change in the distributor configuration can override the advantages of a deeper bed. However, at the lower aspect ratio, i.e. 1.1, the concentration profiles are similar without a clear developed zone.

Effect of the Jetsam Concentration on the Mixing Profiles

The effect of the jetsam concentration on the mixing profile was studied using the distributor no.9 (9.5/18x1.5). The static bed height in all cases was 20.2 cm, corresponding to an aspect ratio of 1.5. All the experiments were conducted from a segregated mode with the jetsam particles, black ABS cylinders placed on the top. The tests were conducted with 6 different jetsam concentrations, namely 10%, 20%, 35%, 50%, 65% and 80%; for each increase in jetsam concentration a higher superficial air velocity was required to achieve a stable central spout. Table 10.4 presents the basic experimental data.

The mixing profiles for the 6 different jetsam concentrations are shown in Figure 10.27. The shapes of each are similar, the size of the developed zone increases with the increase in jetsam concentration. The Mixing Number (S) for each profile has been calculated and these are also tabulated in Table 10.4.

The mixing number (S) shows that there is a quantum improvement in the mixing efficiency when the jetsam concentration is $> 50\%$. The system switches from flotsam-rich system over to jetsam-rich one. Kaye et al. (1975) and Nienow et al. (1978a) have observed that the mixing is easier in a jetsam-rich system than in the equivalent flotsam-rich system; they have concluded that with a gas velocity of about 0.3 m/s greater than the U_{mf} of jetsam, jetsam-rich systems are well mixed. This study shows that a suitably designed distributor can make a jetsam-rich system well mixed at a superficial velocity equal to the U_{mf} of jetsam.

Table 10.4: Experimental data and Mixing Numbers

- Study of the effect of Jetsam Concentration o Mixing

Initial Jetsam Concentration (%)	Superficial Velocity (m/s)	Point of intersection at initial conc. line on DAP Scale	Average Jetsam % in D.Z.	Mixing No. (S)
10	0.49	0.38	13.7	1.4
20	0.53	0.33	24.5	1.5
35	0.59	0.28	39.5	1.26
50	0.66	0.23	53.2	0.74
65	0.74	0.13	67.4	0.31
80	0.78	0.09	82.4	0.22

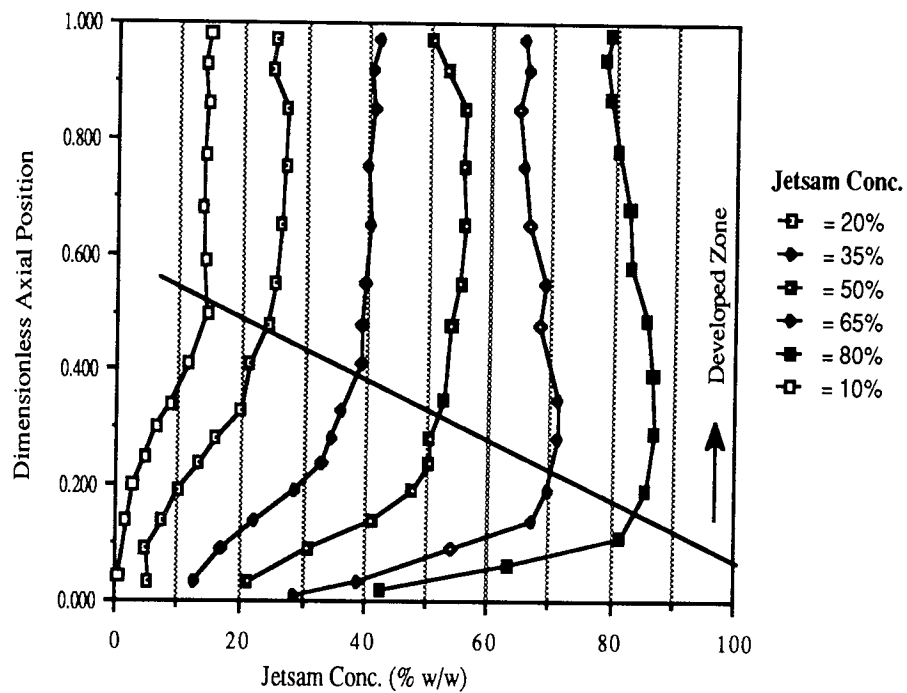


Fig.10.27 : Effect of the jetsam conc. on the conc. profile

10.4.2 The Ballotini 1090 / Ballotini 550 System

This was a binary system of equidensity, spherical particles comprising brown ballotini 1090 and white ballotini 550. The size ratio between jetsam and flotsam was 2 to 1. The system was flotsam rich, having 80% of the flotsam and 20% of the jetsam. The static bed height and aspect ratio were kept constant at 14.2 cm and 1.06 respectively. The experiments were carried out using 6 different distributors.

Two initial conditions were employed: a) the completely segregated mode where the jetsam was neatly placed on the top and the superficial air velocity was 0.4 m/s; and b) the completely mixed mode, where, first, the particles were vigorously mixed at a much higher velocity than the U_{mf} of the jetsam for 15 minutes and then the flow rate was reduced to the desired level of 0.4 m/s.

A typical concentration profile for ballotini 1090 / ballotini 550 is shown in Figure 10.28. The spout-fluid bed column was fitted with distributor no.1 (6/150x1). The shape of the profile is similar to the one obtained with the Polybeads 1090 / ABS Cylinder System and, again, it can be divided into a '*developed*' and an '*undeveloped*' zone.

Effect of Distributor Design

First a set of experiments was carried out with distributors having a common central orifice but varying peripheral orifice sizes and configurations. Three distributors namely distributor nos. 1 (6/150x1), 2 (6/36x2) and 3 (6/13x2/35x1) were used. All experiments were conducted at the superficial air velocity of 0.4 m/s, which produced a neat central spout projecting 4 - 5 cm above the expanded bed surface. The concentration profiles thus obtained are shown in Figure 10.29.

The plot shows that the best profile was obtained with a distributor having a large number of small orifices; as the number of orifices was decreased, so the size of the developed zone decreased. This is also confirmed by the Mixing Numbers, presented in Table 10.5. The undeveloped zones follow a similar pattern and contain similar jetsam concentrations.

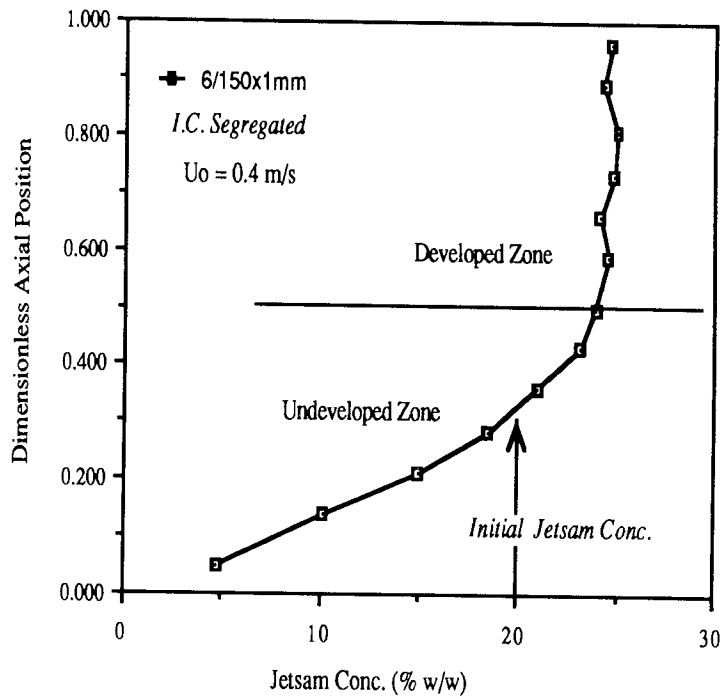


Fig.10.28: A typical concentration profile (Ballotini 1090 / Ballotini 550)

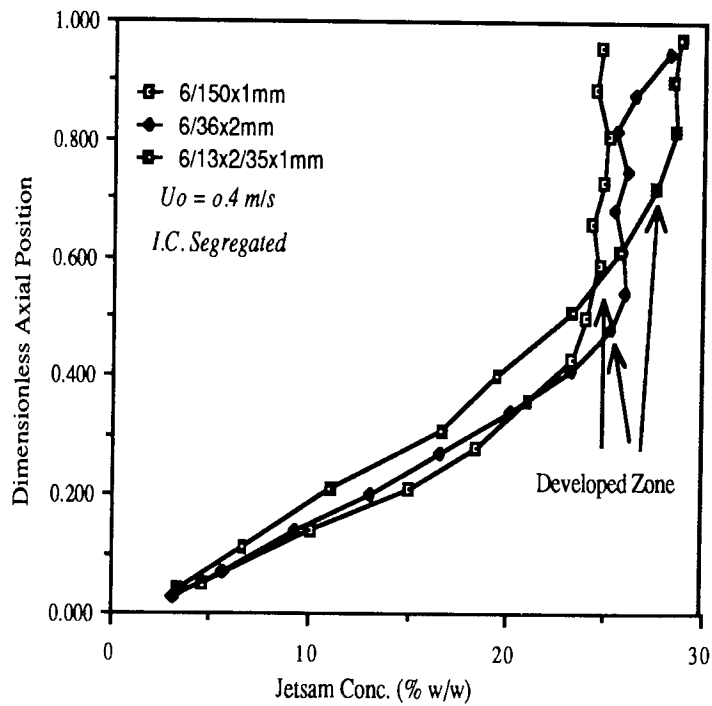


Fig.10.29: Effect of distributor configuration on the conc. profile

Visual observation established that the central spout was mainly responsible for the mixing/segregation mechanism with occasional air bubbles near the column wall. The solid mixture was showered from the central spout on to the bed surface. The large brown particles travelled downward by the column wall and then they seemed to disappear inwardly some 6 - 7 cm above the distributor. The lower section of the bed i.e. about 5cm above the distributor, appeared to be stagnant without any particle movement. This section corresponds to the undeveloped zone. The sizes of these two sections, as visually observed, were slightly different for each distributor and thus producing different sizes of developed zone on the concentration profile graph. (see Figure 10.29).

Next, the effect of the central orifice variation was studied while having the same size and configuration of the peripheral orifices. Three distributors namely nos.6 (6/18x1.5), 7 (10/18x1.5) and 8 (14/18x1.5) respectively were used. The concentration profiles are shown in Figure 10.30.

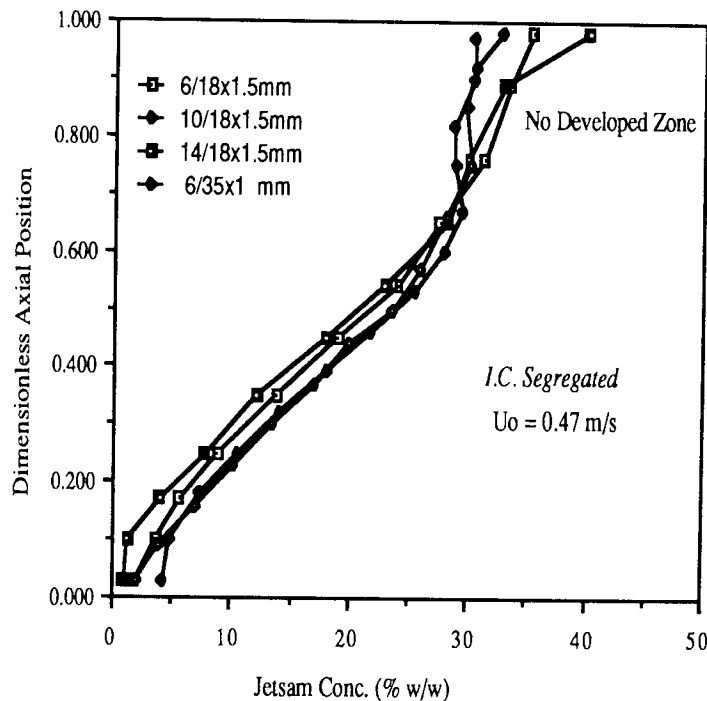


Fig.10.30: Effect of central orifice size on the conc. profile

The figure shows that all the profiles are similar in pattern and without any 'developed' zone. The experimental observations did not show any significant difference between this set and the one previously described, i.e. distributors with

various peripheral orifices. An interesting point to be observed from Table 10.5 is that, when the central orifice size was increased from 6 mm to 10 mm keeping the peripheral pattern the same, the Mixing Number decreased from 4.9 to 3.5. On further increasing the central orifice size to 14 mm it again increased from 3.5 to 5.1, suggesting that the distributor with the 10 mm central orifice was marginally the best among these three.

Figure 10.30 also exhibits a fourth profile which was obtained with Dist.4 (6/35x1); this was added here because of its similarity with the other profiles. The common feature of all these is that they do not exhibit a '*developed*' zone.

Effect of the Initial Condition

This effect was studied by starting from a different initial condition, i.e. from the completely mixed mode. This was achieved by vigorously mixing the particles at a superficial velocity of 2.7 m/s for 15 minutes and then reducing it to the desired superficial air velocity of 0.4 m/s for 10 minutes. The superficial air velocity was kept constant in both the 'segregated' and 'well mixed' cases. A comparison of these concentration profiles is shown in Figure 10.31. The figure shows that one layer in both the beds contains exactly the same concentration of the jetsam particles: this is where the two profiles intersect. Both profiles are similar in shape above the point of intersection but consistently differ in jetsam concentration. Below the intersection, they are different and this confirms the importance of the start-up condition. This confirms the visual observation that there is a little particle movement in the lower end of the bed. The central spout was short and quite sluggish in both cases. The height of the spout was ≈ 4 cm above the expanded bed height.

The effect of the initial condition was further explored with four distributors, each having peripheral orifices of different size, number and configurations. The profiles obtained when operating from the well mixed start are shown in Figure 10.32.

The figure also shows one profile obtained with a distributor differing in both central and peripheral orifice sizes and configuration. All the profiles show the existence of two zones; an upper zone behaving similar to the one obtained with a segregated start but consistently different in jetsam concentration and a lower zone near the distributor very different from the 'segregated start' profile. These plots

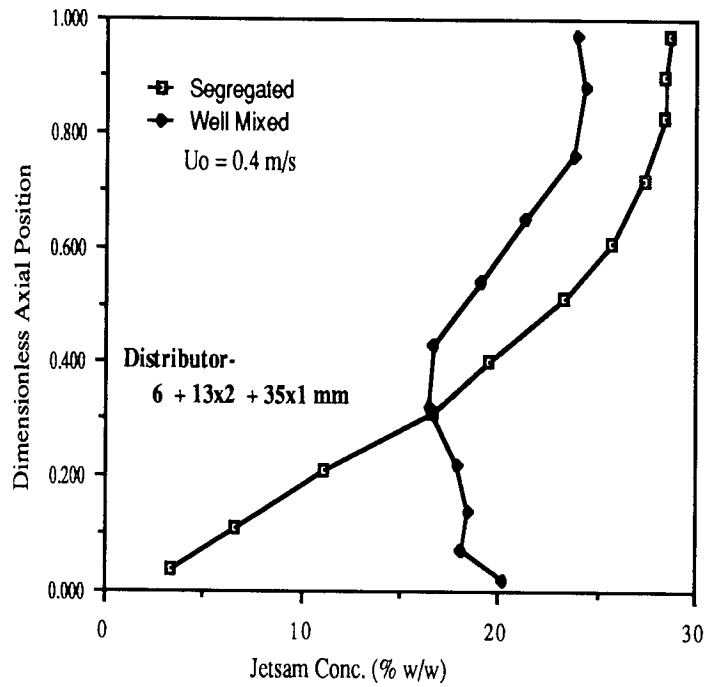


Fig.10.31: Effect of Initial condition on the conc. profile

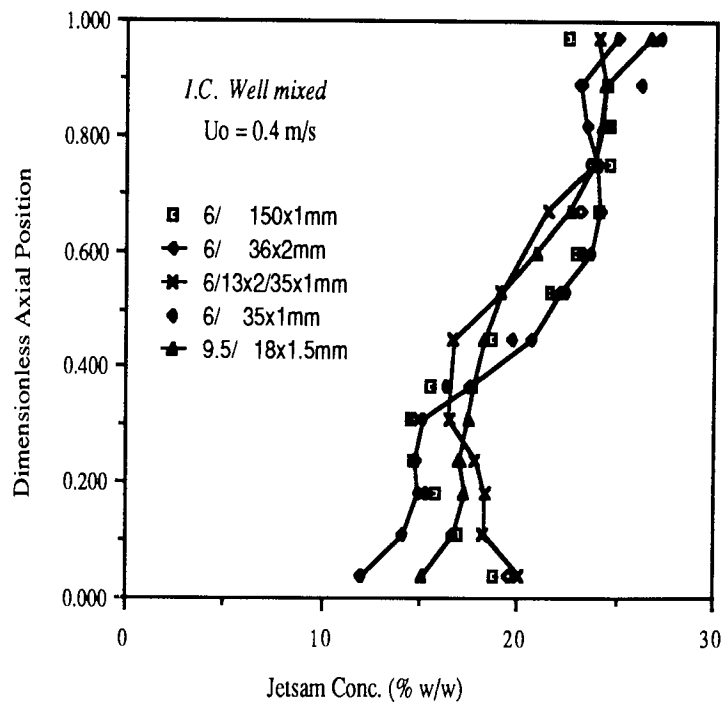


Fig.10.32: Effect of distributor configuration on the conc. profile

further show that the effect of the distributor configuration was far less pronounced when starting from the completely segregated state. Two profiles, one with Dist.2 (6/36x2) and the other with Dist.9 (9.5/18x1.5), showed that the jetsam concentration was a minimum at the distributor level while the other three distributors led to a jetsam concentration at the distributor level of nearly 20%.

Visual observations of developed zones in both cases were similar. The mixture of particles was showered by the spout in the centre of the bed and particles tended to travel downward along the column wall. The path of a few jetsam (brown ballotini) particles was followed and it appeared that these travelled along the column until about 8 cm above the distributor, at which level they were dragged radially inward and disappeared from view. This phenomenon was witnessed regardless of the starting position. Further information was provided on sectioning the bed, and typical results are shown in Figure 10.34. This figure confirms that, irrespective of the starting condition, the radius of spout penetration keeps on reducing from a height of $\cong 7$ cm to a minimum at the distributor level. This again confirms that the solid circulation pattern due to the spout is restricted to the 7 cm level and above. Below this height the particles stay undisturbed in their starting condition. The spout penetration pattern, as observed, is shown in Figure.10.33.

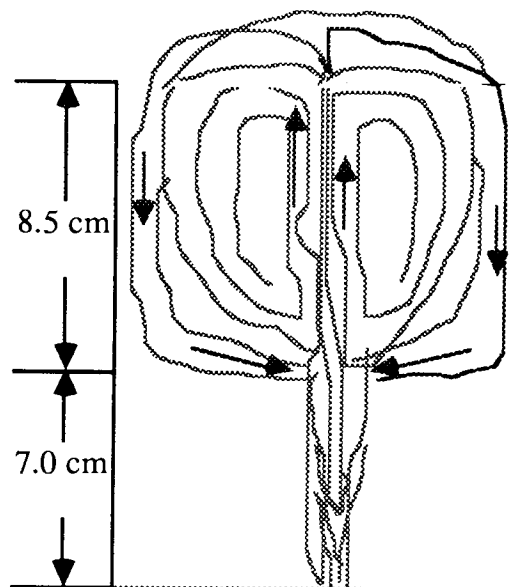


Fig.10.33: Simulation of the solids movement in the bed based on visual observation.

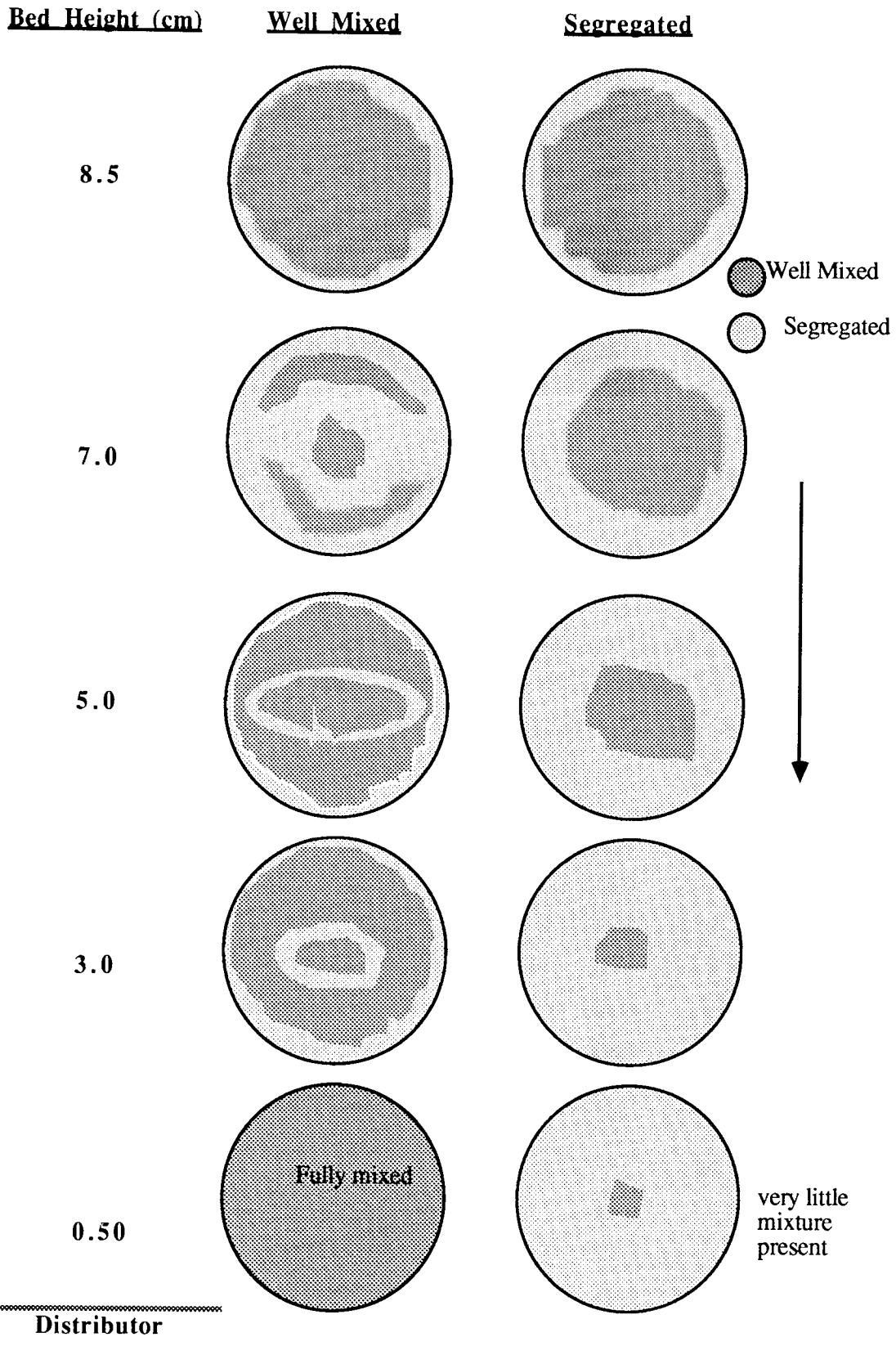


Fig.10.34 Surface appearance of the particles at different bed heights

The figure 10.33 represents the solid circulation path for both cases. The limited radial circulation of the solids in the lower half of the bed is a major concern to the designer. This problem, which is frequently encountered in the spouted bed, has received very little attention (Mathur,1974).

Analysis of the Data - The Mixing Number, S

The performance of the distributors was also judged using the Mixing Number, S, defined in section 10.4.1. The mixing number calculation was restricted to the developed zone only. The details are given in Table 10.5.

Table10.5: Calculation of The Mixing Number, S

System: The Ballotini / Ballotini System.			
(1090) (550)			
Distributor No.	Point of intersection at 20% conc. line on DAP Scale (A)	Average jetsam % in section above 'A' (B)	S = A(B-20)
<i>I.C. Segregated:</i>			
Dist.1 (6/150x1)	0.32	24.0	1.3
Dist.2 (6/36x2)	0.34	25.2	1.8
Dist.4 (6/35x1)	0.44	27.6	3.3
Dist.7 (10/18x1.5)	0.45	27.8	3.5
Dist.3 (6/13x2/35x1)	0.42	28.6	3.6
Dist.6 (6/18x1.5)	0.48	30.3	4.9
Dist.8 (14/18x1.5)	0.47	30.8	5.1
<i>I.C. Well Mixed:</i>			
Dist.2 (6/36x2)	0.50	23.2	1.6
Dist.3 (6/13x2/35x1)	0.60	22.7	1.6
Dist.1 (6/150x1)	0.55	23.5	1.93
Dist.6 (6/18x1.5)	0.55	23.7	2.04
Dist.4 (6/35x1)	0.50	24.2	2.1

The above table lists the distributors according to the value of their Mixing number (S). Dist.1 (6/150x1) tops the performance table when starting from the 'segregated' mode, followed closely by Dist.2 (6/36x2). In the case of the 'well mixed' mode, there is little to choose between the five distributors.

10.4.3. The Ballotini 1090 / Polybeads 1850 System

This was a binary system of spherical particles differing in both density and particle size. The role of flotsam was played by the white Polybeads 1850 with a size range of 1.7 - 2.0 mm and solids density of 0.95 g/cc. The bed contained 80% w/w of flotsam particles. The role of jetsam was played by the yellow glass ballotini particles with a size range of 1.0 - 1.18 mm and particle density of 2.45 g/cc. The bed contained 20% w/w of these particles. In contrast to the difference in both particle size and density, they had similar minimum fluidising velocities, 0.53 m/s for the Polybeads and 0.57 m/s for ballotini particles. The particle to particle size and density ratios were 1.7 and 0.39 respectively.

The static bed height and aspect ratio were 14.5 cm and 1.05 respectively and the superficial air velocity ranged from 0.69 - 0.72 m/s. The experiments were mainly carried out using the completely segregated mode with the jetsam neatly placed on the top of the flotsam.

Effect of the Distributor Design

The effect of the central orifice diameter on the concentration profile was studied with four distributors namely no.6, 7, 8 and 10 containing 6 mm , 10 mm , 14 mm and 17 mm diameter central orifices and 18x1.5 mm orifices in the periphery. The experimental criterion was the establishment of a stable central spout and this was achieved with all the three distributors with only a slight variation in the superficial air velocity. A typical operation of this system is photographically shown in figure 10.35. The concentration profiles obtained with these five distributors is shown in Figure 10.36.

During these experiments, a spout some 12-15 cm tall formed above the bed surface and created a shower of the mixture particles. A band of yellow ballotini particles was formed a short distance above the distributor: the position of this band varied with different central orifice diameters. Initially this yellow band lifted higher with the increase in the central orifice diameter to 14 mm and then it declined when this diameter was further increased to 17 mm. Above the jetsam band, vigorous

mixing of particles each place, the ballbed particles being close to the bed walls and then away from the spray at the longer bed level. Also, below the band, the particles seemed to be almost stationary and relatively well-suspended.

The general shape of the concentration profile was similar to the jetman concentration - gradually increasing from the spray at the 'Peak Point' (band), a short

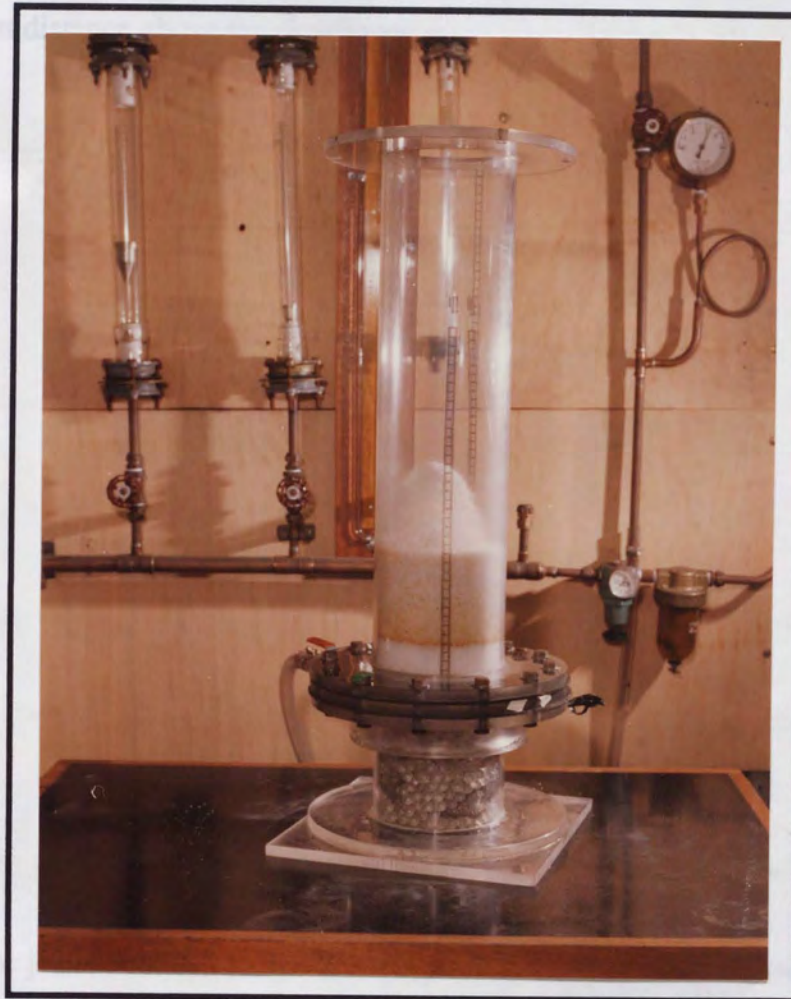


Fig.10.35: Photograph showing Ballotini 1090 / Polybeads 1850 mixture in operation with Dist.8 (6/18 x 1.5)

mixing of particles took place, the ballotini particles being drawn down the bed walls and then swept into the spout at the jetsam band level. However, below the band, the particles seemed to be almost stationary and behaved like a packed bed.

The general shape of the concentration profiles is similar with the jetsam concentration - gradually increasing from the top of the bed to the 'Peak Point' (band), a short distance above the distributor.

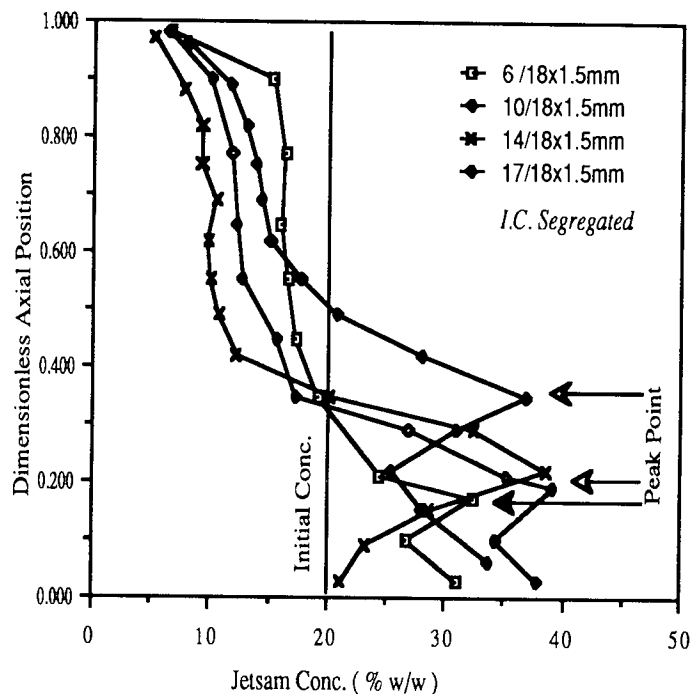


Fig.10.36: Effect of the central orifice diameter on conc. profile

The jetsam concentration at the band is dependent on the superficial air velocity; increasing the air velocity reduces the concentration and eventually it disappears. The position of the concentration band is dependent on the central orifice diameter and a plot describing this relationship is shown in Figure 10.37.

Generally, it is difficult to single out any one distributor configuration as the best due to the complex shape of the profiles. However, from the mixing point of view distributor no.6 (6/18x1.5) gave the best performance. The mixture exhibited a strong tendency towards spouting and fluidisation was completely dominated by the strong central spout. It is possible that some bubbles were formed above the peripheral orifices and that these were quickly swept into the central spout within the bed.

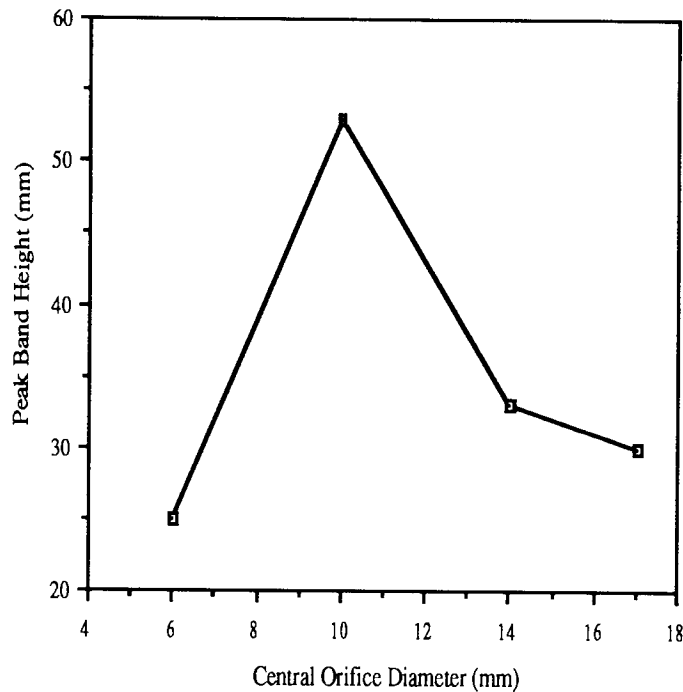


Fig.10.37: Variation of Ballotini peak band height with central orifice diameter

The effect of the peripheral orifices on the concentration profile was studied with four distributors namely no.1(6/150x1), no.2 (6/36x2), no.3 (6/13x2/35x1) and no.6 (6/18x1.5) and the profiles thus obtained are shown in Figure 10.38.

The first observation to be made is that an increase in the number of peripheral orifices has tended to bring the jetsam particles towards the distributor leaving only a small portion of the jetsam to be mixed. The profile obtained with t Dist.1(6/150x1) shows a steady average jetsam concentration of 7% in the main section of the bed but, in the last two layers next to the distributor, it increases from 7% to 32% and then finally to 90%. On comparing this with the profile obtained with Dist.2(6/36x2), it is seen that there was an average concentration of 20% except in the top and bottom layers: the top layer contained only 4.5% of jetsam because of the preferential entrainment of flotsam in the spout, whereas the bottom layer on the distributor contained 24.5% of the jetsam.

The profiles obtained with the other two distributors are similar to each other and also in line with the traditional profile observed with the spout-fluid bed system. Therefore, in systems of density difference but particles having a similar

U_{mf} , mixing can only be improved by limiting the size and configuration of the distributor.

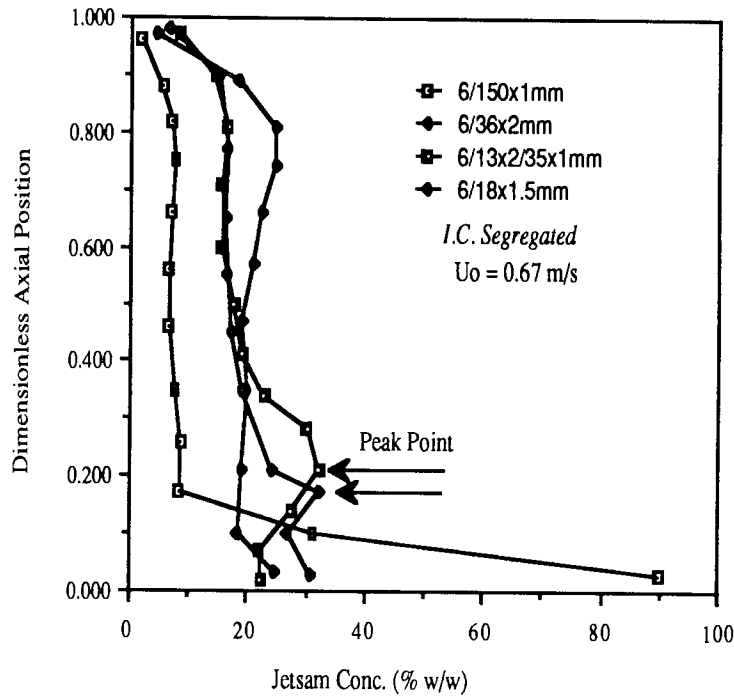


Fig.10.38: Effect of the peripheral orifice variation on conc. profile

Effect of the Initial Condition

The location of jetsam particles in the bed, in the case of a segregated start, could have an effect on the concentration profile. This was studied by placing jetsam particles at different levels in the bed. Three cases were studied with jetsam placed at the top, bottom and in the centre. The static bed height was 15.0 cm, the column was fitted with Dist.7 (10/18x1.5) and experiments were conducted at $U_0 = 0.71$ m/s. In all three experiments, a stable central spout was developed neatly mixing the particles. Figure 10.39 shows the physical appearance of these three cases before and after the experiments. The results showed that with jetsam placed either at the top or in the middle, the final outcome was identical. In both cases, a jetsam band was formed a few centimeters above the distributor: above this band solids were well mixed and below this band solids were segregated especially in a radial direction. In the case of the jetsam placed at the bottom, the majority of the jetsam stayed at the distributor; the mixture was low in jetsam concentration. The concentration profile constructed by sectioning the bed confirms these observation and this is shown in Figure 10.40. These results are very similar to the results obtained with the spouted bed.

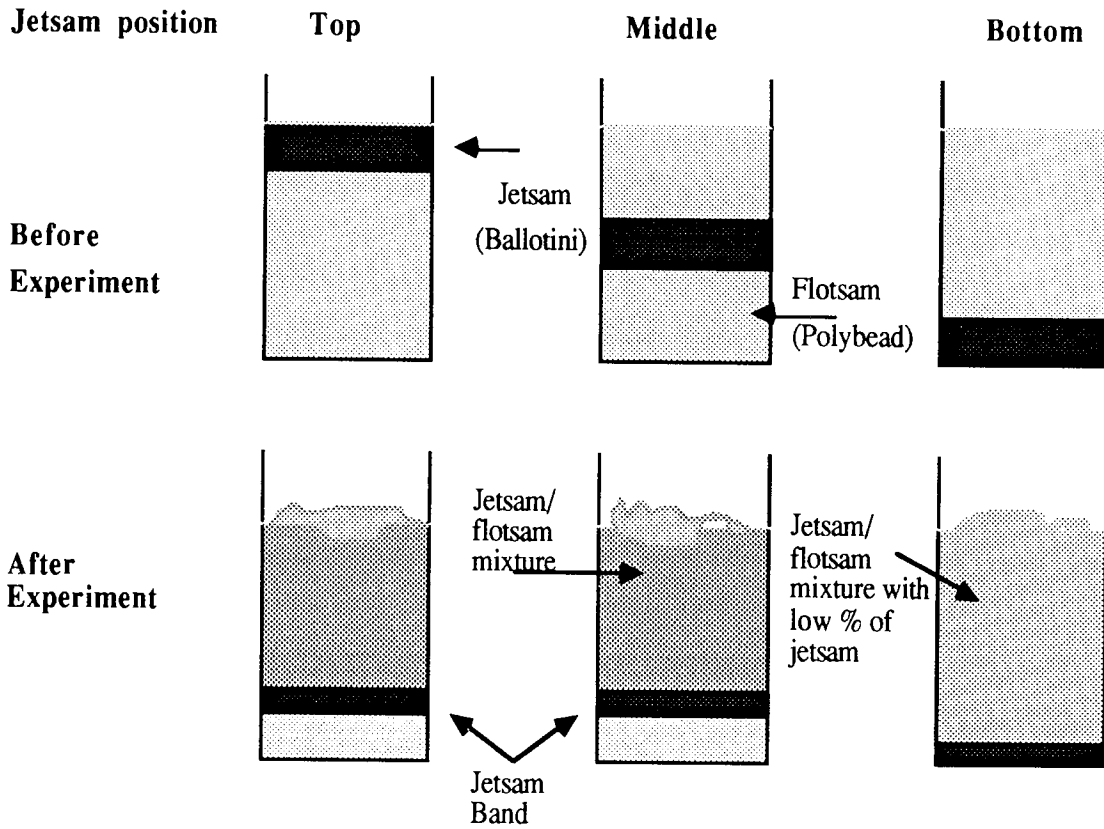


Fig.10.39: Physical appearance of the three locations of jetsam before and after fluidisation.

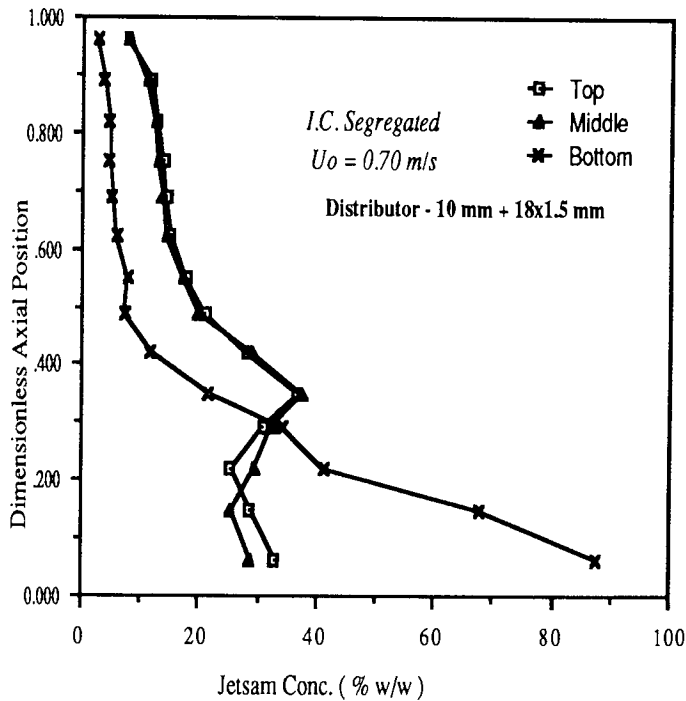


Fig.10.40: Effect of the initial jetsam position on the conc. profile

The effect of the starting position on the concentration profile was studied by conducting the experiment from the 'segregated' and 'well mixed' modes. In the case of a segregated start, the ballotini were neatly placed on top of Polybeads whereas in the well mixed case, 10 equal portions of Polybeads and ballotini solids were hand mixed and carefully placed in the bed. Both the experiments were conducted at the superficial air velocity of 0.67 m/s while the bed was fitted with Dist.2 (6/36x2). The profiles are shown in Figure 10.41.

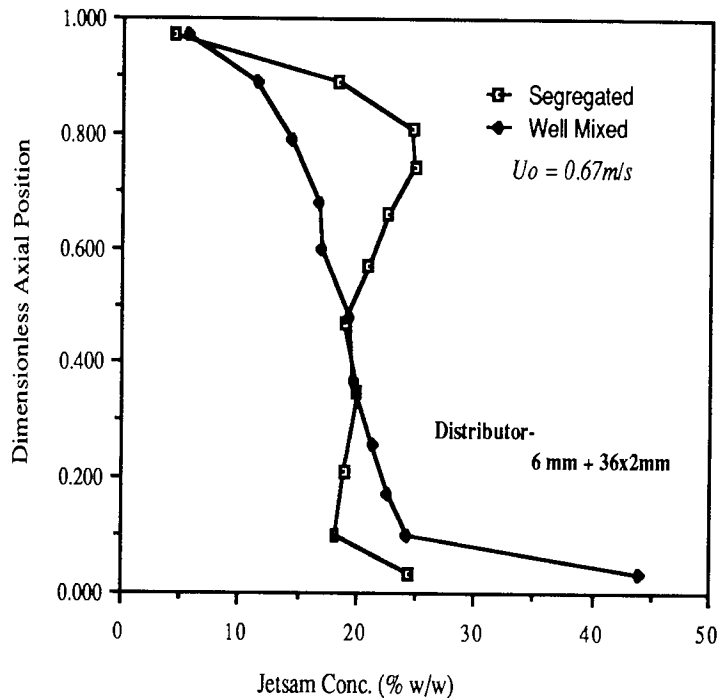


Fig.10.41: Effect of the initial condition on conc. profile

Significant differences in the concentration profiles are noticeable at the two ends. Near the distributor the jetsam concentration is increased by 20% from 25% to 45%, in favour of the 'well mixed' mode. Another big shift was near the surface where jetsam concentration was 25%, with the segregated start, compared with only 15% with the well mixed start.

Effect of the Superficial Air Velocity

The effect of the superficial air velocity on the concentration profiles was explored by conducting the experiments at three different velocities. In all cases the starting condition was the completely segregated mode, ballotini being placed on top of Polybeads. The bed was fitted with Dist.2 (6/36x2). The profiles thus obtained are shown in Figure 10.42.

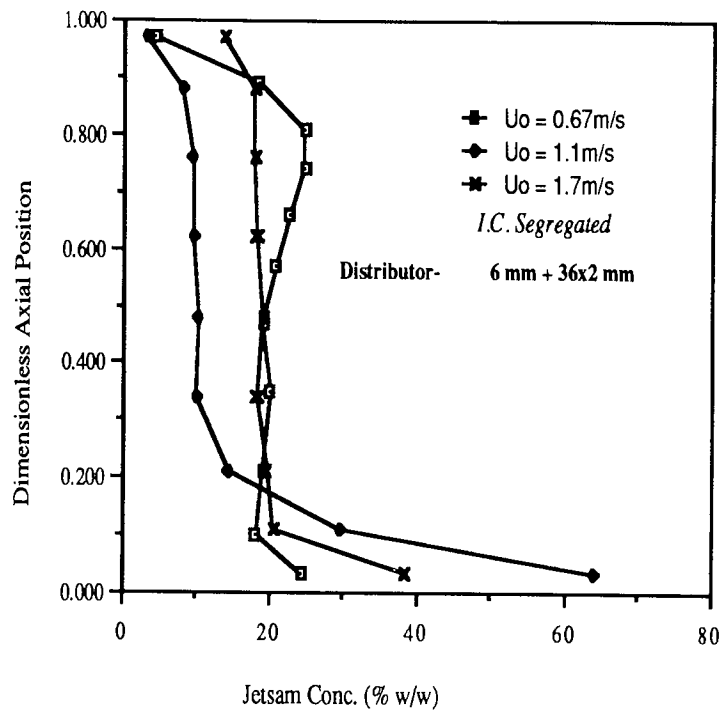


Fig.10.42: Effect of the superficial air velocity on conc. profile

The three profiles were obtained at $U_o = 0.67, 1.1$ and 1.7 m/s; these velocities were chosen arbitrarily but they conveyed a very comprehensive picture. At an initial velocity of 0.67 m/s, a relatively mixed bed was obtained after allowing for the distributor and entrainment effects. The mixing deteriorates substantially when the velocity is increased to 1.1 m/s, perhaps unexpectedly. This shows that, with mixtures of different density, one has to increase the velocity much higher (> 3 times) than the minimum spouting velocity required to achieve good mixing.

On further increasing the velocity to 1.7 m/s, the mixing was improved and a profile slightly better than the one obtained with $U_o = 0.67$ m/s was achieved. The average jetsam concentration in the main section of the bed was $\approx 18\%$. The entrainment effects are less noticeable with a jetsam concentration of $\approx 14\%$ at the surface compared with 4.5% when $U_o = 0.67$ m/s. The distributor effect was more pronounced as $\approx 39\%$ of the jetsam were lying on it.

The effect of superficial air velocity was investigated with another distributor, namely Dist.8 ($14/18 \times 1.5$), again starting from the segregated state with jetsam on the top. The superficial air velocities at 0.71 m/s and 0.95 m/s were used. The concentration profiles are shown in Figure 10.43.

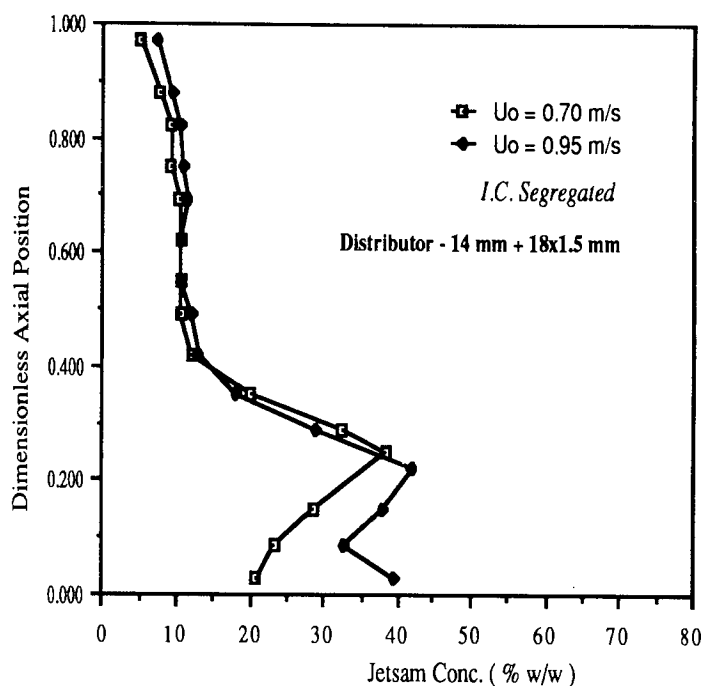


Fig.10.43: Effect of the superficial air velocity on conc. profile

The physical appearance noticed was similar in both cases, except that at the higher velocity the spout was more pronounced and taller and the jetsam band was at a slightly lower position. The spout height was 21 cm and 25 cm and jetsam band height was 3.6 cm and 3.0 cm at 0.71 m/s and 0.95 m/s respectively. The particle movement was more intense at the higher velocity as is to be expected. The figure illustrates a remarkable similarity in the two profiles especially above the peak point. The difference starts to emerge at the peak point level with a slight difference in concentration which increases further in the distributor region. This confirms that the concentrated jetsam band position is only slightly effected by an increase in the superficial velocity but generates a significant change below the jetsam band.

10.4.4. The ABS Cylinder / Polycylinder System

This was again a binary system of equidensity, non - spherical particles. The Polycylinder particles were red expandable polystyrene having a cylindrical shape with an average size of 0.75 mm in diameter by 3.0 mm long; the equivalent spherical particle diameter, based upon surface area, was 3.35 mm. The Polycylinder occupied 90% of the bed and played the role of flotsam. The role of

jetsam was played by the black ABS cylinders; these were 2.4 mm in diameter and 3.0 mm long; the equivalent spherical particle diameter, based upon surface area, was 7.2 mm. This gave the 'equivalent spherical diameter' ratio of 2.15. The bed contained 10% of the ABS cylinders.

The static bed height and the aspect ratio were kept constant at 18.2 cm and 1.3 respectively. The experiments were mainly conducted from the 'segregated' mode with the jetsam neatly placed on the top of the flotsam. In all cases, a central spout was established during operation.

Effect of Distributor Design

The effect of the central orifice diameter was studied with three distributors, namely Dist.6 (6/18x1.5), Dist.7 (10/18x1.5) and Dist.8 (14/18x1.5). The superficial air velocity was 0.46 m/s with all the distributors which produced a well established spout \approx 21 cm above the expanded bed. Figure 10.44 shows a photograph of the spout obtained with Dist.7 (10/18x1.5) when operated at 0.46 m/s superficial air velocity. The concentration profiles obtained with these three distributors are shown in figure 10.45. The mixture stayed badly segregated. The particle movement near the walls was very slow in contrast to the smooth movement observed with spherical particles. There is hardly any difference in the profiles obtained when using distributors with 6 mm and 10 mm central orifices; on increasing the central orifice diameter to 14 mm, the lower portion of the profile was elevated and a small developed zone in the upper two sample layers of the bed was produced.

The effect of peripheral orifice size, number and configuration variation was studied with four distributors, namely Dist.1 (6/150x1), Dist.2 (6/36x2), Dist.3 (6/13x2/35x1) and Dist.8 (6/18x1.5). The concentration profiles are shown in Figure 10.46. All the experiments were carried out from the 'segregated' mode and at a superficial air velocity of 0.46 m/s. Figure 10.46 illustrates that two very different sets of concentration profiles were obtained. The two distributors containing a higher % distributor free area produced profiles with a high portion of jetsam settled at the bottom. The jetsam concentration at the distributor appeared to be related directly to the % free area; the 0.95% free area of Dist.2 (6/36x2) gave 40% concentration whereas the 0.97% free area of Dist.1 (6/150x1) gave 45% concentration.

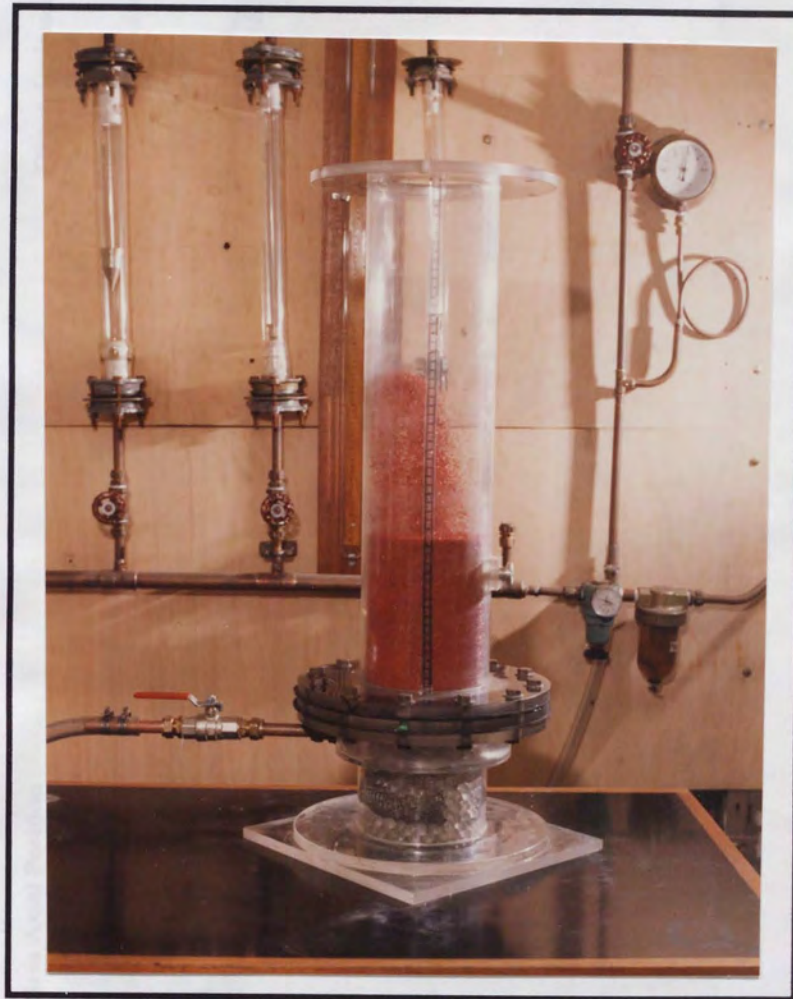


Fig.10.44: *Photograph showing the spout produced with Polycylinder / ABS system with Distributor 7 (10/18x1.5) @ $U_0 = 0.46$ m/s*

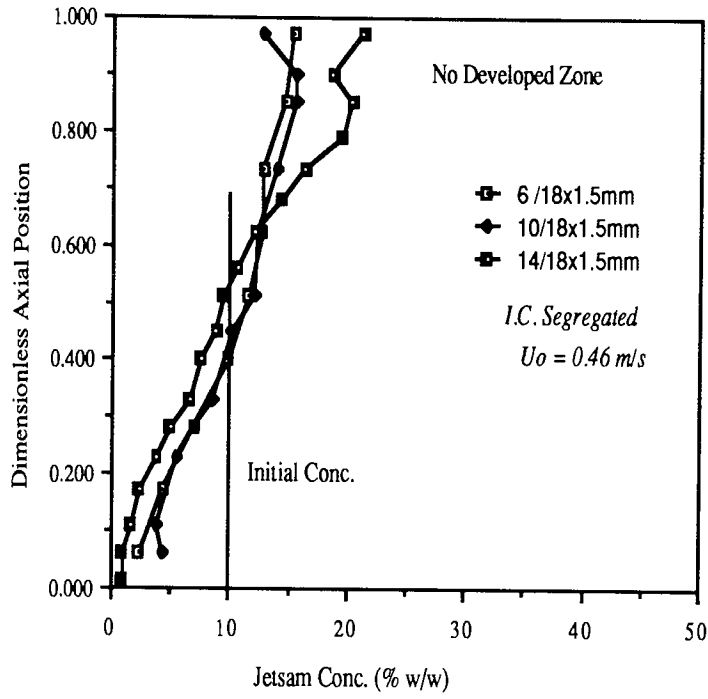


Fig.10.45: Effect of the central orifice diameter on conc. profile

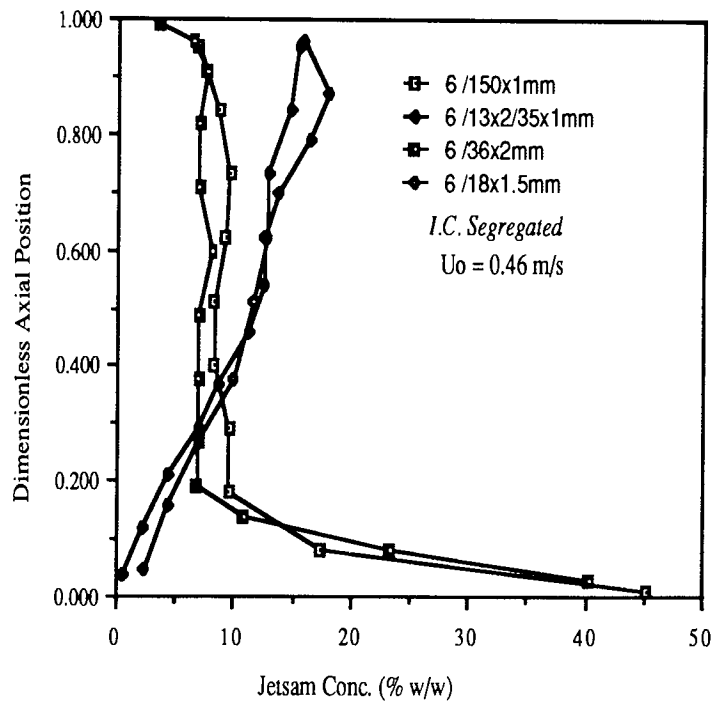


Fig.10.46: Effect of the peripheral orifice on conc. profile

Although the central spout was quite pronounced, some bubbles were seen to be frequently travelling by the column wall, in both cases. Furthermore, in the case of Dist.2(6/36x2) which contained 2 mm diameter peripheral orifices, small jets were observed at the peripheral orifices extending upto 6 cm high in the bed and then converting into bubbles.

The other two profiles, which are very similar to each other, are associated with Dist.3 (6/13x2/35x1) and Dist.6 (6/18x1.5). The % free areas of these two distributor are 0.65% and 0.4% respectively. Although there is a substantial difference in free area, the difference in the concentration profile is small with 0.5% and 2.4% jetsam at the distributor. The spout was again very pronounced \approx 25 cm above the expanded bed surface.

In the author's opinion these data reflect the operability of the peripheral orifices. In the case of the distributors with high free peripheral area, the peripheral air jets and bubbles enable jetsam particles to sink down towards the distributor. This can be attributed to the fluidisation mechanism whereas in the case of the distributors with a low peripheral area, the central spout controls the solids movement with little help from the peripheral holes and so the jetsam stays higher up in the bed, a typical illustration of the spouting mechanism controlling the particle movement. Interestingly, the change in the diameter of the central orifice does not appear to have any effect.

Effect of the Initial Condition

The changes in the concentration profile when starting from the 'segregated' and 'well mixed' modes were studied at a superficial air velocity of 0.46 m/s. The bed was fitted with Dist.2 (6/36x2). In the case of a segregated start, the jetsam was neatly placed on top of the flotsam: a powerful spout was established some 21cm above the expanded bed surface. In the case of a well mixed start, 10 equal portions of hand mixed solids were carefully placed on top of each other: again a spout very similar to the one associated with the 'segregated start' was obtained.

The concentration profiles are shown in Figure 10.47 and they are found to be remarkably similar. The small difference near the top of the bed may be related to the initial starting position. The preferential flotsam entrainment is more pronounced when starting from the segregated mode.

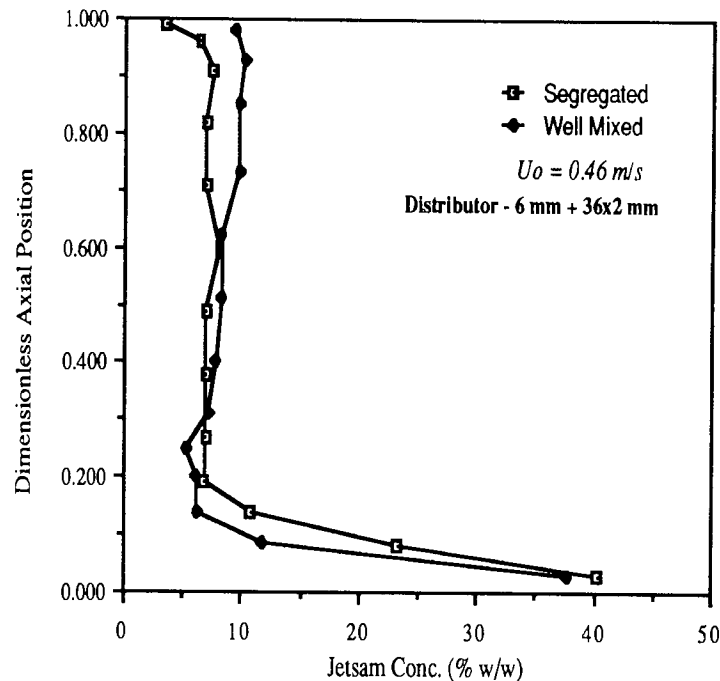


Fig.10.47: Effect of the initial condition on conc. profile

The effect of the initial condition was also examined with Dist.7 (10/18x1.5). Again the experiments were started with mixtures at the two extreme conditions; the superficial velocity was kept constant at 0.46 m/s. The concentration profiles are shown in Fig.10.48. The initial conditions made a considerable impression with this distributor. The jetsam concentration gradually increases upwards but without producing any developed zone with the segregated start. In the well mixed case, the concentration profile lies within about +/- 2% of the initial condition but these variations are difficult to interpret.

The effect of the initial condition with these two distributors is remarkable and once again confirm the importance of distributor design. In the author's opinion, the central spout appears to be causing segregation whereas the fluidisation seems to be promoting mixing for this mixture. Although a central spout was formed with Dist. 2 (6/36x2), generally this distributor leads to peripheral fluidisation. During all the experiments using this distributor it was observed that small jets approximately 3 cm high were formed above the peripheral orifices which were then converted into bubbles. In comparison, no jets above the peripheral orifices were noticed with Dist.7 (10/18x1.5) and it can be assumed that almost all

the superficial air was utilised in the central spout.

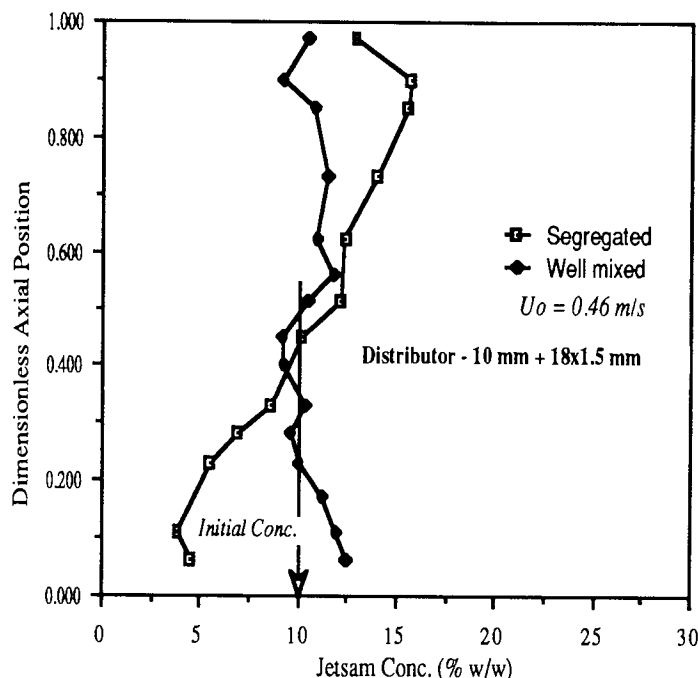


Fig.10.48: Effect of initial condition on conc. profile

Effect of the Superficial Air velocity

The effect of the superficial air velocity on the concentration profile was explored by conducting the experiments at three different velocities using a distributor from each of the two groups as identified earlier. The distributors used were Dist.2 (6/36x2) and Dist.8 (14/18x1.5). All the experiments were carried out from the segregated position with the jetsam placed at the top. The three velocities used were 0.47, 0.61 and 0.76 m/s; whereas the minimum spout fluidisation velocity of the mixture is 0.43 m/s. The concentration profiles obtained at these three velocities are shown in Figures 10.49 and 10.50 representing Dist.2 and Dist.8 respectively. In the case of the Dist.8 (14/18x1.5), the developed zone was only established at the fairly high superficial velocity of 0.76 m/s. The developed zone occupied the top 40% of the bed but the jetsam concentration stayed quite high at about 15.5%. The jetsam concentration in the bottom half of the bed was only 1.2 and 1.3% jetsam at the distributor with gas velocities of 0.61 and 0.76 m/s respectively.

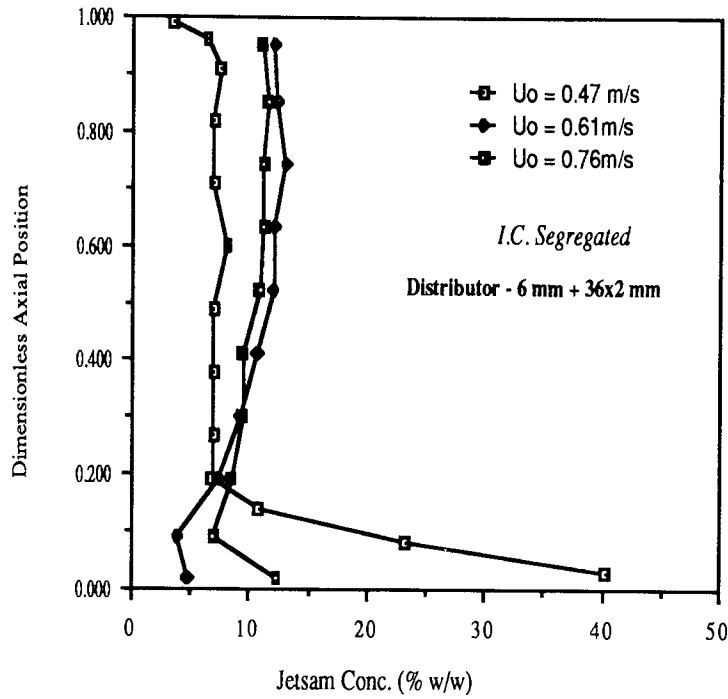


Fig.10.49: Effect of the superficial velocity on the conc. profile

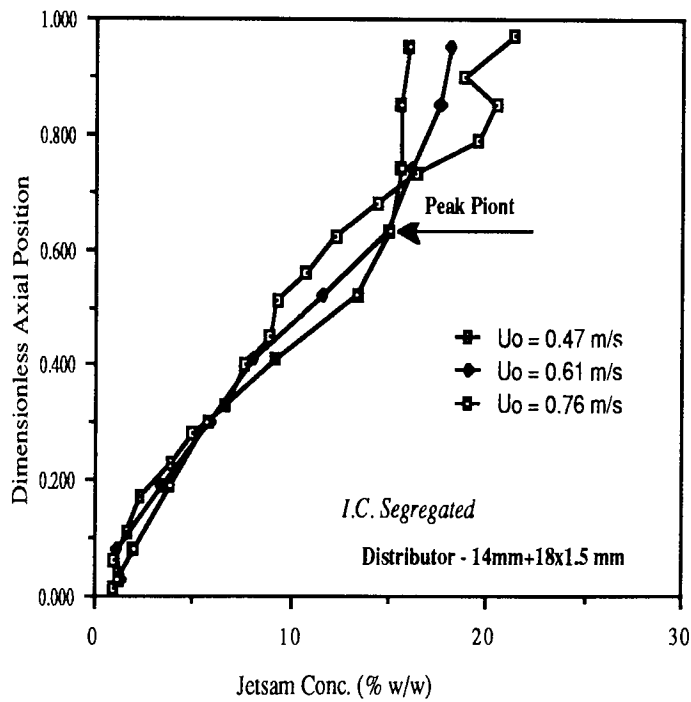


Fig.10.50: Effect of the superficial velocity on the conc. profiles

Effect of the Aspect Ratio (Ra)

The group of distributors with a high central to peripheral free area ratio did not lead to the formation of any developed zone unless the superficial air velocity was high. Another parameter which could help in identifying the existence of any developed zone is the aspect ratio and this was explored in three stages. The distributor used was No.8 containing a 14 mm diameter central orifice and 18x1.5 mm peripheral orifices; this give a central to peripheral free area ratio of 4.9. Earlier work with this distributor showed that the developed zone could only be established with a superficial velocity at 0.76 m/s; therefore a slightly lower superficial velocity of 0.61 m/s was selected to investigate this parameter. All the experiments were carried out from the segregated start with jetsam placed at the top. A series of three experiments was conducted giving aspect ratios of 1.3, 2.0 and 2.6 and the concentration profiles are shown in Figure 10.51.

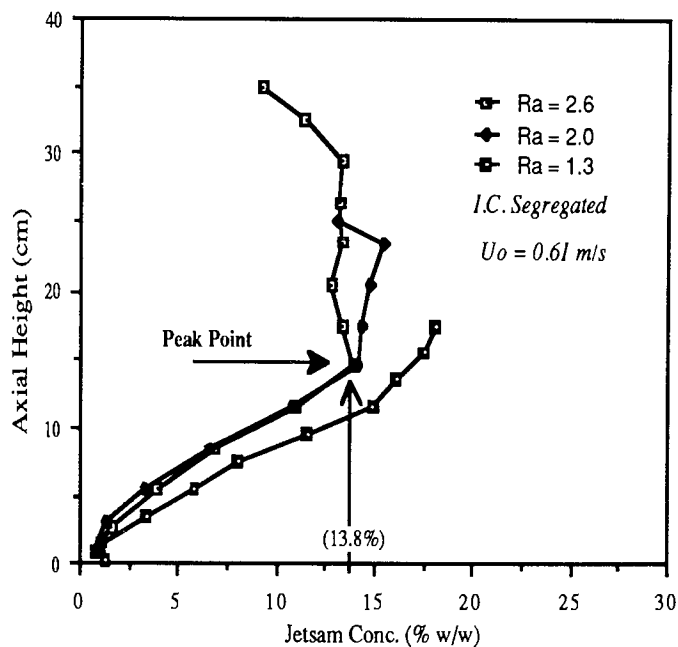


Fig.10.51: *Effect of the aspect ratio (Ra) on the conc. profile*

The concentration profiles illustrate that the developed zone starts to develop at an aspect ratio higher than 1.3 accompanied by a transition from a spout-fluid bed to a slugging bed. The physical appearances of the bed at the three aspect ratios have been reproduced in Figure 10.52. A clear central spout was achieved at an aspect ratio of 1.30, increasing the aspect ratio to 2.0 resulted in deterioration of the spout - the spouting was rather intermittent accompanied by bubbles and slugs. The spout was completely lost at an aspect ratio of 2.6 and the bed behaved as a slugging bed.

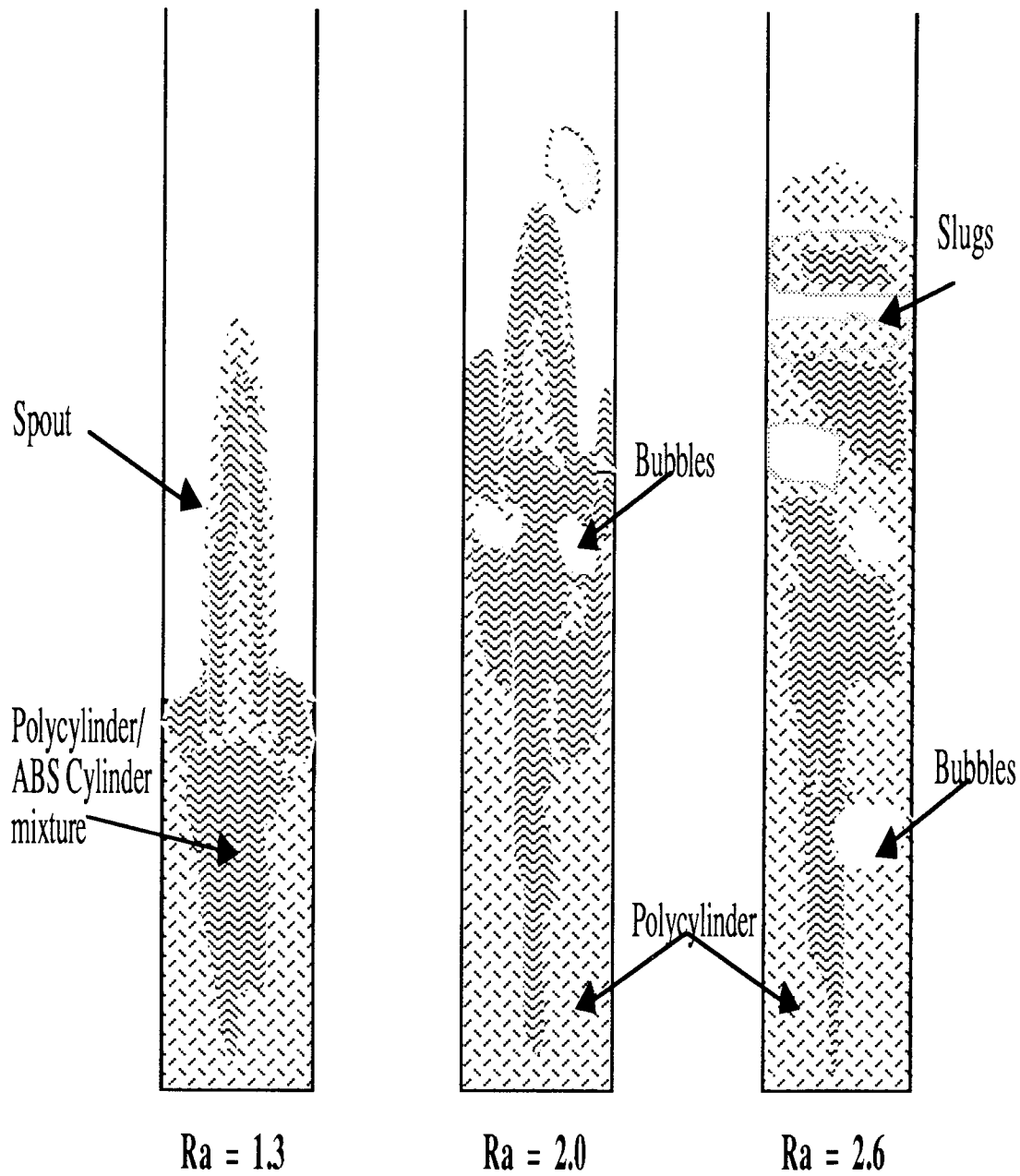


Fig.10.52: Physical appearance of the bed at three different aspect ratios

10.4.5. The Polybeads 1550 / Polybeads 925 System

This is a binary system of equidensity spherical particles employing white Polybeads 1550 with a size range of 1.4 - 1.7 mm and olive green Polybeads 925 with a size range of 0.85 - 1.00 mm. The system was jetsam rich containing 90% of the jetsam particles and 10% of flotsam. The jetsam to flotsam size ratio was 1.7. The static bed height was kept at 22.4 cm with an aspect ratio of 1.6.

Effect of Distributor Design

This aspect of the work was carried out with eight distributors differing in central and peripheral orifice size, number and configuration. Most of the experiments were carried out from the completely segregated mode with the flotsam on the top; mixing then took place for 10 minutes.

This first set of experiments was carried out at superficial air velocities of 0.5 - 0.6 m/s. The test with Dist.1 (6/150x1) at a superficial air velocity of 0.59 m/s failed to induce a central spout and any mixing. The flotsam on the top was fluidising but the jetsam was mainly acting as a fixed bed with very little solid inter-mixing of jetsam and flotsam. The bed was then sectioned and the profile is shown in Figure 10.53.

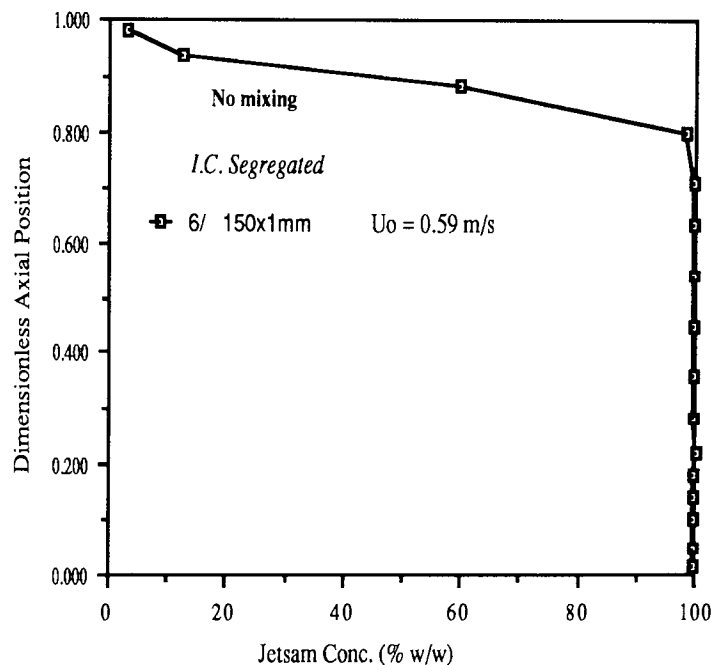


Fig.10.53: Concentration profile showing no mixing

On further increasing the superficial air velocity to 0.63 m/s, the bed started fluidising but without any central spout. The bed was thus behaving as a typical fluidised bed without any of the features of the spout-fluid beds observed in the various flotsam rich systems. The final appearance of the beds at these two superficial velocities is shown in Figure 10.54 b and c respectively.

Dist.1 - 6 mm + 150x1 mm

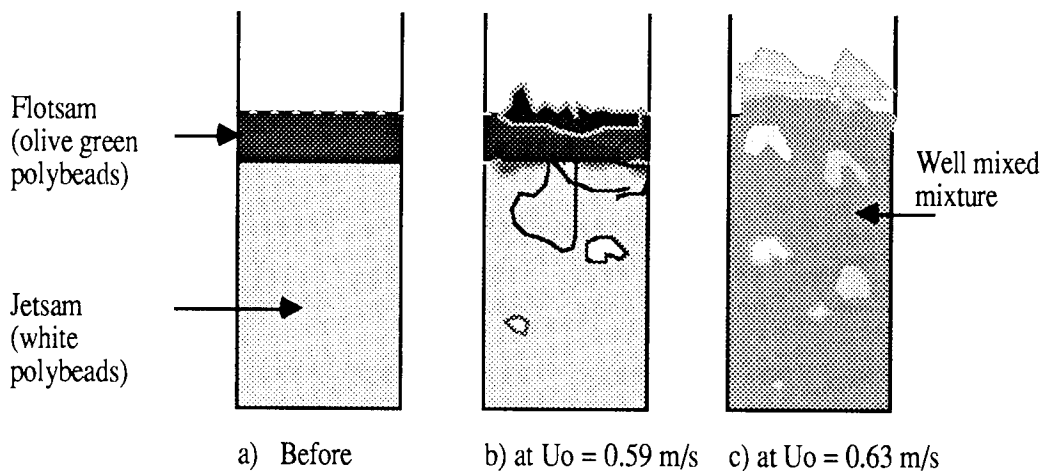


Fig. 10.54: Physical appearance of the three experimental stages

This compares remarkably with the concentration profile obtained with another distributor, namely Dist. 2 (6/36x2), which has a similar free area but different peripheral orifice size and configuration. This comparison is shown in Figure 10.55. The free area of Dist.2 (6/36x2) is 0.95% compared with a figure of 0.98% for the first distributor. The physical appearance of the beds before and after each experiment is presented in Figure 10.56.

The profile obtained with Dist.2 (6/36x2) shows a higher flotsam concentration at a band 6 cm above the distributor. During the experiment it was observed that two distinctly separate zones existed around this band as shown in Figure 10.56b. The dividing band was mainly in the form of a concentrated flotsam layer; below this band, it appeared from visual observation that the bed mainly comprised jetsam particles. The layer by layer analysis, however, shows a contrary picture: the lower section was quite rich in flotsam but the radius defining the mixture gradually decreased downwards.

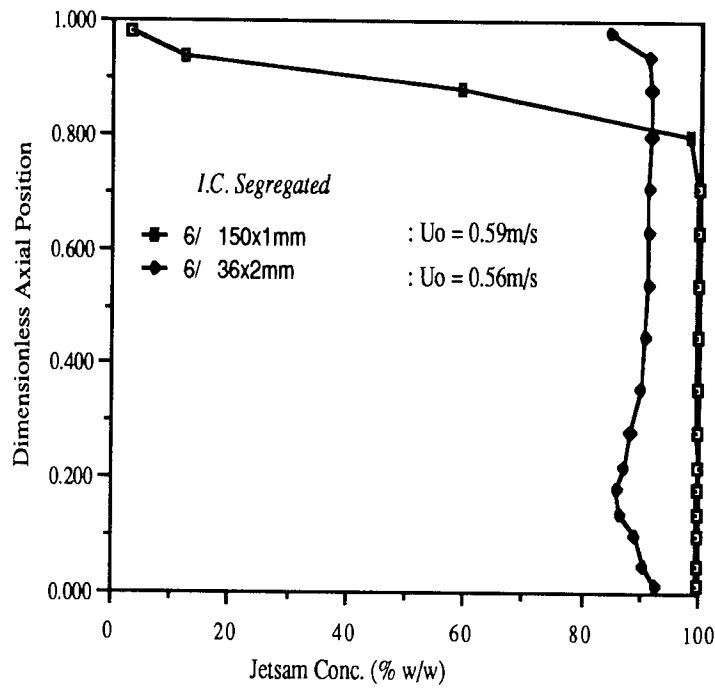


Fig.10.55 Effect of the peripheral orifice configuration on conc. profile

Dist.2 - 6 mm + 36x2 mm

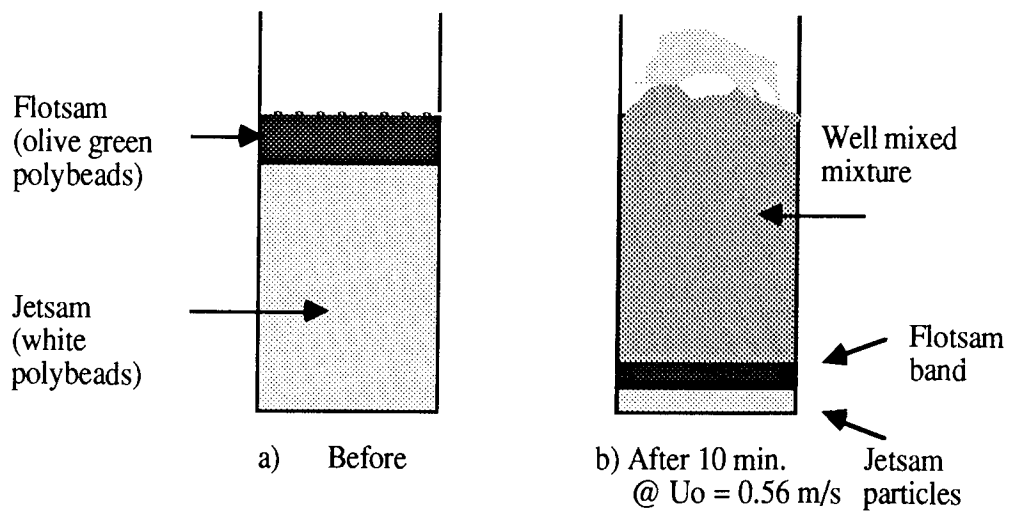


Fig.10.56 Physical appearance of the bed before and after the experiment.

The zone above the band showed intensive mixing of white and green polybeads, in line with the observation that the mixture of particles spouted up from the centre and was drawn down near the bed walls. Also, visual observations revealed that the flotsam tended to move upwards within the jetsam voids and was entrained in the downward flow of the jetsam particles. The spout height was 5 to 6 cm above the surface of the expanded bed.

This set of experiments again reveals that spouting and/or fluidisation can be extremely sensitive to distributor design. Furthermore, the configuration and size of the peripheral orifices would appear to be more important than the total free area. In the case of Dist.1(6/150x1), the peripheral holes promoted fluidisation at the expense of spouting, whereas with Dist.2 (6/36x2) the reverse was true.

The effect of peripheral orifice size, number and configuration was further studied with three other distributors namely No.3 (6/35x1), 4 (6/18x1.5) and 5 (6/13x2/35x1). The concentration profiles obtained with these four distributors are shown in Figure 10.57.

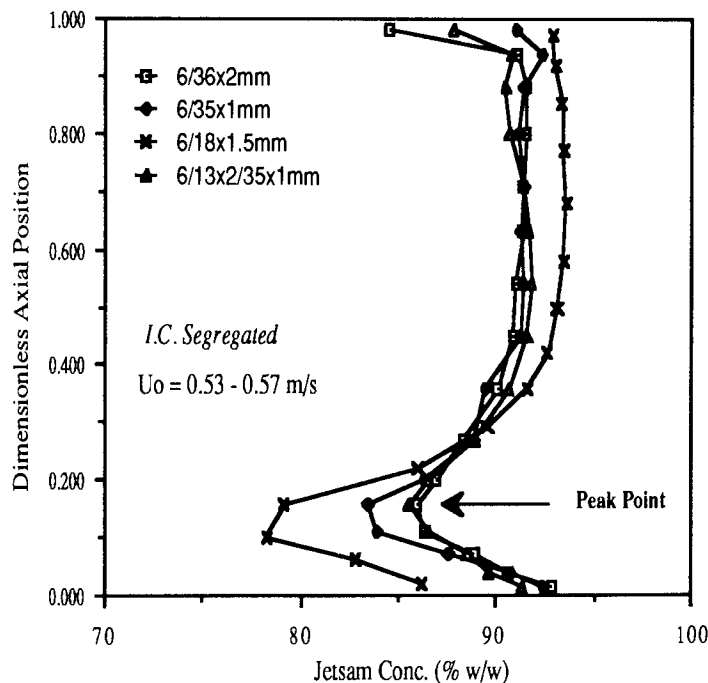


Fig.10.57: Effect of the peripheral orifice design on conc. profile

The figure shows that these profiles are very similar in shape to each other; the sizes of the two zones are almost the same. This means that the concentration profiles are virtually unaffected by the difference in the peripheral orifice size, number and configuration, even though the % free area relative to the total distributor area is substantially different i.e. 0.95%, 0.70% and 0.37% respectively. This observation is contrary to the one made earlier. However, it does help to clarify understanding of the mixing/segregation phenomenon. It appears that there is a dividing line and the distributor will favour either fluidisation or spouting depending on which side of this dividing line it falls. The only single parameter which can help pinpoint the behaviour of the distributor appears to be the free area. In this system, it seems to lie between 0.95% and 0.98%.

The difference in flotsam concentration at the band is also apparent (shown as the peak point in Figure 10.57); Dist.2 (6/35x2) and Dist.3 (6/13x2/35x1) with a % free area of 0.95% and 0.65% respectively contain the same level of flotsam, whereas the concentration decreases gradually with Dist.4 (6/35x1), 0.37% free area, and Dist.6 (6/18x1.5), 0.4% free area, to 85% and 78% respectively. Therefore, it can be concluded that the level of flotsam concentration at the band is loosely related the % free area of the distributor.

The effect of the central orifice diameter was studied with four distributors having 6, 10, 14 and 17 mm orifice diameters while having the same peripheral configuration of 18x1.5 mm holes at 1.5 cm Δ pitch. The profiles are shown in Figure 10.58.

The most noticeable difference is the position of the 'peak point' on the vertical scale. The height of the band increases with the increase in central orifice diameter until it reaches a value of 5.8 cm with the distributor having a 14 mm diameter central orifice. A further increase in the central orifice diameter to 17mm lowers the position of the flotsam band to 5.5 cm, thus revealing an optimum level of central orifice diameter for the flotsam band height. The relationship between the central orifice diameter and flotsam band height is shown in Figure 10.59.

During all these experiments, the spouting mechanism was predominant and formation of jets and bubbles was not witnessed above the peripheral orifice. Again it is expected that some bubbles might have been formed at the periphery but these would have been quickly swept into the central spout.

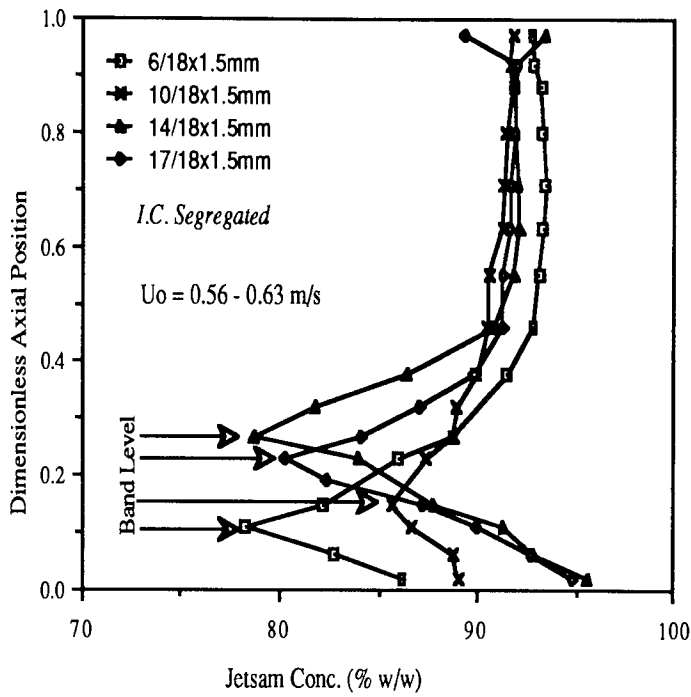


Fig.10.58: Effect of the central orifice diameter on conc. profile

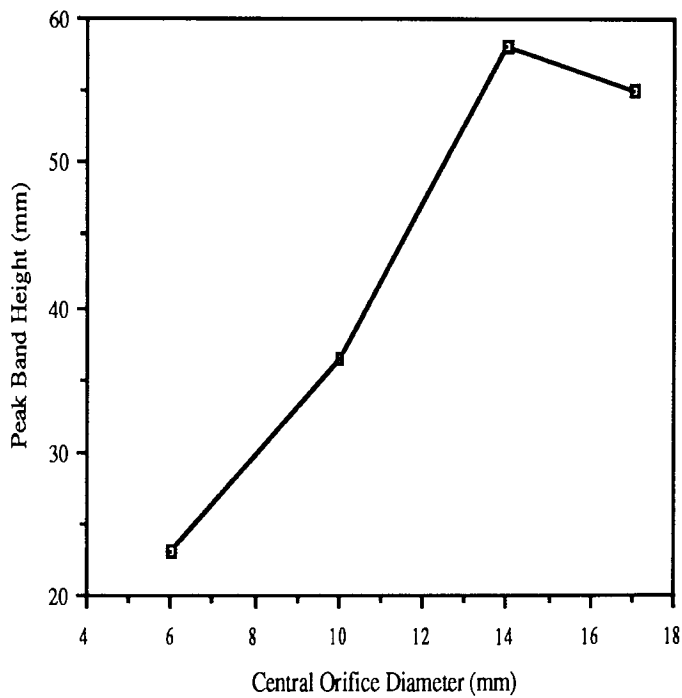


Fig.10.59: Flotsam concentration band height vs central orifice diameter

Effect of the Initial Condition

This effect was studied with two distributors namely Dist.2 (6/36x2) and Dist.4 (6/35x1), both having a common central orifice diameter of 6 mm but differing in peripheral layout. The difference in concentration profile was recorded with experiments starting from the completely 'segregated' and 'well mixed' states and the profiles obtained are shown in Figures 10.60 and 10.61 respectively.

Generally, with both distributors, the profiles obtained from the two different starting positions are similar in shape. In both cases it was observed that, even with a well mixed start, the bed developed a flotsam concentration ring above the distributor dividing the bed into two sections. However, in the case of the well mixed start, this ring was found to be established relatively closer to the distributor .

Figure 10.60 also shows that, when operating with Dist.2 (6/36x2), there was an increase in flotsam concentration at the bed surface. The concentrated flotsam band is shown photographically in Figure 10.62 and 10.63. These photographs were taken when the column was fitted with Dist.2 (6/36x2), while operating from the two starting positions i.e. a) segregated and b) well mixed. The location of this band within the bed was only slightly effected by the initial conditions. This is quite different from the observation made with the Ballotini 1090 / Ballotini 550, which was a flotsam rich system; the difference in jetsam concentration was substantial. A conclusion which can be drawn from this observation is that with a flotsam rich system the effect of the initial starting condition on the concentration profile is substantial, whereas with a jetsam rich system this effect is very minor.

Effect of the Superficial Air Velocity

The flotsam concentration at the band level and its relationship with the superficial air velocity also needed critical examination. Preliminary work showed that the flotsam position is unaffected unless the air velocity is substantially increased ($< 2x$ minimum spout-fluid velocity) so the bed is completely fluidised. Figure 10.64 and 10.65 show photographs of the band taken at $U_0 = 0.59\text{m/s}$ and 0.75m/s ; the position of the band appeared to be unaffected. However, the concentration reduces with an increase in the air velocity until the bed converts to the completely fluidised state and the band completely disappears.

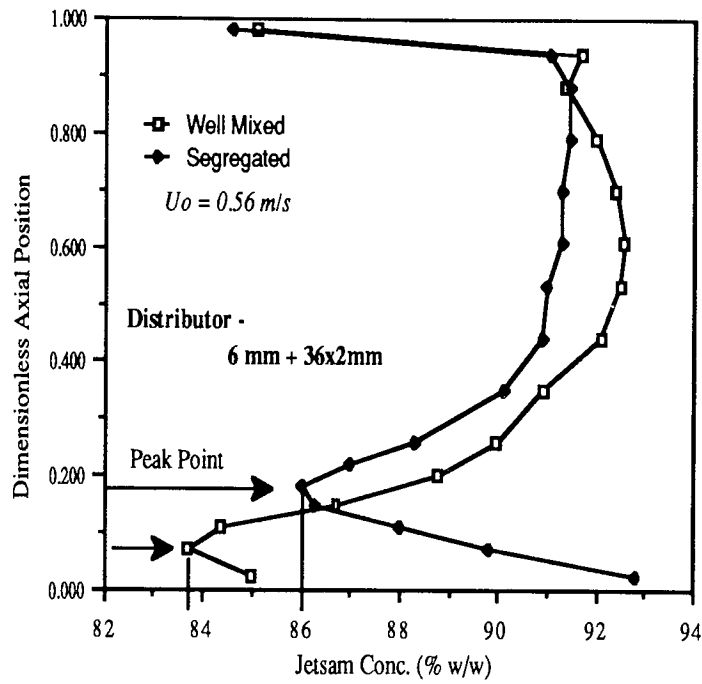


Fig.10.60: Effect of the initial condition on conc. profile

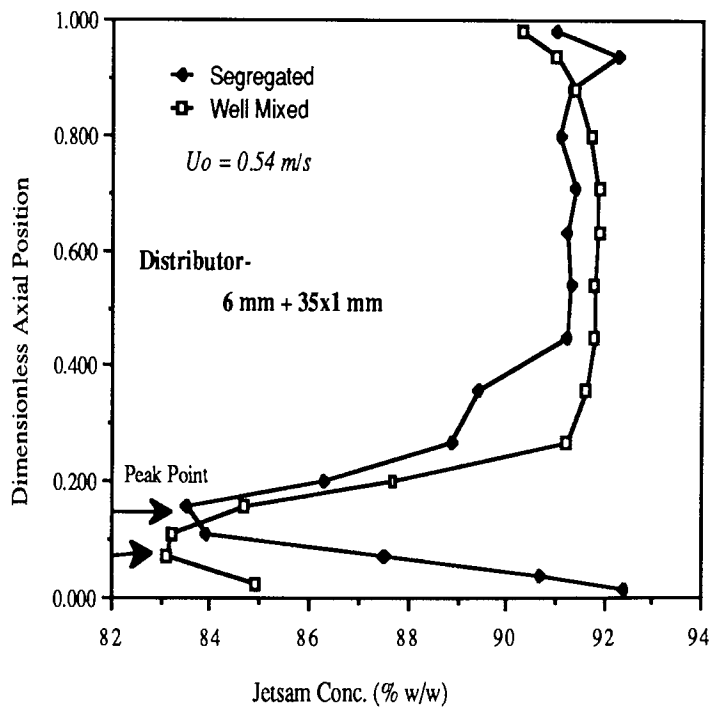


Fig.10.61: Effect of the initial condition on conc. profile



Fig.10.62: Position of the flotsam band when started from "well mixed" state.

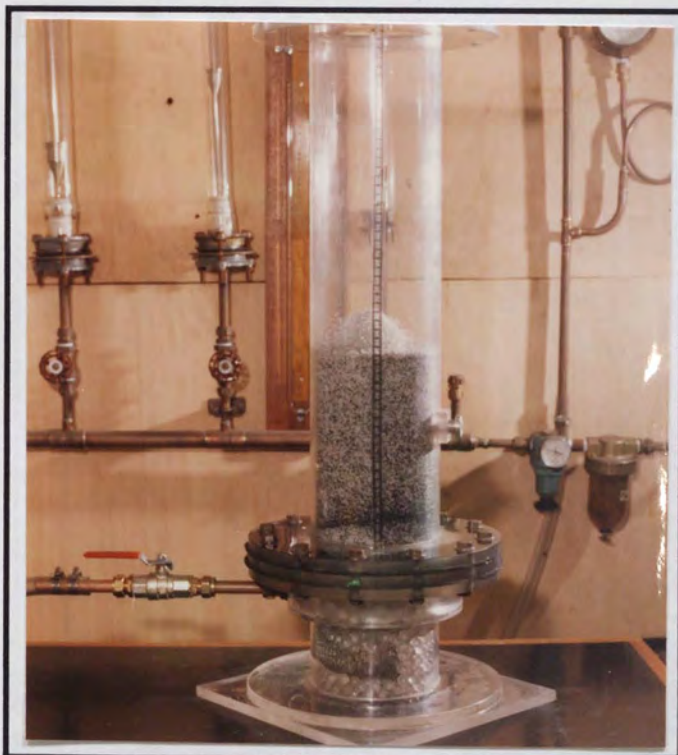
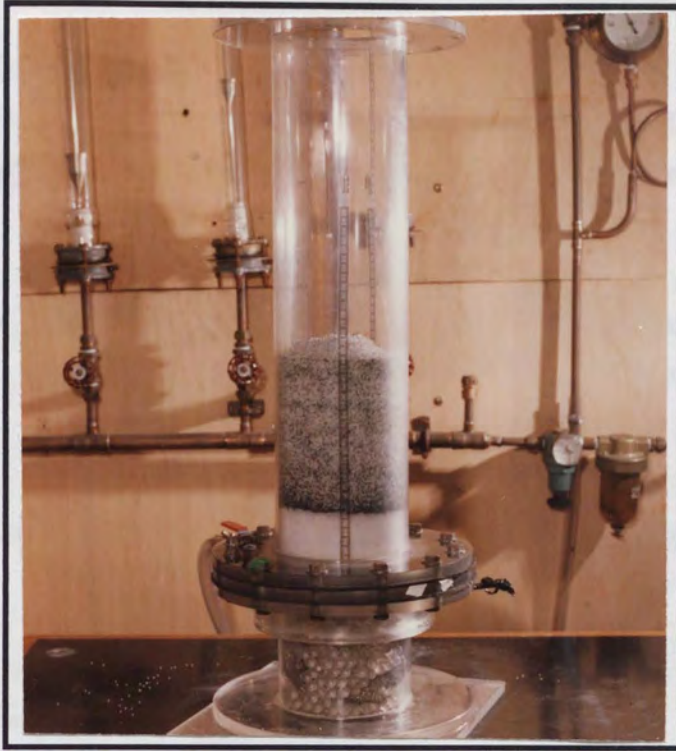
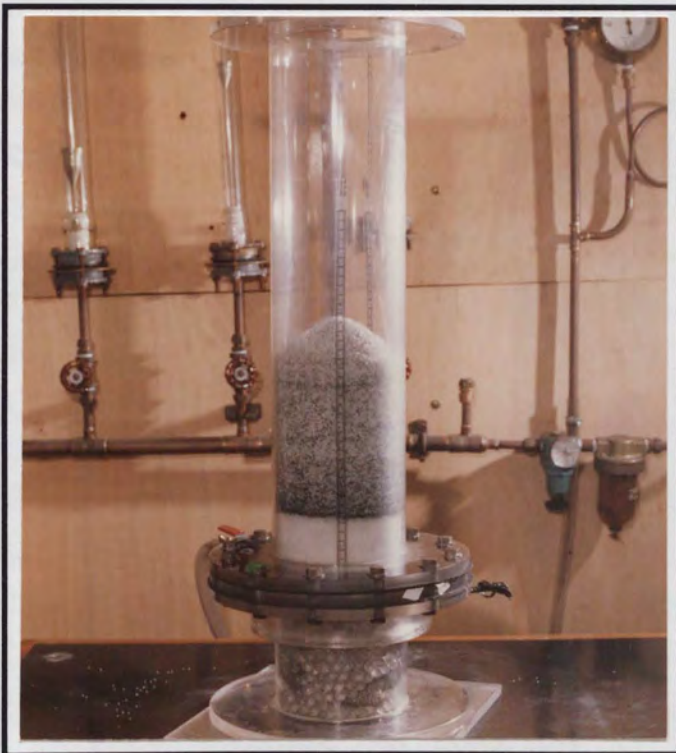


Fig.10.63: Position of the flotsam band when started from "well mixed" state.



*Fig.10.64: Position of the flotsam band @ $U_o = 0.59$ m/s
The column was fitted with Dist.8 (6/18x1.5)*



*Fig.10.65: Position of the flotsam band @ $U_o = 0.75$ m/s
The column was fitted with Dist.8 (6/18x1.5)*

Calculation of the Mixing Number, S

The mixing number, S, was calculated as described in section 10.1., in order to assess the best distributor. The data are shown in Table 10.6.

Table: 10.6 Experimental Data and Mixing Number Calculations for the system Polybeads 1550 / Polybeads 925

Distributor No.	Point of intersection at 90% conc. line on DAP scale (A)	Average Jetsam conc. (B)	Mixing No. $S=A(B-90)$
<i><u>I.C. Segregated</u></i>			
Dist.1 (6/150x1)	No Mixing		
Dist.2 (6/36x2)	0.36	90.4	0.14
Dist.3 (6/13x2/35x1)	0.36	90.7	0.25
Dist.4 (6/35x1)	0.42	91.5	0.63
Dist.5 (6/18x1.5)	0.32	93.0	0.96
Dist.7 (10/18x1.5)	0.38	91.2	0.46
Dist.8 (14/18x1.5)	0.42	92.0	0.84
Dist.9 (17/18x1.5)	0.40	91.5	0.60
<i><u>I.C. Well Mixed</u></i>			
Dist.2 (6/36x2)	0.26	91.1	0.28
Dist.4 (6/35x1)	0.27	91.5	0.41

Dist.2 (6/36x2) gave the best performance in terms of the Mixing Number, (S). Dist.7 (10/18x1.5) gave the best performance among the four distributors when the central orifice diameter was varied.

CHAPTER 11

DISCUSSION, CONCLUSIONS AND RECOMMENDATIONS

11.1 Discussion

A different version of the spout-fluid bed has been developed and tested by the author. This version uses the distributor to establish spouting and fluidisation simultaneously. One advantage of this system is that air can be supplied from a common plenum chamber, thus simplifying the bed construction. Initially, at low flowrates, spouting is initiated but on increasing the flowrate, both mechanisms operate. It has also been established that changes in the distributor design can superimpose either spouting or fluidisation. Therefore, a careful balance between the central orifice and peripheral orifices is required. The most common parameter which can be used for this balance is the free area. The type of solids to be handled plays a significant role; the particle size, diameter, density and shape factor are all important in determining the correct distributor for the required final results.

A disadvantage is that the flow rate for spouting and fluidisation cannot be individually controlled without altering the distributor configuration. Further work on the hydrodynamics of this system could help overcome these difficulties.

Although the work carried out with five binary systems is presented here, experience was also gained with a number of other binary and tertiary systems. Four of these systems were flotsam rich (or flotsam was the major component and jetsam was the minor component) and one system was jetsam rich. Attention was concentrated on unidensity systems with only one exception.

The first system considered was the *ABS Cylinders / Polybeads 1090* where flotsam was the major component. Although the jetsam particles (ABS Cylinders) were cylindrical, their shape did not seem to have any effect on the mixing/segregation results. It was seen that the system divides itself into two zones designated the '*developed zone*' and the '*undeveloped zone*'. The size and shape of the undeveloped zone can be related to the design of the lower section of the conventional spout-fluid bed and it is in the developed zone where the mixing and segregation phenomenon are most significant. The work showed that the size of the developed zone is directly affected by the configuration/size of the peripheral orifices, i.e. the section producing the fluidisation effect. Figure 10.7 confirms that

changes in the central orifice did not alter the size of the developed zone but did affect the jetsam concentration; there appears to be an optimum value (10 mm diameter in this case) which gives the most uniform concentration. This conclusion is independent of the initial condition of the solids.

The effect of the aspect ratio experiments showed that there is a limit to the height of a stable spout. If the bed height is greater than this, then the spout is converted into bubbles. An increase in the superficial velocity did not increase the height of the spout and the bubbles became slugs in the case of the deep beds; the jetsam stayed fairly well mixed in the developed zone of these deep beds. The size (height) of the undeveloped zone was independent of the bed depth. With a shallow bed, the spout was established but the bed stayed badly segregated. Therefore, there is a minimum and maximum aspect ratio within which the spout-fluid bed behaves as a good mixer and these are 1.5 to 2.5.

The study to determine the effect of the jetsam concentration on the mixing mechanism shows that a higher flowrate is required to establish the central spout, which is to be expected, and that mixing improves with higher jetsam concentrations.

Another system similar in behaviour to that of *ABS Cylinder/Polybeads* was *Ballotini1090 / Ballotini550*. The distributor containing a high peripheral free area produced a profile exhibiting both developed and undeveloped zones, whereas distributors with a lower peripheral free area did not produce any developed zone. This effect was not observed with the polymer system and can only be attributed to the higher density of the ballotini. This means that with denser solids the mixing can best be achieved with the fluidisation mechanism rather than the spouting mechanism. This conclusion is applicable regardless of the initial conditions. One point to note is that although the average diameter of the major component put it in Geldart's group 'D', it was quite small i.e. 500 - 600 μm .

The binary system with particles differing in both size and density was *Ballotini 1090/ Polybeads 1850*. These particles were selected due to their similarity in the minimum fluidising velocity. The central spout with this mixture was generally well distinguished and relatively tall. The physical appearance of the bed was very different from that of the two systems described above. Within a few

seconds of operation the minor component (jetsam - ballotini) concentrated in the form of a band a few centimeters above the distributor; it appeared that below this band the ballotini did not penetrate whereas above the band the particles were well mixed. The central orifice diameter had a direct influence on the height of this band; the band was elevated initially with an increase in the orifice diameter but then dipped and stabilised. This is in contrast with the observation made with the Polybead/ABS Cylinder system where changes in the central orifice diameter did not alter the size of the developed zone.

The variation in the size and the configuration of peripheral orifices showed that when the peripheral free area is substantially greater than the central orifice free area (≈ 3 times), the bed behaves more like a fluidised bed. Bubbles were frequently observed beside the central spout with these distributors. When the peripheral free area to central free area ratio is < 3 , the bed develops a central spout without any bubbles.

The effect of placing the ballotini at various positions in the bed confirmed that the concentration profile is unaffected if the ballotini are placed anywhere above the band. This shows that the spouting mechanism predominates and principally determines the mixing/segregation mechanism. The showered solids travel downwards in the annulus and are pulled into the spout at some stage in the bed. The position where they are pulled into the spout determines the height of the band. Figure 10.39 schematically shows this mechanism. Patrose and Caram (1984) in their study of the mechanics of particle motion in a grid jet have found that the solids drain down from the packed annulus, into the jet, all along the jet length. The author's investigation suggests that the solids do not drain down all along the jet length; this transfer process stops at some distance above the distributor and that is where the band is formed. Inside the spout, the mixing continues which is in line with Patrose and Caram's finding that ' the inlet grid jet is not a hollow gas cavity, but a region of active solids motion'. However, if the ballotini are placed at the distributor, then only part of the solid participates in the mixing mechanism.

The effect of the superficial velocity showed that particles are best mixed at the minimum velocity required to produce a central spout. Increasing it further will promote segregation and then at even higher velocities mixing again predominates.

The above system can be compared with the jetsam-rich Polybeads/Polybeads System. Although this is a unidensity system and the particle size ratio difference is 1.7, its general behaviour is very similar to that of the Polybeads/Ballotini system, especially with a distributor where the ratio between the peripheral and central free area is less than 3. The minor component (flotsam in this case) behaves similarly to the minor component (jetsam) in the Polybeads/Ballotini system. In both cases a band containing a high percentage of the minor component is formed a few centimeters above the distributor. The vertical height of this band can be directly related to the central orifice diameter. The effect of the peripheral free area is limited to the concentration of the minor component in this band.

By contrast, with distributors having a peripheral to central free area ratio between 3 to 4, the behaviour is substantially different. In the case of the Polybead/Polybeads system, the minor component (flotsam) still forms the band a few centimeters above the bed, whereas with the Polybead/Ballotini system the minor component (jetsam) does not form the band and its general behaviour is like a fluidised bed even though a spout is formed. When this peripheral to central free area ratio becomes greater than 4, once again the behaviour becomes similar and both beds behave as a fluidised system with a central spout. The best performance was achieved with Dist.2 (6/36x2).

The initial condition had only a limited effect. The general behaviour of the bed was similar and the band was approximately at the same height. However, the minor component concentration at the distributor increased as a result of a 'well mixed' start.

The fifth system reported in this study was used mainly to examine the effect of particle shape. In the case of the Polybeads/ABS Cylinder System (see above), the minor component was cylindrical and it was concluded that the shape factor did not contribute to the mixing/segregation phenomenon. In the study with Polycylinder / ABS Cylinders, both the major and minor components were cylindrical and of the same density. Both particles had the same cylindrical length of 3 mm but differed in the cylindrical diameter by 3.2 to 1. This study showed that when the major components are non spherical, the shape factor makes an important contribution. Under normal operating conditions, i.e. at a superficial velocity which produces a stable central spout, the bed stayed badly segregated. The changes in the

central orifice diameter did not produce any improvement in the concentration profiles. However, changes in the peripheral orifices split the distributors into two categories. Distributors with a peripheral to central free area ≤ 3.4 failed to produce any developed zone and the bed stayed badly segregated. Distributors where the peripheral to central free area was > 3.4 produced a developed zone which occupied nearly 80% of the bed. The only drawback with these distributors was that a high percentage of the minor component (jetsam) was pushed on the distributor. Changing the initial condition when using a distributor where the peripheral to central free area ratio was > 3.4 (Dist.2 6/36x2) showed that bed behaviour was not affected.

11.2 Conclusions

While this study must be considered preliminary, the following important conclusions can be drawn from the results.

1. The modified version of the spout-fluid bed, where gas is supplied from the common plenum, has opened up a new dimension in gas-solid reactor systems where changes in the mixing and segregation pattern can be controlled by the distributor design. The heart of this spout-fluid bed is the use of the new type of distributor, which contains a large orifice in the centre with no orifice in the vicinity but a number of smaller peripheral orifices of different size and configuration. Operating information was collected with five systems covering a wide spectrum of particle variables. A stable spout (fountain) was created in all the cases and this operating condition provided a common datum.
2. The mixing curve obtained by plotting minor component concentration versus the dimensionless axial position showed that two distinct zones exist in the bed. Zone I occupies the lower section of the bed and is where segregation phenomena dominate. Zone II occupies the upper part of the bed and here mixing phenomena dominate. These zones clearly occur, in the case of flotsam-rich systems, if the superficial gas velocity is less than the jetsam minimum fluidising velocity (U_{mfj}) but greater than the flotsam minimum fluidising velocity (U_{mff}). In the case of jetsam-rich systems, the superficial gas velocity needs to be

greater than the jetsam minimum fluidising velocity to establish these two zones. However, the experience has shown that these regions, although sometimes quite ill-defined, always exist.

3. The relative size of these two regions and their composition depends mainly on the distributor configuration and more particularly the free area ratio of the central and peripheral orifices. Operating factors such as gas velocity, the particle densities and diameters, overall bed composition and initial conditions play only a small part.

4. In Zone I (*undeveloped zone*), the bed stays fairly segregated. In the case of an initially segregated start, the minor component concentration is low at the distributor and slowly increases along the axial length of the bed until it reaches the developed zone. In the case of an initially mixed start, the minor component concentration is about average at the distributor, drops to its minimum value along the axial length, then picks up and gradually reaches an average value before reaching developed zone.

5. In Zone II (*developed zone*), a variety of axial concentration profiles can occur, depending mainly on the peripheral orifice diameter and configuration supplemented by the superficial gas velocity, the particle densities and diameters, the aspect ratio and overall bed composition. The pattern of the final steady-state concentration profile does not depend on the initial condition.

6. A distributor performance criterion has been established based on the Mixing Number for unidensity, spherical rich systems. The Mixing Number $S = A \cdot (B - C_{i,\text{major component}})$ is a good indicator of the degree of mixing or segregation and provides a convenient means to quantify the effect of distributor design. This mixing number represents the variation of the jetsam concentration along the bed height. The mixing number, S, has zero value in the ideal case.

The main findings for the systems employed are now summarised below for comparative purposes.

7. ***Unidensity Flotsam Rich System:***

Particle density - $< 1.1 \text{ kg/m}^3$

Shape factor - Flotsam - Spherical

Jetsam - Spherical or non spherical

- a) The mixing process appeared to be controlled by the spouting mechanism for peripheral to central orifice (cross sectional area) ratios of < 3 : if this ratio is > 3 , the fluidisation mechanism dominates .
Dist.7(10/18x1.5) seems to fall out of the above range.
- b) The size of Zone II (developed zone) is directly proportional to the free area occupied by the peripheral orifices.
- c) The variation in the size of the central orifice will affect the jetsam concentration in the developed zone.
- d) The establishment of a stable spout is limited to the aspect ratio of 2.5 and above that the spout is converted into bubbles.
- e) Dist. 1 (6/150x1) attained the lowest mixing number followed closely by Dist 2 (6/36x2). Dist 8 (14/18x1.5) scored the highest mixing number.

8. ***Unidensity Flotsam Rich System:***

Particle density - $> 1.1 \text{ kg/m}^3$

Shape factor - Flotsam - Spherical

Jetsam - Spherical

- a) The mixing is mainly controlled by the fluidisation mechanism.
- b) Zone II (developed zone) can only be established with distributors containing a high peripheral free area. The size of this zone is directly proportional to the peripheral free area.
- c) The jetsam concentration in the developed zone is independent of the central orifice diameter.
- d) It is assumed that the establishment of the stable spout is limited to the aspect ratio of 2.5.
- e) Dist 1 (6/150x1) and Dist 2 (6/36x2) achieved the lowest mixing

number whereas Dist 8 (14/18x1.5) scored the highest .

9. ***Different Density Flotsam Rich System:***

Shape factor - Flotsam Spherical

Jetsam Spherical

- a) The mixing process appeared to be controlled by the spouting mechanism for peripheral to central orifice (cross sectional area) ratios of <3 : if this ratio is > 3 , the fluidisation mechanism dominates .
- b) A concentrated band of the minor component is formed just above the distributor in all cases except when this component is initially placed at the distributor. The height of this band is closely related to the central orifice diameter. The 10 mm diameter was found to be optimum.
- c) Effective mixing is achieved at the superficial gas velocity that is required to establish the spout. The superficial gas velocity is slightly higher than the composite minimum spout-fluidising velocity of the mixture.
- d) The minor component concentration at the band is dependant on the superficial gas velocity.
- e) Distributors containing a large number of small orifices in the periphery promote segregation.
- f) Dist. 2 (6/36x2) gave the best performance in promoting mixing where as Dist. 1 (6/150x1) promoted segregation.

10. ***Unidensity Flotsam Rich System:***

Shape factor - Flotsam Cylindrical

Jetsam Cylindrical

Equivalent Spherical Diameter Ratio: 2.15

- a) The spouting mechanism appeared to be controlling the mixing mechanism. Generally a tall and well pronounced spout was obtained with this cylindrical system unlike the spherical system.
- b) Stable spouting is achieved at a slightly higher superficial gas velocity than the minimum spout-fluidising velocity.
- c) Distributors containing a high peripheral free area promote segregation regardless of the orifice diameter and configuration.

- d) Distributors containing low peripheral free areas promote mixing.
- e) Variation in the central orifice diameter has no bearing on the mixing or segregation phenomenon.
- f) Zone I (developed zone) does not exist under normal operating conditions.
- g) Zone II is only established in deep beds with aspect ratio of >2 , or with superficial gas velocity $> 1.4 \times U_{sfav}$.

11. ***Unidensity Jetsam Rich System:***

Shape factor - Flotsam Spherical

Jetsam Spherical

Particle Size Ratio: 1.7

- a) The presence of a large number of peripheral orifices hinders the establishment of the central spout. Otherwise the spouting mechanism appears to control the mixing.
- b) This system behaved in a similar way to different density systems in that a band containing a high percentage of the minor component was formed a few centimeters above the distributor.
- c) The height of the band is related to the central orifice diameter with no optimum diameter.
- d) The concentration of the minor component in the band is related to the free area of the peripheral orifices.
- e) Initial conditions had little effect on the final concentration profile.
- f) Dist 2 (6/36x2) gave the best performance.

12. Dist 2 having a 6 mm diameter central orifice and 36 x 2mm diameter peripheral orifices appeared to perform best for the five systems employed. Obviously the spouting and fluidising mechanisms have been active, side by side, to create this desirable situation. Analysis of the orifice diameter and configuration shows that the best result for spouting can be achieved when

$$D_c / D_b = 0.04 \quad (11.1)$$

where

D_c = Column diameter (mm)

D_b = Central orifice diameter (mm)

For the spouting mechanism to be active, the centre of the bed should be free of orifices other than the central one: the small orifices for fluidisation should be drilled near the periphery. The exact size and configuration of these orifices is difficult to define and depends upon a number of variables. The literature fails to provide any clear guidance and so recourse must be made to trial and error methods.

11.3 Recommendations for Future Work

The areas in which it is suggested that further work be carried out are:

- a) establishing the flow regimes
- b) effect of the particle size difference
- c) beds with jetsam-rich systems compared with flotsam-rich systems
- d) effect of both density and particle size difference
- e) bed rich with non-spherical and particularly with cylindrical particle
- f) development of general correlations to determine the effects of the distributor design related to particle properties, gas velocity, bed height and bed composition
- g) basic mechanism
- h) overall bed behaviour
- i) experiments to determine scale-up effects.

A systematic study is now needed to exploit these preliminary findings. Flow regime maps for various solids systems alongwith the effect of the distributor design need to be developed. This work should be carried out on similar lines to Sutanto's (1983) work. Initial work should be concentrated only on one type of solid system i.e. unidensity particles. Experiments should be conducted with a wide range of particle sizes covering binary mixtures of various densities. The configuration of the distributor design should be examined thoroughly. The effect of the central spout on the rest of the bed and its

interaction with the peripheral orifices needs to be carefully examined.

The difference between the flotsam rich and jetsam rich systems and their effect on the final concentration needs to be fully exploited, especially the concentration band of minor component in the jetsam rich and different density systems.

After the initial study with the unidensity system, the work should be extended to different density systems to find common areas in order to establish overall rules for particle interaction. It would be interesting to examine the factors which catalyse the formation of the concentrated band of the minor component in two systems.

The author's study has shown that beds containing cylinders behave somewhat differently from those made up of spheres, the mixing phenomenon being completely dominated by the spouting mechanism. Further work is required to validate this initial finding.

The effect of distributor design and other operating parameters needs to be explored to develop empirical correlations. The finding that $D_c / D_b = 0.04$ is best in spout-fluidised bed needs to be thoroughly investigated, as this ratio is lower than the ratio widely used in the design of the spouted bed. The interaction of the central orifice and standpipe type orifices in the periphery needs to be investigated.

One of the fundamental areas for future research is the distribution of superficial gas between the central orifice and the peripheral orifices. It will be worthwhile to study the effects of the central and peripheral orifices in isolation and then superimpose these on each other to complete the picture.

Development of more rapid methods for measuring solids distribution is an important consideration, because of the time consumed in layer-by-layer, slumped-bed sampling. Radioactive tracer methods such as that used by Chen and Chao (1982) appear to have considerable promise.

Scale-up has always been the most common and the most frustrating concern for designers of gas-solid reactors. Mixing or segregation behaviour is likely to be strongly influenced by the size of the bed, especially with regard to the large-scale convection parameters. Therefore, some large-scale experiments will be essential in establishing the validity of laboratory and bench-scale data. Because of the difficulties in evaluating mixing/segregation in a large bed, development and application of radioactive tracers or similar techniques could result in saving of time and labour.

REFERENCES

REFERENCES

- Agarwal, J. C., W. L. Davies, Jr., and D. T. King, "Fluidized Bed Coal Dryer," *Chem. Eng. Prog.*, **58**, No. 11, 85 - 90 (1962)
- Agbim, A. J., "The Mechanism by which Particles Segregate in Gas Fluidised Beds," *Ph. D. Thesis, University of London*, (1971)
- Beeckmans, J. M and B. Stahl, "Mixing and Segregation Kinetics in a Strongly Segregated Gas-Fluidized Bed", *Powder Tech.*, **53**, 31 - 38, (1987)
- Berquin, Y. F., "Method and Apparatus for Granulating Melted Solid and Hardenable Fluid Products," *British Patent No. 962 265*, (1964).
- Berquin, Y. F., "Propects for full-scale Development of Spouting Beds in Fertilizer Granulation". *Proc. First Int. Conf. on Fertilisers, London, Paper 23*, 296 - 304, (1977)
- Botterill, J.S.M. and P.D. Bloore, "Channels and Chains of Bubbles in Gas Fluidised Bed," *Can. J. Chem. Eng.* **41**, 111 - 115, (1963)
- Burgess, J. M., A. G. Fane and C.J.D. Fell, "Measurement and Prediction of the mixing and segregation of solids in Gas Fluidized Beds", *Second Pachec Conference, Denver*, 2, 1405 (1977).
- Canada, G.S., M. H. McLaughlin, and F.W. Staub, "Flow Regimes and Void Fraction Distribution in Gas Fluidization of Large Particles with and without Tube Banks", in "Fluidization: Application to coal Conversion Processes," *AIChE Symposium Series No. 176*, **74**, 14 - 26, (1978).
- Chavarie, C. and J. R. Grace, "Performance Analysis of a Fluidizes Bed Reactor, II. Observed Reactor Behavior Compared with Simple Two-Phase Models," *Ind. Eng. Chem. Fund.*, **14**, 79 - 91, (1975)

Catapovic, N. M., N. G. Jovanovic, and T. J. Fitzgerald, "Regions of Fluidization for Large Particles," *AIChE J.*, **24**, 543 - 547, (1978).

Chen, J.L.-P. and D. L. Keairns, "Particle Segregation in a Fluidized Bed," *Can. J. Chem. Eng.*, **53**, 395 - 402, (1975).

Chatterjee, A., "Spout-Fluid Bed Technique", *Ind. Eng. Chem. Process Des. Develop.*, **9**, No.2, 340 - 341, (1970).

Cheung, L.Y-L., "A Quantitative Analysis of the Mixing of Two Segregating Powders of Different Density in a Gas-Fluidised Bed," *Ph.D. Thesis, University of London*, 1976.

Clift, R., M. Filla, and L. Massimilla, as in "Chapter 3 -Gas Jets in Fluidised Beds" 133 - 171, in "*Fluidisation*", Edited by R. Clift, J. F. Davidson and D. Harrison, second edition, Academic Press, New York, (1985)

Cook, H. H., and J. Bridgwater, "Segregation in Spouted Beds", *Can. J. Chem. Eng.*, **56**, 636 - 639, (1978).

Cowan, C. B., W. S. Peterson and G. L. Osberg, "Spouting of Large Particles" *The Engineering Journal*, **May**, 60- 64, (1958)

Cranfield, R. R., "Solids Mixing in Fluidized Beds of Large Particles," in "Fluidization: Application to coal Conversion Process," *AIChE Symposium Series No. 176*, **74**, 54 - 59, (1978)

Cranfield, R. R., "Solids Mixing in Fluidized Beds of Large Particles," in "Fluidization: Application to Coal Conversion Process," *AIChE Symposium Series No. 176*, **74**, 54 - 59, (1978).

Cranfield, R. R. and D. Geldart, "Large Particle Fluidization", *Chem. Eng. Sci.*, **29**, 935 - 947, (1974).

Davidson, J. F. and D. Harrison, *Fluidised Particles*, Cambridge University Press, Cambridge, (1963).

Davidson, J. F., as in " *Chapter 3 - Gas Jets in Fluidised Beds* " 133 - 171, in " *Fluidisation* " , Edited by R. Clift, J. F. Davidson and D. Harrison, second edition, Academic Press, New York, (1985)

Davidson, J. F., D. Harrison, and R. Clift, " *Fluidization* " Second Edition, Academic Press, London, (1985).

Daw, C.S., "Solids Segregation in Gas-Fluidized Beds of Large Particles", *Ph.D. Thesis, The University of Tennessee, Knoxville*, (1985).

Fan, L. T. and Y. Chang, "Mixing of Large Particles in Two-Dimensional Gas Fluidized Beds," *Can. J. Chem. Eng.*, **57**, 88 - 97, (1979).

Feng, D., H. Chen and W. B. Whiting, "The Effects of Distributor Design on Fluidized-Bed Hydrodynamic Behavior," *Chem. Eng. Commun.*, **36**, 317 - 332, (1985).

Fryer, C. and O. E. Potter, "Countercurrent Backmixing Model for Fluidized Bed Catalytic Reactions," *Ind. Eng. Chem. Fund.*, **11**, 338 - 344, (1972)

Geldart, D., " *Gas Fluidization Technology* ", John Wiley & Sons, (1986).

Geldart, D., "Types of Gas Fluidisation" , *Powder Tech.*, **7**, 285 - 292, (1973)

Geldart, D. and J. Baeyens, "The Design of Distributors for Gas-Fluidized Beds", *Powder Tech.*, **42**, 67 - 78, (1985).

Geldart, D. and J. R. Kelsey, "The Influence of the Gas Distributor

on Bed Expansion, Bubble Size, and Bubble Frequency in Fluidised Beds", *I.Chem. E. Symposium Series No. 30*, 114 - 125 (1968).

Geldart, D., J. Baeyens, D. J. Pope, and P. Van De Wijer, "Segregation in Beds of Large Particles at High Velocities," *Powder Tech.*, **30**, 195 - 205, (1981).

Gibilaro, L. G. and P. N. Rowe, "A Model for a Segregating Gas Fluidised Bed," *Chem. Eng. Sci.*, **29**, 1403 - 1412, (1974).

Groshe, E. W., "Analysis of Gas Fluidized Solid System by X-ray Absorption," *AIChE J.*, **1**, 358 - 365, (1955)

Jovanovic, G. N. "Gas Flow in Fluidized Beds of Large Particles; Experiment and Theory," *Ph.D. Thesis, Oregon State University. Corvallis, Oregon*, (1979)

Kato, K. and C.Y.Wen, "Bubble Assemblage Model for Fluidized Bed Catalytic Reactors," *Chem. Eng. Sci.*, **24**, 1351 - 1369, (1969)

Keceioglu, I., Yang, W. C., and Keairns, D.L., *74th AIChE Annu. Meet. AIChE J.*, **30**, 99 - 110, (1984).

Kutluoglu, E., J.R.Grace, K.W. Murchie, and P. H. Cavanagh, "Particle Segregation in Spouted Beds", *Can. J. Chem. Eng.*, **61**, 308 - 316, (1983).

Kunii, D. and O. Levenspiel, *Fluidization Engineering*, R. E. Krieger Publishing Company, Huntington, New York (1969).

Latham, R., C. Hamilton, and O.E.Potter, "Back-Mixing and Chemical Reaction in Fluidised Beds," *Brit. Chem. Eng.*, **13**, 666 - 671, (1968).

Lefroy, G. A. and J. F. Davidson, "The Mechanics of Spouted Beds," *Trans. Instn. Chem..Engrs.*, **47**, T120 - T128, (1969)

Markhevka, V.I., Basov, V.A., Melik-Akhnazarov, T.Kh., and Orochko, D.I. *Theor. Found. Chem. Eng. (English Translation)*, **5**, 80 - 85, (1971)

Mather, K. B., "A New Technique for Grinding of Particulate Solids. Patent proposal", 1972, as in "*Spouted Bed*," by Mathur and Epstein, Academic Press, New York, (1974).

Mathur, K. B. and Epstein, N., "*Spouted Beds*", Academic Press, New York, (1974).

Madonna, L. A., Bensel, B. K. , Boornazian, L., Geveke, D., Nixon McGowan, G., "Some Characteristics of a Spout-Fluid Bed," *Proceedings of 3rd International Conference on Alternative Energy Sources, Miami Beach, Ed. by T.N. Veziroglu Hemisphere, Washington D.C. , 3*, No.6, 257 - 282 (1980)

Massimilla, L, in " Chapter -3, Gas Jets in Fluidised Beds ", in "*Fluidization* " by Edited by R. Clift, J. F. Davidson and D. Harrison, Second Edition, Academic Press, London, 133 - 171, (1985).

Mori, S. and C. Y. Wen, "Estimation of Bubble Diameter in Gaseous Fluidized Beds," *AICh J.*, **21**, 109 - 117, (1975).

McNab, G. S., and J. Bridgewater, "Solid Mixing and Segregation in Spouted Beds," *Proc. 3rd Europ. Conf. on Mixing, BHRA Fluid Engineering*, 125 - 140, (1979)

McGrath, L and R. E. Streatfield, "Bubbling in Shallow Gas-Fluidised Beds of Large Particles, " *Trans. Inst. Chem. Eng.*, 49, T70 - T79, (1971)

Naimer, N. S., " Studies of Segregating Fluidised Beds: Batch and Continuous Operations", *Ph.D. Thesis, University of London*, (1982)

Naimer, N. S., T. Chiba and A W Nienow, "Parameter Estimation for a

Solids Mixing / Segregation Model for Gas Fluidised Beds," *Chem. Eng. Sci.*, **37**, No.7, 1047 - 1057, (1982)

Nicklin, D. J., "Two-Phase Bubble Flow," *Chem. Eng. Sci.*, **17**, 693 - 702, (1963).

Nienow, A. W. and D. J. Cheeseman, "The Effect of Shape on the Mixing and Segregation of Large Particles in a Gas-Fluidized Bed of Small Ones," in *Fluidization*, J. R. Grace and J. M. Matsen ed., Plenum Press, New York, 373 -379, (1980).

Nienow, A.W. and T. Chiba, "Fluidization of Dissimilar Materials" in "*Fluidization*" by Davidson, Harrison and Clift, Academic Press, London, (1985).

Nienow, A. W., P. N. Rowe, and L. Y.-L. Cheung, "A Quantitative Analysis of the Mixing of Two Segregating Powders of Different Density in a Gas-Fluidised Bed," *Powder Tech.*, **20**, 89 - 97, (1978a)

Nienow, A. W., P. N. Rowe, and T. Chiba, "Mixing and Segregation of a small proportion of Large Particles in Gas Fluidized Beds of Considerably Smaller Ones", in *Fluidization: Application to Coal Conversion Process*, AIChE Symposium Series No. 176, Vol. **74**, 45 - 53, (1978).

Piccinini, N., A. Bernhard, P. Campagana and F. Vallana, "Segregation Phenomenon in a Spouted Beds, " *Can. J. Chem. Eng.*" , **55**, 122 - 125, (1977)

Piccinini, N., "Particle Segregation in Continuously Operating Spouted Beds," in *Fluidization*,. Edited by R. Grace and J. M. Matsen , Plenum Press, New York, 373 - 381, (1980).

Pyle, D. L. and P. I. Rose, "Chemical Reaction in Bubbling Fluidized Beds," *Chem. Eng. Sci.*," **20**, 25 - 31, (1965)

Partridge, B. A. and P. N. Rowe, "Chemical Reaction in a Bubbling

Gas-Fluidised Bed," *Trans. Inst. Chem. Eng.*," **44**, T335 - T348, (1966)

Qureshi, A. E. and D. E. Creasy, "Fluidised Bed Gas Distributors", *Powder Tech.* , **22** , 113 - 119, (1979).

Rice, R. W. and J. F. Brainovich, Jr., " Mixing / Segregation in Two- and Three-Dimensional Fluidized Beds: Binary Systems of Equidensity Spherical Particles", *AIChE J*, **32**, 7 -16, (1986)

Robinson, T. and B. Waldie, "Particle Cycle Times in a Spouted Bed of Polydisperse Particles, *Can. J. Chem. Eng.*, **56**, 632 - 635, (1978)

Rowe, P. N., in "*Fluidisation* " , Edited by J.F. Davidson and D. Harrison, Academic Press, New York, (1971).

Rowe, P. N., "Gas-Solid Reaction in a Fluidised Bed," *Chem. Eng. Prog.* , **60**, No.3, 75 - 80, (1964).

Rowe, P. N., and A. W. Nienow, "Particle Mixing and Segregation in Gas Fluidised Beds. A Review", *Powder Tech.*, **5**, 141 - 147, (1976).

Rowe, P. N., A. W. Nienow, and A. J. Agbim, "The Mechanism by which Particles Segregate in Gas Fluidised Beds," *Trans. Inst. Chem. Eng.*, **50**, 310 - 323, (1972a).

Rowe, P. N., A. W. Nienow, and A. J. Agbim, " A Preliminary Quantitative Study of Particle Segregation In Gas Fluidsed Beds," *Trans. Inst. Chem. Eng.*, **50**, 324 - 335, (1972b).

Shakhova, N.A., and Minaev, G.A. , "*Heat Transfer - Sov.*", Res. 4, No.1, 133 - 142, (1972).

Sutanto, W., N. Epstein and J.R. Grace, "Hydrodynamics of Spout-fluid bed", *Powder Technology*, **44** , 205 - 212, (1985).

Sutherland, J.P. and K.Y. Wong, "Some Segregation Effects in Packed-Fluidized Beds," *Can. J. Chem. Eng.*, **42**, 163 - 167, (1964).

Tanimoto, H. , S. Chiba, T. Chiba and H. Kobayashi, "Mechanism of Solid Segregation in Gas Fluidized Beds," *in Fluidization*, Edited by R. Grace and J. M. Matsen ed., Plenum Press, New York, 381 - 387, (1980).

Toomey, R.D. and H.F. Johnstone, "Gaseous fluidization of solid particles", *Chem. Eng. Prog.*, **48**, No. 5, 220 - 226 (1952).

Uemaki, O., R. Yamada and M. Kugo, "Particle Segregation in a spouted Bed of Binary Mixtures of Particles", *Can. J. Chem. Eng.*, **61**, 303 - 307, (1983).

Wen, C.Y., Deole, N.R., and Chen, L.h., " A study of jets in a three-dimensional gas fluidised-bed", *Powder Technology*, **31**, 175 - 184, (1982)

Wen, C. Y. and Y. H. Yu , " A Generalised Method of Predicting the Minimum Fluidization Velocity," *A.I.Ch.E.J.*, **12**, 610 - 612, (1966)

Whitehead, A. B., D. C. Dent, and R. Close, "*Some Effects of Distributor type on Size Segregation in Gas-Solid Fluidized Beds*", in *Fluidization IV*, 515 - 523, (1986)

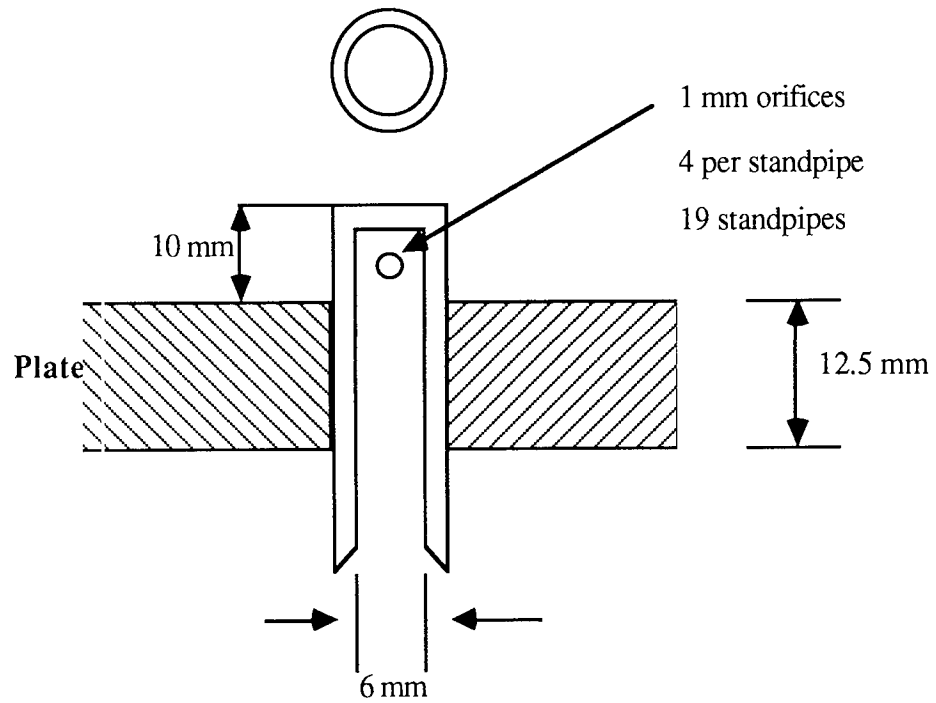
Yoshida, K., H. Kameyama, and F. Shimizu, "Mechanism of Particle Mixing and Segregation in Gas Fluidized Beds," *in Fluidization*,. R. Grace and J. M. Matsen ed., Plenum Press, New York, 389 - 396, (1980).

Zenz, F. A. , "Bubble Formation and Grid Design," *Tripartate Chem. Eng. Conf. Symp. of Fluidization II p. 136, Inst. Chem. Eng.* (1968)

APPENDICES

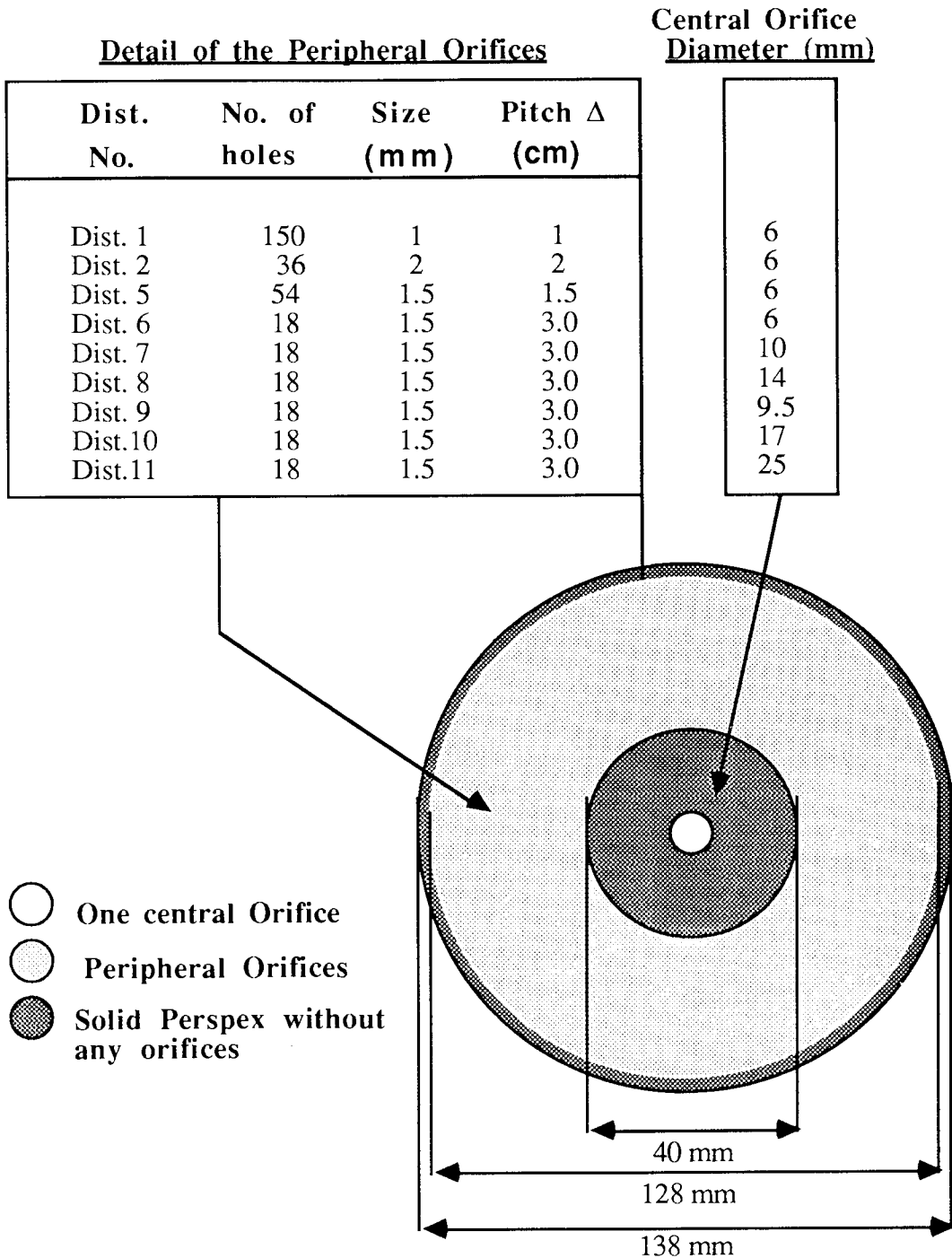
A P P E N D I X 1

Drawing of the standpipes used for standpipe
type Distributor



A P P E N D I X 2

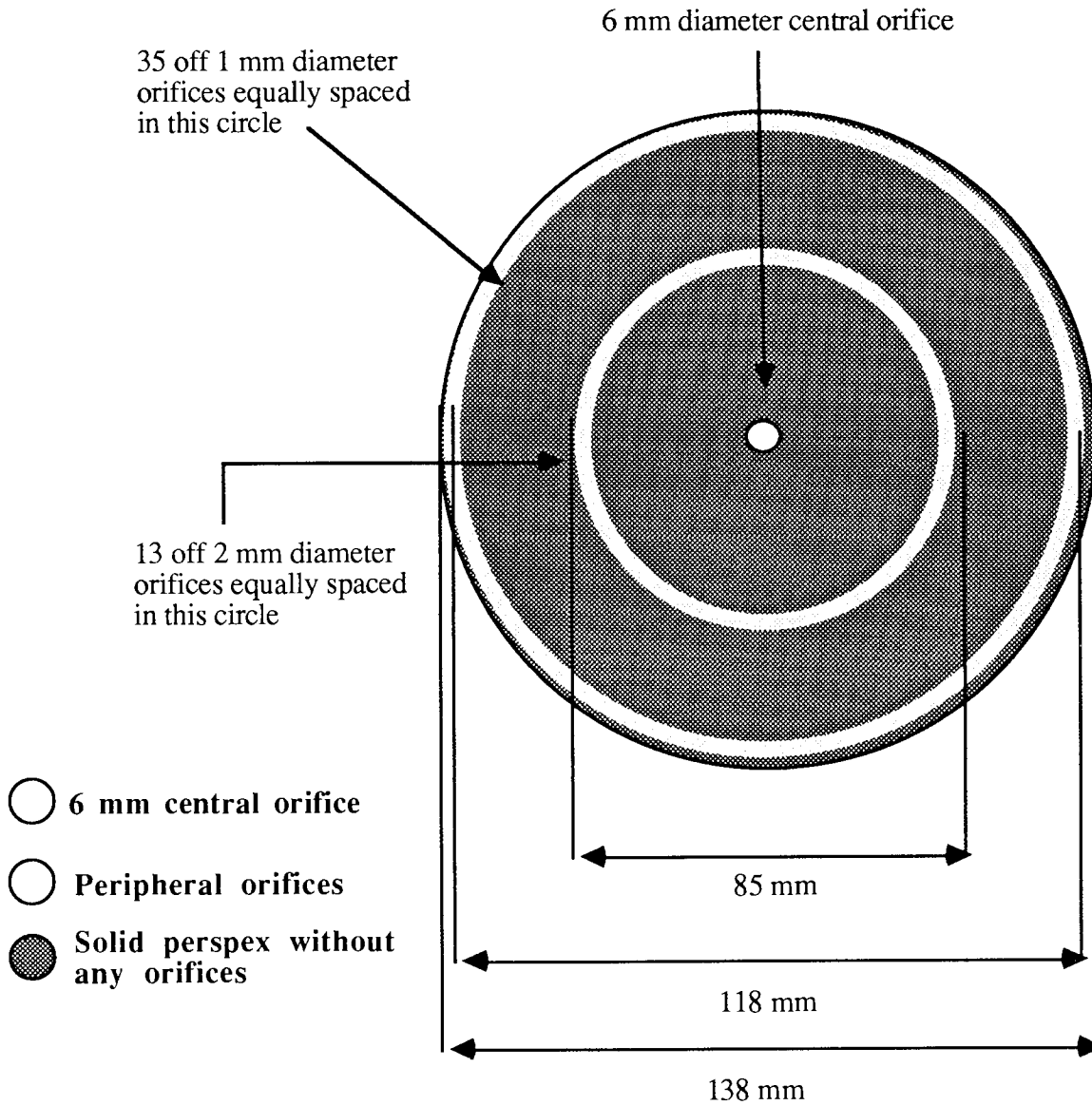
Detail of Distributors used in Spout-fluid Bed experiments



A P P E N D I X 3

Drawings of Distributor No.3 and 4

Distributor 3:



Distributor 4 : This distributor is identical to the shown above except that it does not contain 2 mm diameter orifices.